Investigating the effects of PARP and ATR inhibition for the treatment of high-risk neuroblastoma

Harriet Elizabeth Dinah Southgate

A thesis submitted to the Faculty of Medical Sciences, Newcastle University for the degree of Doctor of Philosophy

December 2020

Wolfson Childhood Cancer Research Centre

Abstract

Neuroblastoma (NB) is the commonest extra-cranial malignant solid tumour of childhood and one of the most difficult to cure. Long term survival of high-risk NB (HR-NB) currently remains less than 50% at 5 years despite intensive high-dose multimodal treatment. DNA damage response (DDR) defects are frequently observed in HR-NB including allelic deletion and loss of function mutations in key DDR genes, leading to cell cycle checkpoint dysfunction, and oncogene induced replication stress (RS). Cancer cells with defective cell cycle checkpoint signalling and/or increased oncogene-driven RS are acutely dependent on the DNA damage sensor kinase ATR.

The aim of this thesis is to identify determinants of sensitivity to ATR and PARP inhibition, alone and in combination, in preclinical models of NB. The baseline level of RS and activity of DDR kinases ATM and ATR was characterised in a panel NB cell lines as well the mutation and/or deletion status of genes previously reported to be synthetically lethal with PARP or ATR inhibition. MYCN-induced RS resulted in vulnerability to ATR and PARP inhibition, by VE-821 and olaparib, respectively. ATM deficiency was also associated with sensitivity to ATR inhibition. VE-821 sensitised NB cell lines to olaparib cytotoxicity, which was synergistic in all cell lines. There was a significant positive correlation between fold sensitisation by VE-821 and MYCN protein expression.

To obtain greater mechanistic understanding of the synergy between ATR and PARP inhibition, the effect of dual inhibition on markers of RS, cell cycle checkpoints and DNA repair were measured. VE-821 abrogated olaparib-induced S and G2 checkpoint arrest, increased olaparib-induced markers of RS and reduced homologous recombination repair foci.

Taken together the work presented in this thesis provides strong rationale for the introduction of ATR and PARP inhibitors for the treatment of HR-NB exhibiting high levels of RS.

Acknowledgements

First of all, I would like to thank my supervisors, Professor Deborah Tweddle, Professor Nicola Curtin and Dr. Lindi Chen, for all their guidance, support and confidence in me throughout this project, and for reading endless drafts for annual reviews, publications and ultimately this thesis. I am particularly grateful to Lindi for teaching me various techniques and helping me to find my feet at Newcastle University.

My thanks go to Emily Beckett, Dr. Alem Gabriel and Dr. Lisa Allison and all the previous members of the group for providing me with a wealth of genetic data relating to the cell lines, which was invaluable to this study.

Thank you to all my friends and colleagues at the Wolfson Childhood Cancer Research Centre for allowing me to borrow reagents, offering advice and making me feel so welcome during the last 3 years, it has been a privilege to work with you all. Special thanks go to Emma and Nefeli for keeping me sane when it all got a bit much with a cup of tea and the odd KitKat.

I also owe a great deal to Rory, my Mum and Dad, and my sister for always supporting me on my adventures and listening to me ramble on about science.

Finally, I would like to thank the Children's Cancer and Leukaemia Group (CCLG) and the Little Princess Trust for funding this study.

Contents

List of Figures

List of Tables

List of abbreviations

A-T	Ataxia telangiectasia
ATM	Ataxia telangiectasia mutated
ATR	Ataxia telangiectasia and Rad 3 related
ATRX	Alpha-thalassemia/mental retardation syndrome, X-linked
BER	Base excision repair
BrdU	Bromodeoxyuridine
BSA	bovine serum albumin
CDK	Cyclin dependent kinase
DDR	DNA damage response
DNA	Deoxyribose nucleic acid
DSB	Double strand break
ECL	Enhanced chemiluminescence
EFS	Event-free survival
FA	Fanconi anaemia
GN	Ganglioneuroma
GNB	Ganglioneuroblastoma
HR-NB	High risk neuroblastoma
HRP	Horse radish peroxidase
HRR	Homologous recombination repair
ICL	Interstrand crosslink
IDRF	Image derived risk factor
Indel	Insertions and deletions
INRG	International Neuroblastoma risk group
INRGSS	International Neuroblastoma risk group staging system
LOH	Loss of heterozygosity
PIKK	Phosphatidylinositol-3-kinase-like kinase
MAPK	Mitogen-activated protein kinase
MMR	Mismatch repair
MRN	Mre11-Rad50-Nbls1

NB	Neuroblastoma
NER	Nucleotide excision repair
NGS	Next generation sequencing
NHEJ	Non-homologous end joining
PAGE	polyacrylamide gel electrophoresis
PAR	Poly (ADP) ribose
PARP	Poly (ADP) ribose polymerase
PBMC	Peripheral blood mononuclear cell
PBS	Phosphate buffered saline
PCNA	Proliferating cell nuclear antigen
PI	Propidium Iodide
RPA	Replication protein A
RS	Replication stress
RT	Room temperature
RTK	Receptor tyrosine kinase
SCA	Structural chromosome alteration
SEM	Standard error of the mean
SIOPEN	European Society of Paediatric Oncology Neuroblastoma
SNP	Single Nucleotide polymorphism
SNV	Single nucleotide variant
SSB	Single strand break
TBST	Tris buffered saline, 0.5% tween 20
TLS	Trans-lesion synthesis
Top1	Topoisomerase I
TOPBP1	Topoisomerase 2-binding protein 1
WT	Wild type

Chapter 1: Introduction

1.1 Introduction

Neuroblastoma (NB) is a rare childhood cancer derived from cells of the developing sympathetic nervous system. Like many cancers, NB tumours present with numerous genetic abnormalities, including chromosomal rearrangements, focal amplifications, gains and losses of whole or parts of chromosomes or changes to the nucleic acid sequence. This dynamic process, known as genome instability, is described as an enabling characteristic promoting the acquisition of six major hallmarks of cancer, first proposed by Hanahan and Weinberg in 2000 and updated in 2011, including infinite replication, evasion of apoptosis, self-sufficiency in growth signals, insensitivity to anti-growth signals, angiogenesis, and tissue invasion and metastasis (Hanahan and Weinberg, 2000; Hanahan and Weinberg, 2011).

Defects in the DNA damage response (DDR), a highly co-ordinated network which signals to cell cycle checkpoint arrest and DNA repair pathways in response to DNA damage (**Figure 1.1**), can give rise to genomic instability (Yao and Dai, 2014; Shaltiel *et al.*, 2015). Dysregulation of cell cycle control allows for mutations to accumulate. Loss of G1 checkpoint control, through imbalance in G1/S cyclins, cyclin-dependent kinases (CDKs) and their inhibitors, activation of oncogenes such as *MYC* or *RAS* and mutations in the *TP53* or *RB* tumour suppressor genes, is a common feature of cancer cells (Massague, 2004), resulting in replication stress (RS), a state in which the DNA replication machinery cannot maintain the rate of DNA synthesis. RS causes increased replication fork stalling and collapse, rendering cells dependent on the S and G2 checkpoints for survival after DNA-damaging treatments (Zeman and Cimprich, 2014; Gaillard *et al.*, 2015). Targeting DDR defects may not only exploit cancer specific vulnerabilities but also overcome resistance to cytotoxic chemo- and radiotherapy resulting from upregulation of DNA repair pathways (Gavande *et al.*, 2016).

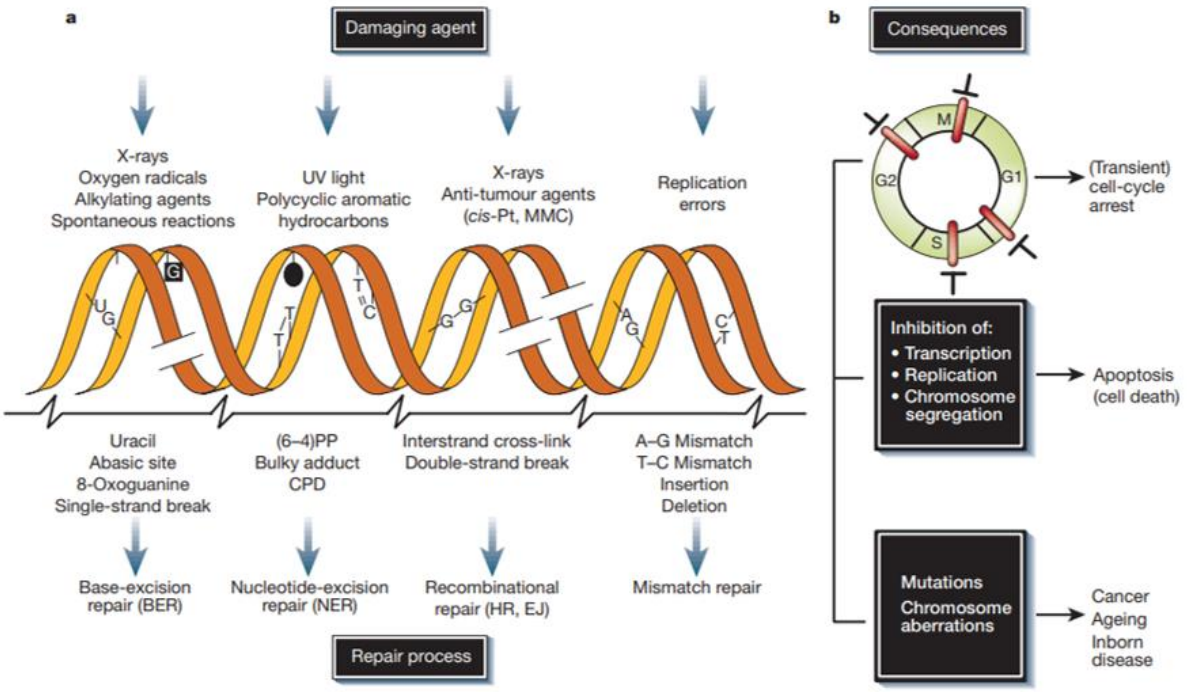

***Figure 1.1**: From (Hoeijmakers, 2001). Overview of the DNA damage response. A) DNA lesions induced by common DNA damaging agents are repaired by appropriate DNA repair pathways. B) Consequences of DNA damage. In the short term, the DDR signals to cell cycle arrest (top), and changes to DNA metabolism (middle). Persistent DNA damage can result in permanent changes in the DNA sequence, which can lead to cancer, ageing and inborn disease (bottom). Abbreviations: cis-Pt: cisplatin; MMC: mitomycin C; (6–4)PP: 6–4 photoproduct; CPD: cyclobutane pyrimidine dimer; HR: homologous recombination; EJ: end joining.*

1.2 Neuroblastoma

NB accounts for 8% of all childhood (0-14 years) cancers in the UK and is the commonest extra-cranial malignant solid tumour of infancy (Stiller, 2007). Around 100 new cases are diagnosed each year in the UK, with the median age of diagnosis being 17 months (Maris, 2010). NB is a neuroendocrine tumour derived from undifferentiated or precursor cells of the sympathetic nervous system resulting in tumours in the adrenal glands or sympathetic ganglia, presenting in the abdomen, neck, chest or spine (Matthay *et al.*, 2016). Tumours are highly heterogeneous both phenotypically and clinically and outcome can vary from maturation or spontaneous regression to aggressive progression (Shimada *et al.*, 1999). Pathologically, tumours show varying degrees of differentiation ranging from NB, which is mainly composed of poorly or undifferentiated small round tumour cells, ganglioneuroblastoma intermixed, consisting of both immature cells and terminally differentiated ganglion tumour cells, to a mature ganglioneuroma (Matthay *et al.*, 2016). Tumours showing a higher degree of cell differentiation tend to have a better prognosis than

undifferentiated tumours. Tumour differentiation, age at diagnosis, tumour stage and molecular abnormalities are used to stratify NB into risk groups which determine treatment strategies (discussed in 1.2.2).

1.2.1 Genetics of Neuroblastoma

1.2.1.1 *MYCN* amplification

Amplification of the *MYCN* oncogene, either as extrachromosomal double minutes or intra-chromosomal homogenously staining regions (Brodeur, 2003), is one of the strongest unfavourable prognostic markers, observed in around 20% of NB cases (Cohn *et al.*, 2009). The frequency of *MYCN* amplification increases to around 50% in the high-risk group (Brodeur *et al.*, 1984). *MYCN* is a member of the *MYC* family of basic-helix–loop–helix-leucine zipper (bHLH-LZ) transcription factors, which also includes c-*MYC* and MYCL (Collins and Groudine, 1982; Schwab *et al.*, 1983; Nau *et al.*, 1985). **Figure 1.2** shows the structure of the MYCN protein.

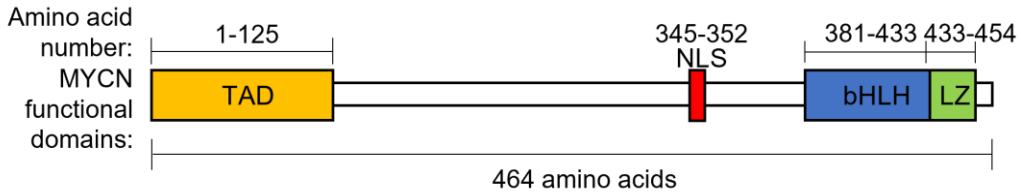

Figure 1.2: Schematic representation of MYCN functional domains. TAD: transcriptional activation domain; NLS: nuclear localization signal; bHLH: basic-helix-loop-helix; LZ: leucine zipper

MYC family transcription factors mediate mitogen signalling by regulating transcription of target genes involved in cell cycle regulation, cell adhesion, protein biosynthesis, metabolism, and the cytoskeleton (Dang *et al.*, 2006; Eilers and Eisenman, 2008). Increased expression of *MYC* family proteins have a critical role in cell proliferation, differentiation, apoptosis, and oncogenesis. *MYCN* expression is restricted to the developing nervous system and only a few other sites (Downs *et al.*, 1989; Hirning *et al.*, 1991; Ma *et al.*, 2014). Ectopic expression of *MYCN* drives cell proliferation but results in sensitisation to apoptosis through activation of the p53 tumour suppressor pathway (Chen *et al.*, 2010). Mechanisms to escape MYCN induced apoptosis are essential for the development of NB tumours (reviewed by (Hogarty, 2003)), which may be achieved by loss of expression of the initiator caspase, caspase 8 (Teitz *et al.*, 2001; McKee and Thiele, 2006; Stupack *et al.*, 2006), a mediator of the extrinsic death

receptor apoptosis pathway (Crowder and El-Deiry, 2012; Kaufmann *et al.*, 2012). A functional MYCN/c-MYC signature also characterizes a fraction of aggressive neuroblastoma without *MYCN* amplification (Westermann *et al.*, 2008; Valentijn *et al.*, 2012), suggesting that increased MYC activity is a main driver of aggressiveness in neuroblastoma. Overexpression of *MYC* oncogenes drives rapid, erroneous replication leading to RS (Rohban and Campaner, 2015).

Direct therapeutic targeting of MYCN is hindered by the lack of appropriate small molecule binding surfaces in its DNA binding domain (Prochownik and Vogt, 2010), therefore most strategies to regulate MYCN are indirect by targeting proteins involved in the transcription or stabilization of MYCN and inhibiting downstream targets or synthetically lethal pathways (Bell *et al.*, 2010; Barone *et al.*, 2013; Esposito *et al.*, 2017). Targeting MYCN-induced RS with DDR inhibitors may provide a novel treatment strategy for *MYCN* amplified NB.

1.2.1.2 DNA ploidy

Normal human cells have a diploid genome consisting of 2 copies of each of the 23 chromosomes. However, in NB, changes to DNA ploidy are frequently observed. The DNA index of a tumour is the ratio of the number of chromosomes present compared to a diploid genome, and hence diploid cells have a DNA index of 1. DNA index is an important prognostic marker of disease in infants. Typically, patients with near-triploid tumours have a better survival rate than patients with near diploid or near tetraploid tumours (Look *et al.*, 1991), although this association is lost in children older than 2 years of age.

1.2.1.3 Segmental chromosome alterations

Many NB tumours present with numerous “typical” structural chromosome alterations (SCAs), such as gain of 1q, 2p, and 17q, and deletion of chromosomes 1p, 3p and 11q (Schleiermacher *et al.*, 2011; Schleiermacher *et al.*, 2012; Defferrari *et al.*, 2015). Gain of chromosome 17q and loss of chromosome 1p, observed in half and a third of NB cases respectively, correlate with *MYCN* amplification and poor prognosis (Bown *et al.*, 1999; Attiyeh *et al.*, 2005). Loss of 11q is also observed in about third of NB tumours and is a marker of poor prognosis independent of *MYCN* status (discussed in 1.2.1.4) (Attiyeh *et al.*, 2005).

Both the *MYCN* and the *ALK* genes (discussed 1.2.1.7) are located on chromosome 2p (Mossë *et al.*, 2008) and gain of this region is associated with their overexpression. Generally, the presence of SCAs is associated with advanced stage of disease and inferior outcome (Schleiermacher *et al.*, 2012).

1.2.1.4 11q loss

Loss of chromosome 11q is observed in around 30-40% of NB tumours and is present in many non-*MYCN* amplified high-risk tumours. *MYCN* amplification and 11q loss rarely occur together, and prognosis is especially poor for the 2% of cases of NB patients who present with both abnormalities (Spitz *et al.*, 2006; Villamón *et al.*, 2013). The smallest region of overlap in 11q deletions has been reported between 11q14 and 11q23 (Maris *et al.*, 2001) and includes 4 DDR genes, *ATM* (11q22.3), *CHK1* (11q24.2), *MRE11* (11q21) and *H2AFX* (11q23.3) (**Figure 1.3**) (Mlakar *et al.*, 2017). In most cases, no mutation or hyper-methylation was found in the remaining allele of these genes (Mlakar *et al.*, 2017), but loss of one copy through 11q deletion could contribute to tumorigenesis due to haploinsufficiency.

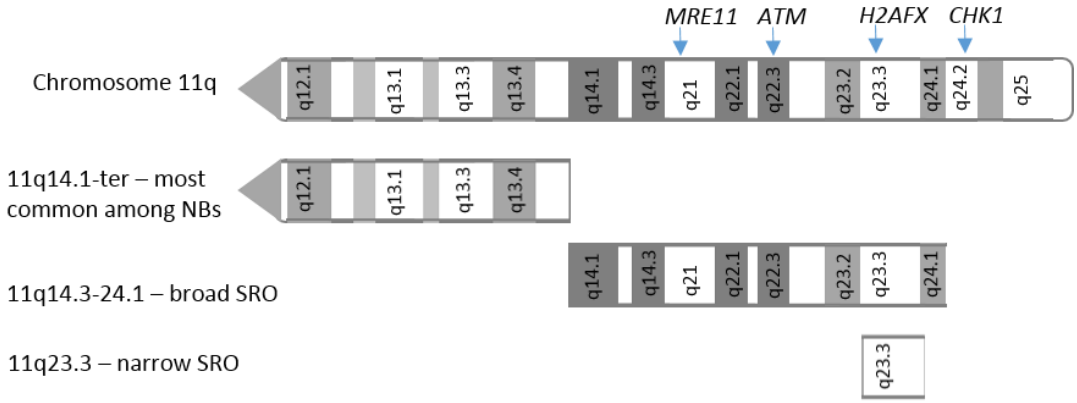

***Figure 1.3**: from (Southgate et al., 2020). Location of 11q arm deletions observed in neuroblastoma tumours. SRO: shortest region of overlap.*

Homozygous germline mutations in *ATM* (ataxia-telangiectasia mutated) cause ataxia telangiectasia (A-T), a recessive genetic disease characterised by cerebellar degeneration, chromosomal instability and cancer predisposition. ATM has a key role in signalling to DNA repair machinery and cell cycle arrest in response to DNA double strand breaks (DSBs) (reviewed in (Maréchal and Zou, 2013)). Somatic *ATM* mutations have been identified in many cancer types (Choi *et al.*, 2016), suggesting that ATM loss contributes to tumorigenesis.

CHK1, MRE11 and *H2FAX* encode proteins integral to the DDR. CHK1 is the primary target of ataxia-telangiectasia and rad3-related (ATR) kinase which has a pivotal role in the regulation of DNA replication, repair and cell cycle checkpoint arrest in response to RS. Mre11 is part of the Mre11-Rad50-Nbls1 (MRN) complex, which is involved in the identification and repair of DSBs. *MRE11* is essential for cell survival and homozygous, hypomorphic *MRE11* mutations result in ataxia telangiectasia-like disorder, a genetic disease which is phenotypically similar to A-T (Delia *et al.*, 2004). *H2AFX* encodes a variant of histone 2A which can be phosphorylated. Phosphorylation of H2AX by DDR kinases, such as ATM and ATR, in response to DNA damage results in the recruitment of DNA repair machinery and chromatin remodelling complexes, and the amplification of the signal along chromatin (Podhorecka *et al.*, 2010).

In summary, heterozygous loss of these genes through 11q deletion could result in defective DDR, increasing chromosome instability and tumourigenesis.

1.2.1.5 p53 pathway

The tumour suppressor gene *TP53* is frequently mutated in many human cancers (Rivlin *et al.*, 2011). The p53 protein is a transcription factor which is activated in response to a variety of intra- and extracellular stresses, including DNA damage, oncogene activation, ribonucleotide depletion, deficient growth factors/signals, and hypoxia (Horn and Vousden, 2007) and has a crucial role in maintaining genome integrity and tumour suppression. Activated p53 regulates transcription of genes involved in cell cycle arrest, DNA repair, metabolism, apoptosis, senescence, differentiation, angiogenesis and metastasis (Vogelstein *et al.*, 2000; Bieging *et al.*, 2014; Liu *et al.*, 2015).

Loss of p53 function is also seen in tumours with wild type p53 (Vogelstein *et al.*, 2000), through upregulation of *MDM2*, an E3 ubiquitin ligase which targets p53 for degradation (Zhao *et al.*, 2014), or loss of $p14^{ARF}$ function, which inhibits MDM2 (Agrawal *et al.*, 2006; Ozenne *et al.*, 2010) (**Figure 1.3**).

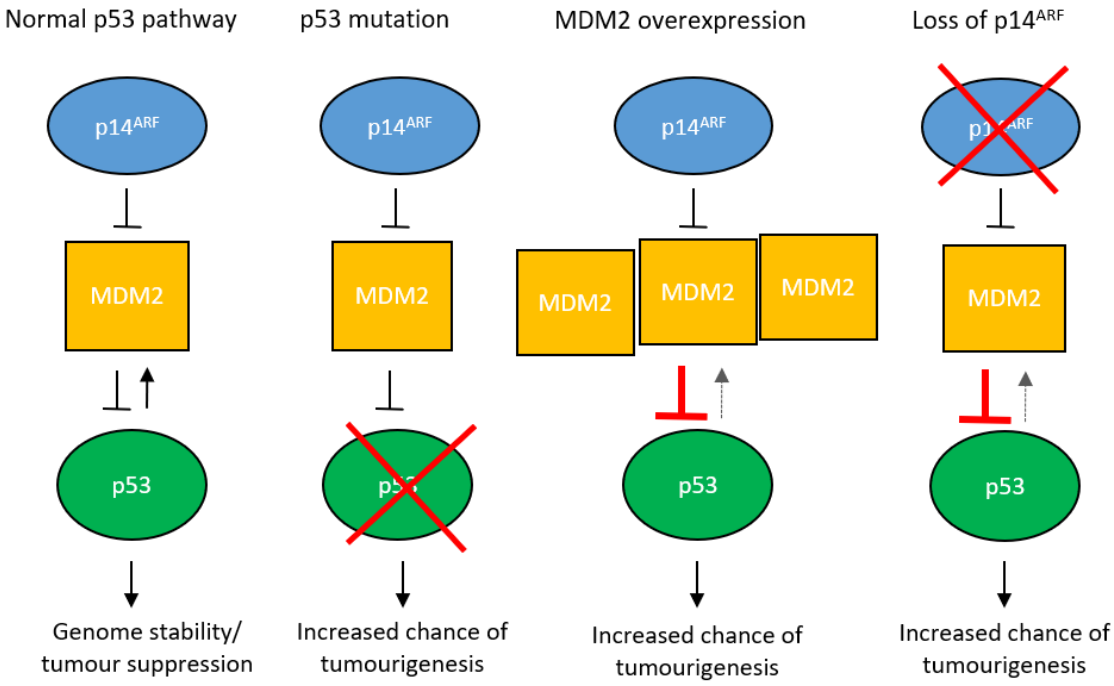

Figure 1.4: *from Southgate et al. 2020. The p53 tumour suppressor pathway can be disrupted in neuroblastoma by mutation of the gene coding for p53, overexpression of MDM2 e.g. by gene amplification, or loss of p14^{ARF} expression by gene methylation or homozygous deletion.*

TP53 mutations are rare in NB at diagnosis, however p53 pathway aberrations are observed more frequently at relapse (Tweddle *et al.*, 2001; Carr *et al.*, 2006; Carr-Wilkinson *et al.*, 2010), where around 50% of relapsed cases analysed show *TP53* mutation, *MDM2* amplification or *p14^{ARF}* deletion, suggesting that p53 inactivation could be a contributor to drug resistance. In addition, *TP53* is located on chromosome 17p13.1 and allelic loss of 17p has been observed in both NB cell lines and tumours (Schleiermacher *et al.*, 2004; Vandesompele *et al.*, 2008), indicating that 17p loss could contribute to loss of p53 function.

Targeting the MDM2-p53 interaction with MDM2 antagonists such as Nutlin-3, MI-63 and idasanutlin, have been shown to have anti-tumour activity in NB cell lines with wild type p53, as single agents and in combination with conventional chemotherapies (Van Maerken *et al.*, 2009; Van Maerken *et al.*, 2011; Gamble *et al.*, 2012; Chen *et al.*, 2015a; Lakoma *et al.*, 2015). As most NB tumours retain wild-type p53, the use of MDM2 inhibitors have the potential to be an excellent therapeutic tool for the treatment of HR-NB.

1.2.1.6 Telomere maintenance

Telomeres are regions of repetitive DNA sequences at the ends of eukaryotic chromosomes. At each cell division, some telomeric repeats are lost due to the end replication problem and telomere length is decreased. At a critical length, short telomeres trigger senescence, a state of permanent cell cycle arrest where the cell will cease to divide (Bernadotte *et al.*, 2016). Cancer cells must maintain telomere length in order to achieve unlimited replicative potential, a hallmark of cancer (Hanahan and Weinberg, 2011). In most human cancers, telomeres are maintained by the activation of telomerase, a large RNA-dependent reverse transcriptase responsible for the progressive synthesis of telomeric DNA repeats (Shay and Bacchetti, 1997). Telomerase expression is usually repressed in somatic cells (Ulaner *et al.*, 1998) and is activated by upregulation of *TERT,* the gene encoding the catalytic protein subunit (Hahn and Meyerson, 2001). In many of those cancer cells which do not express telomerase, telomere length is maintained through another mechanism known as alternate lengthening of telomeres (ALT). The ALT pathway is a recombination mediated mechanism of DNA replication which lengthens telomeres by using telomeric DNA as a template (Dunham *et al.*, 2000).

Telomere maintenance is essential in the establishment of HR-NB (**Figure 1.5**) (Hertwig *et al.*, 2016). High telomerase expression indicates increased invasiveness and poor prognosis (Onitake *et al.*, 2009), comparable to *MYCN* amplified tumours (Kawashima *et al.*, 2016). Rearrangements at the *TERT* gene locus (5p15.33) are frequent in NB resulting in overexpression of the *TERT* gene and subsequent telomerase expression (Valentijn *et al.*, 2015; Kawashima *et al.*, 2016). *TERT* is known to be a transcriptional target of MYCN (Mac *et al.*, 2000), and, in the absence of *TERT* rearrangements, *MYCN* amplified NB cells show increased *TERT* expression compared to non-*MYCN* amplified cells (Peifer *et al.*, 2015). In light of this, telomerase inhibitors could contribute to the personalised treatment of a subset of NB cases (Binz *et al.*, 2005; Duan and Zhao, 2017).

In HR-NB tumours that do not express telomerase, the ALT pathway is activated. ALT activity in NB is associated with mutations to the α-thalassaemia/mental retardation syndrome X-linked (*ATRX*) gene (Bower *et al.*, 2012; Cheung *et al.*, 2012; Napier *et al.*, 2015). *ATRX* encodes an RNA-helicase which plays a role in chromatin remodelling, nucleosome assembly and telomere maintenance (Clynes *et al.*, 2013). Loss of function mutations or intragenic deletions

in *ATRX* is associated with older age of diagnosis (>5 years) and a chronic or indolent, but ultimately fatal, disease course (Cheung *et al.*, 2012; Molenaar *et al.*, 2012). Loss of ATRX function is mutually exclusive with *MYCN* amplification, and is incompatible with MYCN overexpression due to intolerable levels of RS (Pugh *et al.*, 2013; Zeineldin *et al.*, 2020). Identifying *ATRX* mutations or intragenic deletions could define a subset of NB cases in which the ALT pathway could be targeted to improve treatment.

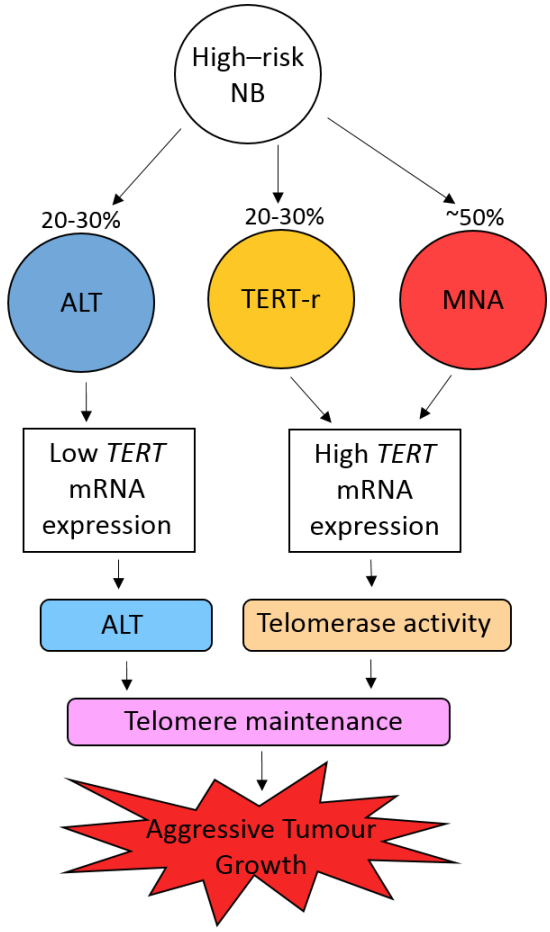

***Figure 1.5**: Telomere maintenance by alternate lengthening of telomeres (ALT) or by telomerase activation as a result of TERT rearrangements (TERT-r) or MYCN amplification (MNA) leads to aggressive tumour growth seen in high risk NB tumours.*

1.2.1.7 ALK

Activating anaplastic lymphoma kinase (*ALK*) mutations have been reported in between 8-10% of sporadic NB and up to 50% of familial NB (familial NB is rare accounting for around 2% of NB cases), across all risk groups and occurring more frequently at relapse (Carén *et al.*, 2008; Janoueix-Lerosey *et al.*, 2008; Mossë *et al.*, 2008; Pugh *et al.*, 2013; Schleiermacher *et*

al., 2014). ALK is a receptor tyrosine kinase (RTK) which is specifically expressed in the developing nervous system (Iwahara *et al.*, 1997; Morris *et al.*, 1997). Like other RTKs, ligand binding leads to receptor activation by dimerization and auto-phosphorylation, recruitment of adaptor proteins and downstream signal transduction through pathways such as PI3K/AKT, RAS/MAPK, and JAK/STAT (George *et al.*, 2008; Azarova *et al.*, 2011; Hallberg and Palmer, 2013). In NB, constitutive activation of ALK, and subsequent downstream pathways, has been shown to be involved in cell proliferation, migration and invasion (Bresler *et al.*, 2014). There are three mutational hotspots in the tyrosine kinase domain which evoke constitutive activation, F1174, R1275 and F1245, and collectively account for around 85% of reported *ALK* mutations in NB (Chen *et al.*, 2008; George *et al.*, 2008). As well as mutations, aberrant ALK activity has also been reported through *ALK* amplification in a further 2% of NB (Mossë *et al.*, 2008; Bresler *et al.*, 2014). *ALK* amplification has been shown to be accompanied by *MYCN* amplification and there is evidence that ALK activation accelerates MYCN-driven tumorigenesis in animal models (Berry *et al.*, 2012; Zhu *et al.*, 2012). Inhibitors of the ALK tyrosine kinase have been developed but, although promising in preclinical models, have had limited success in the clinic as monotherapy, with resistance being a major hurdle (Carpenter and Mossé, 2012; Mossé, 2016; Berlanga *et al.*, 2017).

1.2.1.9 MAP Kinase pathway

Mitogen-activated protein kinase (MAPK) signalling pathways encompass different signalling cascades which regulate processes such as cell proliferation, differentiation and survival (Morrison, 2012). One of these pathways, the RAS-ERK/MAPK pathway, also known as RAS-RAF-MEK-ERK, is one of the most frequently dysregulated in human cancer (Santarpia *et al.*, 2012). In NB, the RAS-ERK/MAPK pathway is activated by constitutive ALK activation (see previous section) and mutation in components of the RAS-ERK/MAPK pathway are frequently observed in relapse, likely contributing to therapy resistance (Eleveld *et al.*, 2015). These mutations include activating mutations in *BRAF, RAS* (*KRAS* and *HRAS*) and *PTPN11* oncogenes (Pugh *et al.*, 2013), the latter encodes the tyrosine phosphatase SHP-2, and inactivating mutations in the *NF1* tumour suppressor gene (Eleveld *et al.*, 2015), a negative regulator of RAS (Bollag *et al.*, 1996). Preclinical studies have shown that NB cell lines with activated RAS-ERK/MAPK pathway are sensitive to MEK inhibitors (Tanaka *et al.*, 2016; Woodfield *et al.*,

2016). Activation of the RAS signalling pathway leads to RS by driving DNA replication, analogous to MYCN overexpression, and highlights another subset of patients which may benefit from DDR inhibitors (Primo and Teixeira, 2020).

1.2.2 Neuroblastoma Risk Stratification

At diagnosis, NB cases are categorised into three risk groups, low, intermediate and high risk, on the basis of age at diagnosis, histopathology, tumour stage and molecular abnormalities including *MYCN* status and chromosome copy number alterations according to the International Neuroblastoma risk group (INRG) classification system (**Table 1.1**) (Cohn *et al.*, 2009). Tumour stage is determined based on the presence or absence of several image defined risk factors (IDRFs) or metastases present at the time of diagnosis according to the International Neuroblastoma risk group staging system (INRGSS), which was designed to identify consistent pre-treatment risk groups to allow comparison in clinical trials (Monclair *et al.*, 2009) (**Table 1.2**). The probability of disease free survival for low, medium and high risk groups is 95% to 100%, 85% to 90%, and less than 50% respectively (**Figure 1.6**) (Davidoff, 2012; Park *et al.*, 2013). HR-NB accounts for around 50% of all NB cases (Cohn *et al.*, 2009) and, despite intensive multi-modal therapy, 50% of patients with HR-NB will relapse, with a 5 years survival rate of 20% after initial relapse (London *et al.*, 2011; Cheung and Dyer, 2013; Basta *et al.*, 2016; London *et al.*, 2017). New treatments and a better understanding of drug resistance are needed before these survival rates can significantly improve.

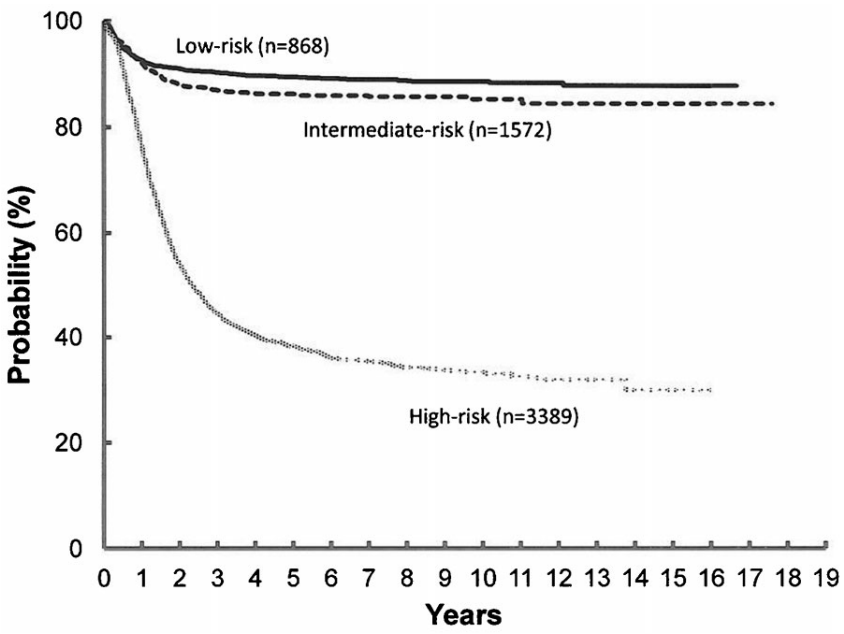

***Figure 1.6**: (from (Park et al., 2013)) Event free Kaplan-Meier survival plots of children with neuroblastoma classified as low, intermediate, and high risk at time of diagnosis.*

Table 1.1: International Neuroblastoma Risk Group Classification System

Pre-treatment Risk Group	INRG stage	Age (months)	Tumour Histology	Tumour Differentiation	*MYCN* status	11q Aberration	DNA Ploidy
Very low	L1/L2	Any	GN maturing GNB intermixed	Any	Any	Any	Any
Very low	L1	Any	Any*	Any	Non-amp	Any	Any
Very low	MS	<18	Any	Any	Non-amp	No	Any
Low	L2	<18	Any*	Any	Non-amp	No	Any
Low	L2	≥18	GNB nodular, NB	Differentiating	Non-amp	No	Any
Low	M	<18	Any	Any	Non-amp	Any	Hyper-diploid
Intermediate	L2	<18	Any*	Any	Non-amp	Yes	Any
Intermediate	L2	≥18	GNB nodular, NB	Differentiating	Non-amp	Yes	Any
Intermediate	L2	≥18	GNB nodular, NB	Poorly or undifferentiated	Non-amp	Any	Any
Intermediate	M	<18	Any	Any	Non-amp	Any	Diploid
High	L1	Any	Any*	Any	Amp	Any	Any
High	L2	Any	Any	Any	Amp	Any	Any
High	M	<18	Any	Any	Amp	Any	Any
High	M	≥18	Any	Any	Any	Any	Any
High	MS	<18	Any	Any	Amp	Any	Any
High	MS	<18	Any	Any	Any	Yes	Any

GN, ganglioneuroma; GNB, ganglioneuroblastoma; NB, neuroblastoma; Amp, amplified *Except GN maturing, GNB intermixed.
Adapted from (Cohn *et al.*, 2009)

Table 1.2: International Neuroblastoma Risk Group Staging System

Stage	Features
L1	Localised tumour not involving vital structures as defined by the list of image-defined risk factors (IDRFs) and confined to one body compartment
L2	Localised tumour with the presence of one or more IDRFs
M	Metastatic disease not including MS
MS	Metastatic disease in children <18 months of age at diagnosis with metastases limited to skin, liver and/or bone marrow
Adapted from (Monclair *et al.*, 2009)	

1.2.3 Current Treatment of Neuroblastoma

Treatment strategies in NB are defined by risk classification and an overview is given in **Table 1.3**. Low risk disease will often spontaneously regress and generally show a good outcome with clinical observation or surgical resection alone. For intermediate risk, treatment regimens are response dependent and vary from 4 to 8 cycles of chemotherapy, often at lower doses than high risk regimens, followed by surgical resection of the primary tumour where possible.

HR-NB is currently treated with a number of different DNA damaging agents during induction and consolidation according to the previous European High Risk NB trial (HR-NBL1, NCT01704716), including cisplatin, carboplatin, etoposide, topotecan, doxorubicin, cyclophosphamide and vincristine during induction, and high dose busulfan and melphalan myeloablative therapy with autologous stem cell rescue and radiotherapy to the site of the primary tumour during consolidation.

A second European High Risk NB trial (HR-NBL2, NCT04221035), is expected to open in the UK in 2021 and will include cisplatin, carboplatin, etoposide, cyclophosphamide, vincristine, ifosfamide, dacarbazine and doxorubicin during induction, and high dose thiotepa, busulfan and melphalan myeloablative therapy with autologous stem cell rescue during consolidation. Radiotherapy is also directed to site of primary tumour during consolidation.

In 2015, immunotherapy with the anti-GD_2 chimeric mono-clonal antibody Dinutuximab (United Therapeutics) was approved by the Food and Drug Administration (FDA) for maintenance treatment in combination with granulocyte-macrophage colony-stimulating factor (GM-CSF) and 13-cis retinoic acid for paediatric HR-NB patients (Gur *et al.*, 2017). The

National Institute for Health and Care Excellence (NICE) recommended Dinutuximab beta (Eusa Pharma) for maintenance treatment of HR-NB in 2018.

Table 1.3: Neuroblastoma treatment overview by risk group

	Treatment		
Risk Group	Induction	Consolidation	Maintenance
Low	Clinical Observation/ Surgical resection		
Intermediate	2-8 cycles chemotherapy (response dependent) and surgical resection		
High	Induction chemotherapy and surgical resection	Autologous stem cell transplant and radiation to site of primary tumour	GD_2 immunotherapy and isoretinoin

With these regimens the majority of patients will respond to treatment but over 50% of cases will relapse and very few relapsed patients can then be cured (Cheung and Dyer, 2013; Basta *et al.*, 2016). Presently at relapse patients are given a backbone chemotherapy of irinotecan with temozolomide, topotecan with temozolomide, topotecan with cyclophosphamide or topotecan, vincristine and doxorubicin, to which new agents are added.

Surviving patients often suffer from multiple sequelae caused by the intensive treatment regimens (Perwein *et al.*, 2011). Exploiting cancer specific vulnerabilities with selective inhibitors has the potential to replace conventional chemotherapeutics or decrease the dose required for therapeutic effect, thus reducing the toxic side effects of HR-NB treatment.

1.3 The DNA damage response

The DDR is a highly orchestrated network which detects DNA damage and signals to cellular responses including cell cycle checkpoint arrest, DNA repair and apoptosis (Harper and Elledge, 2007). It has evolved to allow cells to recover from high levels of endogenous and environmental DNA damage and prevent damaged DNA from being passed on to daughter cells. Types of DNA damage include base modification/loss, bulky abducts, single strand break (SSB), double strand break (DSB), inter-/ intra-strand crosslinks and mismatched bases (Ciccia

and Elledge, 2010). Dysfunction of the DDR network is common in cancer as it leads to genomic instability that enables cellular transformation and tumour development. The differential responses to current anti-cancer therapies is likely to be dependent on the DDR. Although some DDR dysfunction enables cancer development and increases therapeutic resistance (Bouwman and Jonkers, 2012), defects in particular pathways are exploitable with the appropriate conventional therapy or novel agents targeting components of the DDR (reviewed by (Curtin, 2012)), selectively killing cancer cells.

Table 1.4 outlines the mechanism by which cytotoxic agents used in the treatment of HR-NB inflict DNA damage and the pathway involved in subsequent DNA repair (described in section 1.3.4).

Table 1.4: DNA damaging mechanism of chemotherapeutic agents used in the treatment of HR-NB (Payne and Miles, 2008).

Therapy	Mechanism of action	Pathways involved in repair
Cisplatin, carboplatin	Platinum based crosslinking agent	FA pathway including NER and HRR
Cyclophosphamide, busulfan, melphalan, thiotepa, ifosamide, dacarbazine	Crosslinking agent (nitrogen mustard)	FA pathway including NER and HRR
Etoposide, doxorubicin	Topoisomerase II poison	DSBR
Topotecan, irinotecan	Topoisomerase I poison	HRR
Temozolomide	DNA methylating agent	BER
Abbreviations: BER: base excision repair, DSBR: double strand break repair, FA: fanconi anaemia, HRR: homologous recombination repair, NER: nucleotide excision repair		

1.3.1. Replication stress

RS occurs when the DNA replication programme is disrupted. It is a state in which the DNA replication machinery cannot maintain the rate of DNA synthesis resulting in increased replication fork stalling (Zeman and Cimprich, 2014; Gaillard *et al.*, 2015), and is a primary cause of chromosome instability (Burrell *et al.*, 2013). Physical blockages to DNA replication machinery, such as unrepaired DNA damage, stable secondary DNA structures (hairpins or G-

quadruplex structures) or collision with transcription machinery, impair replication fork progression. Limited availability of resources, for example diminished nucleotide pools, also slows down replication fork progression and can lead to fork stalling. In addition to physical impediments to fork progression, dysregulated replication origin firing leads to RS. DNA replication in eukaryotes is initiated at multiple sites along chromosomes known as origins. Origin firing is temporally regulated with some origins firing early or late in each replication cycle. Origins can also be dormant whereby they are not fired unless replication fork progression is impeded (Alver *et al.*, 2014). Both insufficient and excessive origin firing can lead to RS (Taylor and Lindsay, 2016). A common feature of cancer cells is that development is driven by the overexpression of oncogenes such as cyclin E, RAS and MYC. Overexpression of oncogenes causes RS by initiating premature S-phase, driving rapid, erroneous DNA replication, and increasing origin activity (Koppen *et al.*, 2007; Kotsantis *et al.*, 2018). As the *MYCN* oncogene is amplified in ~50% of HR-NB (Brodeur *et al.*, 1984), oncogene-induced RS is a potential target in the treatment of this type of NB.

1.3.2. The Cell Cycle

Cell division in normal cells is tightly regulated by the cell cycle, which is divided into four phases: gap 1 (G1), synthesis (S), gap 2 (G2) and mitosis (M). Transition into each phase requires the activation of CDK, which is controlled by oscillating concentrations of cyclins. CDK activity requires cyclin binding, but is additionally regulated by both activating and inhibitory phosphorylation of serine, threonine and tyrosine residues (Hochegger *et al.*, 2008).

There are 3 checkpoints within interphase, G1, intra-S and G2, in which the cell cycle can be arrested to protect genome integrity by preventing cell cycle progression with damaged DNA. Checkpoint activation by the DDR results in cell cycle arrest by the activation of CDK inhibitory kinases (WEE1 and Myt1), inactivation of phosphatases (cdc25) and the upregulation of CDK inhibitors (e.g. p21). The G1 checkpoint prevents the replication of damaged DNA by restricting entry into S-phase. If damage occurs at the beginning of S phase or has evaded the G1 checkpoint, then further replication is blocked by activation of the intra-S phase checkpoint. If damage occurs after this point, the G2 checkpoint is activated which prevents entry into mitosis with damaged DNA. If irreparable damage is sustained, the cell will undergo apoptosis (Shaltiel *et al.*, 2015).

1.3.3. Cell cycle checkpoint signalling

DNA damage sensors initiate cell cycle arrest by the activation of downstream signalling pathways. Two of these sensors are ATM and ATR, which are members of the phosphatidylinositol-3-kinase-like kinase (PIKK) family. ATM is activated in response to DSBs whereas ATR is activated by regions of single-stranded DNA (ssDNA), such as ssDNA regions at stalled replication forks or formed by end resection during HRR (Maréchal and Zou, 2013). The primary targets of ATM and ATR are the checkpoint kinases CHK2 and CHK1, respectively, which signal to checkpoint arrest by regulation of the proteins involved in cell cycle progression, as demonstrated in **Figure 1.6**. One target of CHK1 and CHK2 is the cdc25 family of phosphatases which remove inhibitory phosphorylation on CDKs. Inhibitory phosphorylation of cdc25 prevents them dephosphorylating and activating CDKs resulting in cell cycle arrest. In addition to inactivation of cdc25, activation of WEE1 kinase maintains the inhibitory phosphorylation of CDKs, preventing entry into mitosis. In undamaged cells, ATM exists as a dimer. Upon recruitment by the MRN complex to DSBs, ATM autophosphorylates resulting in monomerisation and activation (Paull, 2015). ATM is also activated in response to oxidative stress. Active ATM phosphorylates many target proteins regulating DNA repair, cell cycle arrest and apoptosis including CHK2, p53, MDM2, H2AX, MRN, BRCA1 and BLM (Shiloh and Ziv, 2013). ATM plays a crucial role in the activation of the G1/S cell cycle checkpoint which is primarily mediated through p53 activity. ATM can also signal to S and G2/M checkpoints via CHK2, which phosphorylates cdc25A, preventing S phase progression, and cdc25C, preventing the transition into mitosis (**Figure 1.7**) (Weber and Ryan, 2015).

ATR is activated by ssDNA structures arising at resected DSBs or stalled replication forks. The ssDNA is bound by the RPA (replication protein A) complex which recruits ATRIP, the constitutive binding partner of ATR, and hence ATR to the damage. The Rad17-RFC is also recruited to RPA and recruits the Rad9-Rad1-Hus1 (9-1-1) complex. The 9-1-1 complex is a sliding clamp, related to the replication sliding clamp proliferating cell nuclear antigen (PCNA), and recruits DNA topoisomerase 2-binding protein 1 (TOPBP1) to the site of damage which is required for full ATR activation (Cimprich and Cortez, 2008). ATR phosphorylates many downstream targets including Rad17. Phosphorylated Rad17 recruits the mediator protein Claspin which regulates ATR-dependent phosphorylation of CHK1 (Wang *et al.*, 2006). Activation of CHK1 by ATR leads to inhibition of cdc25A and cdc25C (Karnitz and Zou, 2015),

preventing S phase progression and G2/M transition respectively. Despite overlapping downstream targets, loss of ATM is viable, whereas loss of ATR is embryonic lethal, suggesting some roles of ATR are essential. One of the essential functions is the role of ATR in survival following RS. In addition to inducing cell cycle arrest, ATR signalling prevents replication origin firing, maintains stability of stalled replication forks and promotes replication restart (Saldivar *et al.*, 2017).

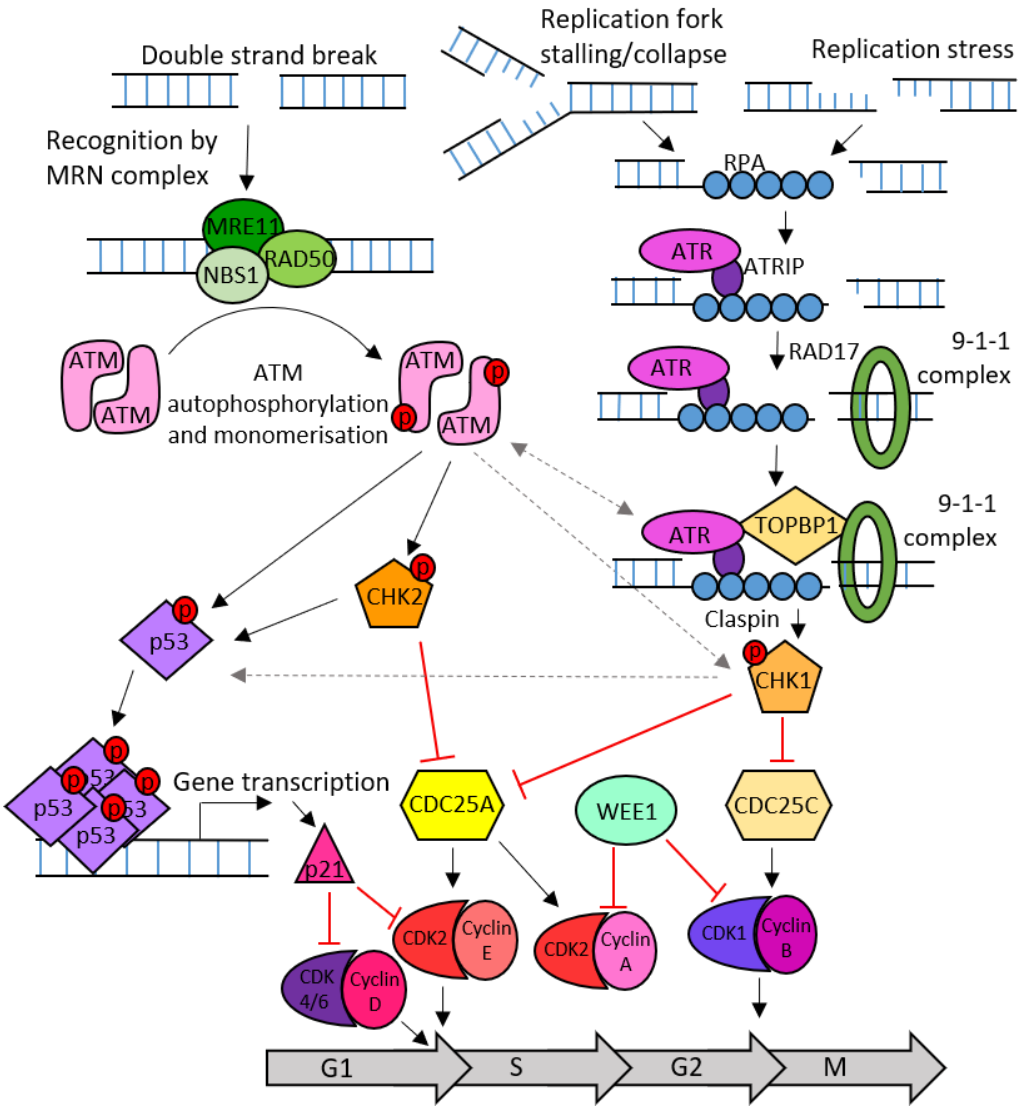

***Figure 1.7**: Overview of ATM and ATR signalling to cell cycle checkpoint arrest. Recruitment of ATM to DNA double-strand breaks (DSBs) leads to ATM activation, which activates CHK2. CHK2 phosphorylates and inactivates cdc25A, preventing it from removing the inhibitory phosphate on CDK2, inhibiting S-phase entry and progression. Both ATM and CHK2 phosphorylate p53 resulting in transactivation of p21 to inhibit CDK2. Regions of single strand DNA (e.g. at stalled replication forks or resected DSBs) are coated by RPA, which recruits ATR via ATRIP and other factors which lead to full activation of ATR, which activates CHK1. CHK1 phosphorylates and inactivates cdc25C, preventing it from removing the inhibitory phosphate on CDK1, inhibiting G2/M progression. There is substantial cross-talk between these pathways. CHK1 is also a target of ATM and cdc25A a target of CHK1. Both ATR and CHK1 also target p53. In addition, DNA damage activates WEE1 which phosphorylates and inactivates both CDK1 and CDK2. Black arrows indicate main activation pathways, dashed lines are secondary pathways and red lines indicate inhibition.*

1.3.4. DNA repair pathways

1.3.4.1 SSBR/BER

Single strand breaks (SSBs) are the most frequent form of endogenous DNA damage. Tens of thousands of SSBs arise per cell per day as a result of spontaneous DNA decay, direct oxidative attack or indirectly by enzymes involved in base excision repair or release of DNA torsion (Caldecott, 2008).

Base excision repair corrects small base lesions such as base deamination, oxidation or methylation, and abasic sites (base loss) arising spontaneously or caused by radiation or cytotoxic chemicals (Krokan and Bjørås, 2013). Essentially, there are five steps to BER, detection and removal of the damaged base, cleavage of the abasic site, end processing, gap filling and ligation. Glycosylases cleave the damaged base from the backbone resulting in an abasic site. An incision is made at the abasic site by AP endonuclease (APE1) creating a single strand break. Processing of DNA ends by APE1, polymerase β, polynucleotide kinase (PNPK) and Aprataxin (APTX) restore the 3' hydroxyl and 5' phosphate allowing gap filling by activation of short-patch repair (major pathway) or long-patch repair and any nicks are sealed by XRCC1-ligase (Fortini and Dogliotti, 2007).

Poly (ADP-ribose) polymerases 1 and 2 (PARP1 and PARP2) detect SSBs and become activated. Activated PARP ADP-ribosylates itself and other proteins forming long chains of poly ADP-ribose (PAR) (Caldecott, 2008). PARP recruits XRCC1, a scaffold protein which interacts with, stabilizes and stimulates proteins in the SSB repair pathway (Caldecott, 2003), including end processing, gap filling and ligation. The BER/SSB repair pathway is illustrated in **Figure 1.8**.

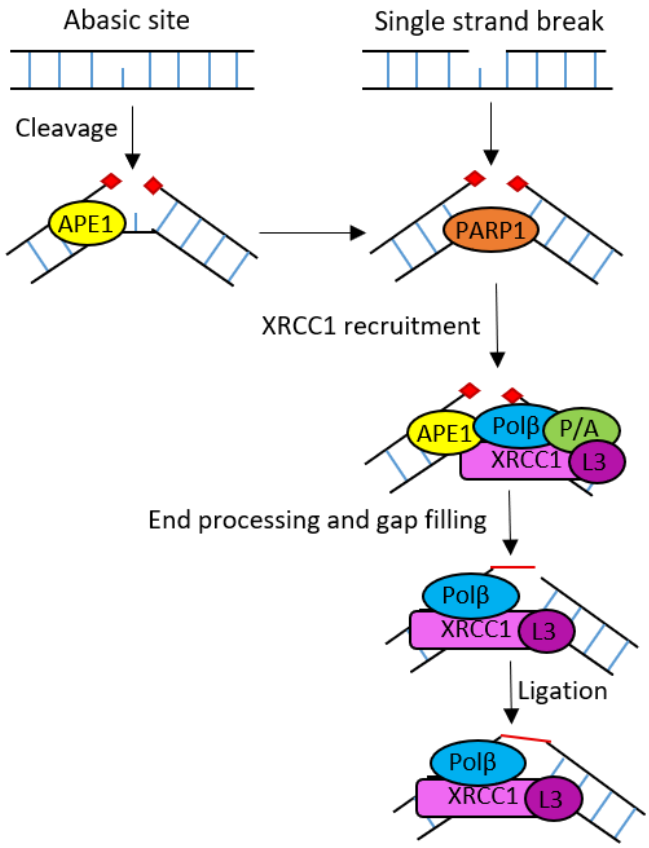

Figure 1.8: *Schematic diagram of short patch base excision and single stand break repair. Abasic sites arise via spontaneous hydrolysis or removal of damaged bases. Cleavage of the sugar backbone at an abasic site by AP endonuclease (APE1) result in a single strand break. Single strand breaks are recognised by PARP which recruits the protein scaffold XRCC1. XRCC1 recruits DNA polymerase β (Polβ), the end processing factors PNPK (P) and Aprataxin (A), and ligase 3 (L3). After end processing, DNA polβ fills the gap with a single nucleotide and the DNA is ligated by the XRCC1-ligase3 complex.*

1.3.4.2 Double strand break repair

DNA double strand breaks (DSBs) occur spontaneously at a frequency of about 10 per cell per day and are also generated by ionising radiation or chemotherapeutic drugs. Although they occur a thousand fold less frequently than SSBs, DSBs are much more toxic and can cause genetic instability if repaired incorrectly (Aparicio *et al.*, 2014). DSBs are repaired by one of two mechanisms (**Figure 1.9**) depending on which stage of the cell cycle the break occurs. HRR is a recombination dependent DNA repair mechanism which uses an undamaged template to restore DNA loss at a DSB. The template sequence is provided by the sister chromatid thus repair by HRR occurs during late S and G2 phase when the DNA has been replicated. DSBs in G1 and early S phase are repaired by a recombination independent mechanism called non-homologous end joining (NHEJ), although this pathway

also functions in G2 if the break occurs in regions of euchromatin (Kakarougkas and Jeggo, 2014). Pathway choice is also mediated by p53-binding protein 1 (53BP1) which suppresses DNA end resection required for HRR therefore promoting repair by NHEJ.

NHEJ repairs DSBs by “sticking together” the DNA ends. The Ku70/Ku80 heterodimer recognises the DSB and recruits the DNA-dependant protein kinase catalytic subunit (DNA-PKcs). Binding of Ku70/Ku80 and DNA-PKcs results in the activation of the DNA-PK holoenzyme which phosphorylates targets leading to ligation of the DNA ends by the XRCC4-ligase 4 complex (Mahaney *et al.*, 2009).

Alternatively, DSBs recognised by the exonuclease MRN complex trigger HRR. DNA ends are resected by MRN exonuclease activity which exposes 3’ ends of the DNA. RPA binds to the 3’ single-stranded overhang and is then replaced by Rad51. The resulting Rad51 filament promotes strand invasion into the sister chromatid so that the lesion can be repaired correctly.

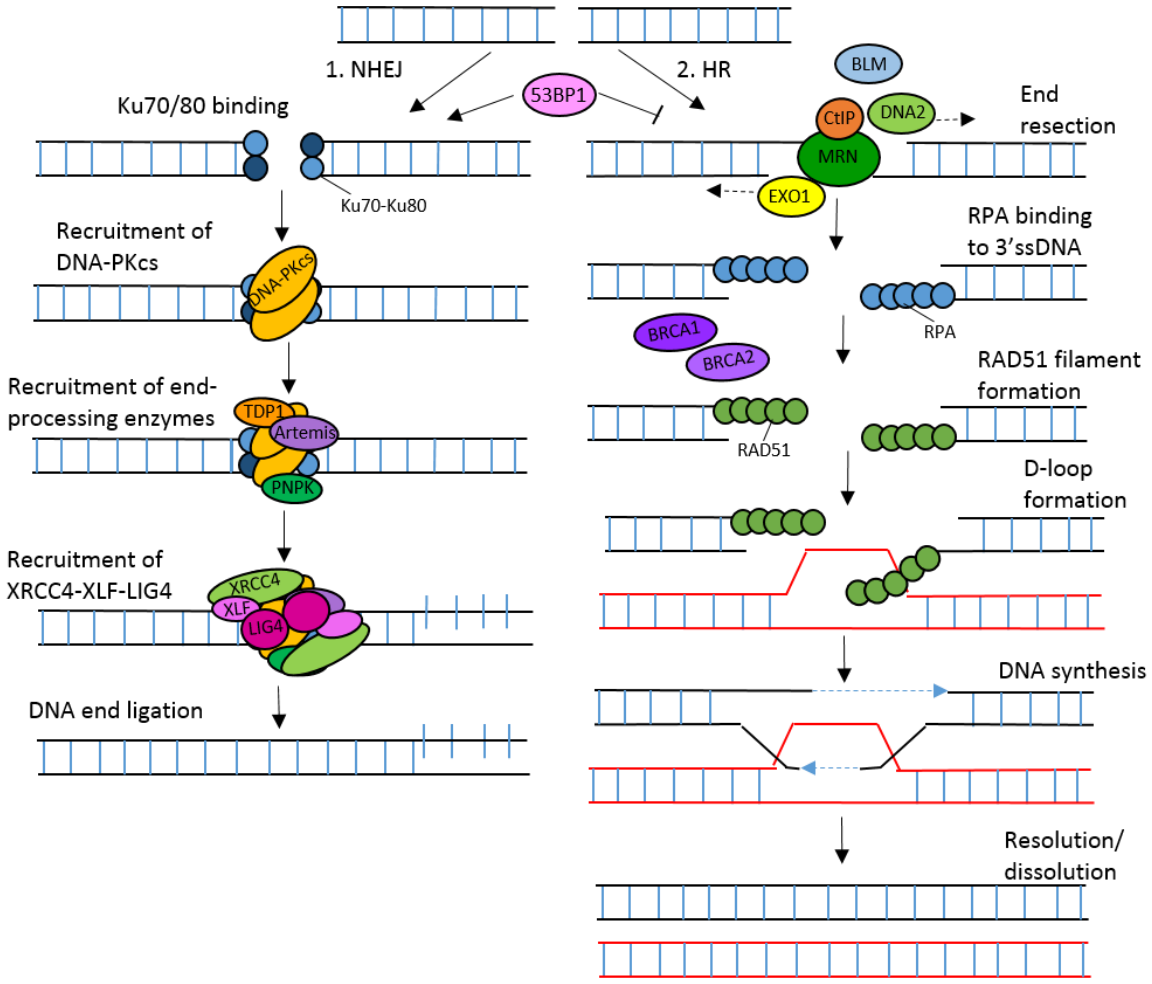

***Figure 1.9**: Overview of DNA double strand break (DSB) repair. In the homologous recombination (HR) repair pathway the single-stranded portion of the resected DSB is coated in RPA which facilitates Rad51 filament formation. DNA from the damage chromosome invades the sister chromatid which is used as a template for DNA synthesis. In the non-homologous end joining (NHEJ) pathway the Ku70/80 components of DNA-PK bind the ends of the DSB and the catalytic subunit (DNA-PKcs) recruits the XRCC4-ligase4 complex to join the ends together.*

1.3.4.3 Mismatch repair

The mismatch repair (MMR) pathway corrects DNA base mispairing and insertion/deletion (indel) loops that arise during DNA replication, recombination and repair (Liu *et al.*, 2017a). MMR is strand-specific, correcting the daughter strand, and has 3 main steps, recognition, excision and gap filling DNA synthesis (**Figure 1.10**). DNA mismatches are recognised by MSH2-MSH6 heterodimers which primarily binds to base mismatches or small indels up to 3 nucleotides long, or MSH2-MSH3 heterodimers which binds to large indels, of up to 13 nucleotides. Downstream processing requires PMS2 and MLH1–MLH3 heterodimers.

Components of other DNA repair pathways such as endonuclease 1, RPA, PCNA, replication factor C (RFC), DNA polymerase-δ (Pol δ) or Pol ε and FEN1 have also been reported to be involved in excision of the lesion and resynthesis of DNA.

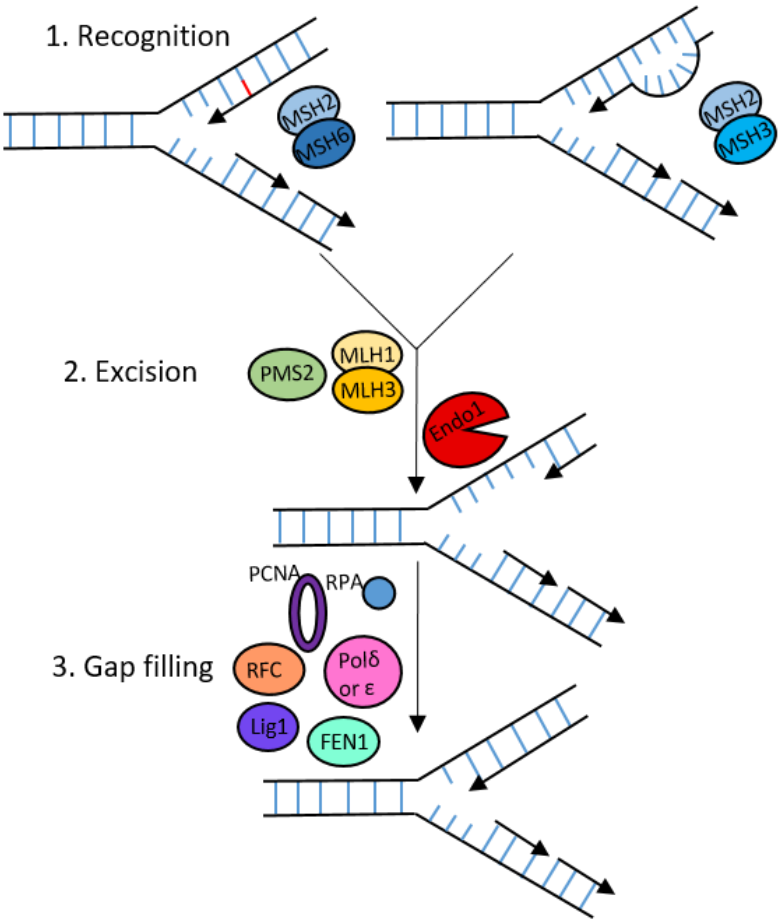

Figure 1.10: Schematic diagram of the mismatch repair pathway. Mismatched DNA is recognised by MSH2-MSH6 or MSH2-MSH3 heterodimers (1). Excision of lesion (2) and resynthesis (3) of DNA requires PMS2, MLH1–MLH3 heterodimers, endonuclease 1 (Endo 1), RPA, PCNA, replication factor C (RFC), DNA Pol δ or Pol ε, Lig1 and FEN1.

1.3.4.4 Removal of bulky lesions

The nucleotide excision repair (NER) pathway removes helix distorting DNA lesions and structures, such as cyclobutane pyrimidine dimers induced by UV radiation, as well as intra-strand cross links from the genome (Spivak, 2015). Two NER pathways are functional in human cells, global genome (GG-NER) and transcription coupled (TC-NER) which differ only in the damage recognition mechanism. Both pathways recruit the TFIIH complex to unwind about 30 nucleotides of DNA either sides of the damage. RPA binds to the exposed single

stranded DNA to prevent reannealing so the damage can be removed and repaired. The resulting gap is then filled by DNA polymerases (Marteijn *et al.*, 2014). **Figure 1.11** illustrates how both GG-NER and TC-NER repair damage.

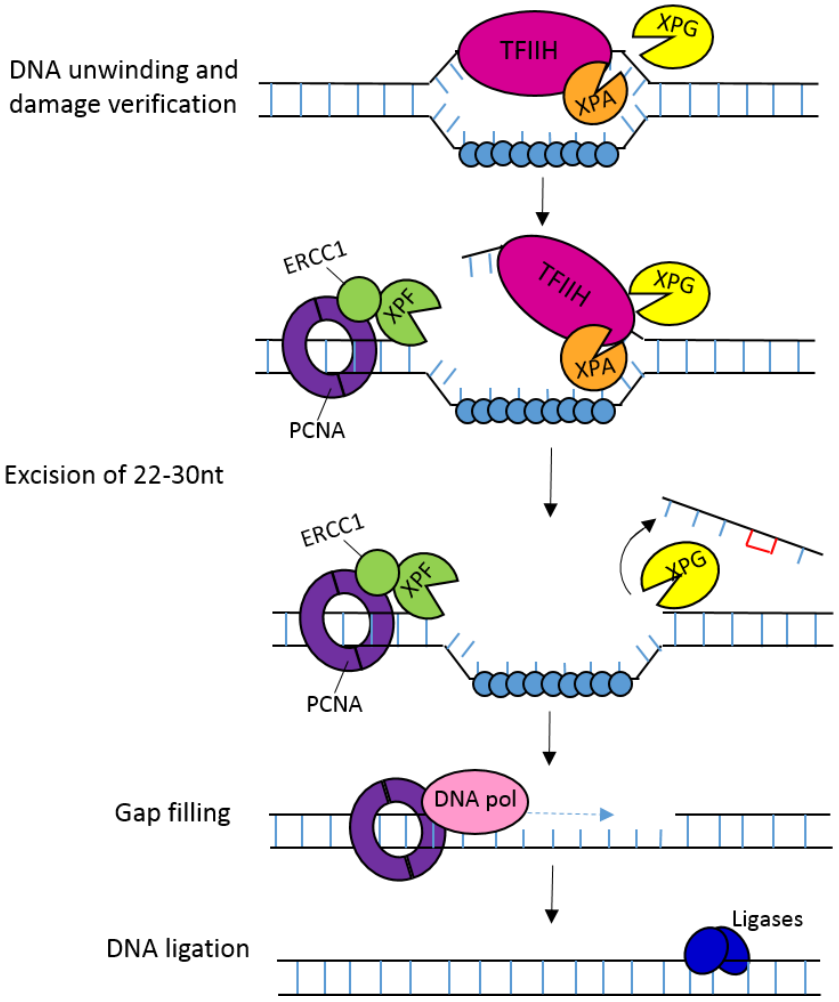

Figure 1.11: *Schematic diagram of nucleotide excision repair. DNA is unwound by helicase subunits of the transcription factor TFIIH. Damage is confirmed by XPA and RPA binds the ssDNA portions to prevent re-annealing. XPG and XPF endonucleases cleave a 22-30 nucleotide section containing the damage. The resulting gap is filled by replication factors.*

Bulky abducts which remain unrepaired at DNA replication are bypassed by a process known as translesion synthesis (TLS), which allows restoration of the DNA duplex before NER can occur. TLS relies on specialised polymerases, such as the Y-family of polymerases, which have an active site that can accommodate distorted templates and incorporate nucleotides opposite them. TLS polymerases show reduced fidelity compared to replicative polymerases and potentially introduce mutations through higher probability of misincorporation of bases (Sale, 2013).

1.3.4.5 Crosslink repair

The Fanconi anaemia (FA) pathway is important in the removal of DNA inter-strand crosslinks (ICLs) and is mediated by the large multimeric FA complex. This pathway also employs the TLS, HRR and NER pathways to repair the DNA after excision of the ICL from one DNA strand (Deans and West, 2011; Mouw and D'Andrea, 2014) (**Figure 1.12**).

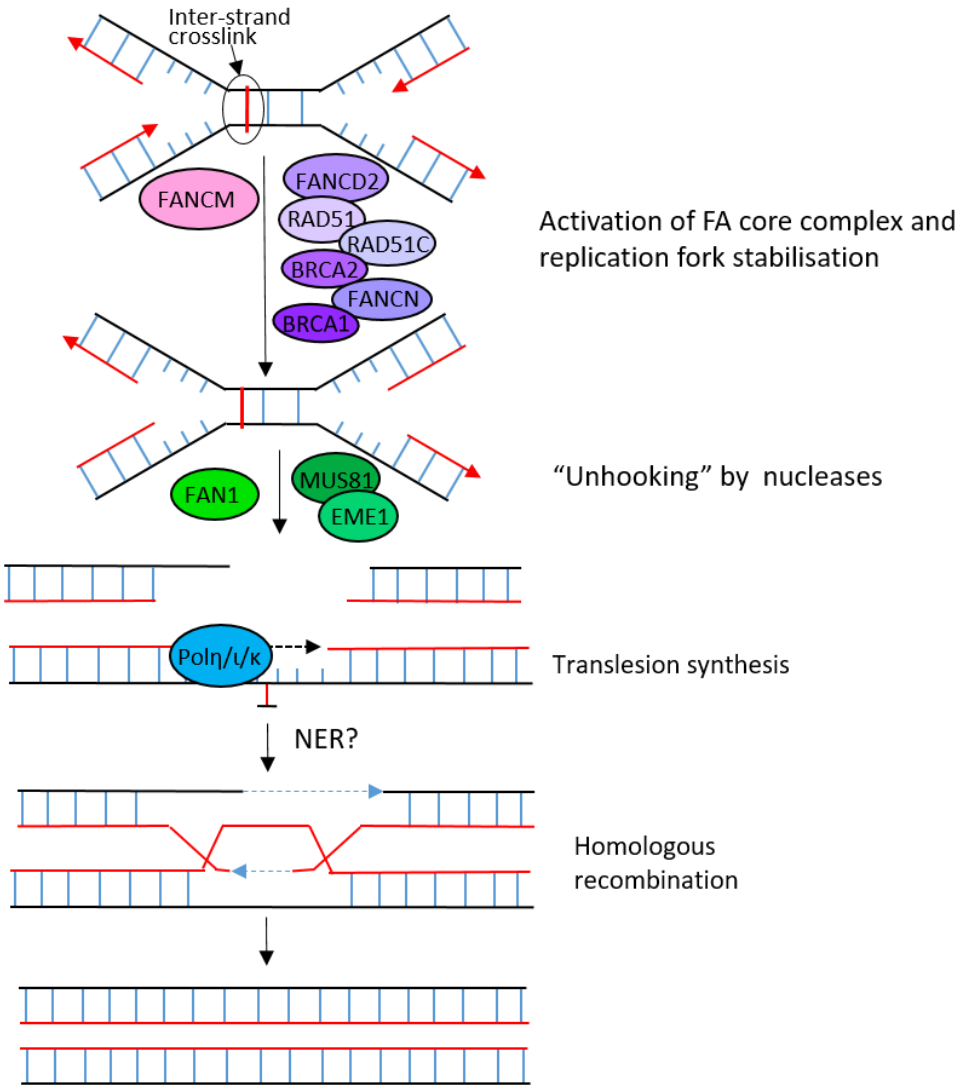

Figure 1.12: Repair of inter-strand crosslinks (ICLs) by the fanconi anaemia pathway. The FA core complex is recruited to the damage and recruits multiple nucleases which co-ordinate incisions required to "unhook" the ICL. The intact strand is replicated by translesion synthesis, bypassing unhooked ICL. The remaining unhooked ICL is removed by NER and the DSB formed by unhooking is repaired by HRR.

1.4 Targeting the DDR in High Risk Neuroblastoma

Consistent with other types of cancers, DDR defects are common in NB tumours. Amplification of *MYCN* oncogene (section 1.2.1.1) or allelic loss of chromosome 11q, which encodes many proteins involved in the DDR (section 1.2.1.4), are commonly observed in NB.

MYCN transcriptionally upregulates the cell cycle checkpoint protein CHK1 (Cole *et al.*, 2011; Gu *et al.*, 2015), and many proteins involved in DNA repair, including PARP (Colicchia *et al.*, 2017), components of the MRN complex (Petroni *et al.*, 2016; Petroni *et al.*, 2018), alternative NHEJ (alt-NHEJ) (Newman *et al.*, 2017), and Bloom syndrome (BLM) helicase (Chayka *et al.*, 2015). Upregulation of these genes likely promotes effective repair of DNA damage allowing MYCN driven tumours to tolerate increased RS.

Loss of G1 checkpoint control, through overexpression of MYCN (promotes premature S phase entry), reduced ATM expression or loss of p53 function (more frequent at relapse) render intra-S and G2/M checkpoint dependency in order to maintain genome integrity and are especially vulnerable to its inhibition, by targeting ATR, CHK1 and/or WEE1 kinases. Targeting tumour specific defects with DDR inhibitors for the treatment of HR-NB could potentially increase the survival in this risk group, which account for > 50% of all NB and for which long term survival is still unacceptably poor.

1.4.1. PARP inhibitors

Inhibition of PARP, the enzyme which promotes the repair of DNA single strand breaks, selectively kills cells defective in HRR, due to BRCA mutation, for example. This is due to synthetic lethality when the function of two complementary pathways are inactivated. PARP inhibition blocks the repair of SSBs and generates a bulky DNA-PARP adduct. These lesions block the progression of DNA replication machinery during replication, resulting in a single ended DSB, which is then repaired by HRR. Cancer cells defective in HRR are unable to repair this break resulting in cell death (**Figure 1.13**). Four PARP inhibitors have been approved to date, Lynparza (olaparib, Astra Zeneca), Rubraca (rucaparib, Clovis Oncology) and Zejula (niraparib, Tesaro), for the treatment of *BRCA* mutated and platinum sensitive ovarian cancer and Talzenna (talazoparib, Pfizer) for the treatment of germline *BRCA* mutated, HER2 negative breast cancer (reviewed by (Curtin and Szabo, 2020). Two other PARP inhibitors, veliparib

(Abbvie), and pamiparib (BeiGene) are being investigated in clinical trials, with veliparib having advanced to phase 3.

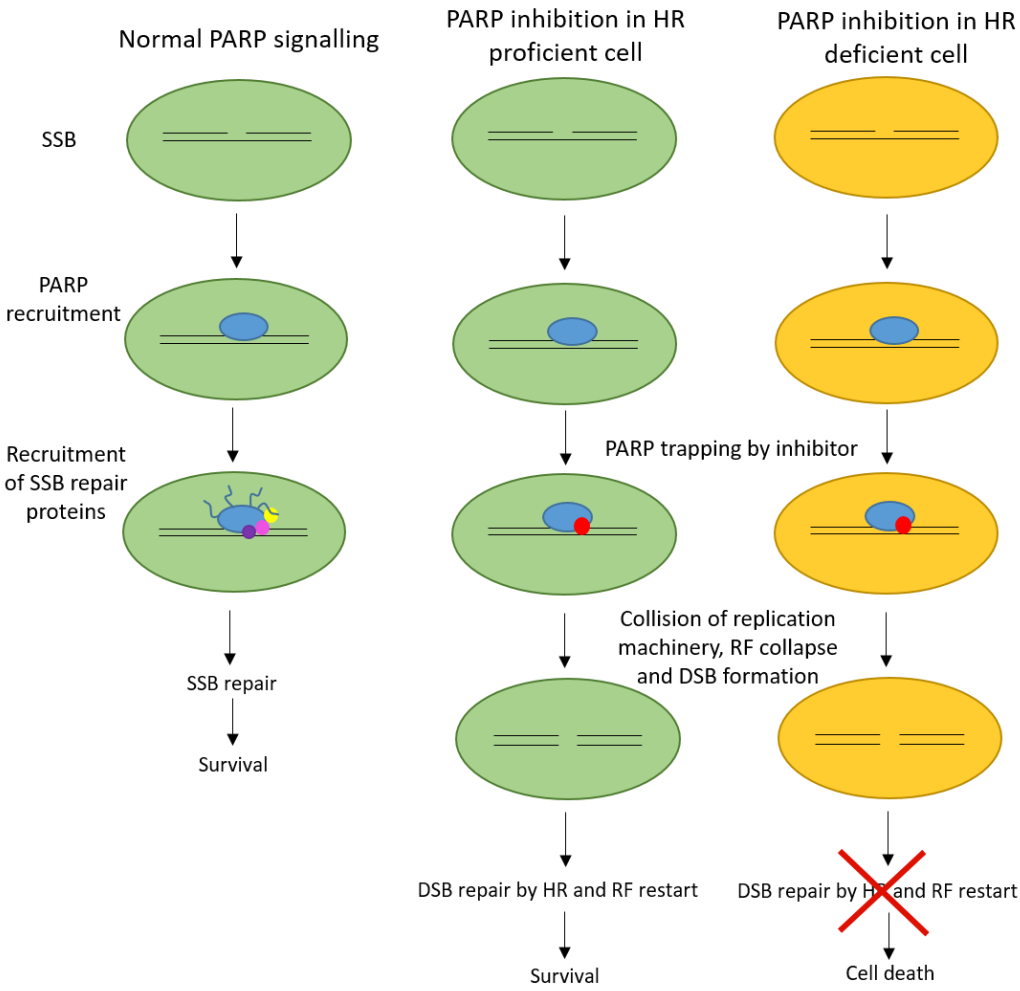

Figure 1.13: *PARP inhibition can result in synthetic lethality. PARP signalling is required for repair of DNA single strand breaks (SSBs). Unrepaired SSBs lead to the formation of double strand breaks (DSBs) during DNA replication, repair of which requires the homologous recombination (HR) DSB repair pathway. Cells which have lost HR function cannot efficiently repair the damage acquired from PARP inhibition, leading to cell death. RF=replication fork*

PARP activity is upregulated in many cancer types (Ossovskaya *et al.*, 2010). PARP1 deficient cell lines are extremely sensitive to DNA damaging agents and ionising radiation (Morales *et al.*, 2014), suggesting that PARP inhibition may provide therapeutic benefit in combination with chemotherapeutic agents or radiotherapy. A number of clinical trials are ongoing investigating the effect of PARP inhibitors in the potentiation of chemotherapy and radiotherapy or increasing the efficacy of immune checkpoint inhibitors (https://clinicaltrials.gov/).

Evidence in favour of introducing PARP inhibitors to HR-NB treatment regimens has been accumulating. In 2009, our group demonstrated potentiation of temozolomide and topotecan cytotoxicity by rucaparib in both *in vitro* and *in vivo* models of NB (Daniel *et al.*, 2009). Subsequent studies have also shown that PARP inhibition increases sensitivity to a variety of chemotherapeutic agents and to ionising radiation and targeted radiotherapy with iodine-131-labelled meta-iodobenzylguanidine (^{131}I-mIBG), which specifically targets neuroendocrine cells expressing the noradrenaline transporter, in preclinical models of NB (Norris *et al.*, 2014; Nile *et al.*, 2016).

PARP inhibitors have been reported to be synthetically lethal in cells with 11q deletions and *ATM* mutations in lymphoid tumours (Weston *et al.*, 2010). Studies in preclinical models of NB have also showed that 11q loss confers sensitivity to PARP inhibitors (Sanmartín *et al.*, 2017; Takagi *et al.*, 2017), further supporting the idea that heterozygous loss of *ATM* and other DDR genes determines sensitivity to PARP inhibition.

In addition to 11q, PARP inhibition has been shown to enhance RS in *MYCN* amplified cells, leading to increased cell death through replication and mitotic catastrophe as DNA damage persists through S phase and mitosis (Colicchia *et al.*, 2017; King *et al.*, 2020).

Clinical trials in adults have shown that combining PARP inhibitors with conventional chemotherapy results in increased haematological toxicity (Zhou *et al.*, 2017), with doses of the PARP inhibitor and cytotoxic chemotherapy combination subsequently being reduced. This observation was also reflected in the results of a trial combining veliparib with temozolomide in paediatric brain tumours (Su *et al.*, 2014), and the results of a trial testing talazoparib in combination with irinotecan in refractory or recurrent paediatric solid tumours (Federico *et al.*, 2020), where dose limiting gastrointestinal toxicities were also observed due to the toxicity profile of irinotecan.

Results from the ongoing trial of olaparib in combination with irinotecan in children with relapsed or refractory tumours with mutations in gene affecting HRR, as part of the European Proof of Concept Therapeutic Stratification Trial (ESMART), reported dose limiting gastrointestinal or haematological toxicities in 30% of patients (Gatz *et al.*, 2019). Partial responses were also confirmed in 3/24 patients, one of whom had NB, and 8/24 patients experienced disease stabilisation.

For NB (and other paediatric tumours), a reduction in chemotherapy doses when combined with a PARP inhibitor might be advantageous in reducing the long term sequelae of these drugs, if efficacy is maintained. In addition, current clinical trials give the maximum tolerated dose of PARP inhibitor, which may result in a much higher concentration than is necessary for enzyme inhibition. Reducing the concentration of inhibitor to a level required for maximal inhibition of PARP activity may result in less toxicity.

Ongoing early phase international clinical trials testing the efficacy of PARP inhibitors for the treatment of childhood solid tumours, including NB, are listed in **Table 1.5**.

Table 1.5: Current paediatric clinical trials investigating PARP inhibitors in neuroblastoma

Inhibitor	Combined with	Disease	Trial phase	Trial number	Expected end date	Status
Olaparib (Astra Zeneca)	N/A	Relapsed or refractory solid tumours, non-Hodgkin lymphoma, or histiocytic disorders with defects in DDR genes	2	NCT03233204 (Pediatric MATCH)	Sept 2024	Recruiting
	Irinotecan	Relapsed or refractory tumours with molecular abnormities	1/2	NCT02813135 (E-SMART)	Jan 2022	Recruiting
Niraparib (Tesaro)	Dostarlimab (PD-1 inhibitor)	Recurrent or refractory solid tumours	1	NCT04544995	Jul 2030	Recruiting
https://clinicaltrials.gov/ accessed December 2020						

1.4.2. ATR inhibitors

Many features of cancer cells have been described as synthetically lethal with ATR inhibition, such as RS and defects in G1 cell cycle control (Rundle *et al.*, 2017). Four inhibitors of ATR are currently being tested in adult clinical trials: Berzosertib (M6620, Merck), M4344 (Merck), Ceralasertib (AZD6738, Astra Zeneca) and BAY1895344 (Bayer). There are currently no trials of ATR inhibitors in paediatric patients, but an additional arm of the ESMART trial investigating ceralasertib in combination with olaparib in paediatric patients is due to open soon.

NB tumours frequently present with abnormalities which may result in vulnerability to ATR inhibition. *MYCN* amplification and impaired ATM function, which result in defects in G1 cell cycle control and RS, are known determinants of sensitivity to ATR inhibitors (Murga *et al.*, 2011; Toledo *et al.*, 2011; Kwok *et al.*, 2016). Collectively, *MYCN* amplification and *ATM* loss through allelic 11q deletion are observed in 70-80% of HR-NB tumours (Mlakar *et al.*, 2017) suggesting a large group of patients who may benefit from inhibitors of ATR.

There is some evidence that chemosensitisation by ATR inhibitors relies on a dysfunctional p53 pathway, and therefore a defective G1/S checkpoint (Schoppy and Brown, 2012; Karnitz and Zou, 2015). Defects in the p53 pathway are rare in NB at diagnosis but abnormalities are observed frequently at relapse (Carr-Wilkinson *et al.*, 2010).

Inhibition of ATR has been shown to mediate sensitivity to PARP inhibitors (Turner *et al.*, 2008; Peasland *et al.*, 2011). PARP inhibition results in DNA double strand ends as a result of collapsed replication forks in S-phase, which require activity of ATR for repair. ATR inhibition has also been shown to overcome acquired resistance to PARP inhibitors (Murai *et al.*, 2016; Yazinski *et al.*, 2017). In theory, the combination of PARP and ATR inhibitors should potentiate the cytotoxic effects of PARP inhibitors in the treatment of NB.

It has been suggested that cancer cells which maintain their telomeres by alternative lengthening have increased sensitivity to ATR inhibition (Flynn *et al.*, 2015). ALT is commonly seen in NB cells which harbour loss of function mutations or intragenic deletions in *ATRX* (Bower *et al.*, 2012; Napier *et al.*, 2015), which is observed in around 25% of stage 4 NB tumours (Cheung *et al.*, 2012). However, ALT positive NB cell lines did not show increased sensitivity to ATR inhibition (George *et al.*, 2020b), and a previous study suggests ALT is not an independent determinant of ATR inhibitor sensitivity (Deeg *et al.*, 2016).

The efficacy of the ATR inhibitor clinical candidate from Merck, berzosertib (M6620, formally VX-970, Vertex), has been tested alone and in combination with cisplatin and melphalan in a range of paediatric solid tumour cell lines and xenograft models, including NB, as part of the paediatric preclinical testing programme (Kurmasheva *et al.*, 2018). The results of this study showed that M6620 had limited single agent cytotoxicity but potentiated cisplatin and melphalan cytotoxicity in most of the cell lines tested, including NB, suggesting that combination with ATR inhibitors may increase the efficacy of existing chemotherapeutic regimens.

Further studies are required to identify molecular abnormalities which are predictive of ATR inhibitor sensitivity in NB.

1.4.3. CHK1 inhibitors

CHK1 kinase is the direct downstream effector of ATR. Inhibition of CHK1 also selectively targets cells with increased RS. Studies in NB cell lines have shown that single agent CHK1 inhibition is particularly cytotoxic to *MYCN* amplified cells (Russell *et al.*, 2013; Lowery *et al.*, 2017; Lowery *et al.*, 2019). CHK1 inhibition also sensitised NB cell lines to irinotecan and gemcitabine independent of *MYCN* status (Xu *et al.*, 2011; Russell *et al.*, 2013). CHK1 inhibitors have been in clinical development for many years, but many compounds have been discontinued before phase III trials due to toxicities. Two CHK1 inhibitors, SRA737 (Sierra Oncology) and Prexasertib (LY2606368; Eli Lilley), are currently being tested in clinical trials. Prexasertib is currently being investigated for the treatment of recurrent or refractory paediatric solid tumours in a phase 1 clinical trial (NCT02808650).

1.4.4 WEE1 inhibition

WEE1 activity contributes to activation of the S and G2/M cell cycle checkpoints in response to DNA damage (Squire *et al.*, 2005). Single agent WEE1 inhibition with adavosertib was shown to be effective in both *in vitro* and *in vivo* preclinical NB models, and synergistic with the CHK1 inhibitor MK-8776, irinotecan and gemcitabine (Russell *et al.*, 2013).

Adavosertib is currently the only WEE1 inhibitor in clinical development. Results of a phase 1 clinical trial investigating adavosertib in combination with irinotecan in relapsed and

refractory paediatric solid tumours reported that maximum tolerated doses of adavosertib were lower than what can be achieved in adult trials, which the authors suggest may be due to the toxicity profiles of the chemotherapy used in combination (Cole *et al.*, 2020). This trial has progressed to the phase 2 expansion cohort, including NB, which is ongoing (NCT02095132).

1.4.5. ATR and PARP inhibitor combinations

PARP inhibition increases RS, increasing reliance on the ATR signalling pathway. Synergy between ATR and PARP inhibitors has been reported in pre-clinical models of several different cancers (Schoonen *et al.*, 2019; Kim *et al.*, 2020; Lloyd *et al.*, 2020). These reports have prompted investigation of combined PARP and ATR inhibition in the clinic. A summary of currently listed adult clinical trials involving a combination of PARP and ATR inhibitors is listed in **Table 1.6**. In addition, a new arm of the ESMART trial investigating ceralasertib in combination with olaparib in paediatric solid tumours, including NB, is due to open imminently.

Table 1.6: ATR and PARP inhibitor combinations currently being investigated in adult clinical trials

ATR inhibitor	PARP inhibitor	Disease	Trial phase	Trail number	Expected end date	Status
M6620 (VX-970)	Veliparib	Refractory solid tumours in combination with cisplatin	1	NCT02723864	Dec 2021	Active, not recruiting
AZD6738	Olaparib	Head and neck squamous cell carcinoma (HNSCC)	1	NCT03022409	Dec 2020	Recruiting
		Advanced solid malignancies – HNSCC, non-small cell lung cancer, gastric and breast cancer	1/2	NCT02264678	Jan 2024	Recruiting
		Ovarian high grade serous carcinoma	2	NCT03462342	Dec 2021	Recruiting
		Patients with tumours harbouring mutations in HDR genes, including *ATM, CHK2, APOBEC, MRE11* complex	2	NCT02576444	Dec 2021	Active, not recruiting
		Metastatic triple negative breast cancer with alterations in HRR genes	2	NCT03330847	Mar 2023	Recruiting
		Renal cell carcinoma, urothelial carcinoma, pancreatic ductal adenocarcinoma, or other metastatic solid tumors	2	NCT03682289	Mar 2023	Recruiting
		Relapsed small cell lung cancer	2	NCT03428607	Dec 2020	Active, not recruiting
BAY 1895344	Niraparib	Recurrent advanced solid tumours and ovarian cancer	1	NCT04267939	May 2024	Recruiting
M4344	Niraparib	PARP resistant ovarian cancer	1	NCT04149145	Dec 2027	Not yet recruiting

1.5 Summary and conclusion

Improving survival rates for HR-NB remains a challenge in paediatric oncology. Relapse is common and if long term survival is achieved, high risk patients are often left with severe sequelae as a result of high dose chemotherapy. New treatment strategies are required before survival rates can significantly improve. There are many features of HR-NB which may predict sensitivity to DDR inhibitors. Mutation or loss of genes, such as *ATM,* suggest sensitivity to PARP and/or ATR inhibition. The frequent loss of G1 checkpoint control in HR-NB, by *MYCN* amplification and p53 pathway loss at relapse, gives rationale for treatment with G2 checkpoint targeting agents (ATR, CHK1 and/or WEE1 inhibitors). *MYCN*-amplified tumours may also be vulnerable to ATR inhibition due to oncogene induced RS.

As well as single agent efficacy, there is mounting evidence to suggest that combining DDR inhibitors with conventional chemo- or radiotherapy would permit lower doses to be given with the same effect due to sensitisation.

Exploiting defects in the DDR has the potential to lead to novel therapeutic options for a large subset of HR-NB patients.

1.6 Hypothesis and aims

Hypotheses:

1. *MYCN* amplification, 11q deletion and/or p53 pathway dysfunction will lead to sensitivity to ATR and/or PARP inhibitors in NB cell lines.
2. PARP and ATR inhibition will be synergistic in NB.

Aims:

1. To identify genetic abnormalities in DDR genes in a panel of NB cell lines with known *MYCN*, 11q and *TP53* genetic abnormalities.

2. To determine baseline expression, activity and function of key DDR proteins in the panel of NB cell lines

3. To determine which DDR defects are predictive of sensitivity to single agent ATR and PARP inhibition in NB

4. To investigate the effect of ATR inhibition on cytotoxicity of conventional chemotherapeutic agents

5. To explore the effect of dual ATR and PARP inhibition on cytotoxicity, cell cycle progression and RS

Chapter 2: Materials and methods

2.1 Cell culture

2.1.1 Propagation and maintenance of neuroblastoma cell lines

NB cell lines used in this study are listed in **Table 2.1**. Cell lines were kindly provided by Linda Harris (SJNB1), Penny Lovat (SHSY5Y and IMR32), Rogier Versteeg (NGP), Mirco Ponzoni (GIMEN), John Lunec (N20_R1), Jean Bénard (SKNAS and IGRN91), Garrett Brodeur (NMB) and Michelle Haber (IMR/KAT100). Cell lines were authenticated by karyotyping by Nick Bown and colleagues at the Northern Genetics Service (Centre for Life, Newcastle, UK).

All cell lines were cultured in RPMI-1640 tissue culture media (Sigma-Aldrich) supplemented with 10% (v/v) Fetal Calf Serum (Gibco, Life Technologies Ltd), maintained at 37 °C in a humidified incubator with 5% CO_2 in air, and passaged at >70% confluent. Cells were detached from the growth surface by incubating with 1x trypsin-EDTA (Sigma-Aldrich) until dislodged. The trypsin was neutralised with equal volume of full media and the resulting cell suspension reseeded in fresh tissue culture flasks (Corning Incorporated, New York, USA) at the desired number, and made up to the required volume with full media. Cell density after detachment was determined using a Haemocytometer (Hawksley, Sussex, UK). Cell lines were routinely tested for Mycoplasma using MycoAlert™ detection kit (Lonza, Basel, Switzerland), and confirmed to be negative.

Table 2.1: Origin of neuroblastoma cell lines used in this study

Cell line	Cell type	Origin	Reference
SHSY5Y SHEP	N S	N and S type subclones of SKNSH cell line. Derived from bone marrow of a 4 year old female after relapse.	(Biedler *et al.*, 1978)
SKNAS	S	Derived from a bone marrow metastasis of a 6 year old female after relapse	(Helson *et al.*, 1983)
SJNB1	N	Derived from an adrenal mass of a 2 year old male after relapse.	(Thompson *et al.*, 1997)
GIMEN	S	Derived from bone marrow of a 2 year old female post chemotherapy at relapse.	(Cornaglia-Ferraris *et al.*, 1990)
NGP	N	Derived from metastatic lung deposit of 2 year old male post chemotherapy at relapse.	(Brodeur *et al.*, 1977)
N20_R1	N	Generated from NGP cell line by selecting for resistance to the MDM2 inhibitor nutlin3	(Drummond *et al.*, 2016)
NMB	N	Derived from bone marrow of a 10 month old female post chemotherapy at relapse.	(Brodeur *et al.*, 1977)
IMR32	N	Derived from an adrenal mass of a 13 month old male at diagnosis.	(Tumilowicz *et al.*, 1970)
KAT100	N	Generated from IMR32 cell line by selecting for resistance to 100 µg/ml potassium antimony tartrate (KAT)	(Xue *et al.*, 2007)
IGRN91	N	Derived from bone marrow of an 8 year old male post chemotherapy at relapse.	(Ferrandis and Bénard, 1993)
N: Neuronal, S: substrate adherent			

2.1.2 MYCN expression regulatable cell lines

Two MYCN regulatable expression cell lines, SHEPTet21N and IMR5/75 shMYCN, were kindly provided by Manfred Schwab and Frank Westermann, respectively. These cell lines employ tetracycline controlled transcriptional activation systems (Tet expression system) to downregulate MYCN expression in the presence of tetracycline, or its derivative doxycycline (Dox) (Lutz *et al.*, 1996; Dreidax *et al.*, 2014).

2.1.2.1 SHEPTet21N

SHEPTet21N cells are a sub-clone of the non-*MYCN* amplified SHEP cell line, in which the MYCN gene is under the control of the Tet-OFF expression system. In the Tet-OFF expression system, the Tet repressor DNA binding protein (TetR), from the tetracycline-resistance operon of the *E. Coli* transposon *Tn10,* is fused to the strong transactivating domain of the VP16 protein found in the Herpes Simplex Virus. The fusion converts the TetR from a transcriptional repressor to a strong transcriptional activator (tTA), which regulates expression of genes under transcriptional control of a tetracycline-responsive promoter element (TRE). The TRE is made up of several identical Tet operator (tetO) sequences fused to the minimal CMV promotor. In the absence of tetracycline, or Dox, transcription of the target gene is activated by the binding of tTA to the TRE. In the presence of tetracycline, or Dox, expression of the target gene is repressed as binding of tetracycline to the tTA prevents it from binding to the TRE (Gossen and Bujard, 1992). In the SHEPTet21N cell line, the *MYCN* gene is expressed under the control of the TRE from the pUHD10-3 plasmid (**Figure 2.1A**) and tTA is coded for on pUHD15-1 (**Figure 2.1B**). In the absence of tetracycline (or Dox) MYCN is highly expressed. The addition of Dox prevents transcription from the TRE and MYCN is no longer expressed.

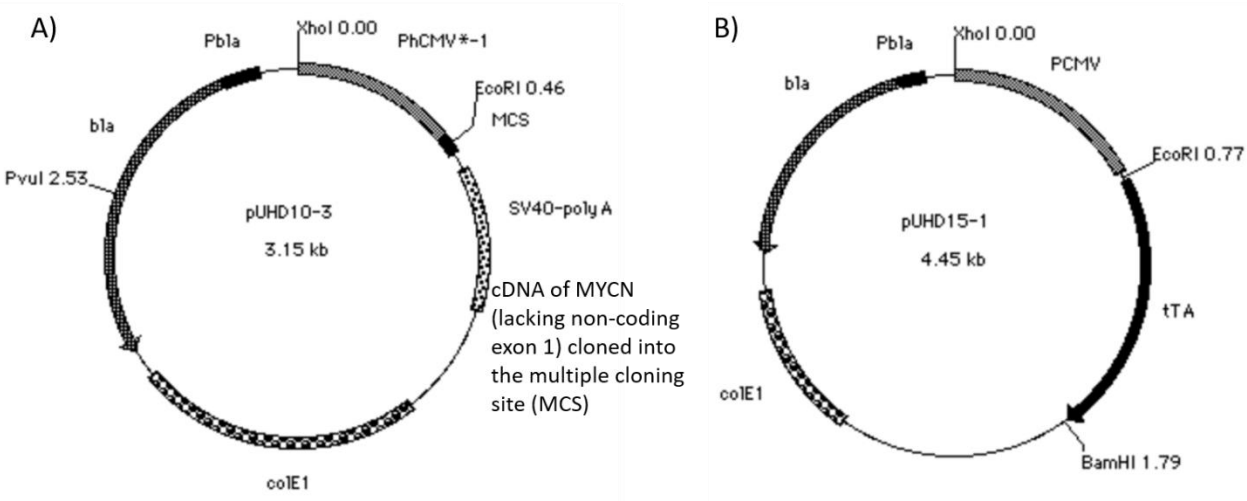

Figure 2.1*: Maps of plasmids used to generate the SHEPtet21N cell line. A) pUHD10-3 contains the MYCN gene under the control of the tetracycline response element (PhCMV*-1). B). pUDH15-1 codes for the tet transcriptional activator (tTA). (https://www.zmbh.uni-heidelberg.de/Bujard/Homepage.html)*

2.1.2.2 IMR5/75 shMYCN

The IMR5/75 shMYCN cell line is a MYCN amplified cell line derived from the IMR32 cell line containing a stably transfected pT-Rex-DEST30 construct (**Figure 2.2A**) consisting of a MYCN targeting small hairpin RNA (shRNA) under the control of a TRE. In the Tet-ON system, a four amino acid change in the TetR DNA binding domain alters the binding characteristics of the tTA so that it recognises the tetO sequences in the TRE when Dox is present. Thus, the introduction of Dox initiates the transcription of the target gene (Gossen *et al.*, 1995). In this cell line, the modified tTA is expressed from the stably transfected pcDNA6/TR plasmid (TetR **Figure2.2B**). The addition of Dox induces the expression of the shRNA which silences MYCN expression through RISC mediated RNA interference. In this system, MYCN expression recovers quickly after the withdrawal of Dox.

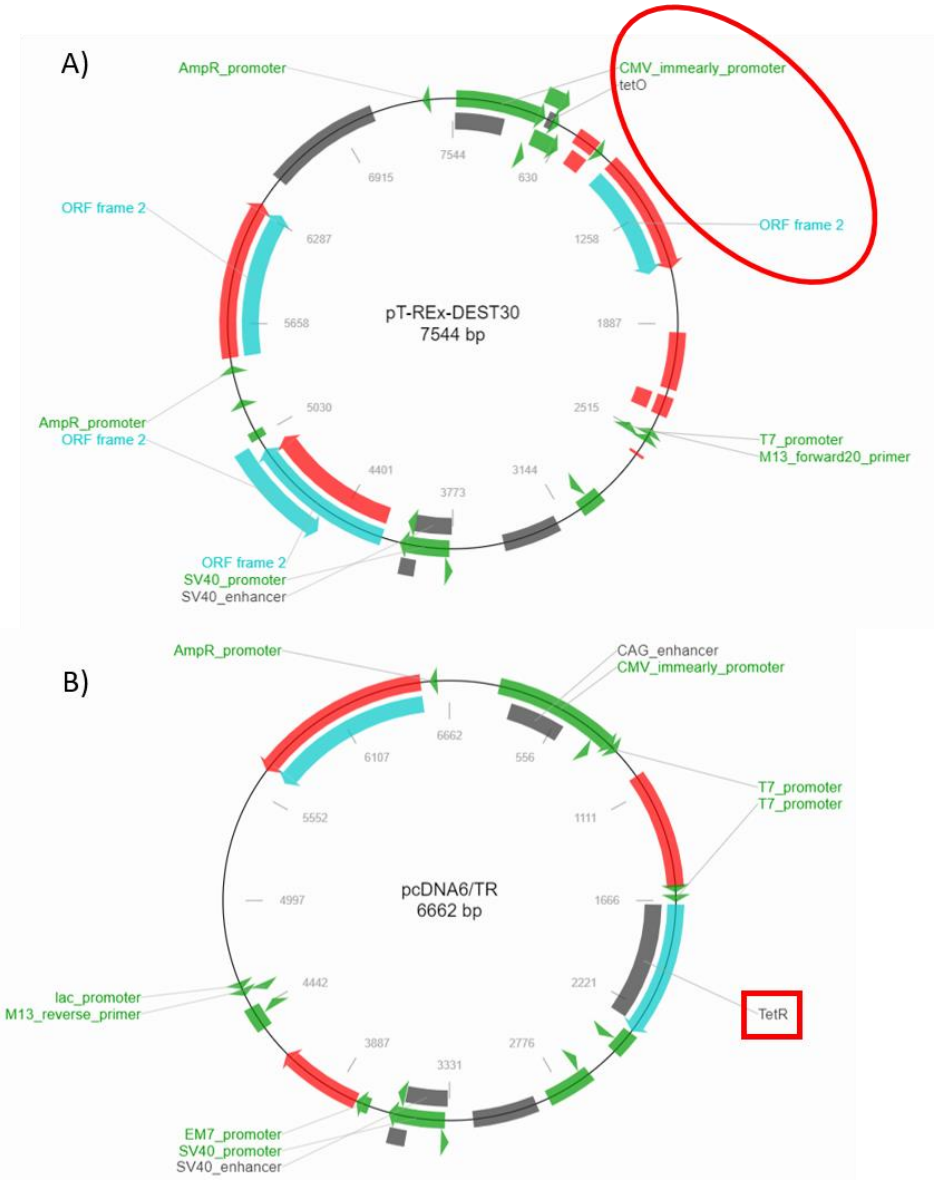

Figure 2.2: *Maps of plasmids used to generate the IMR5/75 shMYCN cell line. A) pT-Rex-DEST30 codes for an shRNA against MYCN under the control of the tetracycline response element (CMV + tetO – red oval). B). pcDNA6/TR codes for the modified TetR (red box), generating a Tet-ON expression system. Restriction sites have been removed to simplify features. (https://www.addgene.org)*

2.1.3 Resurrection of cell lines from -150ºC stocks

Cells were thawed in a 37ºC waterbath and the cell suspension transferred to 25 cm^2 tissue culture flask containing 3 ml fresh full media and incubated at 37 °C, 5% CO_2 in a humidified incubator overnight. The media was replaced with fresh full media the following day to remove media containing dimethyl sulfoxide (DMSO), from freezing.

2.1.4 Freezing cell lines for storage -150ºC

Cells at ~70% confluency in a 150 cm^2 tissue culture flask were detached as described in section 2.1.1, centrifuged at 250 X g and resuspended in 5 ml freezing media containing 10% DMSO (v/v) (tissue culture grade, Sigma-Aldrich), 10% FBS (v/v) and 80% full media (containing 10% FBS). The cell suspension was aliquoted into 5 cryogenic vials (Nunc cryotube vials, Thermo Scientific) and stored at -80ºC for 24 hours prior to transfer to -150ºC.

2.2 Small molecule inhibitors and chemotherapeutic agents

All drugs used to treat cell lines in this study are listed in **Table 2.2.** All stocks were stored in aliquots of up to 1 ml at -20ºC.

Table 2.2: List of small molecule inhibitors and chemotherapeutic agents used in this study

Drug	**Type**	**Supplier**	**Reference number**	**Solvent**	**Stock concentration**
VE-821	ATR inhibitor	Stratech	S8007	DMSO	100 mM
AZD6738	ATR inhibitor	Stratech (Astra Zeneca)	B6007-APE	DMSO	40 mM
Olaparib	PARP inhibitor	Stratech (Astra Zeneca)	S1060	DMSO	20 mM
Doxorubicin	Topoisomerase II poison	Sigma Aldrich	D1515	DMSO	100 mM
Topotecan	Topoisomerase I poison	Sigma Aldrich	T2705	DMSO	100 mM
Temozolomide	Alkylating agent	Sigma Aldrich	T2577	DMSO	100 mM
Doxycycline	Antibiotic – binds Tet repressor	Sigma Aldrich	D9891	PBS	50 mg/ml
DMSO: Dimethyl sulfoxide; PBS: phosphate buffered saline					

2.3 Cytotoxicity assays

2.3.1 XTT cell proliferation assay

The sodium 3´-[1-(phenylaminocarbonyl)-3,4-tetrazolium]-bis(4-methoxy6-nitro)benzene sulfonic acid hydrate (XTT) cell proliferation assay (Roche) was used to determine the growth inhibitory effect of cytotoxic agents. The XTT assay is a colorimetric assay based on the reduction of the yellow tetrazolium salt (XTT) to an orange formazan salt by mitochondrial dehydrogenases, in the presence of an electron coupling reagent, in metabolically active cells. The number of viable cells directly correlates with the amount of formazan salt formed, which is monitored by the absorbance at 450 nM. Before use, the reagents are mixed by combining the XTT reagent with the electron coupling reagent in a 50:1 ratio.

Cells were seeded in 96-well plates (Corning, VWR International Ltd), and allowed to adhere overnight. For single agent treatments, drugs were made up at 200x concentration in DMSO before diluting 200x to give a final DMSO concentration of 0.5%. For combination treatments, drugs were made up at 400x concentration in DMSO before diluting 400x to give a final combined DMSO concentration of 0.5%. Cells were treated with ATR or PARP inhibitors or chemotherapy alone, or in combination for 72 hours. Cells incubated in standard media containing 0.5% DMSO were included as positive controls. Wells containing media only were included as negative controls (no cell control). 50 µl of mixed XTT reagent was added to each well (containing 100 µl media) and incubated for 8-24 hours and absorbance at 450 nm was measured using a FLUOstar® Omega microplate spectrophotometer (BMG Labtech, Buckinghamshire, UK). Absorbance readings were normalised to no cell control. Percentage control growth was determined using the following calculation:

% control growth = (average absorbance drug treated/average absorbance control) x100

2.3.3 Clonogenic survival assay

Clonogenic survival assays measure the ability of an individual cell to survive and replicate to form colonies of >30 cells, or undergo 5 cell doublings, following treatment with a cytotoxic agent. It is thought to be the most robust method of measuring cytotoxicity of drug treatments. The greater the cytotoxicity the fewer cells survive.

Exponentially growing cells were seeded into 6 well plates at varying cell densities and incubated for 24 hours at 37°C. Drugs were made up at 200x concentration in DMSO before diluting 200x to give a final DMSO concentration of 0.5%. Cells were treated with ATR or PARP inhibitors or chemotherapy alone, or in combination for 72 hours. Cells incubated in standard media containing 0.5% DMSO were included as controls. After treatment, cells were washed in PBS and incubated for 14-21 days in fresh media until colonies had formed. Colonies were fixed with Carnoy's fixative (methanol/acetic acid, 3:1) or ice cold methanol and stained with 0.4% (w/v) crystal violet. Colonies were counted manually. Cloning efficiency and cell survival were determined using the following calculations:

Cloning efficiency (%) = (number of colonies counted/number of cells seeded) x100
Cell survival (%) = (cloning efficiency following treatment/ cloning efficiency of DMSO control) x100

2.4 DNA analysis

2.4.1 DNA extraction

Cell line DNA was extracted using DNeasy Blood and Tissue Kit (QIAGEN) according to the manufacturer's protocol. DNA was eluted with water and stored at 4^{o}C to prevent degradation.

2.4.2 DNA quantification

DNA concentration was estimated using a NanoDrop^{TM} 2000 spectrophotometer (ThermoFisher Scientific). After blanking with 1 µl sterile distilled water, 1 µl DNA sample was loaded onto the stage and the absorbance at 260 nm was measured and DNA concentration estimated (ng/µl). An average of 3 measurements was taken.

For whole exome sequencing, DNA concentration was measured by a Qubit^{TM} Assay (ThermoFisher Scientific) to measure double stranded DNA according to the manufacturer's specification. A master solution was created by diluting Qubit^{TM} reagent 1:200 in Qubit^{TM} buffer. A total volume of 200 µl was prepared for each sample in addition to two standards, which were used for calibration. Samples were quantified by taking an average of three

readings measured by a Qubit 3.0 fluorometer (ThermoFisher Scientific) according to the manufacturer's protocol.

2.4.3 SNP array

DNA extracted from cell lines was sent to the Northern Genetics Service for SNP genotyping. Data was generated by Angharad Humphreys and Fiona Harding using Infinium CytoSNP-850k v1.1/1.2 BeadChip array according to the manufacturer's guideline (Illumina Inc, San Diego, CA). Data was returned in the form of a log2-ratio, reflecting the total copy number of the segment, and B-allele frequency, reflecting allele proportion, in the form of an intensity data (IDAT) file. IDAT files were processed using GenomeStudio (Illumina Inc.), according to the user-guide, to generate a final report and analysed using Nexus Copy Number™ (BioDiscovery, Hawthorne, CA) software. Data were normalised to a standard reference human genome (hg19) to extract log2-ratio and B-allele frequency.

2.4.4 Targeted next generation sequencing

DNA extracted from the GIMEN, IGRN91, KAT100, NGP, SHSY5Y, SKNAS and SJNB1 cell lines was sent to the Northern Genetics Service for targeted next generation sequencing (NGS), performed by Angharad Humphreys, on a panel of 38 SIOPEN Biology group agreed genes of established or potential significance in NB (**Table 2.3**). The Illumina Truseq custom amplicon kit was used for NGS library preparation and sequenced using the Illumina NextSeq 550. Analysis was carried out using Illumina TruSeq Amplicon BaseSpace Amplicon software, Illumina Variant Studio software and Alamut® Visual (Interactive Biosoftware, Rouen, France).

Table 2.3: Neuroblastoma sequencing panel (SIOPEN Biology group agreed gene list)

ALK	*CDKN2B*	*MDM2*	*PTCH1*
ARID1A	*ERBB2*	*MDM4*	*PTEN*
ARID1B	*FGFR1*	*MYC*	*PTPN11*
ATM	*FGFR4*	*MYCN*	*PTPRD*
ATRX	*HRAS*	*NF1*	*TENM2*
BRAF	*IDH1*	*NRAS*	*TERT*
CCND1	*KRAS*	*PDE6G*	*TP53*
CDK4	*MAP2K1*	*PDGFRA*	*TSC1*
CDK6	*MAP2K2*	*PHOX2B*	
CDKN2A	*MAP3K13*	*PIK3CA*	

In addition to the NB gene list, targeted NGS, performed by Jonathan Coxhead at the Newcastle University Genomics Core Facility (Institute of Genetic Medicine), on a panel of 63 genes of established or potential significance in medulloblastoma (**Table 2.4**) for all 10 cell lines. A custom SureSelect XT Low input kit (Agilent) was used for NGS library preparation, by Jemma Castle, and sequenced using the Illumina MiSeq system. Analysis was carried out using Illumina TruSeq Amplicon BaseSpace Amplicon software, Illumina Variant Studio software and Alamut® Visual (Interactive Biosoftware, Rouen, France). Mutational analysis was performed following the genome analysis toolkit (GATK) pipeline v3.5 (do Valle *et al.*, 2016), modified by Dr. Matthew Bashton and converted for use on rocket by Dean Thompson. Variants of high significance were identified by Dr. Lisa Allison, using the following *in silico* tools: PolyPhen v2.2.2, SIFT v5.2.2 and CAROL (Lopes *et al.*, 2012; Adzhubei *et al.*, 2013; Vaser *et al.*, 2016).

Table 2.4: Medulloblastoma sequencing panel gene list

ABCA13	*CDKN2A*	*FCGBP*	*LTBP4*	*PRKAR1A*	*TBR1*
AKT1	*CDKN2B*	*FLNA*	*MAN2C1*	*PTCH1*	*TCF4*
ALPK2	*CREBBP*	*GLI2*	*MDM2*	*PTEN*	*TERT**
APC	*CSNK2B*	*GPS2*	*MDM4*	*RYR3*	*TNXB*
ATM	*CTDNEP1*	*GTF3C1*	*MYCN*	*SHH*	*TP53*
BCOR	*CTNNB1*	*KDM6A*	*NBAS*	*SMARCA4*	*TSC1*
BRCA2	*DDX3X*	*KIF26B*	*NEB*	*SMARCB1*	*TSC2*
CACNA1D	*EP300*	*KMT2C*	*NLRP5*	*SMO*	*ZMYM3*
CBFA2T2	*EPPK1*	*KMT2D*	*OTX2*	*SNCAIP*	
CDH7	*EYA4*	*LDB1*	*PALB2*	*SPTB*	
CDK6	*FBXW7*	*LRP1B*	*PIK3CA*	*SUFU*	
*promoter only					

2.4.3 Whole exome sequencing

DNA (50 ng) from NGP, N20_R1, IMR32 and KAT100 cell lines was sent to the Newcastle University Genomics Core Facility for whole-exome sequencing by Rafiqul Hussain. The Exome libraries for sequencing were generated using the Twist Human Core Exome EF Multiplex Complete Kit, according to the manufacturer's protocol. DNA was fragmented to an average target size of 200 bp and ligated to adapters. DNA fragments were bound to probes adhered to streptavidin-coated magnetic beads, for purification. The exome enriched genomic library was loaded onto the Illumina NovaSeq 6000 flow cell (Illumina Inc., San Diego, CA) for paired-end sequencing according to the manufacturer's protocol. Around 100 million reads were generated, resulting in 100x median haploid coverage per genome. Mutational analysis was performed following the genome analysis toolkit (GATK) pipeline v3.5 (do Valle *et al.*, 2016), modified by Dr Matthew Bashton. Variants of high significance were identified by Emily Beckett, under the supervision of Dr. Alem Gabriel (Beckett, 2019, MRes thesis), using the following *in silico* tools: PolyPhen v2.2.2, SIFT v5.2.2 and CAROL (Lopes *et al.*, 2012; Adzhubei *et al.*, 2013; Vaser *et al.*, 2016).

2.5 Protein analysis

2.5.1 Protein extraction and quantification

Cell pellets were collected by using trypsin to detach cells from the tissue culture flask and resuspended in media. Cells were pelleted by centrifugation at 250 X g for 5 minutes at 4°C. Media was removed and the pellet resuspended in 1 ml PBS. Cells were centrifuged at 250 X g for 5 minutes and the PBS removed. Cell pellets were stored at -80^{o}C prior to protein extraction.

Protein was extracted using PhosphoSafe™ Extraction Buffer (Novagen) following the manufacturer's protocol. Cell debris was pelleted by centrifugation for 5 minutes at 16000 x g and the supernatant collected. Lysates (supernatant) were either used immediately or stored at -20°C until required. Protein concentration was quantified using the Pierce BCA protein assay kit (Thermofisher Scientific), a colorimetric assay where the presence of protein generates a purple coloured reaction product in a concentration dependent manner.

Solutions of bovine serum albumin (BSA) at known concentrations were used to generate a standard curve which was used to interpolate the lysate protein concentration.

2.5.2 SDS-PAGE Western blot

The Western blot is a method of analysing protein expression. Proteins are separated by polyacrylamide gel electrophoresis (PAGE), where negatively charged proteins are separated by size, the smallest travelling the furthest and largest travelling the least. Western blotting allows proteins to be detected using antibodies raised to the specific protein or phosphorylation site on the protein. Primary antibodies are then bound by horseradish peroxidase (HRP)-conjugated secondary antibodies, which amplifies the protein signal and oxidises luminol in the enhanced chemiluminescence (ECL) reagent to generate detectable low emission light.

Protein samples were diluted to 40 µg in 4 x XT loading buffer or 4 x Laemmli loading buffer (BioRad, Hemel Hempstead, UK) to give the proteins a negative charge, denatured by heating to 95°C for 10 minutes and loaded immediately into 3–8% Criterion™ XT Tris-Acetate Protein Gel, for proteins up to 300 kDa, or 4–20% Mini-PROTEAN® TGX™ Precast Protein Gel, for protein up to 200 kDa (Bio-Rad Laboratories Ltd, Hemel Hempstead, UK). Proteins were separated by electrophoresis at 100-150V using a Criterion™ cell or Mini-PROTEAN Tetra vertical electrophoresis cell (BioRad) and transferred onto Hybond-C Extra membrane (GE Life Sciences, Little Chalfont, UK) at 100V for 1 hour using a Criterion™ blotter or Mini Trans-Blot module (BioRad). Membranes were stained with Ponceau S (Sigma-Aldrich) as a control for loading, destained in tris buffered saline, 0.5% tween 20 (TBST) and blocked for 1 hour in 5% milk TBST. Proteins were detected using primary antibodies diluted in 5% milk or BSA in TBST overnight at 4°C. Details of primary antibodies are provided in **Table 2.5**. Secondary antibodies used are listed in **Table 2.6**. Proteins were detected by exposing membranes to ECL reagent (Bio-Rad) and imaged using the ChemiDoc imaging system (Bio-Rad). Densitometry was performed using ImageJ image analysis software.

Table 2.5: Primary antibodies for Western blot analysis

Primary Antibody	Molecular Weight (kDa)	Type of antibody	Supplier	Reference Number	Dilution for immunoblotting
ATR	300	Rabbit polyclonal	CST	2790S	1:500 in 5% BSA
ATM	350	Rabbit monoclonal	CST	2873S	1:500 in 5% milk
pATM (Ser1981)	350	Rabbit monoclonal	CST	13050S	1:500 in 5% BSA
PARP	116 (cleaved 109)	Mouse monoclonal	SCBT	sc-8007	1:5000 in 5% milk
PAR	50-250	Mouse monoclonal	SCBT	sc-56198	1:1000 in 5% milk
pCHK1 (Ser345)	56	Rabbit monoclonal	CST	2348S	1:1000 in 5% BSA
CHK1	56	Mouse monoclonal	SCBT	Sc8408	1:1000 in 5% milk
CHK2	61	Mouse monoclonal	SCBT	sc-17747	1:1000 in 5% milk
pCHK2 (Thr68)	61	Rabbit monoclonal	CST	2197S	1:1000 in 5% BSA
p53	53	Mouse Monoclonal	Leica biosystems	NCL-L-p53-DO7	1:1000 in 5% milk
p21	21	Rabbit monoclonal	CST	2947S	1:1000 in 5% BSA
pRPA2 (ser8)	32	Rabbit monoclonal	CST	54762S	1:1000 in 5% BSA
γH2AX	18	Rabbit polyclonal	CST	2577S	1:1000 in 5% BSA
GAPDH	37	Mouse monoclonal	SCBT	sc-47724	1:10000 in 5% milk
CST: cell signalling technology, SCBT: Santa Cruz biotechnology					

Table 2.6: Secondary antibodies for Western blot analysis

Secondary antibody	Type of antibody	Supplier	Reference Number	Dilution
Anti-mouse immunoglobulins HRP conjugate	Goat polyclonal	Dako	P0447	1:2500
Anti-rabbit immunoglobulins HRP conjugate	Goat polyclonal	Dako	P0448	1:2500
Anti-mouse immunoglobulins HRP conjugate	Goat polyclonal	Abcam	ab6789	1:10000
Anti-rabbit immunoglobulins HRP conjugate	Goat polyclonal	Abcam	ab6721	1:10000
HRP: horse radish peroxidase				

2.6 Immunofluorescence

Immunofluorescent labelling allows the detection of a protein of interest in its subcellular location by using specific primary and fluorophore-conjugated secondary antibodies, which are visualised using a fluorescence microscope. Illumination of a fluorophore with wavelengths of light in its excitation spectrum causes it to emit light at a different wavelength, which is measured by a detector. Multiple target proteins can be visualised in the same sample by using different antibodies conjugated to fluorophores with different excitation and emission spectra.

Cells were grown on sterilised coverslips for 24 hours prior to treatment with control vehicle (DMSO 0.5%), or 1 µM VE-821 with or without 10 µM olaparib for 24 hours and then fixed in 4% formaldehyde for 15 minutes at room temperature (RT) and washed 5X with PBS. Cells on coverslips were permeabilised with PBS 0.2% triton-X-100 and blocked in PBS 0.2% triton-X-100 10% goat serum (G6767, Sigma Aldrich), 10% milk, 2% BSA at room temperature for 1 hour. Coverslips were then incubated with primary antibodies diluted in PBS 0.2% triton-X-100 10% goat serum, 10% milk, 2% BSA at 4^{o}C overnight. The primary antibody solution was removed and coverslips were washed 3 times with PBS 0.2% triton-X-100 before incubating

for 1 hour with secondary antibodies, diluted 1:1000 in PBS 0.2% triton-X-100 2% BSA, at RT in dark conditions. Coverslips were washed 3 times and incubated with 0.5 µg/ml DAPI in PBS 0.2% triton-X-100 for 40 minutes at RT in dark conditions. Coverslips were washed again 3 times before mounting cell side down onto glass microscope slide, with VECTASHIELD® Vibrance anti-fade mounting medium (H-1700, Vector Labs, Oxfordshire, UK), and allowed to set in dark conditions before imaging. Antibodies used in immunofluorescent imaging are listed in **Table 2.7**.

Cells were imaged using a Leica DM6 microscope and Leica Application Suite (LAS) X software (Leica Microsystems,Wetzlar, Germany). The number of pRPA2^{S8}, γH2AX and RAD51 foci in each cell were quantified using ImageJ software (Version 1.52p; Java 1.8.0_172 (64-bit)) (Rueden *et al.*, 2017). Total nuclear fluorescence intensity of γH2AX was measured using ImageJ software.

Table 2.7: Antibodies used for immunofluorescent imaging

Primary Antibody	**Type of antibody**	**Supplier**	**Reference Number**	**Dilution**
pRPA2 (ser8)	Rabbit Monoclonal	CST	54762S	1:400
γH2AX	Mouse Monoclonal	SCBT	sc-517348	1:500
RAD51	Rabbit Monoclonal	CST	8875S	1:250
Secondary antibody	**Type of antibody**	**Supplier**	**Reference Number**	**Dilution**
Anti-mouse IgG alexafluor 594 conjugate	Goat polyclonal	Invitrogen (Thermofisher scientific)	A32742	1:1000
Anti-rabbit IgG alexafluor 488 conjugate	Goat polyclonal	Invitrogen (Thermofisher scientific)	A11008	1:1000
CST: cell signalling technology, SCBT: Santa Cruz biotechnology				

2.7 Cell cycle analysis

The cell cycle profile of a population of cells was measured using flow cytometry. The DNA content is estimated by measuring the intensity of a quantitative fluorescent DNA stain, such as propidium iodine (PI) which was used here. Cells in G1 or G0 phase have 2 copies of each chromosome, denoted 2n. Cells that are in G2 phase have 4 copies of each chromosome, denoted 4n, as these are separated when the cell divides during mitosis. The fluorescent intensity measured from cells with 4n DNA is double that of 2n cells. Cells with DNA between 2n and 4n are S-phase cells as these are at various stages of DNA synthesis. S phase cells can also be identified by incubating cells for a short time period with a nucleotide analogue, such as bromodeoxyuridine (BrdU) used here, which gets incorporated into the DNA and can be detected with fluorescently labelled antibodies. Cells with less than 2n DNA are classed as sub-G1 cells, which is often used to estimate the proportion of apoptotic cells, but can also indicate cellular debris (Darzynkiewicz, 2010).

Cell cycle profiles were first measured by staining with PI alone and confirmed by measuring DNA content (PI) and BrdU incorporation to track S phase.

PI alone: Cells were harvested post-treatment, fixed in ice-cold 70% (v/v) ethanol, and stored at -20^{o}C. Prior to analysis, cells were washed with PBS, resuspended in 500 µL PBS with 50 µg/mL propidium iodide (Sigma-Aldrich) and 50 µg /mL RNAse A (Sigma-Aldrich), and incubated at 37 ^{o}C for 30 minutes. Samples were analysed on the Attune NxT Flow Cytometer using Invitrogen Attune NxT Software (Thermo Fisher Scientific). Data were analysed using FlowJo^{TM} (BD Biosciences,Wokingham, UK).

PI and BrdU: Treated cells were incubated with 30 µM BrdU for 1 hour prior to harvest and fixation (as above). Cells were permeabilised in 0.5 ml 2 N HCl/0.5% Triton X-100, incubated 30 minutes at RT, then suspended in 0.5 ml 0.1 M sodium tetraborate for 2 min. Cells were washed with 150 µl PBS/ 1% BSA and resuspended in 50 µl 0.5% Tween 20/1% BSA/PBS and 10 µl FITC conjugated anti-BrdU mouse monoclonal antibody (eBioscience™, Fisher Scientific, catalogue number: 15516556) and incubate for 1 hour at RT. Cells were then washed once in PBS, resuspended in 500 µL PBS with 50 µg/mL propidium iodide (Sigma-Aldrich) and 50 µg /mL RNAse A (Sigma-Aldrich), and incubated at 37^{o}C for 30 min. Samples were analysed as described above.

2.8 Statistics

Where possible, the appropriate statistical tests were performed using GraphPad Prism v8.0 software and p values < 0.05 were taken to be statistically significant. Combination Index (CI) values for evaluation of synergy were determined by the Chou–Talalay method using CalcuSyn v2 software (Biosoft, Cambridge, UK).

Chapter 3: Characterisation of the DNA damage response in neuroblastoma cell lines

3.1 Introduction

HR-NB tumours frequently present with DDR defects including loss or mutation of key DDR genes, oncogene-induced RS and cell cycle checkpoint dysfunction.

Among the most common genetic lesions in NB is allelic loss of chromosome 11q, observed in around 30% of tumours (Mlakar *et al.*, 2017). Many DDR proteins are encoded on 11q and are included within the smallest region of overlap, including *ATM, CHK1, MRE11*, and *H2AFX*. In most cases of 11q deletion, there is no mutation or hyper-methylation (silencing) in the other allele of these genes (Mandriota *et al.*, 2015), however loss of one copy could contribute to tumorigenesis due to haploinsufficiency.

Expression of MYCN also induces downregulation of ATM by the upregulation of the micro RNA, miR-421 (Hu *et al.*, 2010; Mansour *et al.*, 2013). Around 50% of HR-NB tumours have an amplification of the *MYCN* oncogene, which drives proliferation and causes RS (Campbell *et al.*, 2017). 11q deletion and *MYCN* amplification are rarely observed together, but in the 2% of cases which carry both abnormalities, the prognosis is especially poor with 5-year overall survival reported at 25% (Spitz *et al.*, 2006; Villamón *et al.*, 2013).

In addition to *MYCN* amplification, the constitutive activation of ALK, and subsequent downstream pathways, has been shown to be involved in cell proliferation, inducing RS, migration, and invasion (Bresler *et al.*, 2014). Aberrant ALK activity has been reported through *ALK* amplification, which occurs concurrently with *MYCN* amplification in around 2-3% of NB cases, and *ALK* mutation, which occurs in around 14% HR-NB cases (Trigg and Turner, 2018). ALK activation has been shown to accelerate MYCN driven tumorigenesis in animal models (Berry *et al.*, 2012; Zhu *et al.*, 2012), and likely contributes to RS.

Low frequencies of rare single nucleotide variants (SNVs) in other DDR genes, particularly *BARD1* and *CHEK2*, have been identified in NB tumours (Lasorsa *et al.*, 2016; Takagi *et al.*, 2017), but no difference in prognosis was observed between those with and without DDR-associated gene alterations (Takagi *et al.*, 2017). Defects in the p53 tumour suppressor signalling pathway result in chromosome instability from G1 checkpoint dysfunction

(Massague, 2004). Mutant p53 has also been shown to result in aberrant expression of proliferation-driving oncogenes, which could contribute to RS (Freed-Pastor and Prives, 2012). Many mutations in *TP53,* which codes for p53*,* lead to stabilisation of a mutant protein which affects wild-type p53 activity in a dominant negative manner (Freed-Pastor and Prives, 2012). Mutation of *TP53* is rare at diagnosis but is observed in up to 15% of relapsed NB tumours (Carr-Wilkinson *et al.*, 2010).

The impact of SNVs or small insertions or deletions (indels) on protein expression and function can be difficult to predict and largely depend on the protein domain in which the resulting amino acid change(s) reside (Reva *et al.*, 2011; Choi *et al.*, 2012; Sim *et al.*, 2012; Jia and Zhao, 2017). The introduction of a premature stop codon (nonsense mutation) generally leads to loss of mRNA, and subsequent protein, expression through a process known as nonsense mediated mRNA decay, but some stop-gain mutations escape degradation and result in expression of a truncated protein.

In this study, defects in the DDR were characterised in a panel of cell lines by targeted next generation sequencing, analysis of baseline protein expression and activity, and functional analysis of ATR, ATM and p53. The panel of cell lines is listed in Table 3.1 and includes previously reported genetic aberrations which may affect the DDR.

This panel also includes 2 cell line pairs, IMR32 and KAT100, and NGP and N20_R1. The KAT100 cell line was generated by selecting for resistance to potassium acyl trifluoroborate (KAT) in IMR32 cells, which generated mutations in many drug resistance genes including *TP53,* C135F (Xue *et al.*, 2007). The N20_R1 cell line was generated by selecting for resistance to the MDM2 inhibitor nutlin-3 in NGP cells, resulting in two mutations in the *TP53* gene, P98H and P152T (Drummond *et al.*, 2016).

Table 3.1: Cell line reported genetic abnormalities.

Cell line	***MYCN* status**	**11q/ *ATM* status**	***TP53* pathway**	**Other reported DDR defects**	**Reference**
SHSY5Y	Non-amp	No deletion	WT	*CHEK2* (T410fs)* *ALK* (F1174L)	(Ross *et al.*, 1983; George *et al.*, 2008)
SKNAS	Non-amp	Deletion (*MRE11, ATM, CHEK1, H2AFX)*	Mutant Deletion of intron9/exon 10	*ATR* (V2158F) *RB1* (L477P) (COSMIC)	(Van Roy *et al.*, 2001; Goldschneider *et al.*, 2006; Takagi *et al.*, 2017)
SJNB1	Non-amp	Deletion (*MRE11, ATM, CHEK1, H2AFX)*	WT		Van Roy *et al*., 2001
GIMEN	Non-amp	Deletion (*MRE11, ATM, CHEK1, H2AFX)*	WT	*BRCA1* (R466Q) (COSMIC)	Van Roy *et al*., 2001
NGP	amp	Deletion (*ATM, CHEK1, H2AFX)*	WT *MDM2* amp		(Van Roy *et al.*, 2001)
N20_R1	amp	Not reported, assume same as NGP	Mutant P98H P152T *MDM2* amp		(Drummond *et al.*, 2016)
NMB	amp	No deletion	Mutant G245S	*ATM* (S1198F)	(Goldman *et al.*, 1996), Van Roy *et al*. 2001, Takagi *et al.* 2017
IMR32	amp	Deletion (*ATM, CHEK1, H2AFX)*	WT	*ATM* (V2716A)	(Tumilowicz *et al.*, 1970; Mandriota *et al.*, 2015) Takagi *et al.* 2017
KAT100	amp	Not reported, assume same as IMR32	Mutant C135F		(Xue *et al.*, 2007)
IGRN91	amp	No deletion	Mutant Duplication of exons 7-9		(Blanc *et al.*, 2003; Goldschneider *et al.*, 2004)

fs: frame shift
*reported in parental SKNSH cell lines (Sanmartin *et al.,* 2017)
COSMIC database (Tate *et al.*, 2019)

3.2 Chapter aims

The aims of this chapter are as follows:

1. To identify alterations in genes leading to DDR defects in a panel of 10 HR-NB cell lines
2. To characterise the expression and function of key DDR proteins in a panel of HR-NB cell lines

3.3 Methods

3.3.1 Cell culture

Cell lines were cultured and maintained as described in section 2.1

3.3.2 Reagents

Doxorubicin and olaparib were used and stored as described in section 2.2.

3.3.3 Determination of cell lines growth rate

To determine cell doubling time, cells were collected and counted every 24 hours for 5 days (120 hours) and normalised to the number of cells seeded (t=0). Cell number was logged, and doubling time was estimated using the exponential growth function in Graphpad Prism version 8 software.

3.3.4 Calculation of optimal seeding density

To determine cell densities for XTT assays, cells were seeded in 96-well plates, as shown in **Figure 3.1A**, and incubated at 37°C for 96 hours. The XTT reagent (Roche) was added according to the manufacturer's instructions, incubated for 8-24 hours and absorbance at 600 nm was measured using a FLUOstar® Omega microplate spectrophotometer (BMG Labtech, Buckinghamshire, UK). Absorbance readings were normalised to no cell control and plotted. The optimal seeding density was taken as the number of cells seeded before absorbance plateaued e.g. 3000 cells per well for SKNAS (**Figure 3.1B**).

A)

	1	2	3	4	5	6	7	8	9	10	11	12
A	PBS	PBS	PBS	PBS	PBS	PBS	PBS	PBS	PBS	PBS	PBS	
B	PBS	No cells	1000	2000	3000	4000	5000	6000	7000	8000	PBS	
C	PBS	No cells	1000	2000	3000	4000	5000	6000	7000	8000	PBS	
D	PBS	No cells	1000	2000	3000	4000	5000	6000	7000	8000	PBS	
E	PBS	PBS	PBS	PBS	PBS	PBS	PBS	PBS	PBS	PBS	PBS	
F												
G												
H												

B)

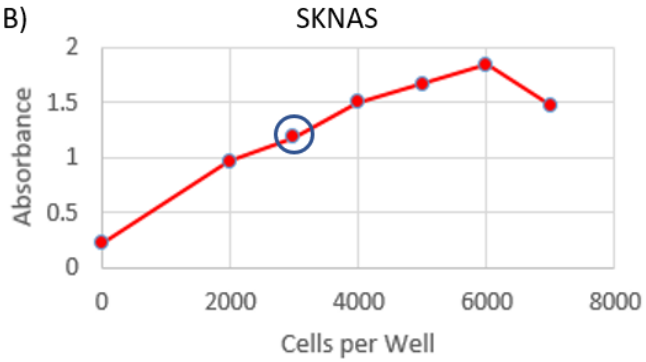

***Figure 3.1**: A) Outline of 96 well plate set up to test optimal seeding density for XTT cell proliferation assay. Numbers indicate the number of cells in that well. Phosphate buffered saline (PBS) surrounds wells containing cells to maintain humidity. B) Cell density optimisation assay for SKNAS cell line. Blue circle indicates number of cells per well used for subsequent experiments.*

3.3.5 Calculation of cloning potential

To calculate cloning potential, 100 exponentially growing cells were seeded into 6 well plates in triplicate and incubated until colonies were visible (around 2 weeks) at 37°C. Cloning potential was calculated as follows: (average number of colonies counted/ number of cells seeded) x100.

3.3.6 DNA extraction

Cell line DNA was extracted using DNeasy Blood and Tissue Kit (QIAGEN) according to the manufacturer's protocol. DNA was quantified as described in section 2.4.2 and stored at 4°C to prevent degradation.

3.3.7 SNP array

DNA extracted from cell lines was sent to the Northern Genetics Service (Centre for Life, Newcastle, UK) for SNP genotyping, as described in section 2.4.3.

3.3.8 Targeted sequencing

Targeted NGS was performed as described in section 2.4.4, on a panel of 38 SIOPEN Biology group agreed genes of established or potential significance in NB (**Table 3.2**) for the GIMEN, IGRN91, KAT100, NGP, SHSY5Y, SKNAS and SJNB1 cell lines. Targeted NGS was also carried out on a panel of 63 genes of established or potential significance in medulloblastoma (**Table 3.3**) for all cell lines.

Table 3.2: Neuroblastoma sequencing panel (SIOPEN Biology group agreed gene list)

ALK	*ERBB2*	*MYC*	*PTPRD*
ARID1A	*FGFR1*	*MYCN*	*TENM2*
ARID1B	*FGFR4*	*NF1*	*TERT*
ATM	*HRAS*	*NRAS*	*TP53*
ATRX	*IDH1*	*PDE6G*	*TSC1*
BRAF	*KRAS*	*PDGFRA*	
CCND1	*MAP2K1*	*PHOX2B*	
CDK4	*MAP2K2*	*PIK3CA*	
CDK6	*MAP3K13*	*PTCH1*	
CDKN2A	*MDM2*	*PTEN*	
CDKN2B	*MDM4*	*PTPN11*	

Table 3.3: Medulloblastoma sequencing panel gene list

ABCA13	*CDKN2A*	*FCGBP*	*LTBP4*	*PRKAR1A*	*TBR1*
AKT1	*CDKN2B*	*FLNA*	*MAN2C1*	*PTCH1*	*TCF4*
ALPK2	*CREBBP*	*GLI2*	*MDM2*	*PTEN*	*TERT**
APC	*CSNK2B*	*GPS2*	*MDM4*	*RYR3*	*TNXB*
ATM	*CTDNEP1*	*GTF3C1*	*MYCN*	*SHH*	*TP53*
BCOR	*CTNNB1*	*KDM6A*	*NBAS*	*SMARCA4*	*TSC1*
BRCA2	*DDX3X*	*KIF26B*	*NEB*	*SMARCB1*	*TSC2*
CACNA1D	*EP300*	*KMT2C*	*NLRP5*	*SMO*	*ZMYM3*
CBFA2T2	*EPPK1*	*KMT2D*	*OTX2*	*SNCAIP*	
CDH7	*EYA4*	*LDB1*	*PALB2*	*SPTB*	
CDK6	*FBXW7*	*LRP1B*	*PIK3CA*	*SUFU*	
*promoter only					

3.3.9 Whole exome sequencing

NGP, N20_R1, IMR32 and KAT100 cell line DNA was sent to the Newcastle University Genomics Core Facility (Institute of Genetic Medicine) for whole-exome sequencing by Rafiqul Hussain, as described in section 2.4.5.

3.3.10 Western blotting

Baseline cell lysates were collected as described in section 2.5.1. Proteins were separated by gel electrophoresis using a 4-20% Tris-acetate or 4-20% Tris-glycine polyacrylamide gel (Bio-Rad, Hemel Hempstead, UK), transferred onto nitrocellulose and detected using Western blotting as described in section 2.5.2. ATR, ATM, pATM^{S1981}, CHK1, pCHK1^{S345}, CHK2, pCHK2^{T68}, MYCN, p53, p21, pRPA2^{S8} and γH2AX were detected using primary antibodies described in **Table 2.5** and the appropriate HRP-conjugated secondary antibodies. Protein expression was measured by chemiluminescence from exposure to ECL detection reagent using a ChemiDoc imaging system and bands were quantified using ImageJ software as described in section 2.5.2.

3.4. Results

3.4.1 Doubling time, cloning potential, and seeding densities of NB cell lines

In order to set up cytotoxicity assays, the growth rate (doubling time), cloning efficiency and optimal seeding density for XTT for each cell line needed to be established. The cloning efficiency, often referred to as plating efficiency, is the percentage of cells seeded which give rise to colonies of more than 50 cells and needs to be taken into consideration when analysing clonogenic survival data. The optimal seeding density for XTT cell proliferation assay is the number of cells seeded in a 96 well plate to give the best XTT absorbance signal without reaching plateau following 96 hours incubation (72 hour drug treatment). All these cell lines are adherent, and growth rate can be restricted by contact inhibition. Cell lines with faster growth rates or volume require fewer cells to be seeded prior to treatment. In addition, cell lines with slow growth rates may require longer treatment incubation times. The doubling time, cloning efficiency, and optimal seeding density for XTT cell proliferation assay for the 10 NB cell lines used in this study are reported in **Table 3.4.**

Table 3.4: The doubling time, cloning efficiency, and optimal seeding density for XTT cell proliferation assay of NB cell lines used in this study.

Cell line	Doubling time (hours)	Cloning efficiency (%)	Seeding density for XTT (cells/well)
SHSY5Y	40.2	50	4000
SKNAS	51.6	16.9	3000
SJNB1	29.2	37.17	4000
GIMEN	25.4	18.25	2000
NGP	40.7	32	4000
N20_R1	31.4	33.05	4000
NMB	62.2	3.83	4000
IMR32	48.2	22.56	5000
KAT100	28.6	38.19	4000
IGRN91	43.9	73.33	4000

3.4.2 Genetics

To confirm and extend the previously reported the genetic abnormalities affecting the DDR in the panel of cell lines, analysis of segmental chromosome aberrations, by SNP array, and targeted panel sequencing was carried out.

3.4.2.1 MYCN amplification and 11q deletion status confirmed by SNP array

The *MYCN* gene is located on chromosome 2 (2p24.3). The reported *MYCN* amplification status of the cell lines was confirmed by SNP array analysis. Figure 3.2 shows the SNP trace of chromosome 2 for each cell line. The *MYCN* gene locus is clearly amplified in 6/10 of the cell lines studied, the IGRN91, NMB, NGP, N20_R1, IMR32 and KAT100 cell lines (**Figure 3.2**, red arrows), but not the GIMEN, SHSY5Y, SKNAS or SJNB1 cell lines, confirming their previously reported *MYCN* status. In addition to *MYCN*, the IMR32 and KAT100 cell lines also have an amplification of the *ALK* gene (**Figure 3.2**, black arrows).

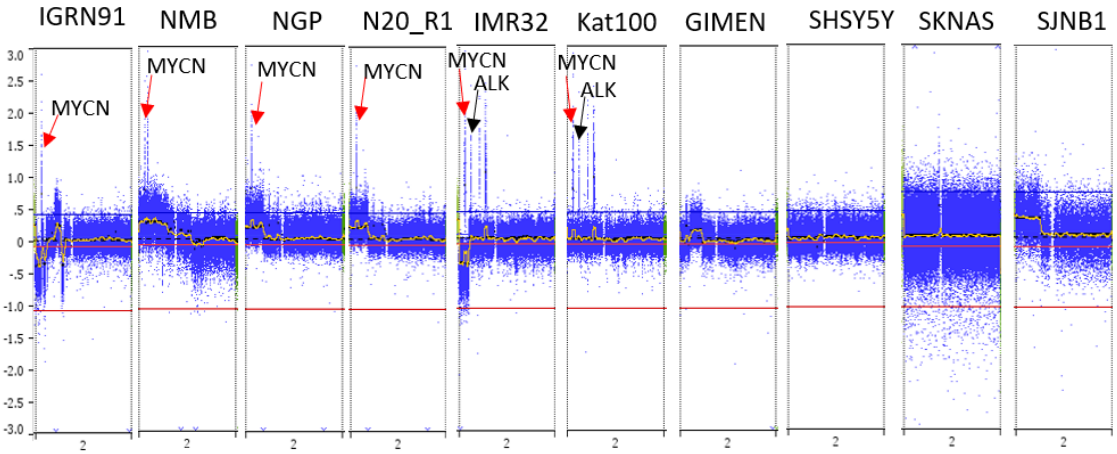

***Figure 3.2**: Analysis of amplicons on chromosome 2 in a panel of 10 NB cell lines by single nucleotide polymorphism (SNP) array using Nexus Copy Number™ software. Log2 ratio of signal intensities between the cell line and normal control. MYCN amplification is confirmed in six cell lines (red arrows), with two also showing ALK amplification (black arrows).*

The 11q status of these cell lines was also confirmed by SNP array. The SNP array trace confirms allelic deletion and loss of heterozygosity (LOH) of 11q in the SKNAS, GIMEN, IMR32, KAT100, NGP and N20_R1 cell lines (**Figure 3.3A**). SJNB1 have a deletion of whole chromosome 11. All 11q deletions included *ATM*, *H2AX* and *CHK1,* but deletion of *MRE11* was only detected in the SKNAS, SJNB1 and GIMEN cell lines (**Figure 3.3B**).

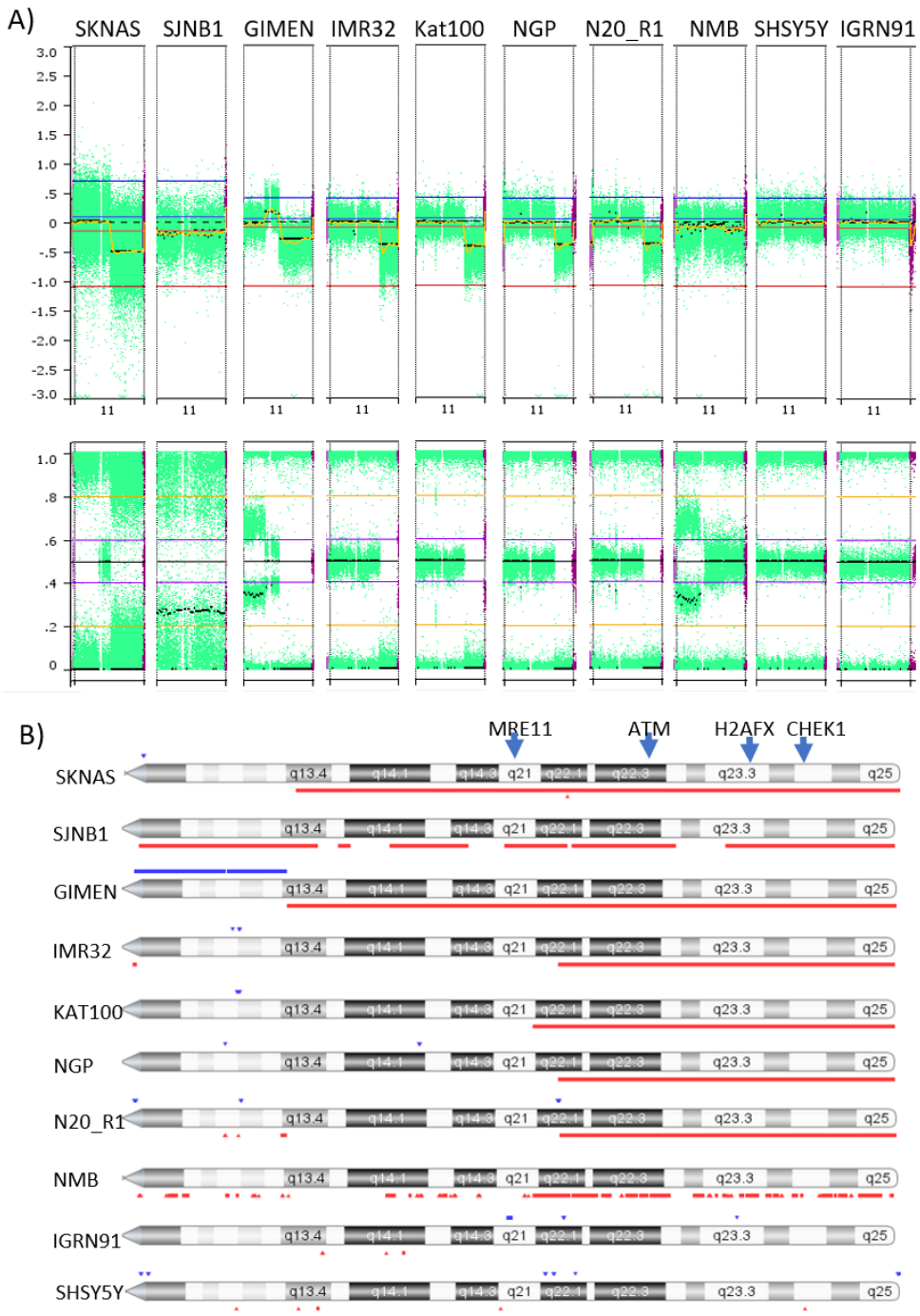

***Figure 3.3**: Analysis of chromosome 11 in a panel of 10 NB cell lines by single nucleotide polymorphisms (SNP) array in Nexus copy number. A) Log2 ratio of signal intensities between the cell line and normal control (top) and the B-allele frequency indicating genotype (bottom). B) Summary of DDR gene loss on chr11q by cell line. Red = loss, blue=gain.*

3.4.2.2 Identification of DDR defects by targeted panel sequencing

To confirm the mutations affecting the DDR in cell lines reported in the literature, cell lines were put through 2 sequencing panels. The panels contained genes which had been shown

to be of prognostic value or predictive of response in either NB or medulloblastoma. DDR mutations discovered in these NB cell lines through targeted sequencing are listed in **Table 3.5**.

Table 3.5: Mutations in genes affecting the DNA damage response in NB cell lines discovered in this study by targeted panel sequencing

Gene	Function	Cell line	Amino acid change	Predicted effect on protein function (PolyPhen, SIFT and CAROL)	Gene panel detected in
ALK	Membrane receptor signalling to MAPK pathway	SHSY5Y	F1174L	Deleterious	NB
ATM	DNA damage sensor kinase, signals to DNA repair and cell cycle arrest	NMB	C532Y	Deleterious	MB
		IMR32	V2716A	Deleterious	NB, MB
		IGRN91	Splice acceptor variant	Deleterious	NB, MB
BRCA2	Orchestrates DSB repair by HR	GIMEN	T2515I	Deleterious	MB
CREBBP	Transcriptional co-activator with lysine acetyltransferase activity involved in regulation of genes involved in the DNA damage response	NGP	S139R	Likely tolerated	MB
		N20_R1	S139R	Likely tolerated	MB
		IMR32	Q1970*	Deleterious	MB
		KAT100	Q1970*	Deleterious	MB
KMT2C	Lysine methyltransferase involved in epigenetic gene regulation	SHSY5Y	P2467R	Deleterious	MB
		NMB	Y2218S	Deleterious	MB
KRAS	RAS GTPase, signal transducer in the MAPK pathway	SHSY5Y	G12V	Deleterious	NB
TP53	Transcription factor involved in signalling to cell cycle arrest and apoptosis in response to DNA damage	SKNAS	R342*	Deleterious	NB, MB
		NMB	G245S	Deleterious	MB
		N20_R1	P98H	Deleterious	MB
		N20_R1	P152T	Deleterious	MB
		KAT100	C135F	Deleterious	NB, MB
*stop codon. NB: neuroblastoma; MB: medulloblastoma.					

Targeted sequencing confirmed the reported *TP53* mutations in SKNAS, NMB, N20_R1 and KAT100 cells. The *TP53* mutation in IGRN91 cells was not identified by targeted sequencing, which is likely due to the mutation being a duplication of exons 7-9, instead a missense mutation. This mutation was originally identified by sequencing *TP53* complementary DNA

obtained from the IGRN91 cell line using the Abiprism 377 Sequencer, a gel electrophoresis based sequencer (Goldschneider *et al.*, 2004).

Although the previously reported *ATM* mutation in IMR32 cells was confirmed (Takagi *et al.* 2017), the *ATM* mutation detected in the NMB cell line by MB panel sequencing differs from what was reported (Takagi *et al.,* 2017). Both *ATM* mutations were predicted to be deleterious to protein function. A mutation in a splice acceptor site was identified in the IGRN91 cell line in both sequencing panels. Splice site variants impair mRNA splicing and can result in exon skipping.

Other mutations affecting the DDR were confirmed through targeted sequencing. Firstly, mutations in *ALK* and *KRAS* were identified in the SHSY5Y cell line. These mutations are thought to lead to constitutive MAPK signalling, contributing to increased RS. A heterozygous mutation in *BRCA2* was identified in the GIMEN cell line.

Deleterious *CREBBP* mutations were identified in the IMR32 and KAT100 cell line pair. *CREBBP* encodes a transcriptional co-activator which is involved in regulation of genes involved in the DDR (Dutto *et al.*, 2018). In addition, mutations in *KMT2C*, which codes for a lysine methyltransferase and is involved in regulation of DDR genes such as *BRCA1* and *RAD51* (Rampias *et al.*, 2019), were found in the SHSY5Y and NMB cell lines.

3.4.2.3 Paired cell lines

Included in this panel of NB cell lines are 2 pairs, IMR32 and KAT100, and NGP and N20R1, which were generated by selecting for resistance to potassium acyl trifluoroborate (KAT) and the MDM2 inhibitor nutlin-3, respectively.

The copy number abnormalities of the KAT100 and N20_R1 cell lines have not been previously reported. Here the segmental chromosome aberrations of each of the paired cell lines was analysed by SNP array and the segmental copy number profiles of the daughter cell lines were compared to the parental, which are summarised in **Table 3.6** (see appendix 1 for full SNP array profile images). The copy number profiles of each of the cell lines in the pairs are largely similar and focal gene amplifications remained unchanged in the daughter cell lines. The difference in copy number loss or gains was greater in the IMR32 cell lines pair than the NGP pair, which is likely due to the mechanism of action of the drugs selected against.

Table 3.6: Copy number alterations in IMR32 and KAT100, and NGP and N20_R1, cell line pairs identified by SNP array. Aberrations specific to one of the pair are in red.

Cell line	Deletion	Gain	Focal amplifications
IMR32	1p, 2p, 11q, 16q	1p, 1q, 4q, 8q, 12p, 15q, 17q	*MYCN, ALK*
KAT100	1p, 11q, 16q	1p, 6q, 7p, 8p, 12p, 15q, 17q	*MYCN, ALK*
NGP	10q, 11q, 12q, 18p	1q, 2p, 17q, 19	*MYCN, CDK4, MDM2*
N20_R1	10q, 11q, 12q, 15q, 18p	1q, 2p, 17q, 19	*MYCN, CDK4, MDM2*
IMR32 and KAT100 cell lines were obtained from different sources and therefore may not reflect parental and daughter cell line pairs			

Whole exome sequencing of these cell line pairs was carried out by Emily Beckett as part of an MRes project (Beckett, 2019, MRes Thesis). Analysis of DDR specific mutations revealed the extent of the single nucleotide alterations generated by selecting for resistance between the parental and the daughter cell lines. The daughter cell lines showed many more cell line specific nucleotide changes than the parental. **Tables 3.7** and **3.8** outline the mutations which are predicted to affect the DDR specific to the parental or daughter cell lines, respectively. The presence of mutations in the parental cell line suggests genetic drift during growth and passage after the generation of the daughter cell line. For the full list of cell line specific mutations from whole exome sequencing see appendix 2.

Table 3.7: Mutations in genes predicted to affect the DNA damage response unique to Parental cell lines identified by whole exome sequencing

Cell Line	Genes	Codes for	AA Change	Variant Effect	SIFT class (score)
IMR32	*RPRD2*	Regulation of nuclear pre-mRNA domain-containing protein 2	S597*	stop_gained	-
IMR32	*YY1AP1*	YY1-associated protein 1	V527F	missense_variant	Deleterious (1.000)
IMR32	*ZSWIM6*	Zinc finger SWIM domain-containing protein 6	R717W	missense_variant	Deleterious (1.000)
IMR32	*PDE6A*	Phosphodiesterase 6A	-	splice_donor_variant	-
IMR32	*PLEKHG 1*	Pleckstrin homology domain-containing family G member 1	E55*	stop_gained	-
IMR32	*ATM***	Serine-protein kinase ATM	V2716A	missense_variant	Deleterious (1.000)
IMR32	*PDE6H*	Phosphodiesterase 6H	-	splice_region_variant,intron_variant	-
IMR32	*RNF6*	Ring Finger Protein 6	R135I	missense_variant	Deleterious (1.000)
IMR32	*IQGAP1*	IQ Motif Containing GTPase Activating Protein 1	E1578G	missense_variant	Deleterious (1.000)
IMR32	*USP32*	Ubiquitin Specific Peptidase 32	A717S	missense_variant	Deleterious (0.989)

*stop codon, ** confirmed by targeted sequencing and previously reported
IMR32 and KAT100 cell lines were obtained from different sources and therefore may not reflect parental and daughter cell line pairs

Table 3.8: Daughter cell line specific mutations in genes predicted to affect the DNA damage response identified by whole exome sequencing

Cell Line	Genes	Codes for	AA Change	Variant Effect	SIFT class (score)
KAT100	*CEP350*	Centrosomal Protein 350	V188F	missense_variant	Deleterious (0.989)
KAT100	*ZNF670*	Zinc Finger Protein 670	S88*	stop_gained	-
KAT100	*CEP120*	Centrosomal Protein 120	K561E	missense_variant	Deleterious (0.999)
KAT100	*MDC1*	Mediator Of DNA Damage Checkpoint 1	Q1463H	missense_variant	Deleterious (1.000)
KAT100	*RUNX2*	RUNX Family Transcription Factor 2	M39R	missense_variant	Deleterious (0.999)
KAT100	*FANCG*	Fanconi anemia group G protein	C75*	stop_gained	-
KAT100	*SRGAP1*	SLIT-ROBO Rho GTPase Activating Protein 1	-	splice_region_variant,intron_variant	-
KAT100	*PLCB2*	Phospholipase C Beta 2	G534V	missense_variant,splice_region_variant	Deleterious (0.999)
KAT100	*TP53***	Tumour suppressor protein 53	C135F	missense_variant	Deleterious (1.000)
KAT100	*RBL1*	RB Transcriptional Corepressor Like 1	L206F	missense_variant	Deleterious (1.000)
N20R1	*RFX5*	DNA-binding protein RFX5	V565G	missense_variant	Deleterious (1.000)
N20R1	*KMT2C*	Lysine methyltransferase 2C	G908C	missense_variant	Deleterious (1.000)
N20R1	*DAGLA*	Diacylglycerol Lipase Alpha	S12Y	missense_variant	Deleterious (1.000)
N20R1	*CDAN1*	Codanin 1	P560Q	missense_variant	Deleterious (1.000)
N20R1	*CENPN*	Centromere Protein N	S195I	missense_variant	Deleterious (1.000)
N20R1	*TP53***	Tumour suppressor protein 53	P152T	missense_variant	Deleterious (1.000)
N20R1	*TP53***	Tumour suppressor protein 53	P98H	missense_variant	Deleterious (1.000)
N20R1	*KHSRP*	Far upstream element-binding protein 2	R394S	missense_variant,splice_region_variant	Deleterious (0.989)
N20R1	*ZC3H4*	Zinc finger CCCH domain-containing protein 4	G431*	stop_gained	-
N20R1	*ZSCAN5A*	Zinc finger and SCAN domain-containing protein 5A	D270G	missense_variant	Deleterious (0.996)
N20R1	*GNAS*	Guanine nucleotide-binding protein G(s) subunit alpha isoforms Xlas	K943N	missense_variant	Deleterious (1.000)

*stop codon, ** confirmed by targeted sequencing and previously reported

IMR32 and KAT100 cell lines were obtained from different sources and therefore may not reflect parental and daughter cell line pairs

3.4.3 Baseline expression of key DNA damage response proteins

To explore the effect of genetic alterations on expression of key DDR proteins, baseline protein expression of each cell line was examined by Western blot (**Figure 3.4**).

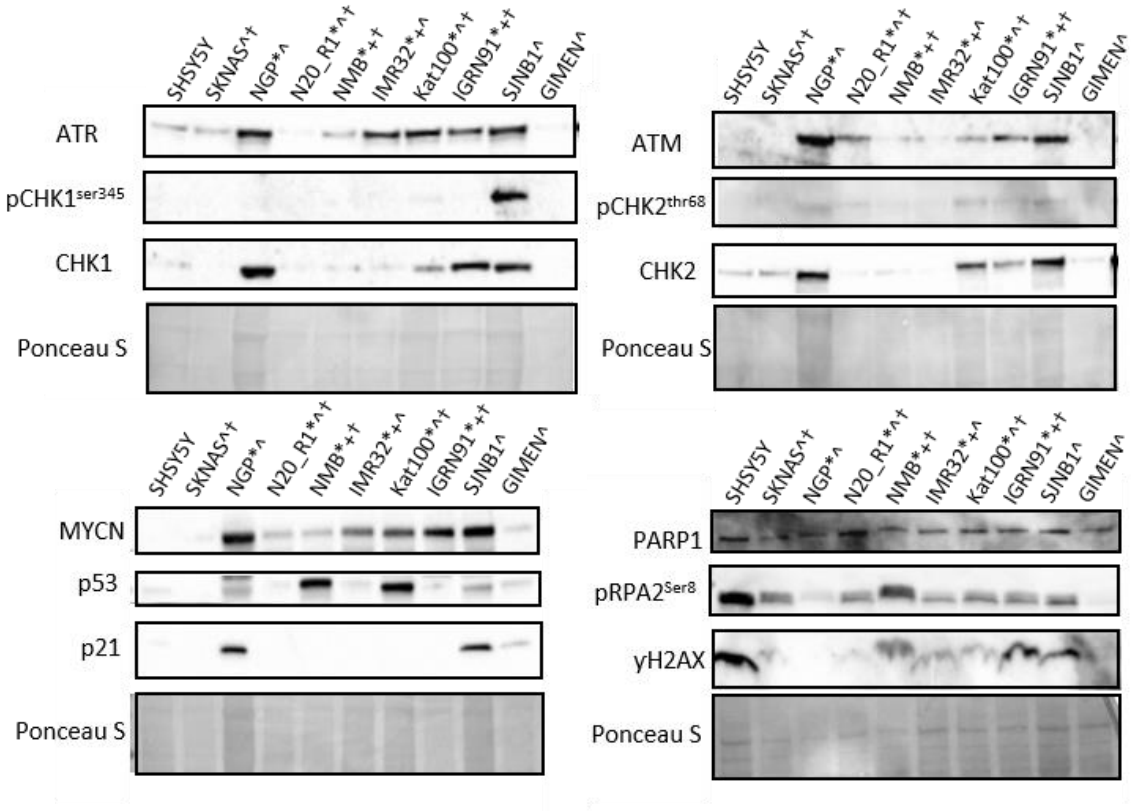

Figure 3.4: *Representative images of baseline expression of DNA damage response proteins ATR, ATM, CHK1, CHK2, phospho-CHK1^{S345}, phospho-CHK2^{T68}, MYCN, p53, p21, PARP1, phospho-RPA2^{S8} and γH2AX from 2 independent Western blot experiments in NB cell lines used in this study. *MYCN amplified, ^11q deleted, +ATM mutant, †TP53 mutant. Ponceau S stain was used as measure of total protein loading for control.*

Baseline expression of MYCN, PARP1, p53, ATR, CHK1, ATM, and CHK2 proteins was quantified for each cell line (**Figure 3.5**).

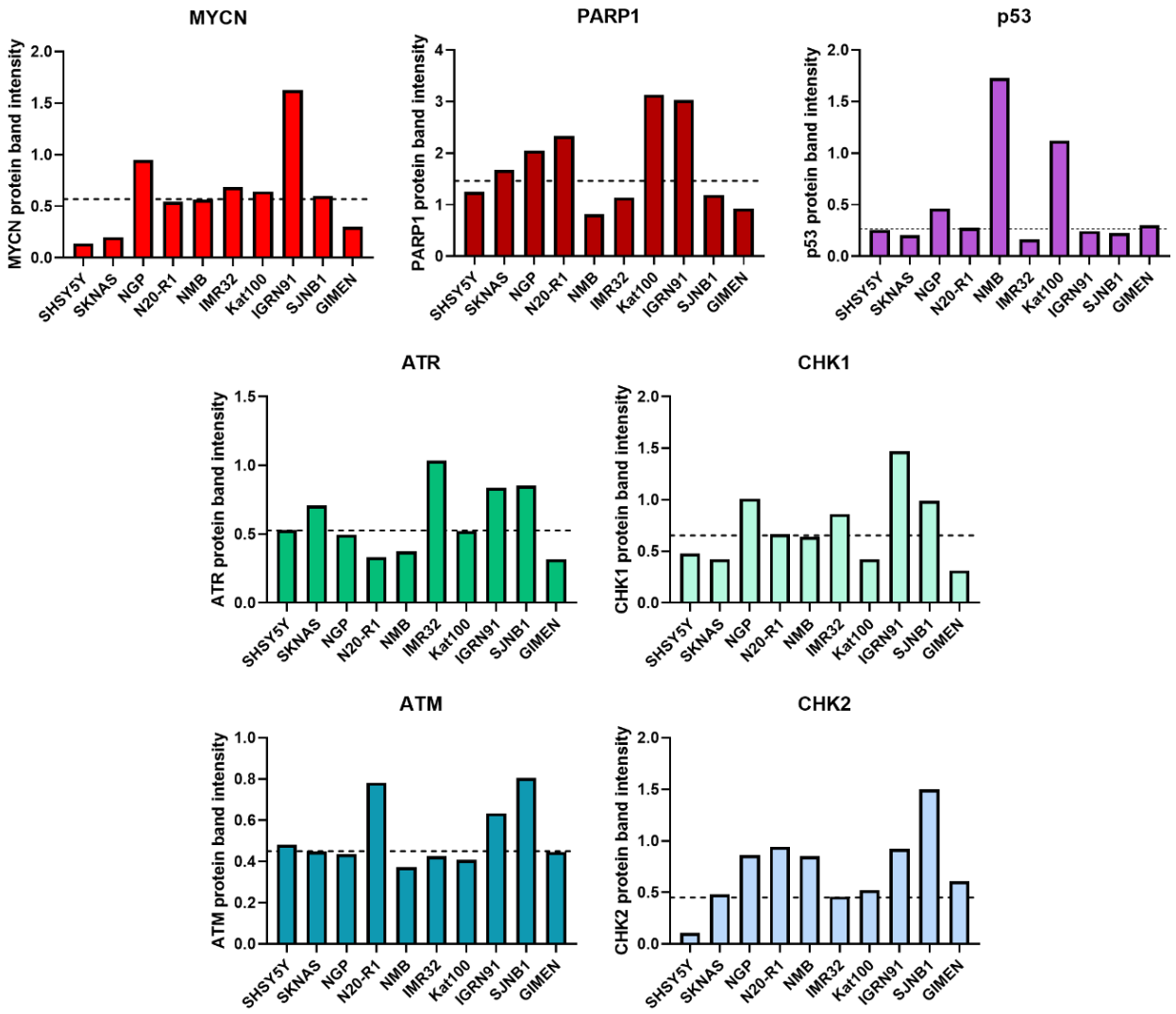

Figure 3.5: *Quantification of baseline expression of DNA damage response proteins MYCN, PARP1, p53, ATR, CHK1, ATM, and CHK2 in NB cell lines by Western blot (representative images Figure 3.4). Band intensity was normalised to total protein (ponceau S). Dashed line represents median expression of each protein. Data shown are mean of 2 independent experiments.*

MYCN, ATM and p53 protein expression was analysed by the corresponding genetic status (**Figure 3.6**). *MYCN* amplified cell lines had a significantly greater level of MYCN protein expression than non-amplified cell lines (**Figure 3.6A**). Interestingly, the SJNB1 cell line had high MYCN protein expression in the absence of amplification. Cell lines with *TP53* mutations show high levels of stabilised p53 protein (NMB and Kat100) or low levels of p53 protein expression (SKNAS, N20R1 and IGRN91) at baseline (**Figure 3.4 and 3.5**), and as expected, there was no significant difference in p53 protein expression between cell lines with or without a mutation in *TP53* (**Figure 3.6B**). There was no difference in ATM protein expression

between 11q deleted cell lines and those without 11q deletion (**Figure 3.6C**), MYCN amplified and non-amplified 11q deleted cell lines (**Figure 3.6D**), or with or without a mutation in *ATM* (**Figure 3.6E**). In addition, there was no difference in CHK1 protein expression between cell lines with and without 11q deletion (**Figure 3.6F**) and no correlation between ATM and CHK1 protein expression (**Figure 3.6G**).

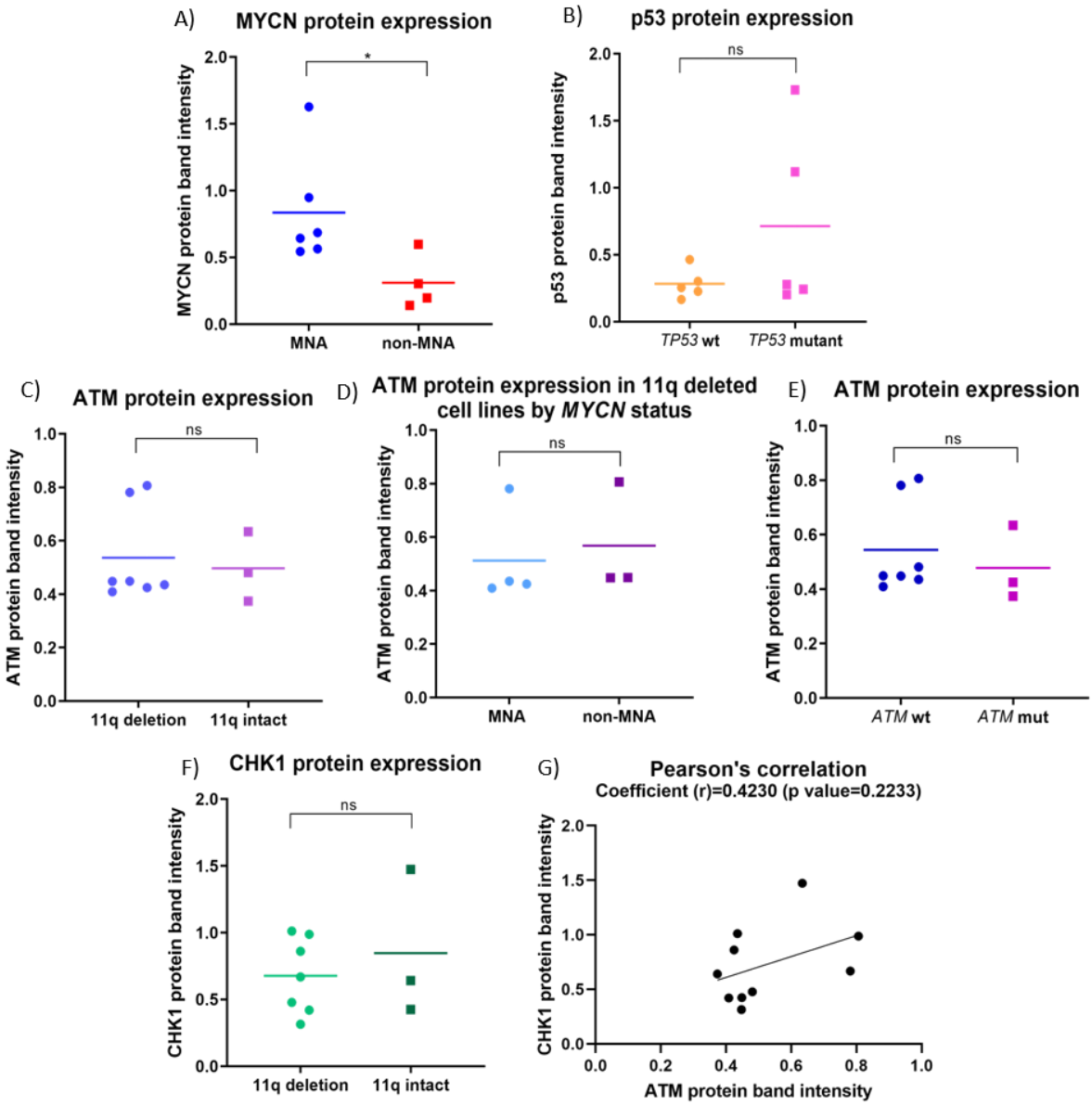

Figure 3.6: *Protein expression by genetic abnormality. A) Analysis of MYCN protein expression of cell lines by MYCN amplification status. B) Analysis of p53 protein expression of cell lines by TP53 mutation status. Analysis of ATM protein expression by chromosome 11q deletion status (C), MYCN amplification status in 11q deleted cell lines (D) and ATM mutation status (E). F) Analysis of CHK1 protein expression by chromosome 11q deletion status and G) Correlation of ATM and CHK1 protein expression. MNA: MYCN amplified. *p<0.05; wt: wild type; ns= not significant Mann Whitney U test.*

As MYCN expression drives proliferation, *MYCN* amplification status and protein expression was correlated with cell doubling time. There was no difference in cell doubling times between *MYCN* amplified and non-amplified cell lines and no correlation between doubling time and MYCN protein expression (**Figure 3.7**). Interestingly, the *MYCN* amplified cell lines with the slowest doubling times, IMR32 and NMB, also have a mutation in *ATM* and low ATM protein expression.

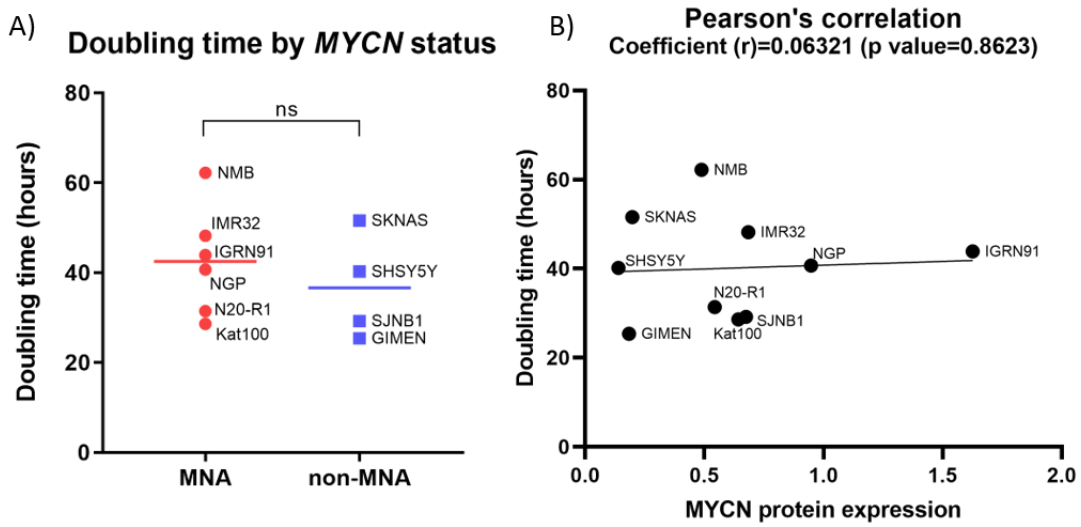

***Figure 3.7**: Relationship between MYCN and growth rate. A) Cell doubling time (Table 3.4) analysed by MYCN amplification status. No significant difference between groups (Mann Whitney U test, Graphpad Prism version 8). B) Correlation of MYCN protein expression in 10 cell lines with cell doubling time. Pearson's rank (r) was tested using Graphpad Prism version 8.*

Baseline expression of DDR proteins was correlated with MYCN protein expression (**Figure 3.8**). There was strong positive correlation between CHK1 and MYCN expression, and slight positive correlation between PARP1 and MYCN expression.

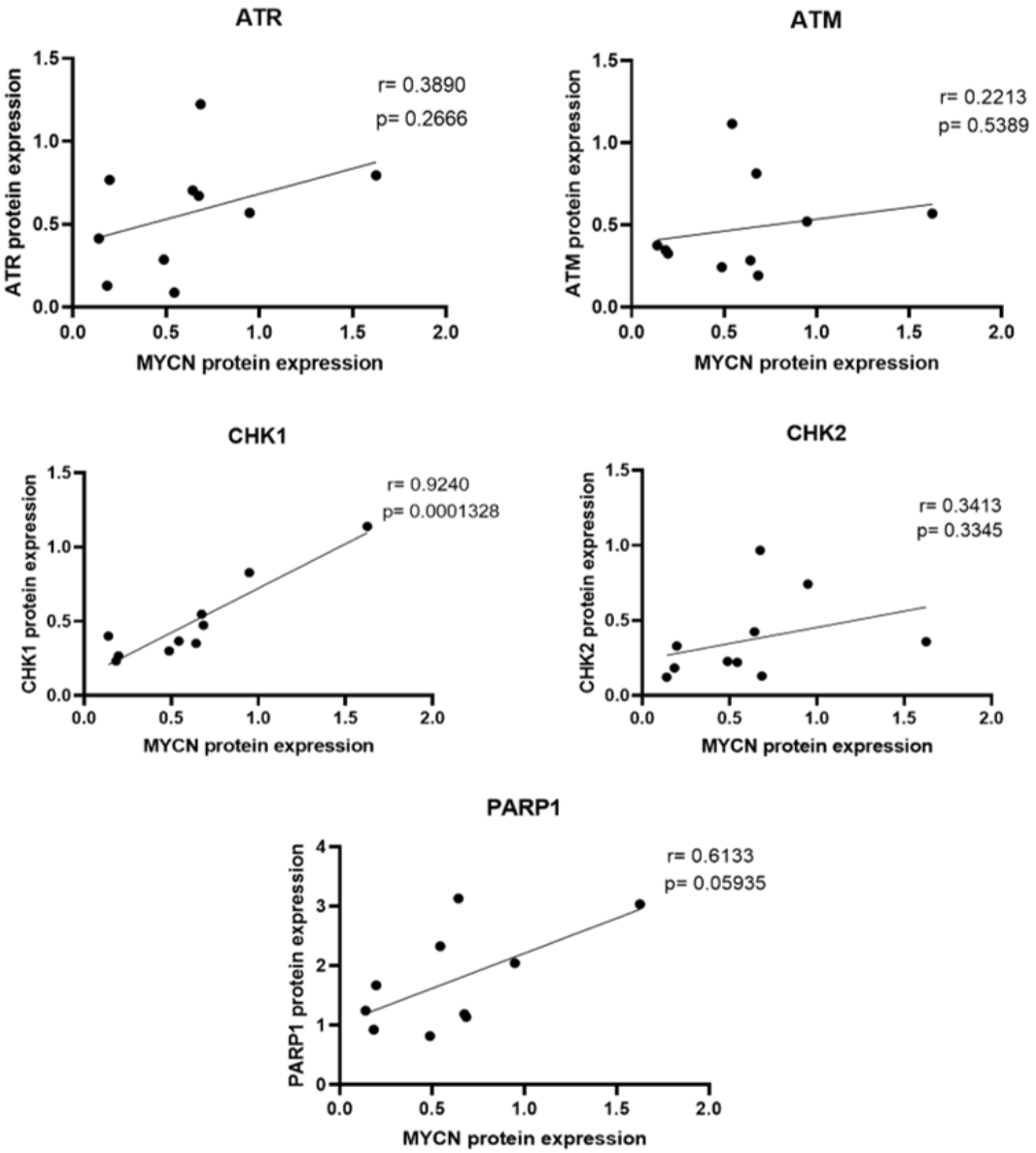

Figure 3.8: *Correlation of MYCN protein expression in 10 cell lines with expression of DDR proteins, quantified in Figure 3.5. Pearson's rank (r) was tested using Graphpad Prism version 8.*

3.4.4 Functional analysis of ATM, ATR and p53

To determine if the level of MYCN protein expression correlated with basal levels of RS, DNA damage and signalling of that damage through ATR and ATM, baseline RPA^{S8}, H2AX^{S139} (γH2AX), CHK1^{S345} and CHK2^{T68} phosphorylation was measured (**Figure 3.9**). None of these markers correlated with MYCN protein levels (**Figure 3.10**).

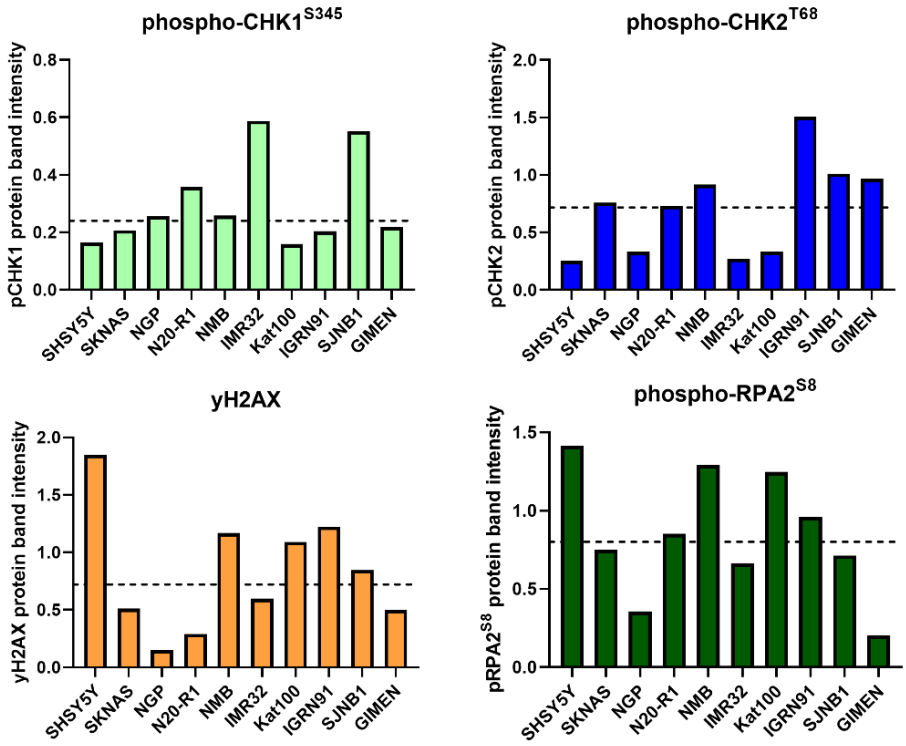

Figure 3.9: *Quantification of baseline expression of phospho-CHK1^{S345} and phospho-CHK2^{T68} (markers of ATR and ATM activity respectively), γH2AX and phospho-RPA2^{S8} (markers of RS), in NB cell lines by Western blot (representative image Figure 3.4). Band intensity was normalised to total protein (ponceau S). Dashed line represents median expression of each protein. Data shown are mean of 2 independent experiments.*

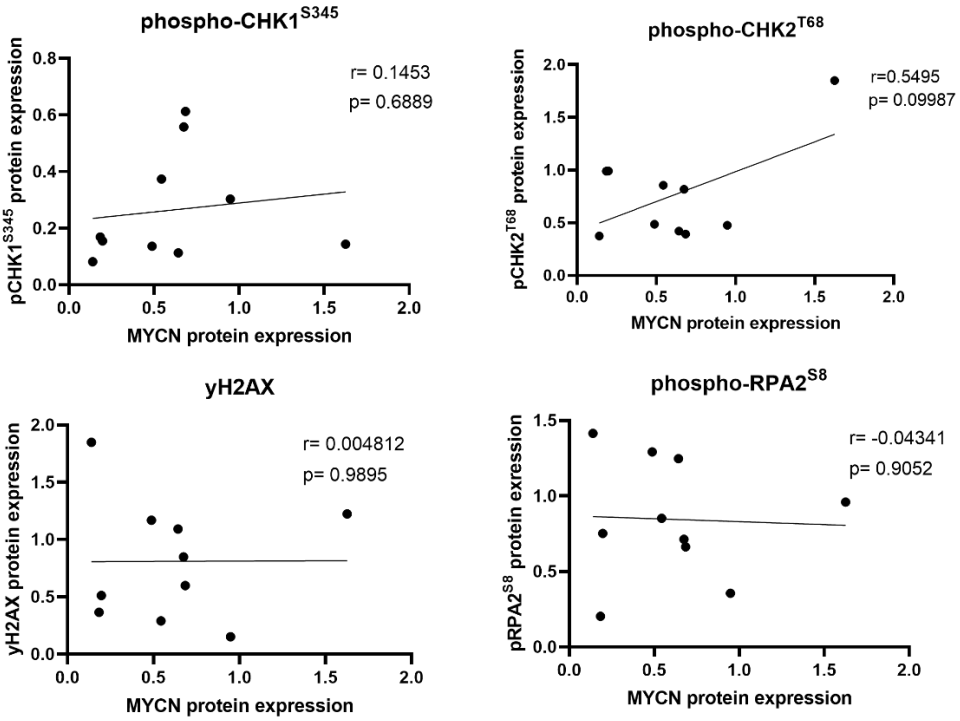

Figure 3.10*: Correlation of MYCN protein expression in 10 cell lines with expression of baseline phospho-CHK1^{S345} and phospho-CHK2^{T68} (markers of ATR and ATM activity respectively) and γH2AX and phospho-RPA2^{S8} (markers of RS) quantified in Figure 3.9. Pearson's rank (r) was tested using Graphpad Prism version 8.*

The function of ATM and p53 was tested in response to treatment with doxorubicin, a topoisomerase II poison which results in double strand breaks (**Figure 3.11A and B**). The function of ATR was tested in response to treatment with the PARP inhibitor olaparib to induce RS (**Figure 3.11 C**). No ATM autophosphorylation or CHK2^{T68} phosphorylation, markers of ATM activity, was observed in the SHSY5Y, IMR32, NMB or IGRN91 cell lines after treatment with doxorubicin (**Figure 3.11 A**), suggesting ATM is not functional in these cells. Induction of p21, a direct transcriptional target of p53 and therefore a marker of p53 activity, was not observed in the *TP53* mutant cell lines, except the IGRN91 cell line which expresses a high molecular weight gene product after activation with doxorubicin (consistent with duplication of exons 7–9), and retained some function (**Figure 3.10 B**). ATR activity was observed in the majority of *MYCN* amplified cell lines after treatment with 10 µM olaparib, but not in the non-amplified SHSY5Y, SKNAS and GIMEN cell lines (**Figure 3.11 C**).

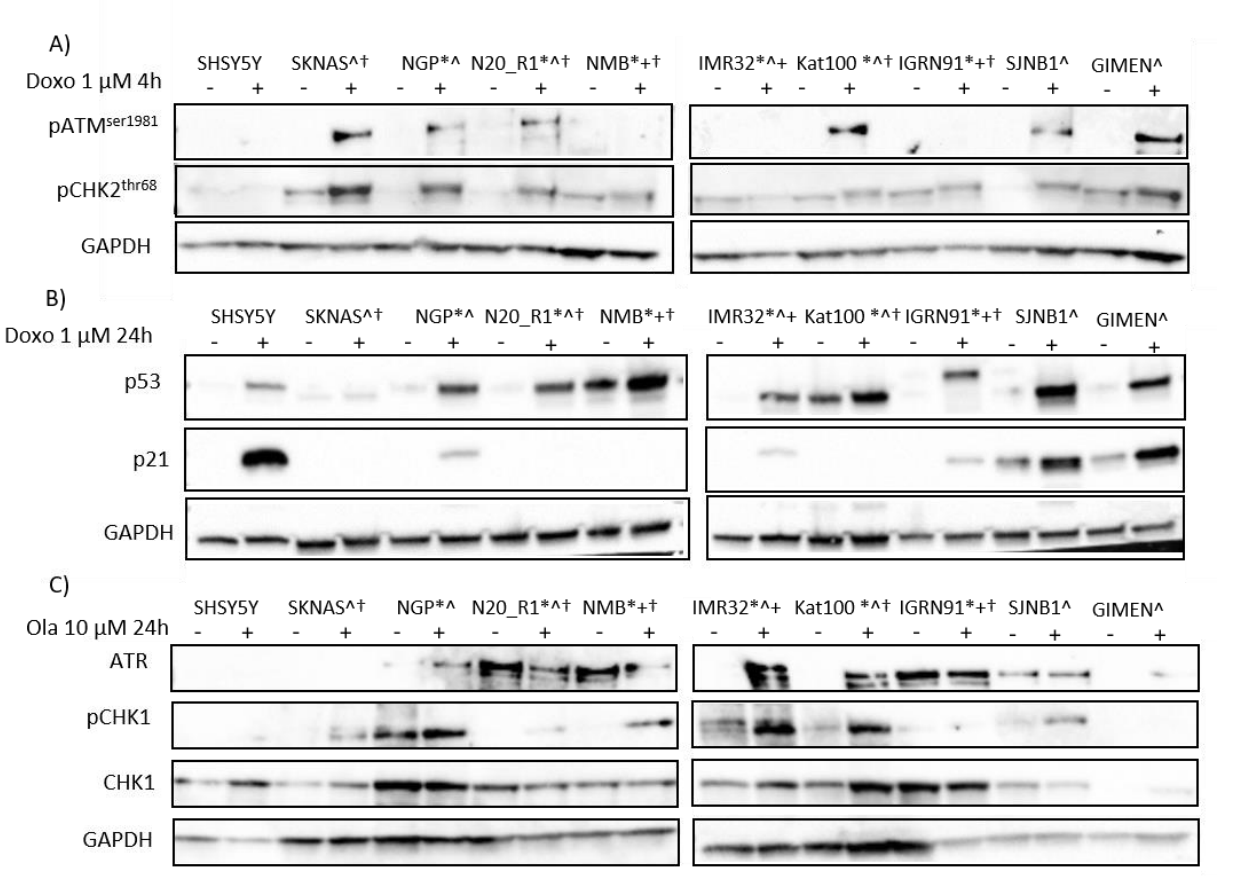

Figure 3.11: *A) ATM function was determined by phospho-ATM^{S1981} and phospho-CHK2^{T68} expression after treatment with 1 µM doxorubicin (doxo) for 4 hours. B) p53 function was determined by p53 and p21 expression after treatment with 1 µM doxo for 24 hours. C) ATR function was determined by phospho-CHK1^{S345} expression after treatment with 10 µM olaparib for 24 hours. Representative images of 2 independent experiments. *MYCN amplified, ^11q deleted, +ATM mutant, †TP53 mutant.*

3.5 Discussion

In this chapter, the defects in the DDR in a panel of NB cell lines were evaluated by next generation sequencing, chromosome copy number analysis and protein expression and function.

3.5.1 *MYCN* amplification is associated with high MYCN protein expression and increased replication stress

MYCN amplification was confirmed in 6 out of the 10 cell lines used in this panel by copy number analysis of SNP array data. *MYCN* amplification was associated with increased MYCN protein expression. *MYCN* amplified cell lines also showed increased PARP1 and CHK1 protein expression compared to non-amplified cell lines, which may be sufficient to counteract RS, thereby limiting the expected increase in RS due to overexpression of MYCN. Correlation between PARP1 mRNA and protein expression and MYCN amplification has been reported previously (Colicchia *et al.*, 2017). MYCN overexpressing cells have been reported to have defective G1 checkpoint arrest (Bell *et al.*, 2006; Ryl *et al.*, 2017), increasing reliance on S and G2 phase checkpoints, which can be activated by CHK1 signalling (Smits and Gillespie, 2015). Previous studies have shown that MYCN transcriptionally upregulates many genes which likely allow the cells to tolerate RS, including *CHK1* (Cole *et al.*, 2011; Gu *et al.*, 2015), and proteins involved in DSB repair, such as components of the MRN complex (Petroni *et al.*, 2016; Petroni *et al.*, 2018), alternative NHEJ (alt-NHEJ) (Newman *et al.*, 2017), and Bloom syndrome (BLM) helicase (Chayka *et al.*, 2015).

3.5.2 11q deletion alone does not predict low ATM expression or loss of ATM function

Partial loss of chromosome 11q, including the *ATM* gene, was observed in 7 of the 10 cell lines in this panel by SNP array. However, loss of *ATM* through 11q deletion was not associated with low ATM protein expression (**Figure 3.6**) or ATM dysfunction in these cell lines (**Figure 3.11A**). Mutation in *ATM* was confirmed in three cell lines, IMR32, NMB and IGRN91. The IMR32 and NMB cell lines had low baseline ATM expression and all 3 *ATM* mutant cell lines showed no ATM activation in response to doxorubicin, suggesting that *ATM* mutation may be a better predictor of ATM deficiency than 11q deletion. ATM functions as a homodimer, therefore mutation in one allele of ATM is likely to be sufficient to reduce ATM function, due

to expression of dominant negative isoforms of ATM protein (Paige, 2003). In contrast to cell lines, ATM mutation is rare in NB tumours. Rare SNVs of unknown significance have been identified in around 7% tumour samples but were mutually exclusive with 11q deletion (Takagi *et al*. 2017). In *MYCN* amplified NB, ATM is downregulated by upregulation of micro-RNA 421 (miR-421) (Hu *et al.*, 2010). Analysis of ATM protein expression in tumour biopsies may identify patients with ATM deficient tumours.

3.5.3 *TP53* mutation is not associated with low p53 expression or loss of p53 function

In the panel studied here, 5/10 cell lines have a mutation in *TP53*. Expression level and function of p53 protein was also examined, as many mutations in *TP53* lead to stabilisation of the mutant protein (Freed-Pastor and Prives, 2012). No association between *TP53* mutation and p53 protein expression was observed in these cell lines, which is expected as some mutations, such as those in the DNA binding domain (Kat100 and NMB cell lines), result in protein stabilisation due to loss of auto-regulatory degradation pathways. *TP53* mutant cell lines failed to show p53 activity in response to doxorubicin, except for IGRN91, which expresses a high molecular weight gene product and retains some function.

TP53 mutations are rare in NB at diagnosis but have been reported in around 15% of relapsed NB tumours (Carr-Wilkinson *et al.*, 2010; Padovan-Merhar *et al.*, 2016), which is thought to contribute to treatment resistance (Keshelava *et al.*, 2000; Tweddle *et al.*, 2001; Xue *et al.*, 2007). However, WES analysis of two pairs of cell lines generated by selecting for drug resistance revealed the acquisition of many new mutations, including *TP53*. Relapsed NB also show numerous genetic changes (Schramm *et al.*, 2015) and it is likely that some of these additional mutations also contribute to treatment resistance.

3.5.4 Other mutations affecting the DDR

Other mutations affecting the DDR in these cell lines were identified by targeted sequencing. Firstly, an activating *KRAS* mutation was identified in the SHSY5Y cell line, in addition to an *ALK* mutation, which has been previously reported (George *et al.*, 2008). These mutations are thought to lead to constitutive MAPK signalling, contributing to increased RS (Prior *et al.*, 2012; Bresler *et al.*, 2014). The *ALK* locus is co-amplified with *MYCN* in the IMR32 and KAT100

cell line pair. *ALK* amplification correlates with ALK overexpression and activity (Osajima-Hakomori *et al.*, 2005). Somatic *ALK* aberration is the most frequent gene alteration in NB, with 7-8% of tumours having an *ALK* mutation and 2-3% amplification (Trigg and Turner, 2018). Targeting *ALK* aberrant NB with ALK inhibitors is promising but, as mechanisms of acquired resistance to these treatments are emerging, targeting RS may provide alternative treatment strategies.

In addition to a *BRCA1* mutation listed on the COSMIC database, a heterozygous mutation in *BRCA2* was identified in the GIMEN cell line. Loss of function in BRCA1/2 proteins leads to HRR deficiency and sensitivity to PARP inhibition (Bryant *et al.*, 2005). However, *BRCA* mutations are very rare in NB and although germline mutations in *BRCA1/2* have been identified in patients with NB, they are not associated with increased risk of NB development (Brooks *et al.*, 2006; Walsh *et al.*, 2017).

Mutations in epigenetic modifiers affect DNA repair efficiency, leading to genomic instability (Karakaidos *et al.*, 2020), and are frequently observed in NB (Durinck and Speleman, 2018). In this study, deleterious mutation of the *CREBBP* gene was identified in the IMR32 and KAT100 cell line pair. *CREBBP* encodes a transcriptional co-activator which is involved in regulation of genes involved in the DDR, such as PARP1 and H2AX (Dutto *et al.*, 2018). In addition, mutations in *KMT2C* were discovered in the SHSY5Y and NMB cell lines. *KMT2C* codes for a lysine methyltransferase and is involved in regulation of DDR genes such as *BRCA1* and *RAD51,* and loss of *KMT2C* has been associated with increased sensitivity to PARP inhibition (Rampias *et al.*, 2019).

3.6 Conclusion

In this chapter, the expression and function of key DDR proteins were characterised and compared with genetic status in a panel of 10 NB cell lines. MYCN protein expression was shown to be higher in *MYCN* amplified cell lines but hemizygous *ATM* loss through 11q deletion was not associated with low ATM protein expression or ATM dysfunction unless an inactivating *ATM* mutation was also present. *MYCN* amplified cell lines also expressed higher levels of CHK1 and PARP1 protein. The DDR defects identified here will be used in the following chapters to identify markers of ATR and PARP inhibitor sensitivity.

Chapter 4: Determinants of ATR inhibitor sensitivity in high risk NB cell lines

4.1 Introduction

As described in Chapter 3, the panel of NB cell lines displayed a range of genetic abnormalities, expression and function in key DDR components. With inhibitors of ATR kinase progressing rapidly through adult clinical trials, robust predictive biomarkers are required to identify which patients will benefit from ATR inhibitors in the paediatric setting. The work described in this chapter aimed to explore if the DDR defects identified in the previous chapter predict sensitivity to ATR inhibition, using the tool compound VE-821 (Merck) and the clinical candidate AZD6738 (Astra Zeneca) for validation.

Proposed biomarkers of sensitivity to single agent ATR inhibition in other cancers include overexpression of oncogenes leading to RS, such as *MYC* and *CCNE1* (cyclin E), and loss of function or reduced expression of tumour suppressors which result in dysfunctional G1 cell cycle arrest, such as ATM and p53 (reviewed in: (Bradbury *et al.*, 2020)).

Amplification of the *MYCN* oncogene is observed in around 50% of HR-NB tumours and is associated with increased MYCN protein expression (Chapter 3 and (Santiago *et al.*, 2019)). Expression of MYCN has been shown to directly decrease replication fork progression and increase fork stalling, a clear indicator of RS (King *et al.*, 2020). *MYCN* amplified cell lines also showed increased ATR activity and CHK1 expression compared to non-amplified cell lines, both of which are required to overcome RS. MYCN transcriptionally upregulates many genes likely allow tolerance of RS, including *CHK1* (Cole *et al.*, 2011; Gu *et al.*, 2015) and proteins involved in DSB repair, such as components of the MRE11-RAD50-NBLS1 (MRN) complex (Petroni *et al.*, 2016; Petroni *et al.*, 2018), alternative NHEJ (alt-NHEJ) (Newman *et al.*, 2017), and Bloom syndrome (BLM) helicase (Chayka *et al.*, 2015).

MYCN overexpressing cells are reported to have defective G1 checkpoint arrest (Bell *et al.*, 2006). Impaired G1 checkpoint control in NB can also occur through deficiencies in ATM or p53 signalling (Kastan *et al.*, 1992; Hyun and Jang, 2015), which leads to increased RS and reliance on the S and G2 checkpoints (Russell *et al.*, 1995; Deckbar *et al.*, 2007; Stolz and Bastians, 2013).

Partial loss of chromosome 11q, including the *ATM* gene, occurs in around 30% of NB tumours. However, data presented in the previous chapter showed that loss of *ATM* through 11q deletion does not correlate with low ATM protein expression or ATM dysfunction in the panel of cell lines tested. Therefore, baseline ATM protein expression may be a better predictor of ATR inhibitor sensitivity.

Defects in the p53 tumour suppressor signalling pathway result in G1 checkpoint dysfunction and escape from proapoptotic signalling (Massague, 2004). Mutation of *TP53*, the gene encoding p53, is rare at diagnosis but is observed in up to 15% of relapsed NB tumours (Carr-Wilkinson *et al.*, 2010). In chapter 3, in addition to *TP53* mutation status, the expression level and function of p53 protein was characterised in the cell line panel, as many mutations in *TP53* often lead to stabilisation of the mutant protein (Freed-Pastor and Prives, 2012).

The current proposed markers of ATR inhibitor sensitivity focus on loss of DNA damage checkpoint control and oncogenic stress. As ATR is activated in response to RS, high levels of endogenous DNA damage or RS may lead to increased sensitivity to ATR inhibition. Baseline expression and activity of ATR, as well as other markers of RS including CHK1, phospho-RPA2^{S8} and γH2AX were examined in chapter 3. In this chapter, expression of these proteins was correlated with sensitivity to ATR inhibition to identify additional predictive biomarkers of response to ATR inhibitors.

4.2 Chapter aims

The aims of this chapter are as follows:

1. To investigate the role of MYCN in sensitivity to ATR inhibition using two MYCN expression regulatable NB cell lines and a panel of NB cell lines with varying genetic abnormalities
2. To determine whether ATM or p53 status confer sensitivity to the ATR inhibitor VE-821 in a panel of NB cell lines
3. To investigate whether markers of RS determine sensitivity to VE-821

4.3 Methods

4.3.1 Cells and cell culture

The 10 cell lines included in the NB cell line panel have been characterised in detail in chapter 3 and were cultured and maintained as described in section 2.1 The MYCN expression regulatable cell lines SHEPtet21N and IMR5/75 shMYCN were maintained as described for the other cell lines but incubated with 1 µg/ml doxycycline for 72 hours for MYCN off states prior to experiments.

4.3.2. Reagents

VE-821, AZD6738 and doxycycline were used and stored as described in section 2.2.

4.3.3 Cytotoxicity assays

XTT cell proliferation (Roche) and clonogenic survival assays were carried out as described in sections 2.3.

4.3.4 Protein expression analysis

Baseline cell lysates were collected as described in section 2.5.1. Proteins were separated using gel electrophoresis using a 4-20% Tris-acetate or 4-20% Tris-glycine polyacrylamide gel (Bio-Rad, Hemel Hempstead, UK), transferred onto nitrocellulose and detected using western blotting as described in section 2.5.2. ATR, ATM, CHK1, pCHK1^{S345}, CHK2, pCHK2^{T68}, MYCN, p53, p21, pRPA2^{S8} and γH2AX were detected using primary antibodies described in **Table 2.5** and the appropriate HRP-conjugated secondary antibodies. Protein expression was measured by chemiluminescence from exposure to ECL detection reagent using a ChemiDoc imaging system and bands were quantified using ImageJ software as described in section 2.5.2.

4.4. Results

4.4.1 Role of MYCN in predicting sensitivity to ATR inhibitors

To examine if *MYCN* amplification or overexpression would predict sensitivity to ATR inhibition, the effect of two ATR inhibitors, VE-821 (Merck) and AZD6738 (Astra Zeneca), was investigated in two MYCN expression regulatable cell line models, and a panel of cell lines with varied genetic characteristics.

4.4.1.1 Characterisation of MYCN regulatable cell lines

Two MYCN expression regulatable cell lines were obtained, SHEPtet21N (Lutz *et al.*, 1996) and IMR5/75 shMYCN (Dreidax *et al.*, 2014), which utilise the tetracycline inducible expression system to modulate *MYCN* expression. The addition of doxycycline, a derivative of tetracycline, results in reduced MYCN expression in both these systems.

SHEPTet21N cells are a sub-clone of the non-*MYCN* amplified SHEP cell line containing a stably transfected tetracycline dependent *MYCN* expression construct. In the absence of tetracycline (or its derivative doxycycline) MYCN is highly expressed. With the addition of doxycycline (dox), MYCN expression is completely repressed within 48 hours (**Figure 4.1A**) and remains repressed for at least 120 hours (**Figure 4.1B**).

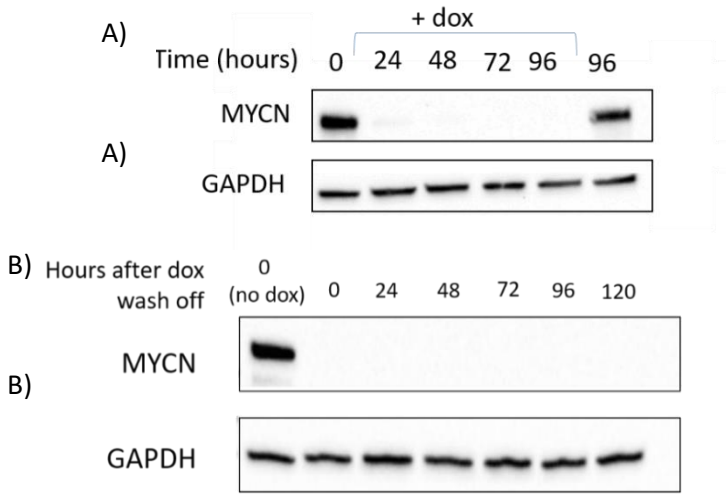

Figure 4.1: MYCN protein expression in the SHEPtet21N cell line A) in response to doxycycline (dox) 1 µg/ml over 96 hours and B) after dox wash off, cells were pretreated with dox for 72 hours.

In contrast, the IMR5/75 shMYCN cell line is a *MYCN* amplified cell line containing a stably transfected construct consisting of a tetracycline inducible *MYCN* targeting small hairpin RNA. The addition of dox activates expression of the shRNA, resulting in around a 40% knockdown of MYCN expression after 72 hours (**Figure 4.2**). For further experiments, this cell line was treated with doxycycline every 72 hours as expression of MYCN recovers if left untreated (**Figure 4.2B**).

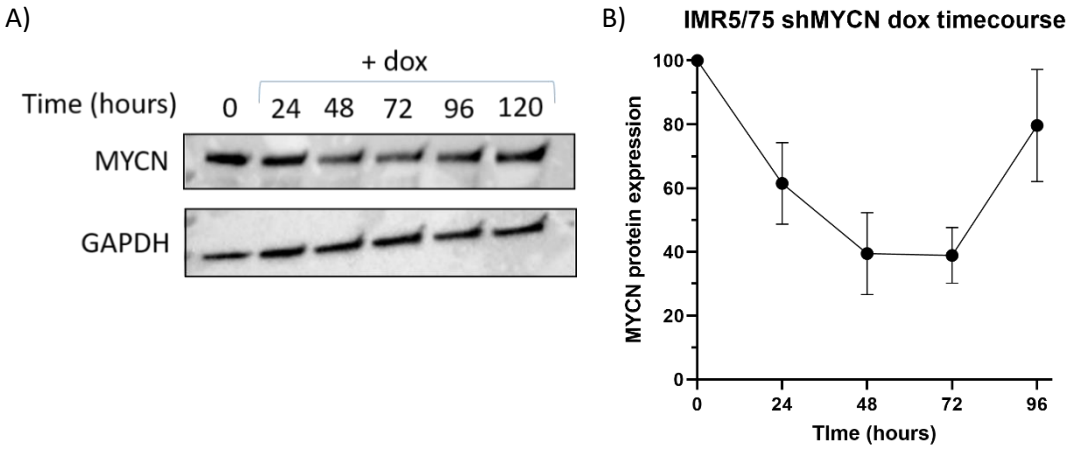

Figure 4.2: MYCN expression in the IMR5/75 shMYCN in reponse to doxycycline (dox). A) representative Western blot image of MYCN expression in response to 120 hours treatment with dox 1 µg/ml over 120 hours (5 days) B) Quantification of MYCN protein expression at 24 hour timepoints over 96 hours of dox treatment. Data are mean ± SEM for 3 independent experiments.

To assess the impact of MYCN expression on the DDR, the expression of key DDR proteins in the SHEPtet21N and IMR5/75 shMYCN cell lines was measured in both MYCN high (no dox) and MYCN low (with dox) states (**Figure 4.3**).

Decreased MYCN expression resulted in decreased expression of ATM, ATR, CHK1 and CHK2 kinases in both cell lines. There was also a decrease in ATR and ATM activity ($CHK1^{S345}$ and $CHK2^{T68}$ phosphorylation respectively) in the MYCN low expression state compared to MYCN high expression in both cell lines. In contrast, there was increased expression of p53 and its target, the CDK inhibitor p21 in the IMR5/75 shMYCN cell line, indicating an increase in G1 and S phase cell cycle checkpoint activation.

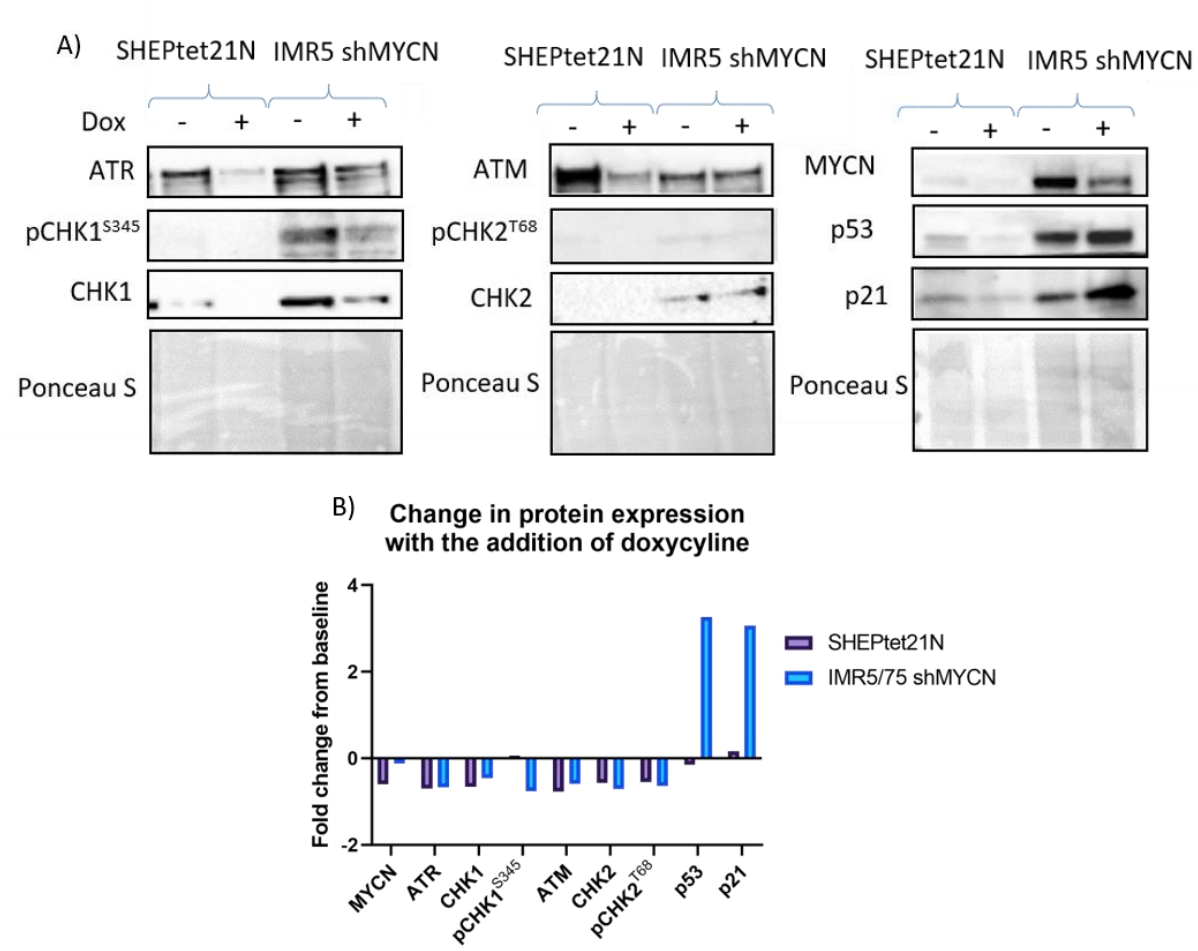

Figure 4.3: *A) Western blot analysis of baseline expression of key DDR proteins in high (no dox) and low (with dox) MYCN states in the SHEPtet21N and the IMR5/75 shMYCN MYCN regulatable cell lines. B) Fold change in expression of DDR proteins from baseline (MYCN on) state after the incubation with 1 µg/ml doxycycline for 72 hours. Data is mean of 2 independent replicates and protein expression was normalised to total protein loaded (Ponceau S).*

The data with these two cell lines confirm that overexpression of MYCN leads to increased expression of ATR and CHK1, and ATM and CHK2, which are required for tolerance of RS and DNA repair.

The doubling time, cloning efficiency, and optimal seeding density for XTT cell proliferation assay for these two MYCN protein regulatable cell lines are reported in **Table 4.1**. Cell doubling time was increased when MYCN was reduced in both cell lines. The IMR5/75 shMYCN cell line did not form colonies so were unable to be used for clonogenic survival assay.

Table 4.1: The doubling time, cloning efficiency, and optimal seeding density for XTT cell proliferation assay of the MYCN expression regulatable cell lines in MYCN on and MYCN off (+ dox) states.

Cell line	Doubling time (hours)	Cloning potential (%)	Seeding density (XTT)
SHEPtet21N (+dox)	34.7 (41.5)	94 (71.9)	2000
IMR5/75 shMYCN (+dox)	43.2 (174.1)	-	4000

4.4.1.2 MYCN overexpressing cells are more sensitive to ATR inhibition

To investigate whether expression of MYCN affects the cytotoxicity of ATR inhibition, the effect of the ATR inhibitors VE-821 and AZD6738 on cell proliferation was first tested in the SHEPtet21N and the IMR5/75 shMYCN cell lines, in both MYCN states, by XTT assay (**Figure 4.4**).

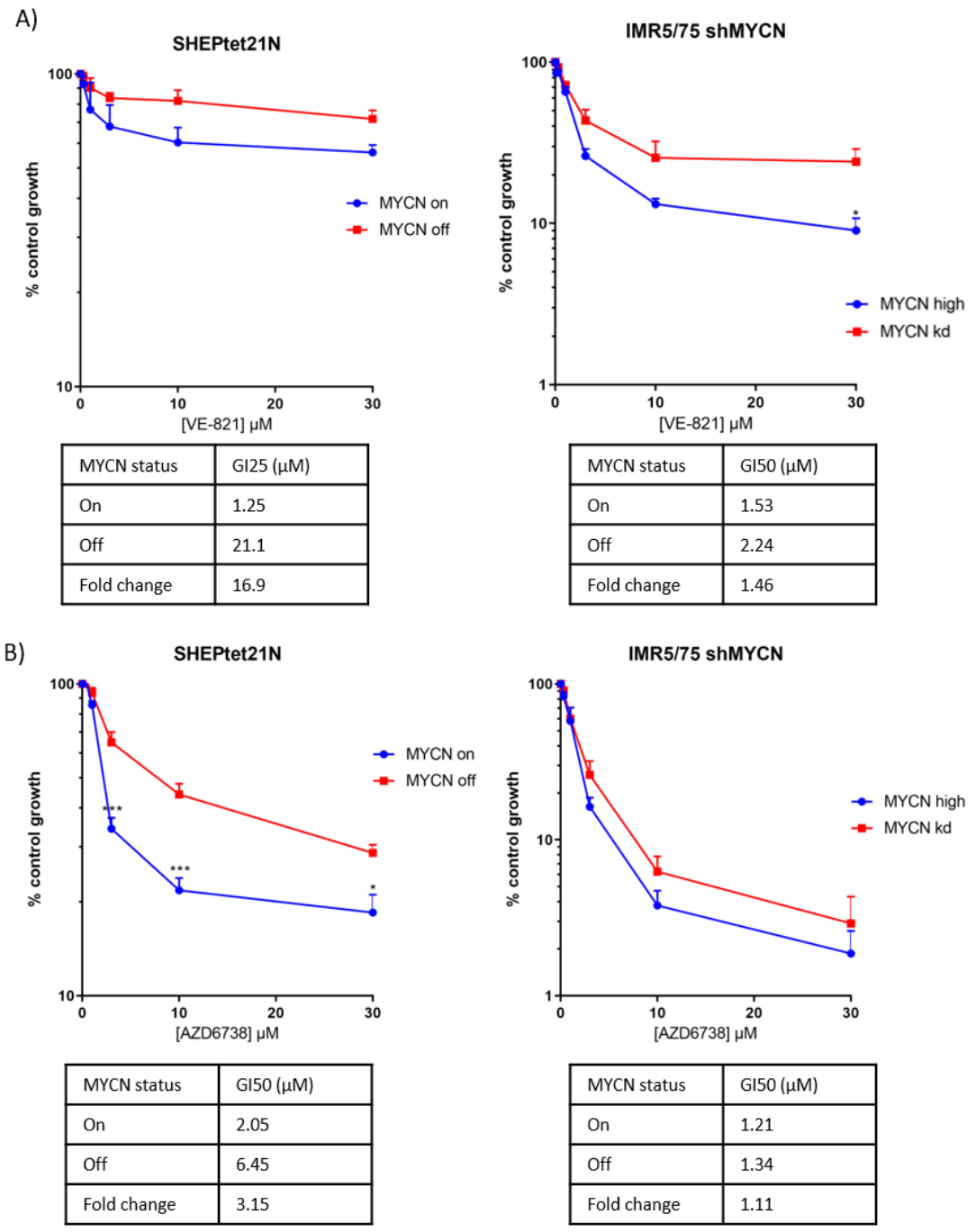

MYCN status	GI25 (µM)
On	1.25
Off	21.1
Fold change	16.9

MYCN status	GI50 (µM)
On	1.53
Off	2.24
Fold change	1.46

MYCN status	GI50 (µM)
On	2.05
Off	6.45
Fold change	3.15

MYCN status	GI50 (µM)
On	1.21
Off	1.34
Fold change	1.11

Figure 4.4: *Effect of ATR inhibition in MYCN regulatable cell lines. Percentage control growth of SHEPtet21N and IMR5/75 shMYCN cell lines in response increasing concentrations of A) VE-821 and B) AZD6738 in MYCN high and low expression conditions (blue and red lines respectively). Data are mean + SEM of 3 independent replicates. *p<0.05, **p<0.01, ***p<0.001 t-test. GI25/50: concentration required to inhibit growth by 25 or 50% respectively. Kd= knockdown*

Both VE-821 and AZD6738 had a greater growth inhibitory effect in MYCN high expressing cells than cells with low MYCN expression, which was most significant at concentrations > 1 µM.

To confirm that MYCN overexpression renders cells sensitive to ATR inhibition, the effect of increasing concentrations of VE-821 was tested on survival of SHEPtet21N cells, in both MYCN states, by clonogenic survival assay. In contrast to the XTT assay, which measures cell viability by metabolic activity, this method measures the ability of single cells to proliferate into colonies. Cytotoxicity of VE-821 was greater in cells expressing high levels of MYCN compared with those with low MYCN expression (**Figure 4.5**).

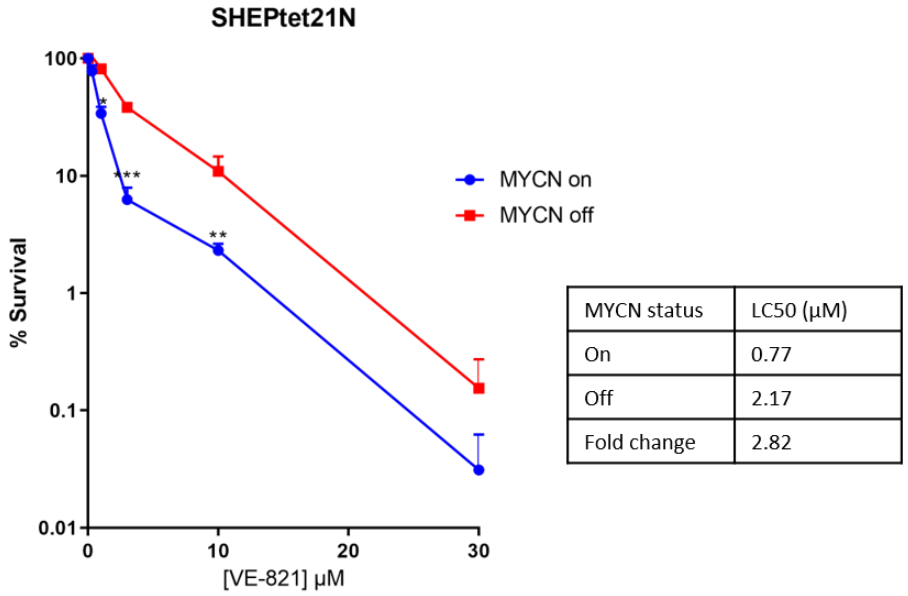

MYCN status	LC50 (µM)
On	0.77
Off	2.17
Fold change	2.82

***Figure 4.5**: Clonogenic survival of the SHEPtet21N cell line in response to increasing concentrations of VE-821 in MYCN high and low conditions (blue and red lines respectively). Data are mean + SEM of 3 independent replicates. *p<0.05, **p<0.01, ***p<0.001 t-test. LC50: concentration required to reduce survival by 50%.*

To test if MYCN expression determines sensitivity to ATR inhibition in the context of additional genetic alterations, sensitivity to VE-821 was tested by XTT cell proliferation assay in the panel of 10 NB cell lines with varying genetic abnormalities (characterised in chapter 3). The growth inhibitory effect of VE-821 in these cell lines varied, with the IMR32 (*MYCN* amplified) cell line showing the greatest growth inhibition and the GIMEN (non-*MYCN* amplified) cell line showing the least in response to 10 µM VE-821 (**Figure 4.6 A and B**). 10 µM VE-821 resulted in significantly greater growth inhibition in *MYCN* amplified cell lines, or cell lines with high MYCN protein expression (above median expression, **Figure 3.5**), than in non-*MYCN* amplified or low expressing cell lines (**Figure 4.6 C and D**). This was confirmed by clonogenic assay (**Figure 4.7**) and shown not to be associated with cloning potential (**Figure 4.7C**).

A summary of percentage control growth and survival in response to 10 µM VE-821 is shown in **Table 4.2.**

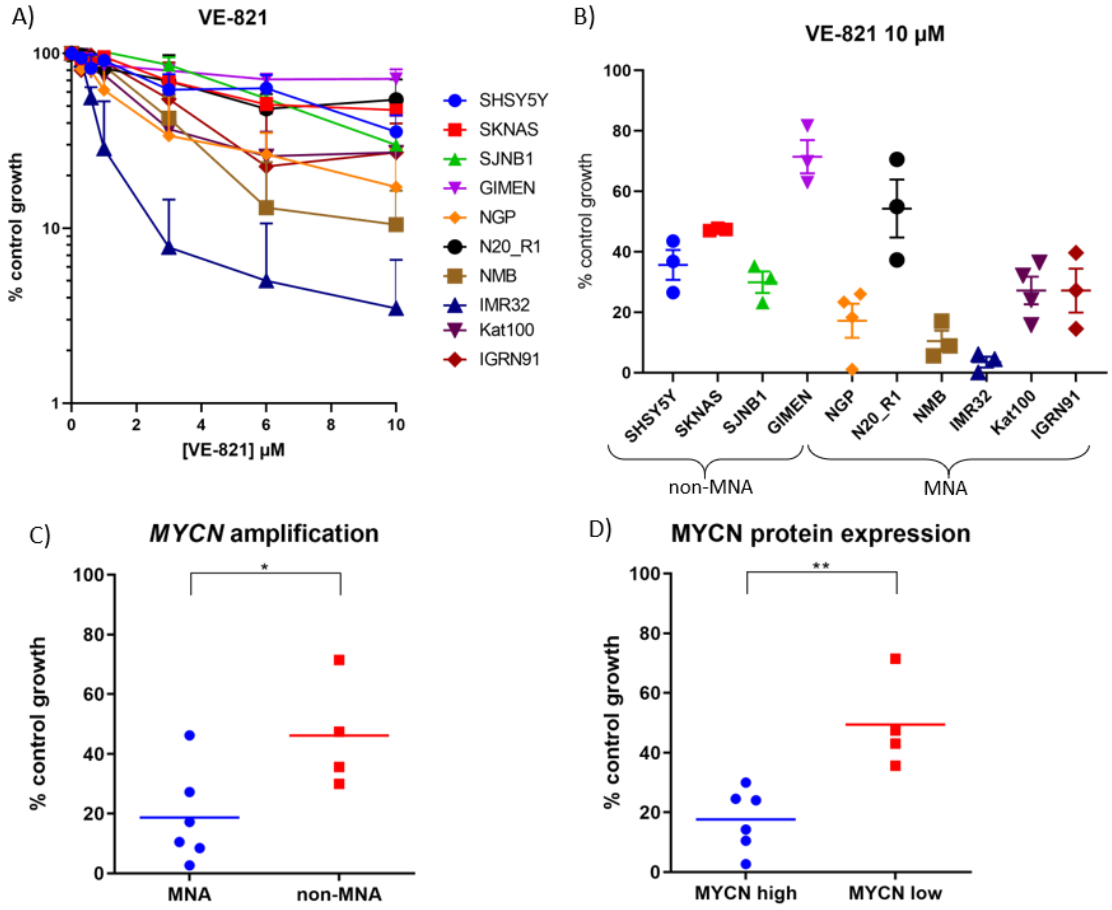

Figure 4.6: *A) Effect of increasing concentrations of VE-821 (ATR inhibitor) by XTT cell proliferation assay in NB cell lines, data are mean + SEM from at least 3 independent experiments. B) Sensitivity to 10 µM VE-821 plotted for each cell line. Bars represent mean +/- SEM from at least 3 independent experiments. Cell lines were split into 2 groups based on MYCN amplification status (C) and MYCN protein expression above (high) or below (low) median expression (D). Average percentage control growth at 10 µM VE-821 (from B) was plotted for cell lines belonging to each group (n=3). *p<0.05, **p<0.01 Mann Whitney U test. MNA: MYCN amplified, non-MNA: non-MYCN amplified.*

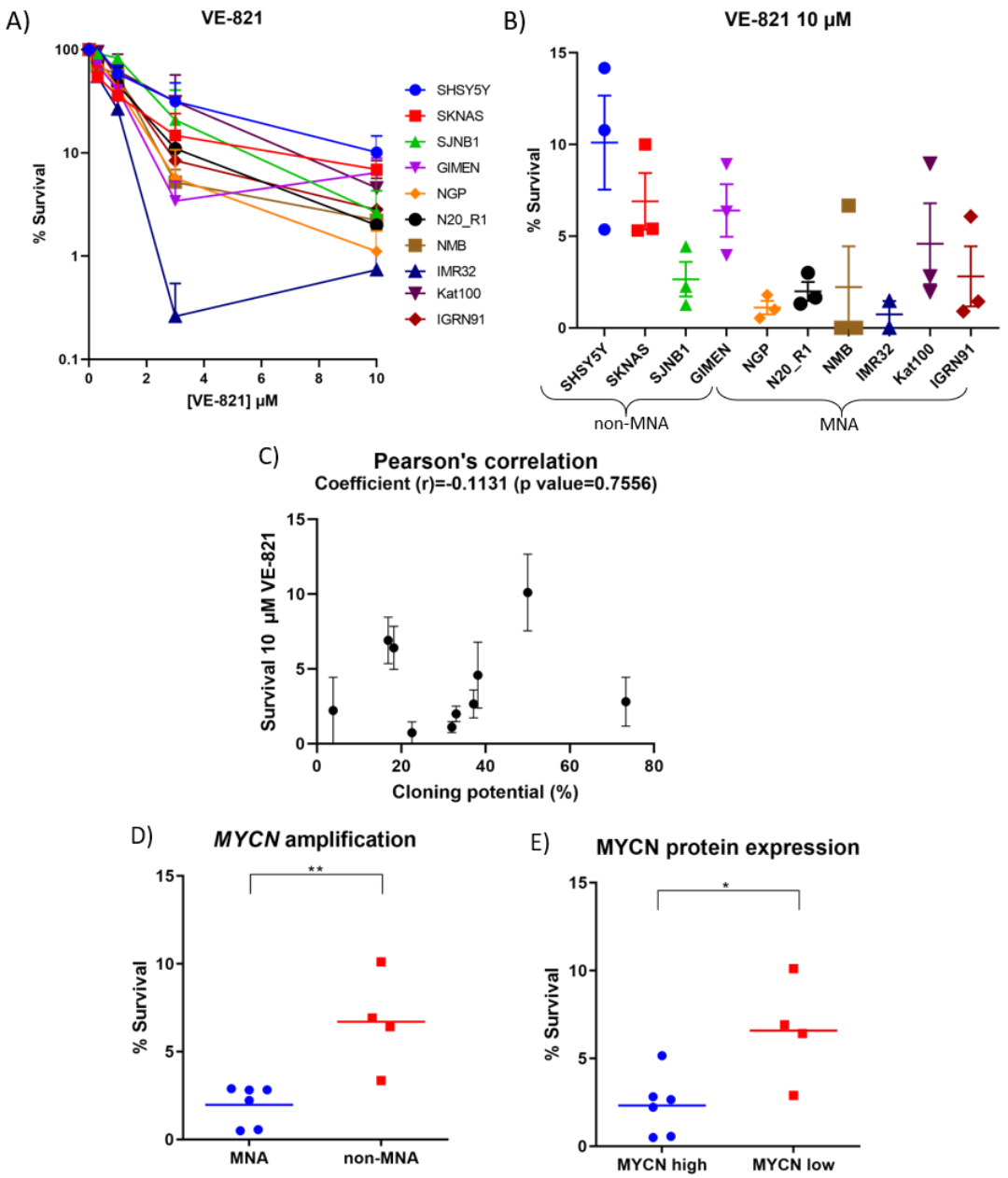

Figure 4.7: *A) Effect of increasing concentrations of VE-821 (ATR inhibitor) by clonogenic survival assay in NB cell lines, data are mean + SEM of 3 independent experiments. B) Sensitivity to 10 µM VE-821 plotted for each cell line. Bars represent mean +/- SEM from at least 3 independent experiments. C) % survival to 10 µM VE-821 correlated with cloning potential. Cell lines were split into 2 groups based on MYCN amplification status (D) and MYCN protein expression above (high) or below (low) median expression (E). Average survival at 10 µM VE-821 (from B) was plotted for cell lines belonging to each group (n=3). *p<0.05, **p<0.01 Mann Whitney U test. MNA: MYCN amplified, non-MNA: non-MYCN amplified.*

Table 4.2: Summary of percentage control growth and survival following treatment with 10 µM VE-821 for 72 hours

Cell line	Percentage of control growth 10 µM VE-821	Percentage survival 10 µM VE-821
SHSY5Y	35.62	10.10
SKNAS	47.39	6.91
SJNB1	17.19	2.66
GIMEN	54.31	6.41
NGP	10.49	1.11
N20_R1	3.48	1.99
NMB	27.17	2.22
IMR32	27.17	0.74
KAT100	29.93	4.59
IGRN91	71.45	2.81

Inhibition of ATR by VE-821 was confirmed by Western blot analysis of CHK1^{S345} phosphorylation in response to 10 µM olaparib, to induce RS, and increasing concentrations of VE-821 in 3 cell lines, NGP, SHSY5Y and SKNAS (**Figure 4.8**). Activity of ATR was reduced after treatment with 1 µM VE-821 in all cell lines.

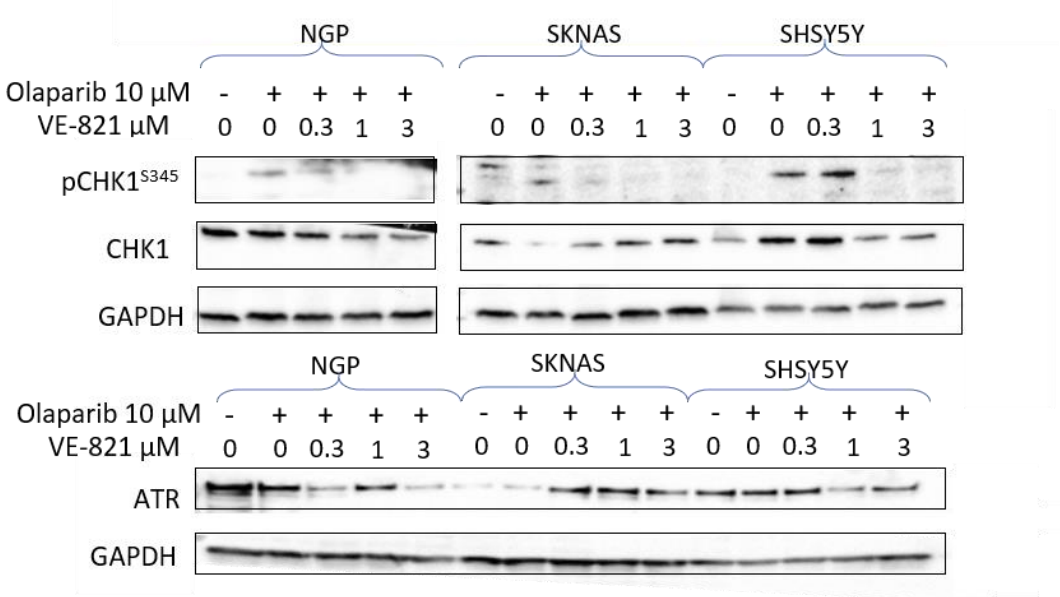

Figure 4.8: *ATR inhibition by VE-821. Western blot analysis of phospho-CHK1^{S345}, CHK1 and ATR in the NGP, SKNAS and SHSY5Y cell lines after treatment with 10 µM olaparib with and without 0.3, 1 or 3 µM VE-821 for 24 hours. GAPDH was used as a control for protein loading.*

The differential cytotoxicity of ATR inhibition was confirmed in 4 cell lines, SHSY5Y and SKNAS (non- *MYCN* amplified), and NGP and N20_R1 (*MYCN* amplified), by testing the effect of increasing concentrations of AZD6738 by XTT cell proliferation assay (**Figure 4.9A**). Growth inhibition caused by 10 µM AZD6738 and 10 µM VE-821 (% control growth) are strongly positively correlated in these 4 cell lines and the MYCN expression regulatable cell lines, SHEPtet21N and IMR5/75 shMYCN (**Figure 4.9B**), suggesting the cytotoxic effect is from ATR inhibition and not the result of off-target effects.

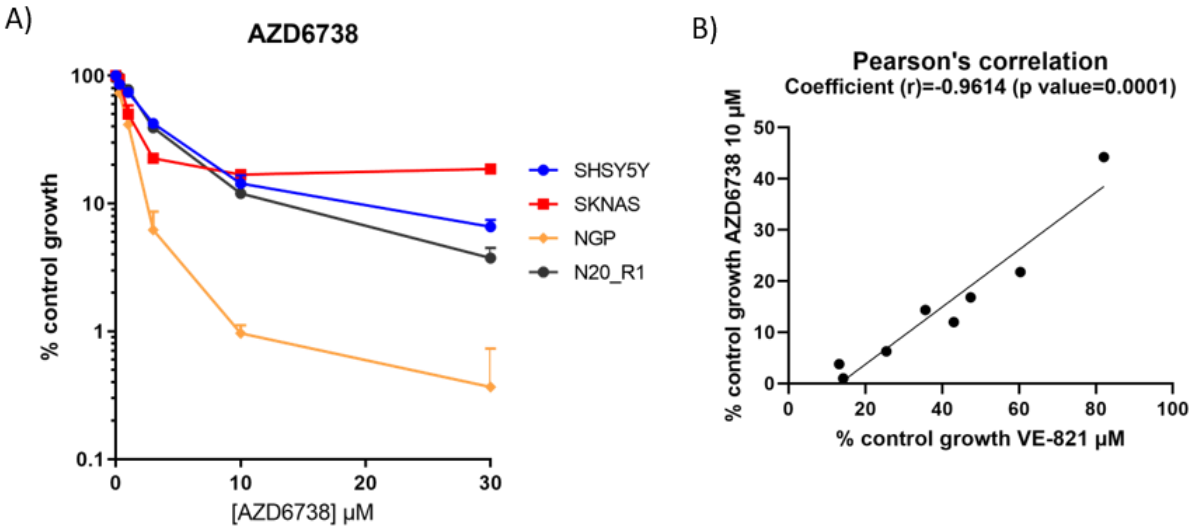

***Figure 4.9**: A) Effect of increasing concentrations of AZD6738 (ATR inhibitor) by XTT cell proliferation assay in NB cell lines, data are mean + SEM from at least 3 independent experiments. B) Correlation of % control growth by 10 µM VE-821 and AZD6738 in cell lines (from A) and MYCN regulatory cell lines (figure 4.4B).*

4.4.2 Role of ATM in determining sensitivity to ATR inhibitors

To determine the role of ATM in sensitivity to ATR inhibition in neuroblastoma, the cytotoxic effect of 10 µM VE-821 was examined by 11q deletion status, which includes hemizygous deletion of *ATM* (**Figure 3.3**), *ATM* mutation status, ATM protein expression and ATM function (**Figures 3.5 and 3.11A**). There was no significant difference in the cytotoxicity of VE-821 between cell lines with and without 11q deletion (Figure 4.10A). Cell lines with mutant *ATM* or low ATM expression (below median expression, **Figure 3.5**) were significantly more sensitive to 10 µM VE-821, compared to cell lines which did not have an *ATM* mutation or expressed high levels of ATM, in both XTT cell proliferation and clonogenic survival assays (**Figure 4.10B and C**).

As *ATM* mutation status or protein expression does not always correlate with protein function, sensitivity to VE-821 by ATM function (shown in **Figure 3.11A**) was analysed. Cell lines lacking ATM function (no ATM^{S1981} autophosphorylation and phosphorylation of $CHK2^{T68}$ in response to doxorubicin) were significantly more sensitive to 10 μM VE-821 by XTT cell proliferation assay (**Figure 4.10D**) and a similar trend was observed by clonogenic survival assay.

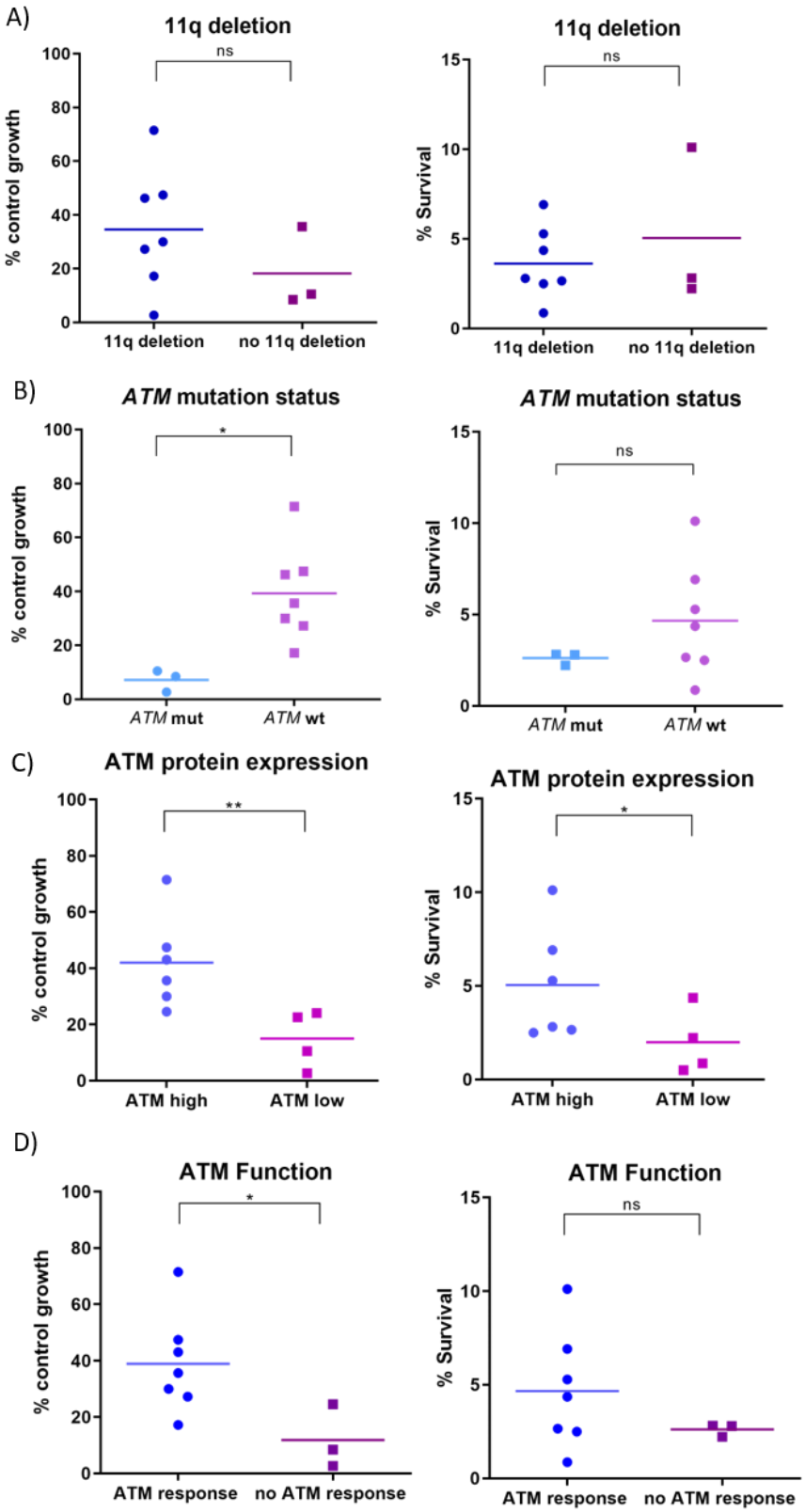

Figure 4.10: *Cell lines were split into 2 groups based on 11q deletion status (A), ATM mutation status (B) ATM protein expression above (high) or below (low) median expression (C) and ATM function in response to 1 µM doxorubicin (Figure 3.11A) (D). Average % control growth and survival at 10 µM VE-821 (from figures 4.6 and 4.7 respectively) was plotted for cell lines belonging to each group (n=3). *p<0.05, **p<0.01, ns: not significant Mann Whitney U test.*

4.4.3 Role of p53 in determining sensitivity to ATR inhibitors

To investigate whether p53 loss of function would increase sensitivity to ATR inhibition, we analysed the sensitivity of two paired cell lines: IMR32 (p53 wild type) and KAT100 (p53 mutant), and NGP (p53 wild type) and N20_R1 (p53 mutant), to increasing concentrations of VE-821. It must be recognised that as these cells were generated by selecting for resistance to drugs, they have additional mutations besides p53, described in chapter 3.

In the case of these cell line pairs, the p53 mutant cell lines were more resistant to VE-821 than the p53 wild type ones (**Figure 4.11**). This is more likely due to these cell lines being generally more drug resistant due to the way they were generated. The effect of p53 mutation alone on ATR inhibitor sensitivity in NB cannot be determined using these cell lines.

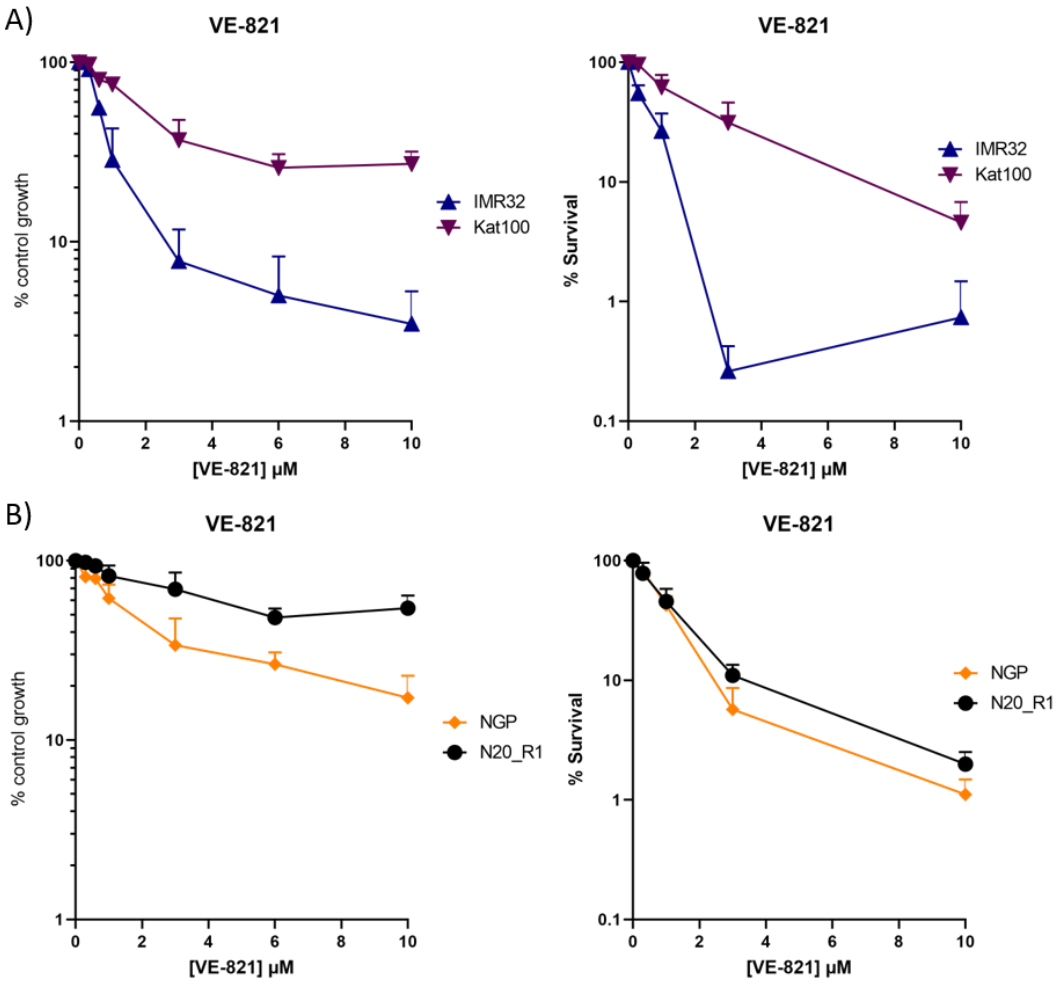

***Figure 4.11**: VE-821 dose response curves by XTT cell proliferation and clonogenic survival assay for A) IMR32 (p53 wild type) and KAT100 (p53 mutant) and B) NGP (p53 wild type) and N20_R1 (p53 mutant) paired cell lines. Data are mean + SEM of 3 independent experiments.*

To further explore the effect of mutant p53 on sensitivity to ATR inhibition, the sensitivity of the panel of NB cell lines to 10 µM VE-821 was analysed by *TP53* mutation status, p53 protein expression and p53 function (**Figures 3.5 and 3.11B**). There was no significant difference in VE-821 sensitivity between *TP53* wild type and mutant cell lines, cell lines with high or low p53 expression or p53 function in response to doxorubicin (**Figure 4.12**).

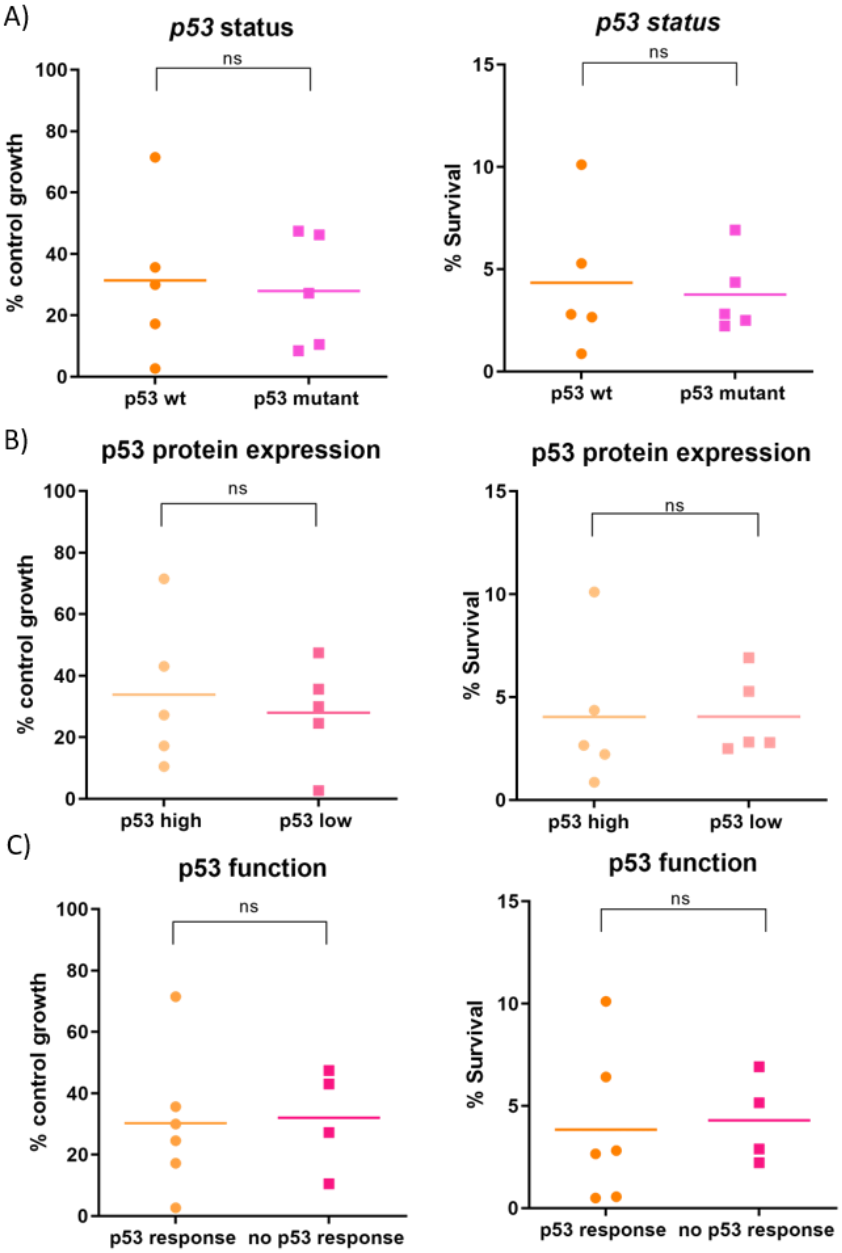

Figure 4.12: *Cell lines were split into 2 groups based on p53 mutation status (A), p53 protein expression above (high) or below (low) median expression (B) and p53 function in response to 1 µM doxorubicin (Figure 11.B) (C). Average % control growth and survival at 10 µM VE-821 (from figures 4.6 and 4.7 respectively) was plotted for cell lines belonging to each group (n=3). wt: wild type, ns: not significant*

4.4.4 Role of replication stress in determining sensitivity to ATR inhibitors

RS occurs when cells enter S phase with unrepaired DNA damage or there is a limited supply of dNTPs, due to defective G1 arrest or by rapid, erroneous DNA replication, often driven by oncogenic signalling, leading to replication fork stalling and collapse. It was hypothesised that cell lines with shorter doubling times will have more RS and, therefore the cytotoxic effect of ATR inhibition by VE-821 will be greater. In contrast, there was no relationship between cell doubling time and percentage control growth (XTT) or survival (clonogenic assay) (**Figure 4.13**).

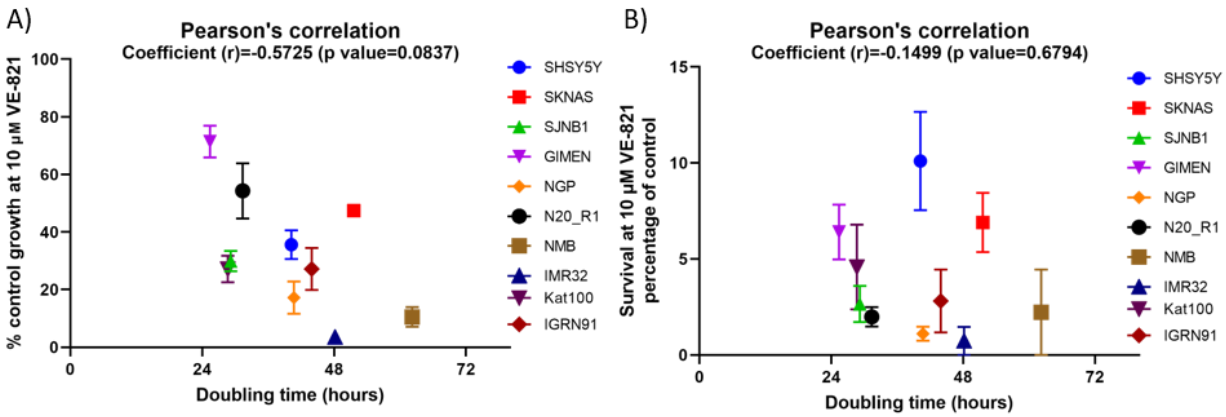

***Figure 4.13**: Sensitivity to 10 µM VE-821 by A) XTT and B) clonogenic survival assays vs. cell doubling time.*

As ATR is activated in response to RS, we analysed the effect of 10 µM VE-821 on growth inhibition and clonogenic survival by baseline protein expression of ATR, CHK1 (downstream target of ATR), and ATR activity (CHK1 serine 345 phosphorylation) in a panel of NB cell lines (**Figures 3.5 and 3.9**), as well as CHK1^{S345} phosphorylation in response to PARP inhibition by 10 µM olaparib (**Figure 3.11C**). There was no significant difference in the cytotoxicity of 10 µM VE-821 between cell lines with high (above median) and low (below median) expression of ATR protein (**Figure 4.14A**). However, when examined by baseline activity of ATR, from pCHK1^{S345} expression, the cytotoxic effect of ATR inhibition by VE-821 was significantly greater in cell lines with higher pCHK1^{S345} (**Figure 4.14B**). Cytotoxicity of 10 µM VE-821 was also significantly greater in cell lines which showed increased ATR activity in response to treatment with 10 µM olaparib (**Figure 4.14C**). In addition, 10 µM VE-821 was significantly more cytotoxic to cell lines with high baseline expression of CHK1 (**Figure 4.14D**).

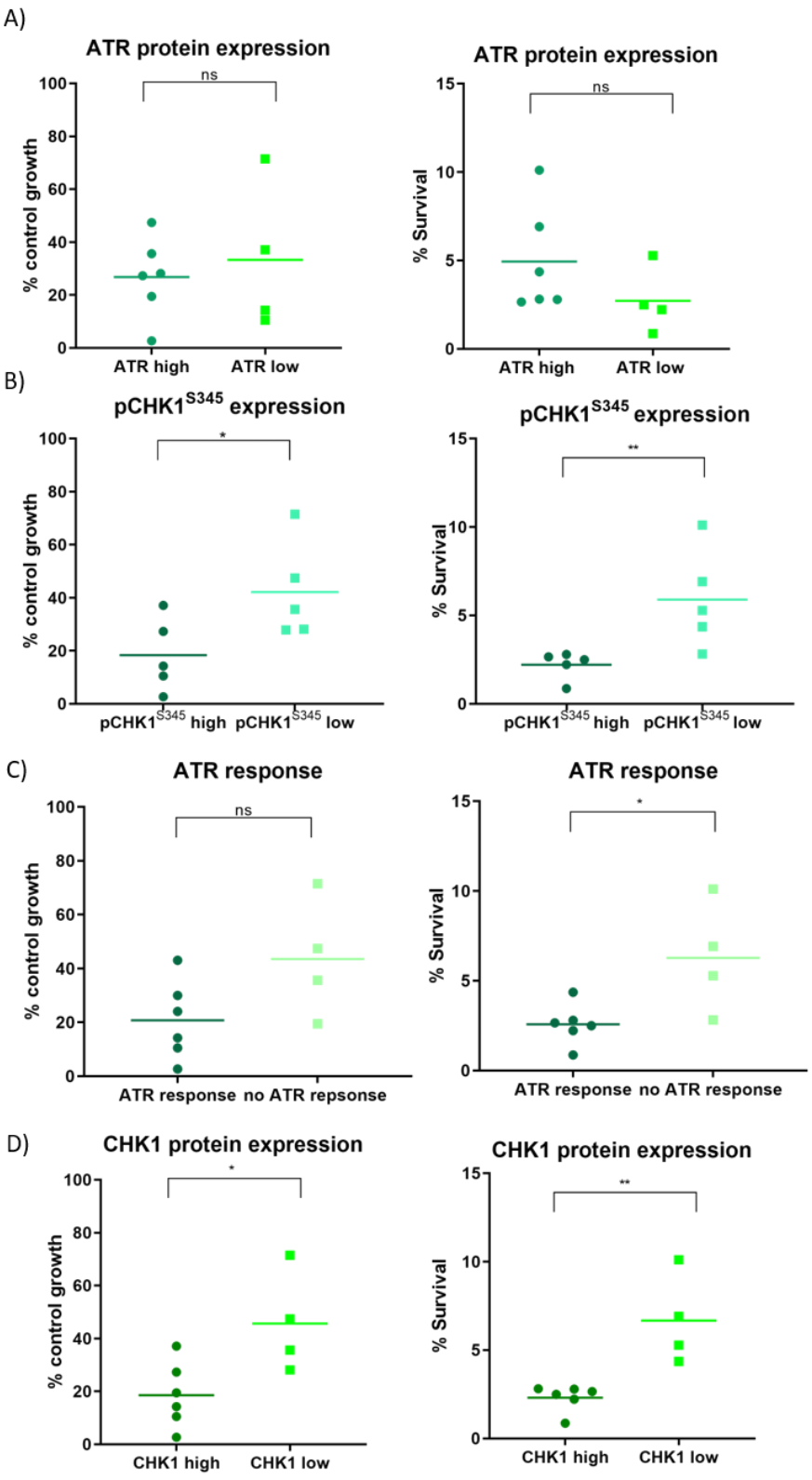

Figure 4.14: *Cell lines were split into 2 groups based on ATR protein expression above (high) or below (low) median expression (A), CHK1^{S345} phosphorylation (pCHK1^{S345}) as a measure of baseline ATR activity (B) CHK1^{S345} phosphorylation in response to PARP inhibition by 10 µM olaparib for 24 hours (C) and CHK1 protein expression above (high) or below (low) median expression (D). Average % control growth and survival at 10 µM VE-821 (from Figures 4.6 and 4.7 respectively) was plotted for cell lines belonging to each group (n=3). *p<0.05, **p<0.01, ns: not significant Mann Whitney U test.*

Cytotoxicity of 10 µM VE-821 was also analysed by ATR independent markers of baseline RS in a panel of NB cell lines. Histone variant 2AX is phosphorylated in response to DNA damage. In the absence of genotoxic agents, histone 2AX phosphorylation (γH2AX) marks endogenous DNA damage, resulting from oxidative and replicative stress. However, there was no significant difference in growth inhibition or clonogenic survival in response to 10 µM VE-821 when cell lines were analysed by γH2AX expression (above and below median expression, **Figure 3.9**) and no correlation between baseline expression of γH2AX and sensitivity to VE-821 (**Figure 4.15**).

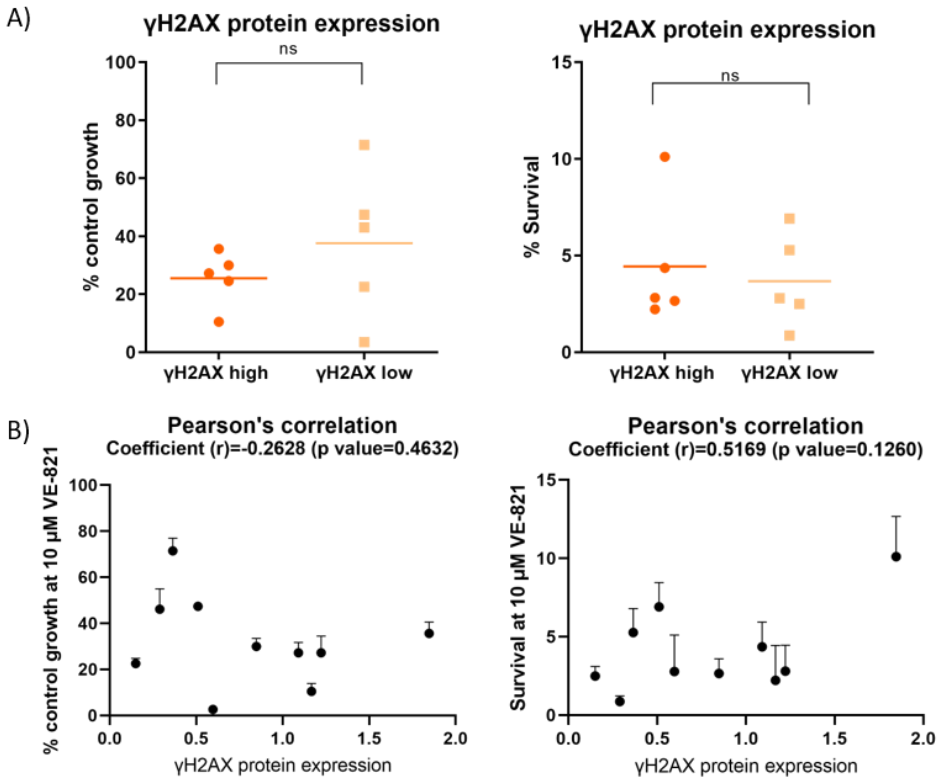

Figure 4.15: *A) Cell lines were split into 2 groups based on γH2AX protein expression above (high) or below (low) median expression. Average % control growth and survival at 10 µM VE-821 (from Figures 4.6 and 4.7 respectively) was plotted for cell lines belonging to each group (n=3). ns: not significant Mann Whitney U test. B) γH2AX protein expression vs. % control growth and survival at 10 µM VE-821.*

Replication protein A (RPA) is another marker of RS. RPA is a trimeric protein which coats single strand regions of DNA and recruits ATR via ATRIP. RPA2 (a subunit of RPA) is phosphorylated at many sites by ATM, ATR, and DNA-PK, and is phosphorylated at serine 8 by DNA-PK and ATM (Liu *et al.*, 2012). Cytotoxicity of 10 µM VE-821 in NB cell lines was analysed according to baseline expression of phopho-RPA2^{S8} (pRPA2^{S8}) as a measure of

endogenous RS. There was no significant difference in growth inhibition or clonogenic survival after treatment with 10 µM VE-821 when cell lines were analysed by pRPA2^{S8} expression (above and below median expression, **Figure 3.9**) and no correlation between baseline expression of pRPA2^{S8} and VE-821 cytotoxicity (**Figure 4.16A and B**).

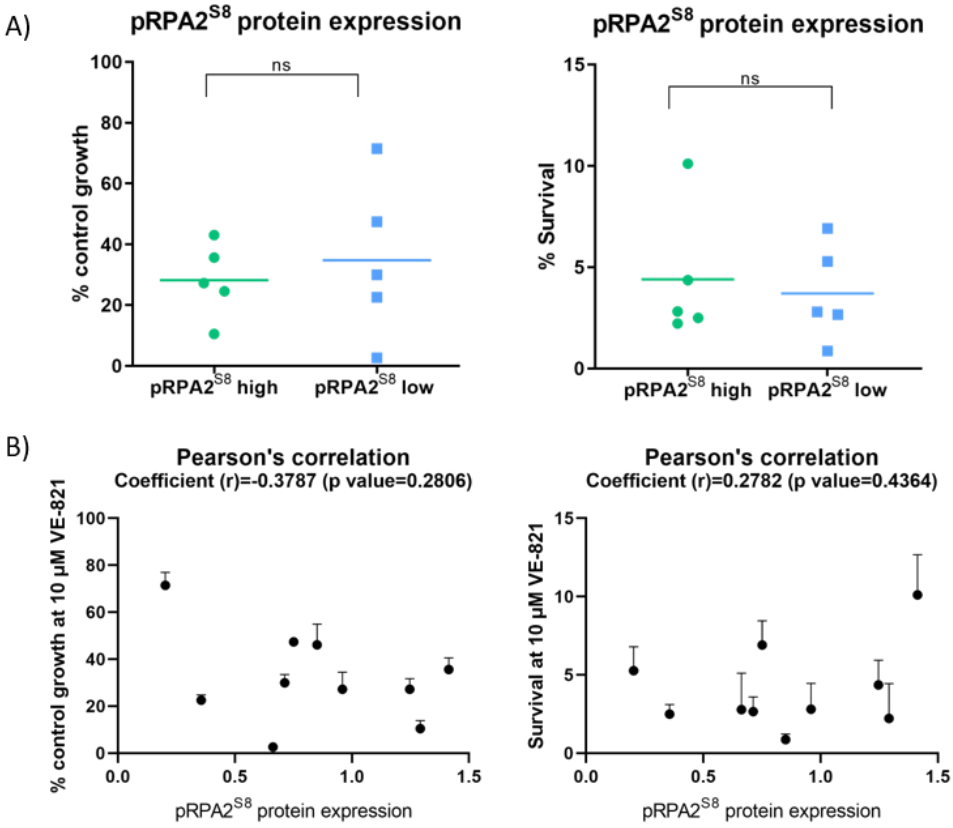

Figure 4.16: *A) Cell lines were split into 2 groups based on phospho-RPA2^{S8} (pRPA2^{S8}) protein expression above (high) or below (low) median expression. Average % control growth and survival at 10 µM VE-821 (from Figures 4.6 and 4.7 respectively) was plotted for cell lines belonging to each group (n=3). *p<0.05, ns: not significant Mann Whitney U test. B) pRPA2^{S8} protein expression vs. % control growth and survival at 10 µM VE-821.*

4.5 Discussion

The aims of this chapter were to investigate if proposed biomarkers of sensitivity to ATR inhibition would determine sensitivity in NB cell lines. The evidence from two MYCN expression regulatable cell lines and a panel of 10 cell lines with varied genetic characteristics, confirm that *MYCN* amplification and subsequent overexpression increases sensitivity to the ATR inhibitors VE-821 and AZD6738. In addition, VE-821 was significantly more cytotoxic in cell lines with low baseline ATM protein expression, high expression of CHK1 protein or high levels of CHK1^{S345} phosphorylation. However, no significant difference in sensitivity to VE-821 was observed when cell lines were analysed by p53 mutation, protein expression or function.

4.5.1 MYCN amplification and overexpression determines sensitivity to ATR inhibition

There is good evidence that overexpression of proliferation-inducing oncogenes leads to RS and dependency on ATR signalling (Kotsantis *et al.*, 2018). In models of Ras- or MYC-driven cancer, signalling through these oncogenes has been shown to lead to sensitivity to ATR inhibition (Murga *et al.*, 2011; Toledo *et al.*, 2011; Schoppy *et al.*, 2012). Overexpression of MYCN has previously been shown to increase replication stress in NB models (Gu *et al.*, 2015; Colicchia *et al.*, 2017). Analysis of two MYCN regulatable cell lines showed that MYCN overexpression results in increased expression of ATR and its downstream effector CHK1, as well as other proteins involved in the DDR such as ATM, CHK2 and p53 (**Figure 4.3**), which likely allows cells to tolerate increased MYCN-induced RS. MYCN overexpressing cells (MYCN on) were more sensitive to ATR inhibition by both VE-821 and AZD6738 in both XTT cell proliferation and clonogenic survival assays.

The role of MYCN expression in sensitivity to ATR inhibition was confirmed in a panel of NB cell lines with varying genetic features. Amplification of the *MYCN* gene is associated with MYCN protein expression, as shown in chapter 3 (**Figure 3.6A**). However, a subset of NB tumours express high levels of MYCN protein in the absence of gene amplification (Valentijn *et al.*, 2012), such as in the SJNB1 cell line (**Figure 3.5**). When analysed by *MYCN* amplification status, *MYCN* amplified cell lines were significantly more sensitive to 10 µM VE-821 than non-amplified cell lines by both XTT and clonogenic assays. Cell lines with high MYCN protein expression (above median expression, **Figure 3.5**), including the SJNB1 cell line, were also

significantly more sensitive to 10 µM VE-821 by both assays, suggesting that MYCN protein expression may provide a useful predictive biomarker for sensitivity to ATR inhibitors, in addition to *MYCN* amplification status, the latter is screened for at diagnosis.

George *et al.* recently reported increased *in vitro* sensitivity to AZ6738 in *MYCN* amplified cell lines, as well as efficacy in the treatment of the MYCN-driven tumours in the Th-*MYCN* transgenic mouse model, providing further evidence of ATR inhibitor vulnerability in MYCN overexpressing tumours (George *et al.*, 2020b).

4.5.2 Markers of ATR activation may provide additional predictive biomarkers for ATR inhibitor sensitivity in neuroblastoma

From studies in two MYCN expression regulatable cell lines, overexpression of MYCN results in RS and increased expression of ATR and CHK1, suggesting increased reliance on the ATR signalling pathway (**Figure 4.3**). Other causes of replication stress include constitutive activation of the RAS-MAPK signalling pathway (Fikaris *et al.*, 2006; Maya-Mendoza *et al.*, 2015) and hypoxia (Pires *et al.*, 2010). Aberrant RAS pathway signalling is frequent in NB caused by activating mutations in *BRAF*, *RAS* (*KRAS* and *HRAS*), and *PTPN11*, and inactivating mutations in the *NF1* tumour suppressor gene (Pugh *et al.*, 2013; Eleveld *et al.*, 2015). In addition, constitutive activation of ALK tyrosine kinase receptor, which signals to the RAS-MAPK pathway, by activating point mutations or amplification of the gene locus, occurs in around 10% of NB (Trigg and Turner, 2018). Studies of hypoxia in NB tumours suggest hypoxic conditions contribute to the aggressive, malignant phenotype observed in high risk disease (Pietras *et al.*, 2008; Zhang *et al.*, 2014; Påhlman and Mohlin, 2018). Measuring endogenous RS in tumours that are not *MYCN*-amplified may identify patients with tumours that may respond to treatment with an ATR inhibitor.

Baseline expression of ATR and CHK1 proteins was measured to quantify endogenous RS, as well as phosphorylation of CHK1^{S345}, a marker of ATR activity, histone 2AX and RPA2^{S8}, which are markers of DNA double strand breaks and single strand regions of DNA respectively. Although there was no significant difference in sensitivity to VE-821 when cell lines were grouped by baseline ATR protein expression, when examined by baseline activity of ATR, cell lines with high pCHK1^{S345} expression were significantly more sensitive to ATR inhibition by VE-821 (**Figure 4.12B**). Interestingly, cell lines with high baseline expression of CHK1 were

significantly more sensitive to 10 µM VE-821 (**Figure 4.12 C**), suggesting that CHK1 protein expression is a better determinant of ATR inhibitor sensitivity than ATR. There was no relationship between endogenous γH2AX or pRPA2^{S8} expression and VE-821 sensitivity in these cell lines. Therefore, baseline ATR activity (by measurement of pCHK1^{S345}) and CHK1 protein expression could be used to identify tumours with high endogenous RS, which are likely to respond to inhibition of ATR.

4.5.3 Low ATM protein expression and ATM dysfunction determine sensitivity to ATR inhibition in neuroblastoma

Studies in adult cancers have identified ATM loss or dysfunction as a marker of sensitivity to ATR inhibition (Reaper *et al.*, 2011; Middleton *et al.*, 2015; Kwok *et al.*, 2016; Min *et al.*, 2017; Schmitt *et al.*, 2017). The results presented in this chapter confirm that *ATM* mutation, low ATM protein expression or loss of ATM function identify cells with increased sensitivity to ATR inhibition in NB.

ATM loss through partial heterozygous deletion of chromosome 11q did not predict sensitivity to ATR inhibition. However, 11q deletion was detected in 7/10 of the cell lines studied here. Deletion of 11q is one chromosomal aberration among many in these cell lines, and the second *ATM* allele is unaffected, except in IMR32 which carries an inactivating *ATM* mutation. As shown in chapter 3, ATM function is retained 5/7 cell lines with 11q deletion when challenged with 1 µM doxorubicin. In a study of 11q deleted chronic lymphocytic leukaemia, a malignancy in which 10-20% of patients present with 11q deletion, mutation in the second *ATM* allele was required to abrogate ATM function in response to ionising radiation, fludarabine, and the alkylating agents chlorambucil and cyclophosphamide (Austen *et al.*, 2007). *ATM* mutations are rare in NB tumours and have been reported to be mutually exclusive with 11q deletion (Takagi *et al.*, 2017) therefore ATM function cannot be determined by hemizygous 11q loss alone.

Interestingly, 2 of the cell lines which showed the greatest sensitivity to VE-821 in both XTT and clonogenic assays, NGP and IMR32, have both *MYCN* amplification and deletion of 11q and express low levels of ATM. *MYCN* amplification and 11q deletion is rarely observed together in NB tumours, and identifies a subgroup with worse outcome than *MYCN* amplified

alone (Villamón *et al.*, 2013). In addition to 11q deletion, loss of ATM can occur in *MYCN* amplified NB by upregulation of the ATM targeting micro-RNA, miR-421 (Hu *et al.*, 2010). ATM silencing is likely contributing to *MYCN*-induced RS through impaired DNA DSB signalling and repair, making these cells especially vulnerable to ATR inhibition.

Overall, *ATM* mutation and reduced ATM function, which can be partially determined by protein level, confers sensitivity to ATR inhibition in NB. Measuring ATM protein expression in NB tumours, by IHC, may identify patients who might respond to ATR inhibitors.

4.5.4 p53 mutation or dysfunction does not determine sensitivity to ATR inhibition in neuroblastoma

Despite some evidence for ATR inhibitor sensitivity in p53 deficient cancers (Kwok *et al.* 2016), no significant difference in sensitivity to VE-821 was observed when analysed by p53 status in our panel of NB cell lines. Using two paired cell lines, the p53 mutant cell lines were more resistant to VE-821 than the p53 wild type ones (**Figure 4.11**). However, the cell lines pairs used in this study were generated by selecting for resistance, and have gained mutations in many genes, including *TP53*. The effect of the other mutations likely contributes to resistance to many other small molecule inhibitors. In NB tumours, mutations in *TP53* are rarely observed at diagnosis, but are more common at relapse (Carr-Wilkinson *et al.*, 2010), suggesting *TP53* mutations contribute to treatment resistance and it is likely that tumours will have acquired other mechanisms of drug resistance.

Middleton *et al.* also demonstrated that defective p53 signalling did not lead to sensitivity to VE-821 alone, but the addition of VE-821 showed greater potentiation of gemcitabine and ionising radiation induced cytotoxicity in p53 deficient cell lines (Middleton *et al.*, 2018). The increased potentiation in the p53 deficient context has also been observed when ATR inhibitors have been combined with cisplatin (Reaper *et al.*, 2011; Sangster-Guity *et al.*, 2011), temozolomide (Peasland *et al.*, 2011) and topoisomerase I poisons (Jossé *et al.*, 2014). The effect of p53 mutations in the potentiation of genotoxic agents by ATR inhibition in NB remains to be explored.

4.5.5 Limitations

There are a number of limitations to this work. Although many cell lines were examined, they were chosen based on their *MYCN* and *TP53* status and 7/10 cell lines had partial 11q loss, 5 of which were *MYCN*-amplified, the combination of which is very rare in patients. From this data, the effect of 11q loss on sensitivity to ATR inhibition could be masked by the RS caused by overexpression of MYCN and therefore the role of 11q loss alone cannot be determined. Further work to examine the effect of 11q deletion in the non-*MYCN* amplified setting would be required to rule this out completely.

Other biomarkers of sensitivity to ATR inhibition which may be important in paediatric solid tumours, including NB, include high expression of *Piggybac transposable element-derived protein 5* (*PGBD5*) and loss of function mutations in *AT-rich interacting domain 1A* (*ARID1A)*. *PGBD5* encodes a DNA transposase and has been shown to be highly expressed in paediatric solid tumours, contributing to tumorigenesis by promoting site-specific genomic rearrangements and mutations of tumour suppressor genes (Henssen *et al.*, 2017a). PGBD5 expressing cells were shown to be dependent on NHEJ and the ATM/ATR signalling pathways and PGBD5 expressing NB cell lines were significantly more sensitive to the AZD6738 than PGBD5 negative cell lines (Henssen *et al.*, 2017b). *ARID1A* encodes a subunit of the SWI/SNF chromatin remodelling complex, a key transcriptional regulator (Mathur, 2018). *ARID1A* is mutated in a wide range of malignancies (Wu *et al.*, 2014) and has been reported in ~5% NB tumours (Sausen *et al.*, 2013; Lee *et al.*, 2017). *ARID1A* loss of function mutation has been shown to impair localisation of topoisomerase 2a to chromatin, leading to increased topological stress and genome instability, and ARID1A-deficient cells have increased sensitivity to ATR inhibition, although the mechanism is unclear (Williamson *et al.*, 2016). Further work to assess the role of PGBD5 and ARID1A in sensitivity to ATR inhibition in NB is required.

4.6 Conclusions

From the results presented in this chapter, it can be concluded that MYCN overexpression leads to increased expression of RS markers and ATR activity. ATR inhibition is more cytotoxic to *MYCN* amplified cells or those with high levels of MYCN protein. *ATM* mutation and

reduced ATM function, which can be partially determined by protein level, also confers sensitivity to ATR inhibition in NB. High CHK1 protein expression and ATR activity ($CHK1^{S345}$ phosphorylation) also identify cells which may be vulnerable to ATR inhibition. Mutations in p53 do not determine sensitivity to single agent ATR inhibitors but may show enhanced sensitisation when combined with conventional chemotherapy.

Chapter 5: Determinants of PARP inhibitor sensitivity in high risk NB cell lines

5.1 Introduction

In the previous chapter, sensitivity to ATR inhibition was analysed by factors involved in the RS and cell cycle checkpoint control responses, including *MYCN* amplification, CHK1 expression, and ATM and p53 deficiency. With increasing evidence of synergism between ATR and PARP inhibitors in pre-clinical models of different cancers (Schoonen *et al.*, 2019; Kim *et al.*, 2020; Lloyd *et al.*, 2020), this chapter aimed to examine whether determinants of sensitivity to ATR inhibitors also confer sensitivity to PARP inhibition.

Previous studies in NB have shown the chemo- and radio-sensitising potential of PARP inhibitors (Daniel *et al.*, 2009; McCluskey *et al.*, 2012; Mueller *et al.*, 2013; Norris *et al.*, 2014; Nile *et al.*, 2016) and PARP inhibitors are currently being evaluated in clinical trials in combination with irinotecan or temozolomide for the treatment of paediatric patients with advanced solid tumours, including NB as part of the E-SMART (Europe) and paediatric MATCH (USA) trials (clinicaltrials.gov: NCT02392793, NCT02813135). Olaparib (Lynparza, AstraZeneca) is also being investigated as monotherapy in children with advanced solid tumours harbouring mutations in genes affecting HRR (NCT04236414, NCT03155620, NCT03233204).

The best characterised marker of PARP inhibitor sensitivity is *BRCA1/2* mutation, which results in defective HRR and synthetic lethality with PARP inhibition (Lord and Ashworth, 2017). Several PARP inhibitors have received FDA approval for *BRCA* mutant gynaecological and breast cancers, including olaparib, which has also been approved for *BRCA* mutant prostate and pancreatic cancers.

There is evidence that other DDR defects affecting HRR, such as loss of ATM (Lord and Ashworth, 2016), lead to PARP inhibitor sensitivity, particularly in ATM-deficient lymphoid (Weston *et al.*, 2010), breast (Gilardini Montani *et al.*, 2013), gastric (Kubota *et al.*, 2014) and colorectal (Wang *et al.*, 2017) cancer cell lines.

In NB, ATM loss through heterozygous deletion of chromosome 11q is commonly observed. Recent studies in preclinical models of NB have shown that 11q loss confers sensitivity to PARP inhibitors (Sanmartín *et al.*, 2017; Takagi *et al.*, 2017). In addition to ATM, other DDR genes located on 11q, including *CHEK1*, *H2AFX* and *MRE11*, are also deleted, perhaps leading to impaired DNA repair.

In addition to 11q loss, recent studies have shown that PARP inhibition is more cytotoxic to NB cells expressing high levels of MYCN (Colicchia *et al.*, 2017; King *et al.*, 2020). *MYCN* amplified tumours have higher PARP1 expression compared to non-*MYCN* amplified tumours (Mueller *et al.*, 2013), suggesting some dependency on PARP1 activity in *MYCN* amplified cells. Inhibition of PARP increases RS in *MYCN* amplified cells, resulting in increased cell death through mitotic catastrophe as these cells enter S-phase with damaged DNA (Colicchia *et al.*, 2017; King *et al.*, 2020).

As PARP inhibition has been shown to increase RS in MYCN overexpressing cells, high levels of endogenous RS may predict sensitivity to PARP inhibitor induced killing. PARP inhibition increases γH2AX foci formation (Michelena *et al.*, 2018), a marker of RS and double strand breaks (Gagou *et al.*, 2010; Lyu *et al.*, 2019). Phosphorylation of RPA2, a subunit of the single strand DNA binding RPA complex, also marks replication stress (Liu *et al.*, 2012).

Here, the role of RS on PARP inhibitor cytotoxicity was analysed using baseline expression of ATR, CHK1, phospho-RPA2^{S8} and γH2AX as markers of endogenous RS and DNA damage.

5.2 Chapter aims

The aims of this chapter are as follows:

1. to investigate the role of MYCN in the sensitivity to PARP inhibition by olaparib

2. to determine whether ATM or p53 status confer sensitivity to olaparib

3. to investigate whether markers of RS, identified as determining sensitivity to ATR inhibition, also confer sensitivity to PARP inhibition

5.3 Methods

5.3.1 Cells and cell culture

The 10 cell lines included in the NB cell line panel have been characterised in detail in chapter 3 and were cultured and maintained as described in section 2.1. The MYCN regulatable cell lines SHEPtet21N and IMR5/75 shMYCN were maintained as described for the other cell lines but incubated with 1 µg/ml doxycycline for 72 hours for MYCN off states prior to experiments.

5.3.2. Reagents

Olaparib, topotecan and doxycycline were used and stored as described in section 2.2.

5.3.3 Cytotoxicity assays

XTT cell proliferation (Roche) and clonogenic survival assays were carried out as described in sections 2.3.

5.4.4 Protein expression analysis

Baseline cell lysates were collected as described in section 2.5.1. Proteins were separated using gel electrophoresis using a 4-20% Tris-acetate or 4-20% Tris-glycine polyacrylamide gel (Bio-Rad, Hemel Hempstead, UK), transferred onto nitrocellulose and detected using Western blotting as described in section 2.5.2. PARP1, poly(ADP-ribose) (pADPr) and GAPDH were detected using primary antibodies described in **Table 2.5** and the appropriate HRP-conjugated secondary antibodies. Protein expression was measured by chemiluminescence from exposure to ECL detection reagent using a ChemiDoc imaging system and bands were quantified using ImageJ software as described in section 2.5.2.

5.4. Results

5.4.1 Role of MYCN

5.4.1.1 MYCN regulatable cell lines

The effect of MYCN overexpression on PARP inhibitor sensitivity was first analysed in the SHEPtet21N and IMR5/75 shMYCN MYCN expression regulatable cell lines described in chapter 4 (section 4.4.1.1).

The growth inhibitory effect of increasing concentrations of the PARP inhibitor olaparib was measured in the SHEPtet21N and the IMR5/75 shMYCN cell lines, in both MYCN states, by XTT assay (**Figure 5.1**).

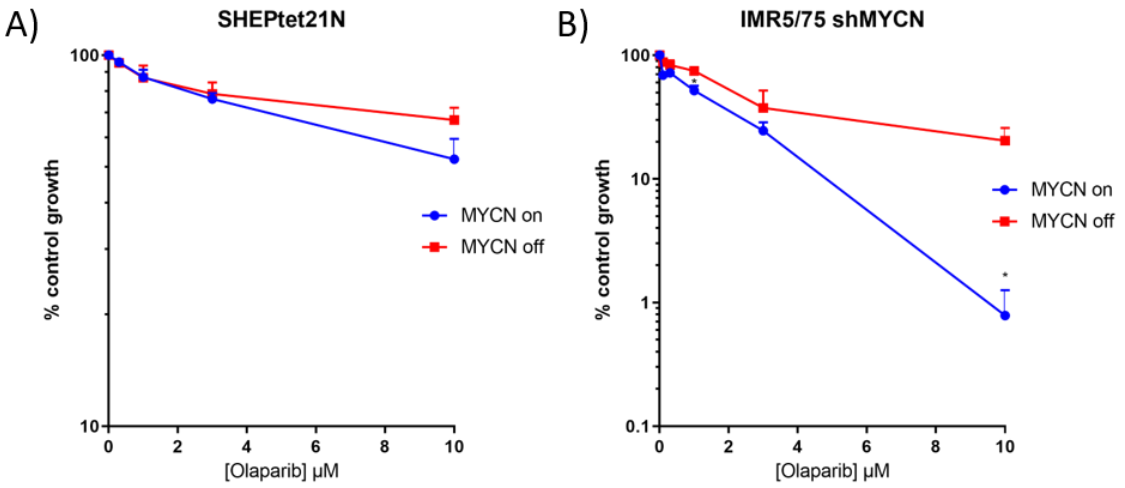

	GI25 (µM)
MYCN on	3.032
MYCN off	4.342
Fold change	1.43

	GI50 (µM)
MYCN on	1.170
MYCN off	2.199
Fold change	1.88

***Figure 5.1**: Effect of PARP inhibition by olaparib in MYCN expression regulatable cell lines. Percentage control growth of A) SHEPtet21N and B) IMR5/75 shMYCN cell lines in response to increasing concentrations of olaparib in MYCN high and low conditions (blue and red lines respectively). Data are mean + SEM of 3 independent experiments. *p<0.05 t-test.*

The growth inhibitory effect of olaparib was greater in MYCN high expressing cells than cells with low MYCN expression, which was most significant at concentrations > 1 µM.

To confirm that MYCN overexpression increases the cytotoxicity of PARP inhibition, the effect of increasing concentrations of olaparib on survival of SHEPtet21N cells, in both MYCN states, was tested by clonogenic survival assay. Cytotoxicity of olaparib was greater in cells expressing high levels of MYCN compared with those with low MYCN expression (**Figure 5.2**).

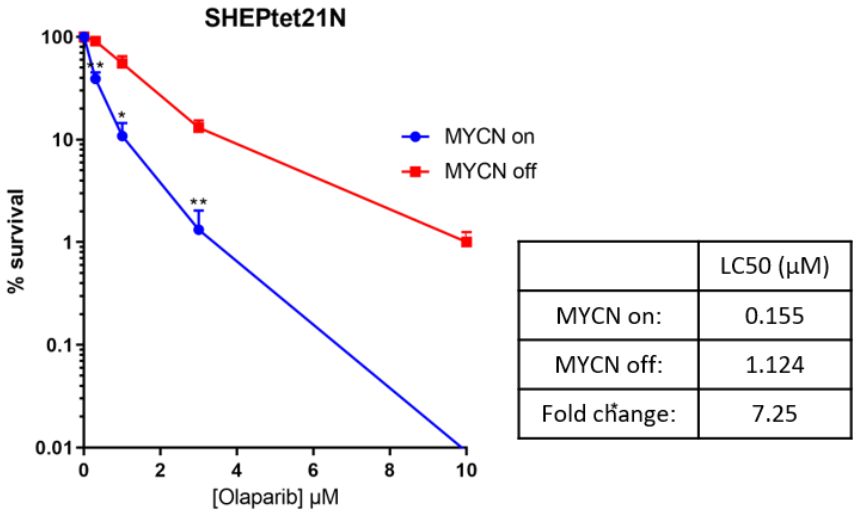

	LC50 (µM)
MYCN on:	0.155
MYCN off:	1.124
Fold change:	7.25

***Figure 5.2**: Clonogenic survival of the SHEPtet21N cell line in response to increasing concentrations of olaparib in MYCN high and low conditions (blue and red lines respectively). Data are mean + SEM of 3 independent experiments. *p<0.05, **p<0.01 t-test.*

5.4.1.2 Role of MYCN in a panel of cell lines

To test if MYCN expression determines sensitivity to PARP inhibitor induced growth inhibition in the context of a more complex phenotype, olaparib-induced growth inhibition was tested by XTT cell proliferation assay in a panel of 10 NB cell lines with different genetic abnormalities, characterised in chapter 3.

The growth inhibitory effect of olaparib in these cell lines was varied, with the IMR32 and NGP cell lines showing the greatest olaparib-induced growth inhibition and SKNAS cells showing the least at 10 µM (**Figure 5.3A and B**). Although *MYCN* amplified cell lines were generally more sensitive than non-amplified cell lines, there was no significant difference in the growth inhibitory effect of 10 µM olaparib between *MYCN* amplified and non-amplified cell lines, or cell lines with high or low MYCN protein expression (above or below median expression,

figure 3.5), (**Figure 5.3 C and D**), which was confirmed by clonogenic assay (**Figure 5.4**) and shown not to be associated with cloning potential (**Figure 5.4 C**).

A summary of percentage control growth and survival in response to 10 µM olaparib is shown in **Table 5.1.**

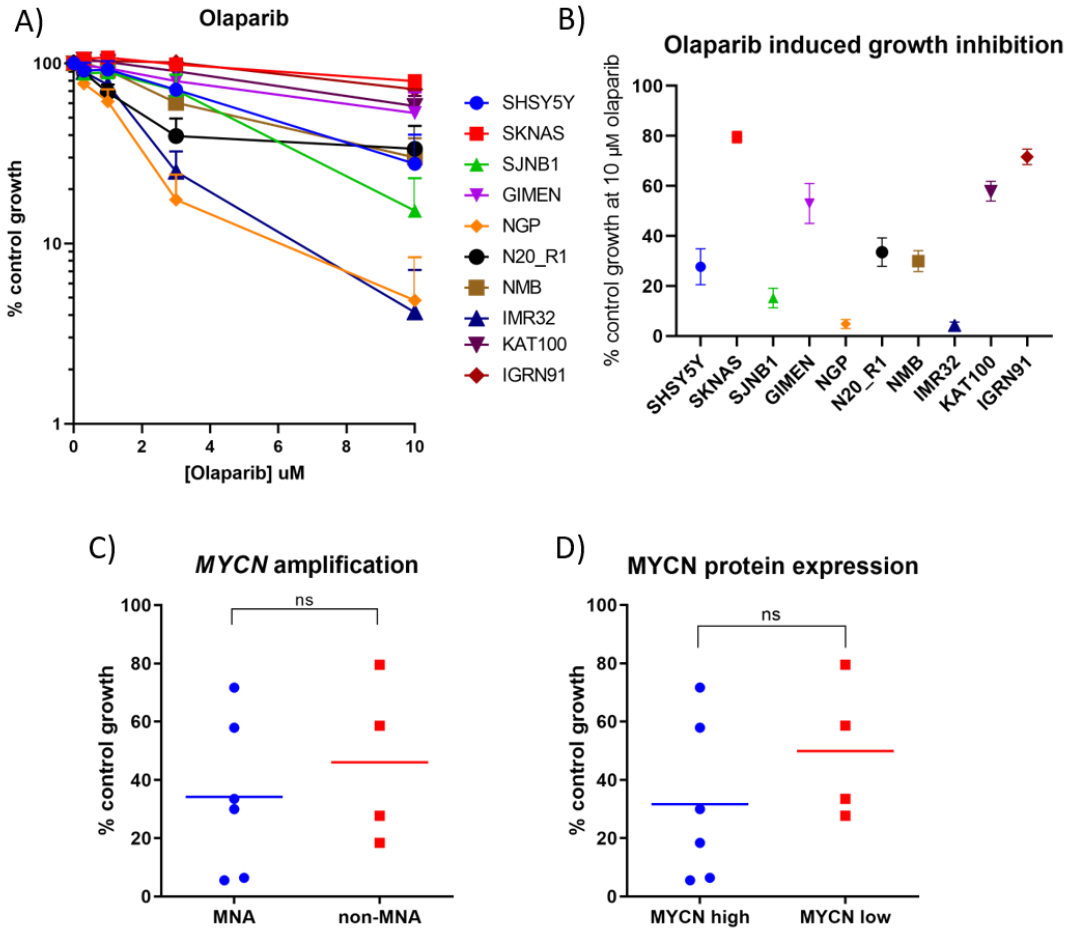

Figure 5.3: *A) Effect of increasing concentrations of olaparib (PARP inhibitor) by XTT cell proliferation assay in NB cell lines, data are mean + SEM from at least 3 independent experiments. B) Percentage control growth when treated with 10 µM olaparib plotted for each cell line. Bars represent mean +/- SEM from at least 3 independent experiments. Cell lines were split into 2 groups based on MYCN amplification (C) and MYCN protein expression above (high) or below (low) median expression (D). Average percentage control growth at 10 µM VE-821 (from B) was plotted for cell lines belonging to each group. Data are mean of 3 independent experiments. ns: not significant Mann Whitney U test. MNA: MYCN amplified, non-MNA: non-MYCN amplified.*

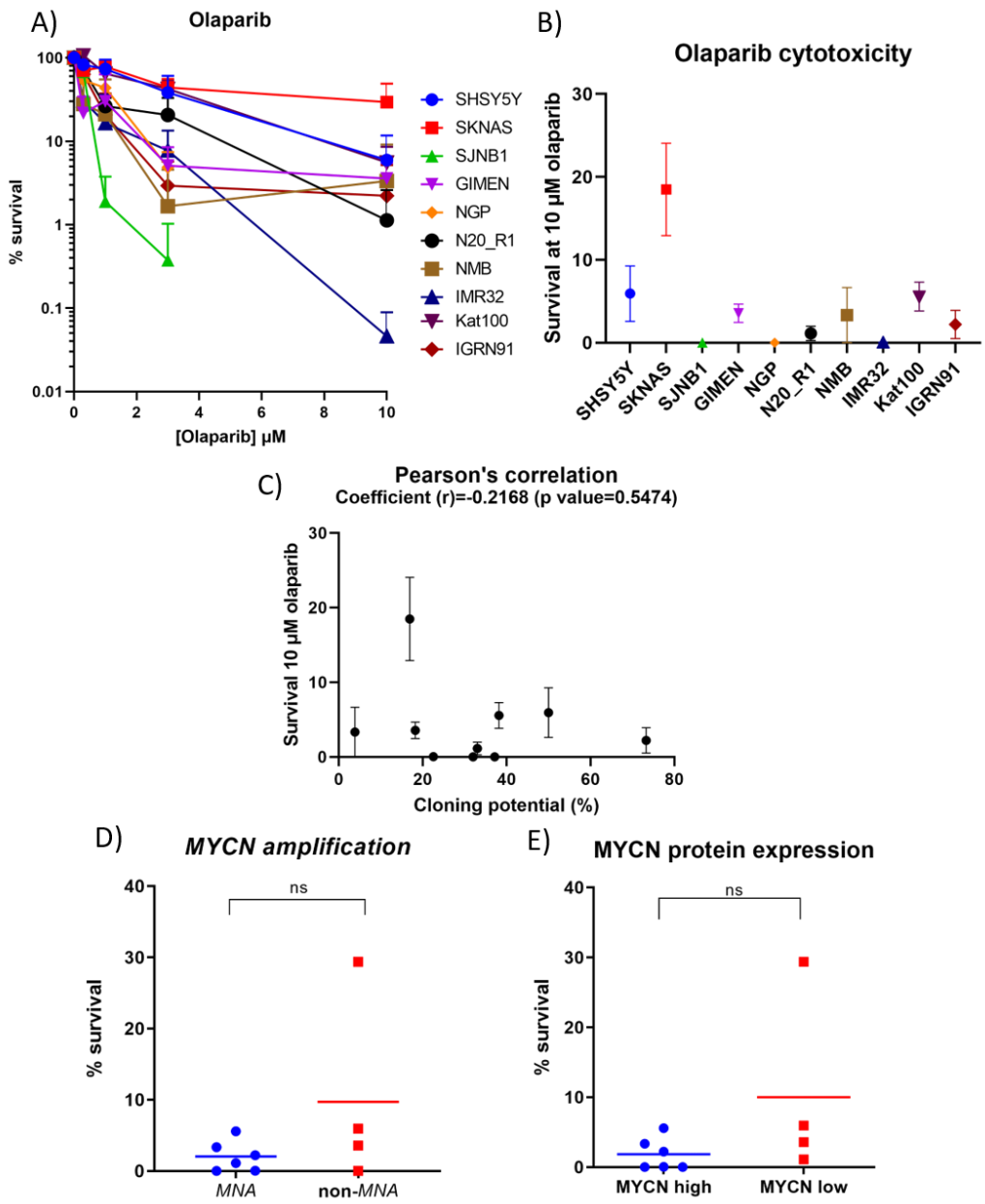

Figure 5.4: *A) Effect of increasing concentrations of olaparib (PARP inhibitor) by clonogenic survival assay in NB cell lines, data are mean + SEM of 3 independent experiments. B) % survival to 10 µM olaparib plotted for each cell line. Bars represent mean +/- SEM from at least 3 independent experiments. C) % survival to 10 µM olaparib correlated with cloning potential. Cell lines were split into 2 groups based on MYCN amplification status (D) and MYCN protein expression above (high) or below (low) median expression (E). Average survival at 10 µM olaparib (from B) was plotted for cell lines belonging to each group. Data are mean of 3 independent experiments. ns: not significant Mann Whitney U test. MNA: MYCN amplified, non-MNA: non-MYCN amplified.*

Table 5.1: Summary of percentage control growth and survival following treatment with 10 µM olaparib for 72 hours

Cell line	Percentage of control growth 10 µM olaparib	Percentage survival 10 µM olaparib
SHSY5Y	27.69	5.93
SKNAS	79.49	29.38
SJNB1	15.19	0.0001
GIMEN	52.99	3.56
NGP	4.84	0.0001
N20_R1	33.52	1.13
NMB	29.96	3.33
IMR32	4.15	0.046
KAT100	57.92	5.57
IGRN91	71.65	2.22

PARP inhibition by olaparib was confirmed by Western blot analysis of poly-ADP ribose (PAR) in response to 0.5 µM topotecan and increasing concentrations of olaparib in 4 cell lines, SHSY5Y, SKNAS, NGP and N20_R1 (**Figure 5.5**). PAR chain formation was significantly reduced after treatment with 0.3 µM olaparib in all cell lines. Additionally, PARP cleavage, a marker of apoptosis (Mullen, 2004), was also observed in the SKNAS and NGP cell lines following combined topotecan and olaparib treatment (PARP1 lower band).

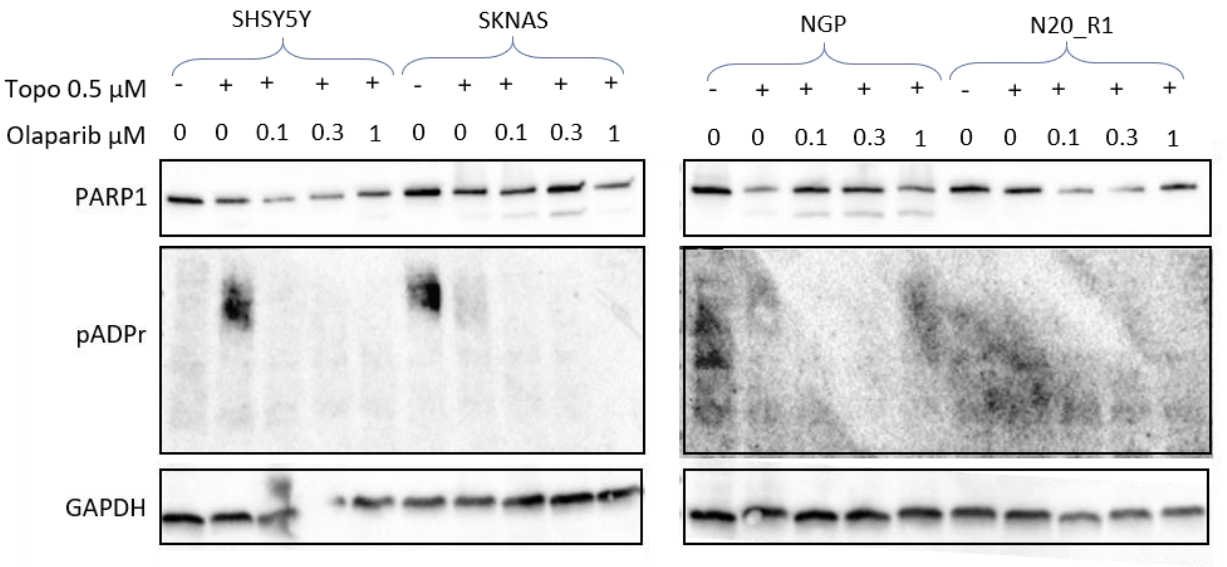

Figure 5.5: *PARP inhibition by olaparib. Western blot analysis of PARP1 and poly-ADP ribose (pADPr) chains in the NGP, SKNAS and SHSY5Y cell lines after treatment with 0.5 µM topotecan (topo) with and without 0.1, 0.3 or 1 µM olaparib for 24 hours. GAPDH was used as a control for protein loading.*

5.4.2 Role of ATM

To examine the role of ATM in sensitivity to PARP inhibition in NB, the cytotoxicity of 10 µM olaparib was examined by 11q deletion status, which includes deletion of *ATM* (**Figure 3.3**), ATM protein expression and ATM function (**Figures 3.5 and 3.11A).** There was no significant difference in the cytotoxicity of 10 µM olaparib between cell lines with and without 11q deletion, although only 3/10 cell lines did not have 11q deletion in this panel (**Figure 3.3**), high and low expression of ATM protein (above and below median expression, **Figure 3.5**), or ATM functional status (ATM^{S1981} autophosphorylation and phosphorylation of $CHK2^{T68}$ in response to doxorubicin, **Figure 3.11A**) (**Figure 5.6**).

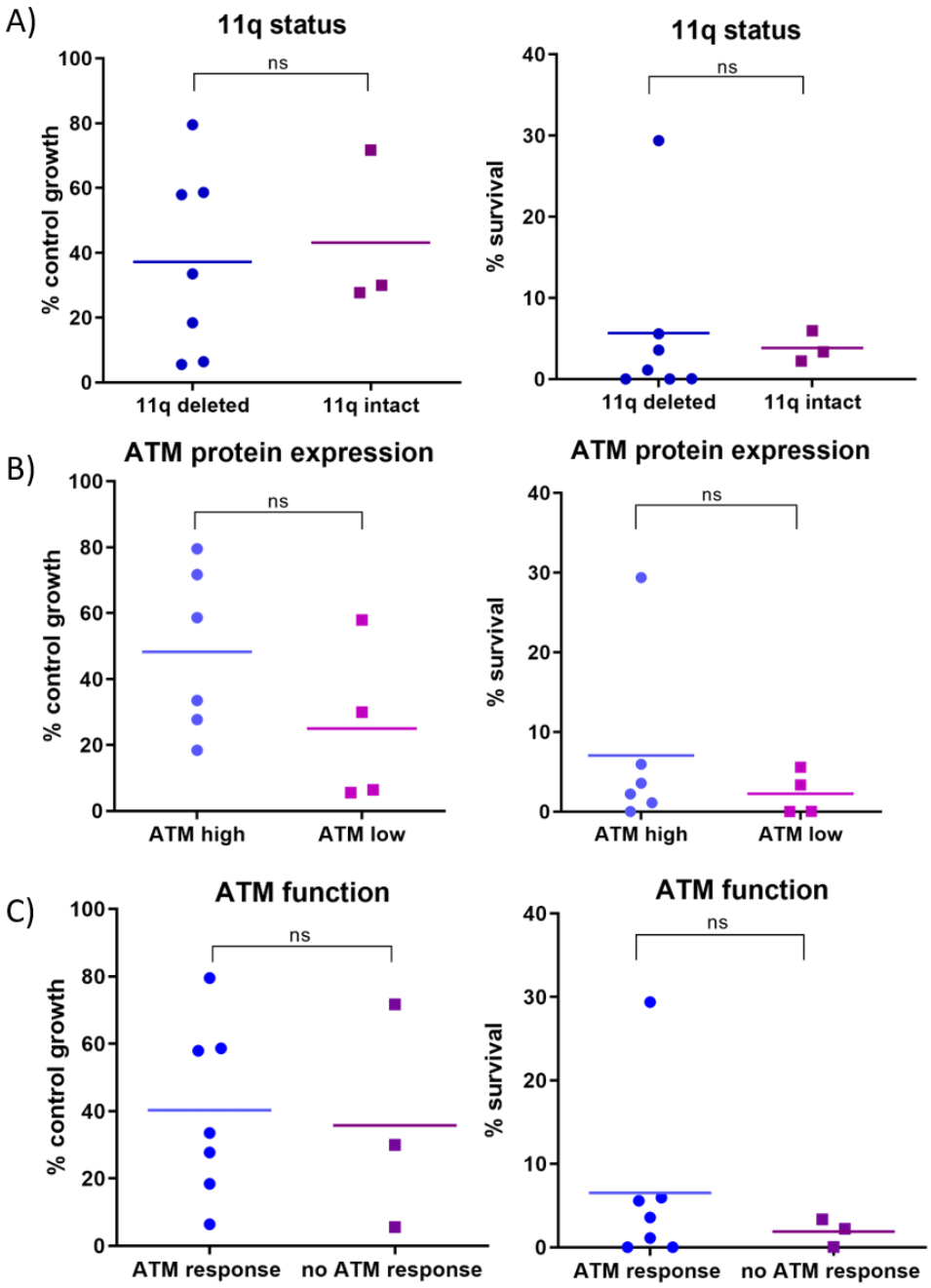

Figure 5.6: *Cell lines were split into 2 groups based on 11q deletion status (A), ATM protein expression above (high) or below (low) median expression (B) and ATM function in response to 1 µM doxorubicin (C). Average % control growth and survival at 10 µM olaparib (from Figures 5.3 and 5.4 respectively) was plotted for cell lines belonging to each group. Data are mean of 3 independent experiments. ns: not significant Mann Whitney U test.*

5.4.3 Role of p53

To investigate whether p53 loss of function would increase PARP inhibitor induced growth inhibition and cytotoxicity, the sensitivity of two paired cell lines: IMR32 (*TP53* wild type) and KAT100 (*TP53* mutant), and NGP (*TP53* wild type) and N20_R1 (*TP53* mutant), to increasing concentrations of olaparib was measured by XTT cell proliferation and clonogenic survival assays.

For both these cell line pairs, the *TP53* mutant cell lines were more resistant to olaparib than the *TP53* wild-type ones (**Figure 5.7**). However, as with ATR inhibition (chapter 4, section 4.4.3) these cell lines are likely to be generally more drug resistant due to the way they were generated. The effect of *TP53* mutation alone on PARP inhibitor sensitivity in NB cannot be determined using these cell lines and would require isogenic pairs.

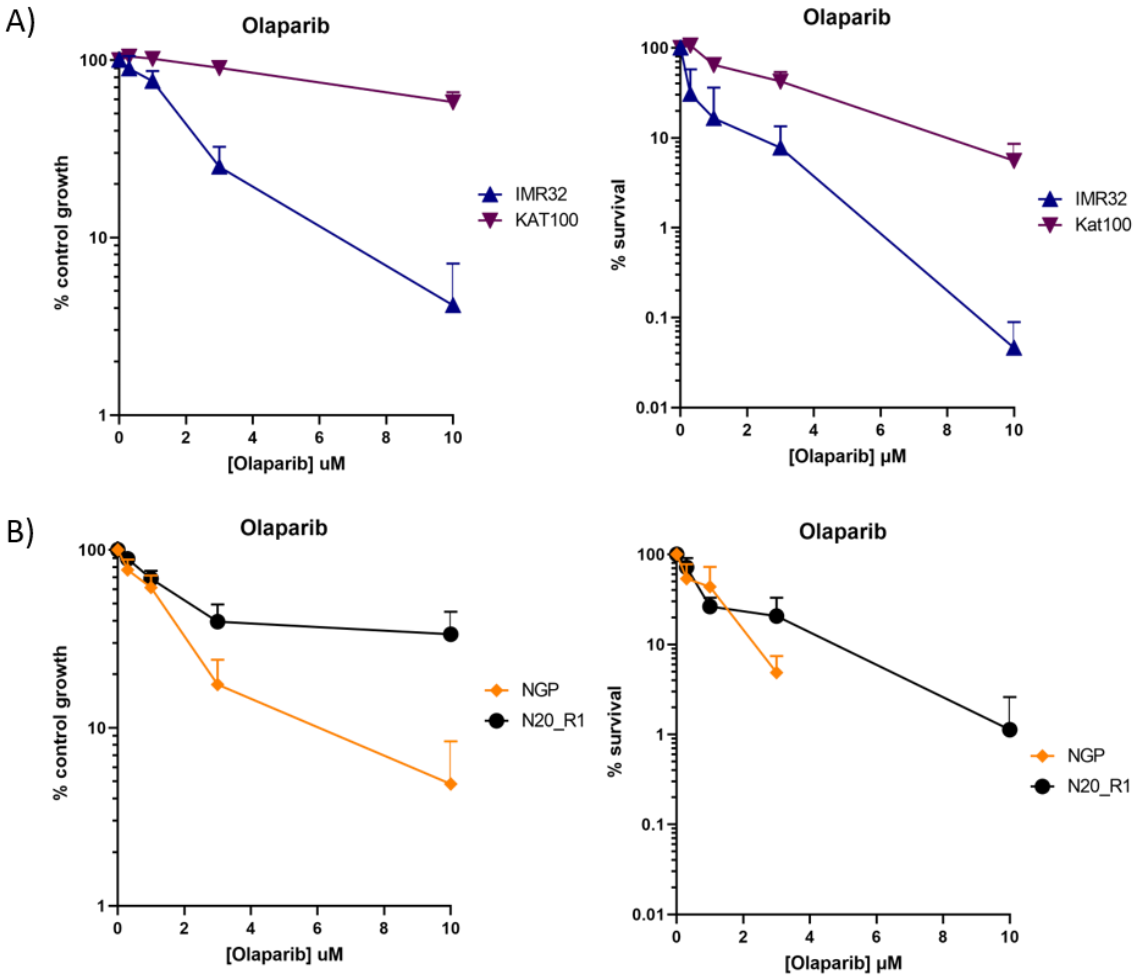

Figure 5.7: *XTT cell proliferation and clonogenic survival assay of increasing concentrations of olaparib in A) IMR32 (p53 wild type) and KAT100 (p53 mutant) and B) NGP (p53 wild type) and N20_R1 (p53 mutant) paired cell lines. Data are mean + SEM of 3 independent experiments.*

To further explore the impact of mutant p53 on cell proliferation and viability in response to PARP inhibition, the sensitivity of the panel of NB cell lines to 10 µM olaparib was analysed by *TP53* mutation status and p53 function (**Figure 3.11B**). Although *TP53* mutant cell lines tended to be more resistant to olaparib cytotoxicity, there was no significant difference in sensitivity between *TP53* wild type and mutant cell lines (**Figure 5.8A**). In addition, no significant difference in olaparib sensitivity was found between cell lines with or without p53 function in response to doxorubicin (**Figure 5.8B**).

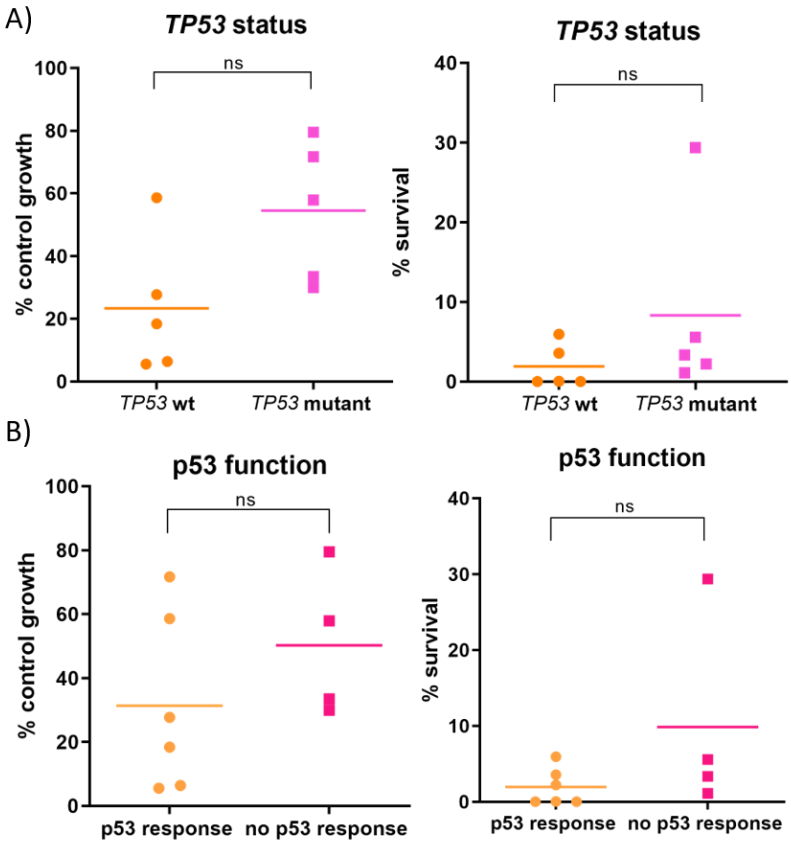

Figure 5.8: *Cell lines were split into 2 groups based on p53 mutation status (A) and p53 function in response to 1 µM doxorubicin (B). Average % control growth and survival at 10 µM VE-821 (from Figures 5.3 and 5.4 respectively) was plotted for cell lines belonging to each group. Data are mean of 3 independent experiments. wt: wild type, ns: not significant Mann Whitney U test.*

5.4.4 Other markers of sensitivity to PARP inhibitor cytotoxicity

Other proposed markers of PARP inhibitor sensitivity include overexpression of PARP1. To determine if PARP1 expression is predictive of sensitivity to PARP inhibition in NB, the sensitivity of the panel of NB cell lines to 10 µM olaparib was analysed by PARP1 protein expression. Sensitivity to olaparib was not increased in cells with high PARP1 expression. In fact, the trend was for cells with lower PARP1 expression to be more sensitive, but this was not significant (**Figure 5.9**).

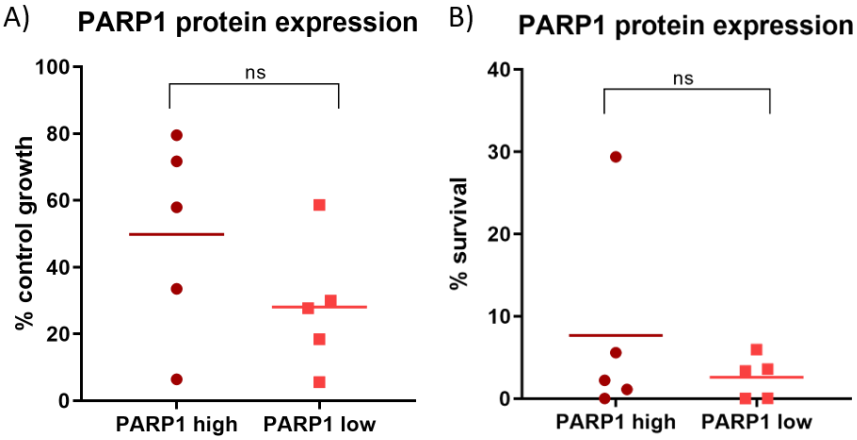

Figure 5.9: *Cell lines were split into 2 groups based on PARP1 protein expression high or low (above or below median expression, figure 3.5). A) Average % control growth and B) survival at 10 µM VE-821 (from Figures 5.3 and 5.4 respectively) was plotted for cell lines belonging to each group. Data are mean of 3 independent experiments. ns: not significant Mann Whitney U test.*

As PARP inhibition has been shown to increase RS, cells which have high endogenous RS may be more sensitive to olaparib cytotoxicity, as further increases could result in intolerable levels of RS. When analysed by two ATR independent markers of endogenous RS, phosphorylation of $H2AX^{S139}$ (γH2AX) and $RPA2^{S8}$ ($pRPA2^{S8}$), there was no significant difference in growth inhibition or clonogenic survival in response to 10 µM olaparib between cell lines with high (above median) and low (below median) baseline expression of γH2AX or $pRPA2^{S8}$ (**Figure 5.10**).

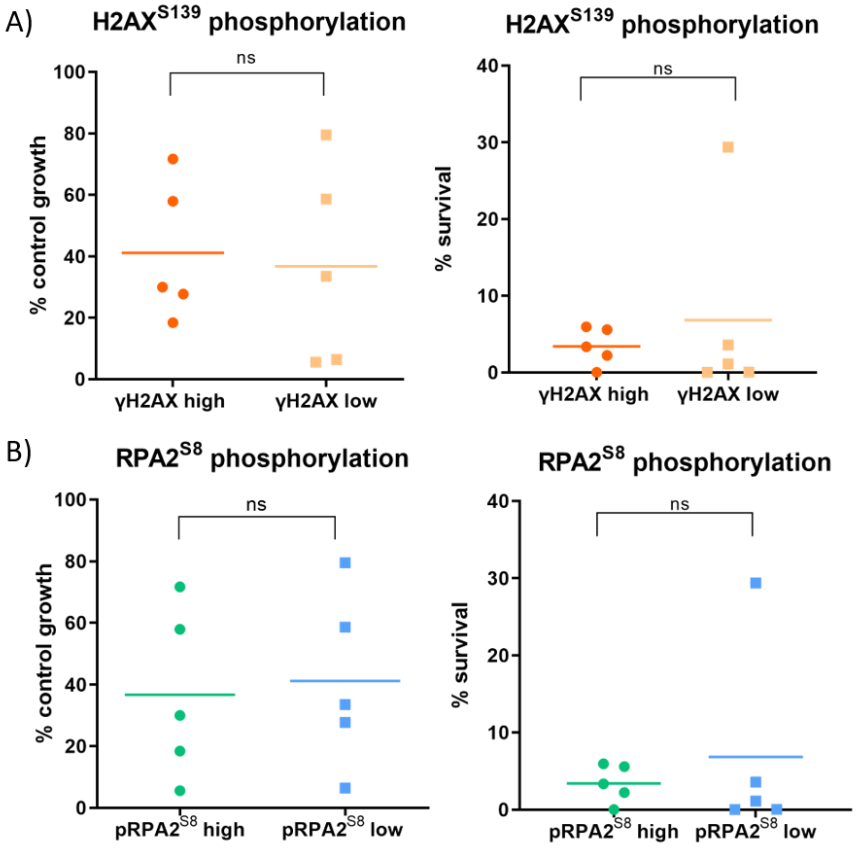

Figure 5.10: *Cell lines were split into 2 groups based on A) γH2AX protein expression and B) phospho-RPA2^{S8} (pRPA2^{S8}) protein expression above (high) or below (low) median expression. Average % control growth and survival following 10 μM olaparib (from Figures 5.3 and 5.4 respectively) was plotted for cell lines belonging to each group. Data are mean of 3 independent experiments. ns: not significant Mann Whitney U test.*

The cytotoxicity of 10 μM olaparib was also analysed by baseline protein expression of ATR and CHK1, and ATR activity (CHK1 serine 345 phosphorylation) in a panel of NB cell lines. There was no significant difference in the cytotoxicity of 10 μM olaparib between cell lines with high (above median expression) and low (below median expression) baseline expression of ATR protein (**Figure 5.11A**). However, when examined by baseline activity of ATR, as indicated by pCHK1^{S345}, the cytotoxicity of 10 μM olaparib was greater in cell lines with higher endogenous pCHK1^{S345} levels (**Figure 5.11B**). 10 μM olaparib was also significantly more cytotoxic to cell lines with high baseline expression of CHK1 when analysed by clonogenic survival, and a similar trend can be seen by XTT cell proliferation (**Figure 5.11C**).

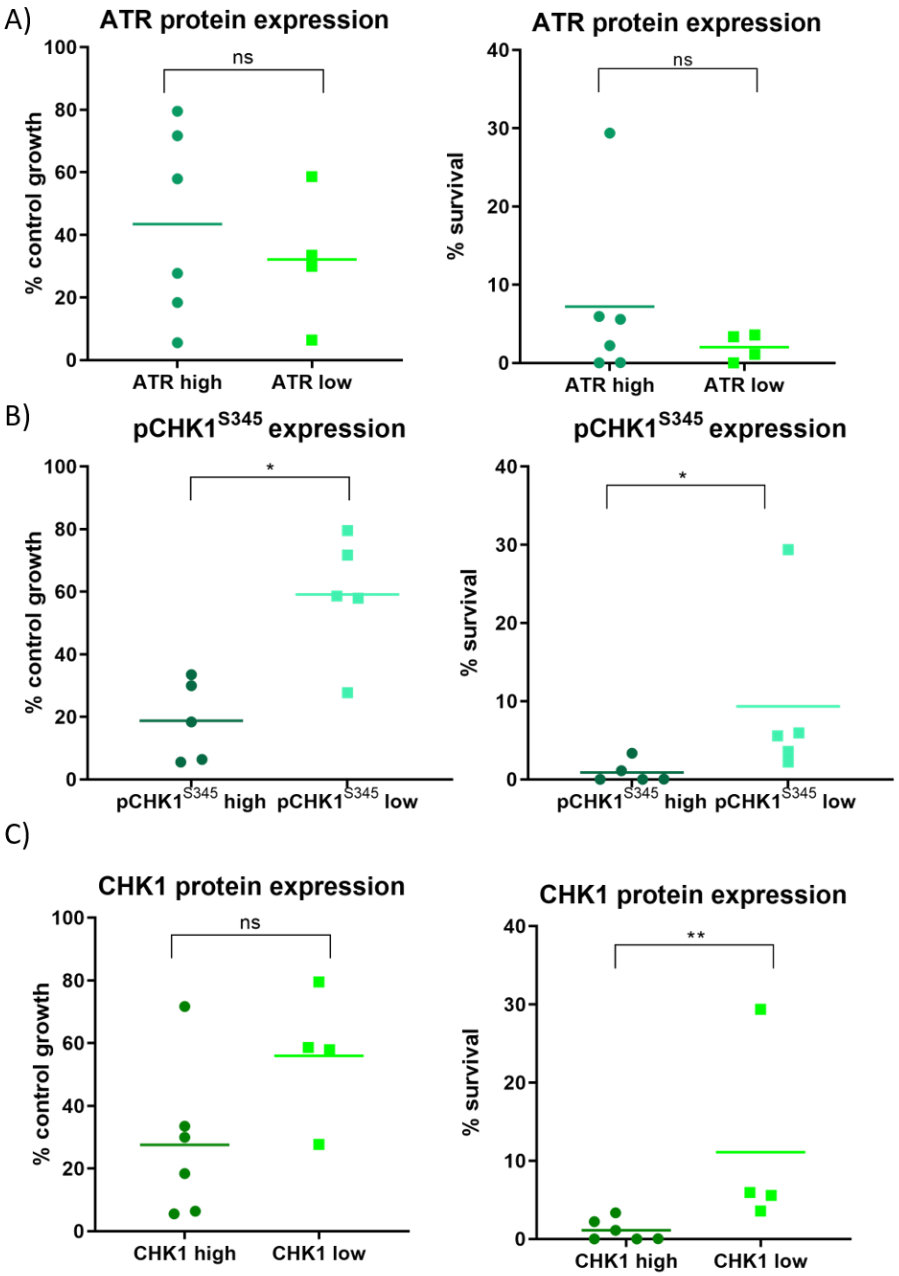

Figure 5.11: *Cell lines were split into 2 groups based on ATR protein expression above (high) or below (low) median expression (A), CHK1^{S345} phosphorylation (pCHK1^{S345}) as a measure of baseline ATR activity (B) and CHK1 protein expression above (high) or below (low) median expression (C). Average % control growth and survival at 10 µM olaparib (from Figures 5.3 and 5.4 respectively) was plotted for cell lines belonging to each group. Data are mean of 3 independent experiments. *p<0.05, **p<0.01, ns: not significant Mann Whitney U test.*

5.5 Discussion

The aims of this chapter were to investigate if the determinants of sensitivity to ATR inhibition identified in the previous chapter would also determine sensitivity to PARP inhibition using a panel of NB cell lines.

In the data presented here, olaparib had the greatest impact on cell proliferation and viability in cell lines which had features contributing to or were indicative of RS, MYCN overexpression, high levels of ATR activity (CHK1^{S345} phosphorylation) and high CHK1 protein expression. However, there was no correlation between olaparib induced growth inhibition or cell death and H2AX or RPA2 phosphorylation. Several previously identified determinants were not confirmed here highlighting the complexity and heterogeneity of cancer cells as described below.

5.5.1 *MYCN* amplification/ expression and RS is not associated with increased sensitivity to PARP inhibition

Here, MYCN overexpression alone was confirmed to result in increased olaparib cytotoxicity in the SHEPtet21N, as well as the IMR5/75 shMYCN cell line models (**Figure 5.1**). However, when analysed in a panel of 10 cell lines, neither *MYCN* amplification nor high MYCN protein expression was associated with increased olaparib cytotoxicity (**Figures 5.3 and 5.4**). *MYCN* amplification and subsequent overexpression in NB cell lines has been shown previously to result in increased sensitivity to PARP inhibition (Colicchia *et al.*, 2017; King *et al.*, 2020). However, in both studies, the researchers utilised the SHEPtet21N MYCN regulatable cell line and confirmed the results in a limited number of cell lines. The suggested mechanism behind sensitivity to PARP inhibition in cells which express high levels of MYCN is increased replication fork stalling, collapse, and subsequent chromosome segregation errors due to intolerable levels of RS. King *et al.* tested the efficacy of olaparib on the growth of MYCN-driven tumours using the transgenic Th-MYCN mouse model, and found that tumours progressed in 2/5 mice treated with olaparib (King *et al.*, 2020). In this model, MYCN is placed under the control of the tyrosine hydroxylase promotor which leads to high MYCN expression in cells of the neural crest lineage specifically and the development of tumours histologically consistent with NB (Weiss *et al.*, 1997). Although there is some debate about the usefulness

of this model, as MYCN expression is driven by the TH promoter, not genomic amplification, and is therefore not a true representation of *MYCN* amplified neuroblastoma, it suggests there may be some inherent resistance mechanisms to PARP inhibition.

Although overexpression of MYCN did not independently determine sensitivity to olaparib in the panel of cell lines analysed here, PARP inhibition with olaparib was significantly more toxic to cell lines which expressed high levels of CHK1 protein or phosphorylated CHK1^{S345}, a marker of ATR activity, compared to cell lines with low expression (**Figure 5.11**). There was a significant positive correlation between CHK1 and MYCN protein expression in these cell lines (Chapter 3) and cell lines expressing high baseline levels of phosphorylated CHK1^{S345} are mostly *MYCN* amplified, with the exception of SJNB1, which expresses high levels of MYCN protein in the absence of amplification. Therefore, cell lines which express high levels of MYCN also expressed high levels of CHK1 and phosphorylated CHK1^{S345}, suggesting that MYCN overexpression does increase olaparib cytotoxicity but too few cell lines have been studied here to see a significant difference. There was no association between ATR independent markers of RS, endogenous γH2AX or pRPA2^{S8} expression, and olaparib sensitivity in these cell lines.

5.5.2 ATM deficiency or p53 loss of function do not determine sensitivity to single agent olaparib

In contrast to previous studies, reduced ATM protein expression or function did not result in significant increase in olaparib cytotoxicity in the cell lines tested here. Sanmartin *et al.* also observed that not all cell lines with reduced ATM expression responded to single agent olaparib treatment (Sanmartín *et al.*, 2017). In 2017, Tagaki *et al.* showed that NB cell lines deficient in functional ATM protein, indicated by the absence of phosphorylated SMC1 after 2 Gy of ionising radiation, were more sensitive to olaparib than cell lines with functional ATM (Takagi *et al.*, 2017), an observation which was also observed in ATM-deficient lymphoid (Weston *et al.*, 2010), breast (Gilardini Montani *et al.*, 2013) gastric (Kubota *et al.*, 2014) and colorectal (Wang *et al.*, 2017) cell lines.

Studies in mantle cell lymphoma and gastric and colorectal cancers have suggested that cells which are deficient in both ATM and p53 are especially sensitive to PARP inhibition

(Williamson *et al.*, 2012; Kubota *et al.*, 2014; Wang *et al.*, 2017). Defects in p53 are more common in these cancer types than in NB, where mutations in *TP53* are rarely observed at diagnosis. The effect of *TP53* mutation and p53 protein function on olaparib cytotoxicity in NB was examined here using a panel of NB cell lines, including 2 paired cell lines. *TP53* mutant cell lines were found to be generally more resistant to olaparib than *TP53* wild type cell lines. However, the *TP53* mutant cell lines were generated by selecting for resistance to other agents, N20_R1 (Drummond *et al.*, 2016) and KAT100 (Xue *et al.*, 2007), or established after treatment with chemotherapy, NMB (Brodeur *et al.*, 1977), SKNAS and IGRN91 (Thiele, 1999), and it is likely that they have acquired other mechanisms of drug resistance, for instance increased expression of drug efflux transporters such as MDR1, which is known to contribute to PARP inhibitor resistance (Lawlor *et al*., 2014). The effect of dual ATM and p53 deficiency on PARP inhibitor sensitivity in NB needs to be analysed further, as only two *TP53*-mutant cell lines have low ATM expression in this panel.

Interestingly, the 2 cell lines which shown the greatest sensitivity to olaparib in both XTT and clonogenic assays, NGP and IMR32, have both *MNA* and deletion of 11q and express low levels of ATM. These cell lines were also very sensitivity to ATR inhibition (Chapter 4), suggesting that MYCN-induced RS, coupled with loss of ATM, render cells extremely sensitive to further RS-inducing treatments, such as PARP inhibition.

Although Sanmartin *et al.* did not observe increased sensitivity to olaparib treatment alone in cells with low ATM expression, they did show that sensitisation of temozolomide or irinotecan cytotoxicity by olaparib was greater in cell lines with low ATM expression compared high ATM expressing cell lines (Sanmartín *et al.*, 2017). Low ATM has also been shown to lead to greater sensitisation of alkylating agents by PARP inhibitors using ATM complemented ataxia-telangiectasia (AT) cell lines (Carrozza *et al.*, 2009), *ATM*$^{-/-}$ mouse embryonic fibroblasts (Löser *et al.*, 2010) and in *ATM* mutant chronic lymphocytic leukaemia (CLL) cells (Weston *et al.*, 2010). Greater sensitisation of irinotecan by PARP inhibition in ATM deficient cells has also been observed in gastric cancers (Subhash *et al.*, 2016). These studies suggest that ATM deficient tumours may be particularly vulnerable to PARP inhibition in combination with conventional chemotherapeutic agents, such as temozolomide and irinotecan, which are currently used to treat NB.

5.5.3 The relationship between PARP expression/activity and sensitivity to PARP inhibition

High PARP1 expression in NB is associated with high disease stage and worse overall survival (Newman *et al.*, 2015; Colicchia *et al.*, 2017; Avitabile *et al.*, 2020). In the current study, high PARP1 protein expression in NB cell lines seemed to indicate resistance to olaparib-induced growth inhibition or cell death, although this was not statistically significant (**Figure 5.9**). A study in AML patient-derived bone marrow cells also found that PARP1/2 expression did not correlate with olaparib sensitivity (Faraoni *et al.*, 2015). However, in small cell lung cancer and CLL, high expression of PARP1 correlated with high PARP1 activity, which was associated with increased cytotoxicity of PARP inhibition (Byers *et al.*, 2012; Cardnell *et al.*, 2013; Herriott *et al.*, 2015). Endogenous PARP activity in this panel of NB cell lines has not been analysed and little correlation between PARP1 protein expression and activity in NB cell lines has been shown previously (Zaremba *et al.*, 2009). Investigating PARP activity using an assay, such as the PARP assay described by (Pfeiffer *et al.*, 1999), or measurement of endogenous PAR levels by Western blot or IHC, is required to determine the role of PARP expression/activity in determining sensitivity to PARP inhibition in NB cell lines.

5.5.4 Strengths and limitations

The strength of this study is that sensitivity to olaparib induced cytotoxicity has been examined in 2 sets of paired cell lines as well as a panel of cell lines with diverse molecular characteristics. Using paired cell lines allows the effect of one gene or protein on sensitivity to PARP inhibition to be interrogated but will not identify a robust biomarker that can be used clinically. Analysing the effect of gene mutations or protein expression level in a panel of cell lines shows that the role of one molecular feature is more complex. The relatively small size of the cell line panel limits this study, and increasing the number of cell lines may have revealed a significant difference in olaparib cytotoxicity between *MYCN* amplified and non-amplified cell lines or cell lines with functional and non-functional ATM.

This study also analysed the function of ATM and p53 using functional read-outs. Although the impact of gene mutation on the function of the protein can be predicted from the amino acid or domain affected (Reva *et al.*, 2011; Choi *et al.*, 2012; Sim *et al.*, 2012), functional read-outs allow for definitive characterisation of protein activity.

Interestingly, the increased cytotoxicity in cell lines expressing high levels of MYCN and ATR pathway activation suggest RS is key to determining response to olaparib. However, when analysed using other markers of RS, H2AX^{S139} and RPA2^{S8} phosphorylation levels, there was no significant difference in the cytotoxicity of olaparib. Correlating endogenous PARP activity with these different indicators of RS may indicate why ATR pathway activation is key to determining response to PARP inhibition.

The work presented in this chapter only investigated the effect of one PARP inhibitor, olaparib. The mechanism of cytotoxicity of PARP inhibitors has been shown to not only be from inhibition of catalytic activity but also from trapping of PARP1/2 on DNA, creating single strand DNA intermediates similar to those generated by topoisomerase I poisons (Ström *et al.*, 2011; Murai *et al.*, 2012; Pommier *et al.*, 2016). Clinical PARP inhibitors show a range of PARP trapping ability (trapping from least to most potent): veliparib < olaparib/ rucaparib < niraparib < talazoparib (Pommier *et al.* 2016). King *et al*. showed that talazoparib is more potent and more cytotoxic than olaparib or veliparib in both *MYCN* amplified and non-amplified cell lines (King *et al.* 2020). The trapping ability of the different PARP inhibitors must be considered when evaluating the efficacy of PARP inhibition in NB, especially in combination with other genotoxic agents. Clinical PARP inhibitors also have different toxicity profiles (LaFargue *et al.*, 2019), which may influence the choice of inhibitor when it comes to combination therapy.

This chapter focused on evaluating the effect of determinants of ATR inhibition in NB, identified in chapter 4, on sensitivity to PARP inhibition and, although there is rationale for using markers such as MYCN and ATM expression as determinants of PARP inhibitor sensitivity, many of the previously validated biomarkers of sensitivity to PARP inhibitors in other tumours, such mutations affecting HRR, have not been evaluated here.

Other proposed markers of PARP inhibitor sensitivity include expression of SLFN11 and mutations in *ATRX* or *ARID1A*. SLFN11 is a nuclear restriction factor which blocks replication forks and induces cell death in response to RS (Murai *et al.*, 2019). SLFN11 expression is associated with sensitivity to PARP inhibitors, whereas lack of expression is associated with resistance across cancer types (Murai *et al.*, 2016). SLFN11 has yet to be evaluated in NB but is now being considered as a pan-cancer biomarker of sensitivity to PARP inhibitors and DNA damaging agents.

ATRX and ARID1A are components of the SWI/SNF chromatin remodelling complex. Mutation or deletion of *ATRX* is reported in around 11% of NB and is associated with older age and an indolent but fatal disease course (Cheung *et al.*, 2012). Recently, George *et al.* identified that *ATRX* mutant cell lines were deficient in HRR and were more sensitive than wild type cell lines to the PARP inhibitors talazoparib, olaparib and rucaparib following a high throughput drug screen (George *et al.*, 2020a). *ARID1A* mutations have been reported in around 5% of NB tumours (Sausen *et al.*, 2013; Lee *et al.*, 2017). ARID1A deficiency has been shown to lead to DNA double strand break repair deficiency and increased olaparib-induced cytotoxicity in isogenic cell lines (Park *et al.*, 2019). Further investigation of the role of ATRX and ARID1A in PARP inhibitor sensitivity in NB may provide additional markers of PARP inhibitor sensitivity.

5.6 Conclusion

From the results presented in this chapter, it can be concluded that high CHK1 protein expression and ATR activity ($CHK1^{S345}$ phosphorylation) may identify cells which are vulnerable to PARP inhibition. Overexpression of MYCN increases sensitivity to olaparib when analysed in MYCN expression regulatable cell lines but did not determine sensitivity when analysed in a panel of NB cell lines with varied genetic characteristics. In addition, reduced ATM expression or p53 mutation did not determine sensitivity to single agent olaparib inhibitors in the panel of cell lines studied here. It may be that in the context of complex genetic alterations, cells may have acquired a spectrum of features leading to resistance, as well as sensitivity, to these inhibitors, making it difficult to predict response.

Chapter 6: Exploring ATR inhibition in combination with conventional chemotherapeutic agents and PARP inhibition

6.1 Introduction

In the previous chapters, RS and increased signalling through ATR, caused by MYCN overexpression or loss of DNA damage signalling through ATM, was identified as a determinant of sensitivity to ATR inhibition and may increase sensitivity to PARP inhibition. Conventional chemotherapeutic agents, such as temozolomide and topotecan currently used to treat NB, increase RS and therefore reliance on ATR signalling (Zhang *et al.*, 2016). Temozolomide is an alkylating agent which leads to accumulation of O6-methylguanine (O6MeG), N7-methylguanine (N7MeG) and N3-methyladenine (N3MeA) lesions, which are removed by base excision repair (BER), generating transient SSB (Fu *et al.*, 2012). Failure to remove these lesions blocks DNA replication and activates ATR (Jackson *et al.*, 2019). Topotecan is a topoisomerase I (Top1) poison, which traps Top1 on the DNA, forming persistent Top1 cleavage complexes resulting in an increase in unrepaired Top1 induced single strand breaks (Staker *et al.*, 2002). Collision between Top1 cleavage complexes and replication or transcription machinery leads to the formation of double strand breaks, repair of which requires activation of HRR through ATR signalling (Jossé *et al.*, 2014). Inhibition of ATR may sensitise NB cells to temozolomide or topotecan, possibly allowing for reduced doses of these agents.

In chapter 3, PARP inhibition by olaparib was shown to increase RS and activate ATR signalling. Olaparib is known to trap PARP1 on DNA, leading to DNA-PARP1 complexes in a similar mechanism to Top1 cleavage complexes (Murai *et al.*, 2012). Inhibiting ATR in combination with PARP inhibition has been shown to overcome replication fork restoration, a key mechanism of PARP inhibitor resistance in *BRCA* deficient ovarian cancer (Yazinski *et al.*, 2017; Kim *et al.*, 2020). The combination of PARP and ATR inhibitors has been shown to be synergistic in ATM-deficient cancers (Jette *et al.*, 2019; Lloyd *et al.*, 2020). Both PARP and ATR have been reported to act at stalled replication forks during RS (Sugimura *et al.*, 2008; Bryant *et al.*, 2009; Saldivar *et al.*, 2017), therefore dual inhibition of PARP and ATR should result in intolerable levels of RS.

Here the effect of MYCN and ATM protein expression, and p53 function on synergism between PARP and ATR inhibition is explored in NB cell lines. The effect of dual PARP and ATR inhibition on cell cycle checkpoint activation, RS and HRR is also investigated in selected *MYCN* amplified and non-amplified cell lines.

6.2 Chapter aims

The aims of this chapter were as follows:

1. To examine the effect of ATR inhibition on temozolomide, topotecan and olaparib cytotoxicity in NB cell lines

2. To examine the effect of dual PARP and ATR inhibition on RS, DNA damage repair and cell cycle checkpoint arrest in NB cells

6.3 Methods

6.3.1 Cells and cell culture

The 10 cell lines included in the NB cell line panel have been characterised in detail in chapter 3 and were cultured and maintained as described in section 2.1. The MYCN regulatable cell lines SHEPtet21N and IMR5/75 shMYCN were maintained as described for the other cell lines but incubated with 1 µg/ml doxycycline for 72 hours for MYCN off states prior to experiments.

6.3.2. Reagents

Temozolomide, topotecan, VE-821, AZD6738, olaparib and doxycycline were used and stored as described in section 2.2.

6.3.3 Cytotoxicity assays

XTT cell proliferation (Roche) and clonogenic survival assays were carried out as described in sections 2.3.

6.3.4 Protein expression analysis

Lysates of NGP, SHSY5Y and SKNAS cell lines were collected as described in section 2.5.1 after treatment with indicated concentrations of olaparib and VE-821. Proteins were separated using gel electrophoresis using a 4-20% Tris-acetate or 4-20% Tris-glycine polyacrylamide gel (Bio-Rad, Hemel Hempstead, UK), transferred onto nitrocellulose and detected using Western blotting as described in section 2.5.2. pRPA2^{S8}, γH2AX and GAPDH were detected using primary antibodies described in **Table 2.5** and the appropriate HRP-conjugated secondary antibodies. Protein expression was measured by chemiluminescence from exposure to ECL detection reagent using a ChemiDoc imaging system as described in section 2.5.2.

6.3.5 Cell cycle analysis

Cell cycle profiles were analysed after treatment with VE-821 and/or olaparib by flow cytometry as described in section 2.7.

6.3.6 Immunofluorescence

Cells were immunostained for pRPA2^{S8}, γH2AX and RAD51 after treatment with 1 µM VE-821 with or without 10 µM olaparib for 24 hours as described in section 2.6. The number of pRPA2S8, γH2AX and RAD51 foci in each cell were quantified and the total nuclear fluorescence intensity of γH2AX was measured using ImageJ software (Version 1.52p; Java 1.8.0_172 (64-bit)).

6.3.7 Data analysis

T-test, 2-way ANOVA and Mann Whitney U statistical tests were carried out using GraphPad Prism v8 software and p values < 0.05 were taken to be statistically significant.

The sensitising effect of VE-821 on olaparib cytotoxicity measured by XTT cell proliferation and clonogenic survival assay was determined by calculating the sensitisation factor (SF).

SF= (effect of 1 µM olaparib)/(effect of 1 µM olaparib +1 µM VE-821 normalised to VE-821 alone).

Combination Index (CI) values for evaluation of synergy were determined by the Chou–Talalay method using CalcuSyn v2 software (Biosoft, Cambridge, UK).

6.4. Results

6.4.1 ATR inhibition in combination with chemotherapeutic drugs

To examine the effect of ATR inhibition on topotecan and temozolomide-induced growth inhibition, XTT cell proliferation assays were carried out on six NB cell lines, the non-*MYCN* amplified SHSY5Y (*TP53* wt) and SKNAS (*TP53* mutant) cell lines and the *MYCN* amplified NGP and IMR32 cell lines and their *TP53* mutant pairs, N20_R1 and KAT100 respectively, treated with increasing concentrations of topotecan or temozolomide alone and with the addition of 1 µM VE-821.

Figure 6.1 shows the sensitisation of topotecan induced growth inhibition by 1 µM VE-821. *TP53* wild type cells were more sensitive to topotecan and were only sensitised by VE-821 when topotecan-induced growth inhibition was <90%. The crossover in the *TP53* wild type cell lines is a function of the normalisation as 1 µM VE-821 alone results in 20% growth inhibition in the SHSY5Y cell line and 40% and 45% in the NGP and IMR32 cell lines, respectively (Chapter 4). Since the *TP53* mutant cells were more resistant to topotecan alone, 1 µM VE-821 sensitised growth inhibition at all concentrations.

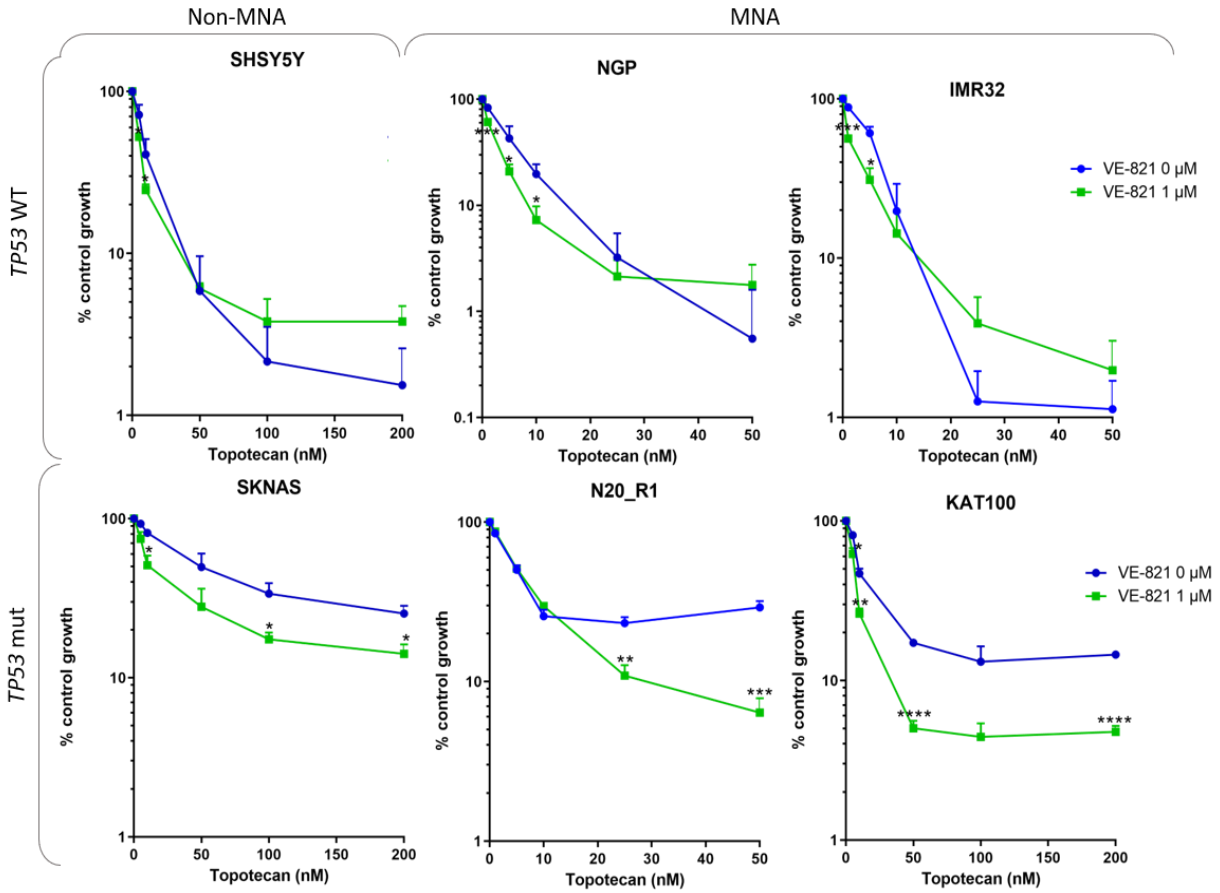

Figure 6.114: *XTT cell proliferation of the SHSY5Y, SKNAS, NGP, N20_R1, IMR32 and KAT100 neuroblastoma cell lines treated with increasing concentrations of topotecan alone (blue) or with the addition of 1 µM VE-821 (green). Percentage control growth was normalised to effect of VE-821 alone. Data shown are the mean + SEM from 3 individual experiments. T-test: *p<0.05, ** p<0.01, ***p<0.001, ****p<0.0001. MNA: MYCN amplified, WT: wild type, mut: mutant.*

These cell lines varied in their sensitivity to temozolomide, with no obvious effect of *TP53* or *MYCN* status (**Figure 6.2**). The concentration range used was not sufficient to cause >90% growth inhibition and an IC50 could not be obtained in the SHSY5Y, SKNAS and N20_R1 cell lines. Sensitisation by VE-821 was generally greater at concentrations of temozolomide that caused >25% growth inhibition in all cell lines and independent of *MYCN* and *TP53*. The addition of 1 µM VE-821 had little effect on temozolomide sensitivity in the SKNAS cell line, which is especially resistant to temozolomide alone.

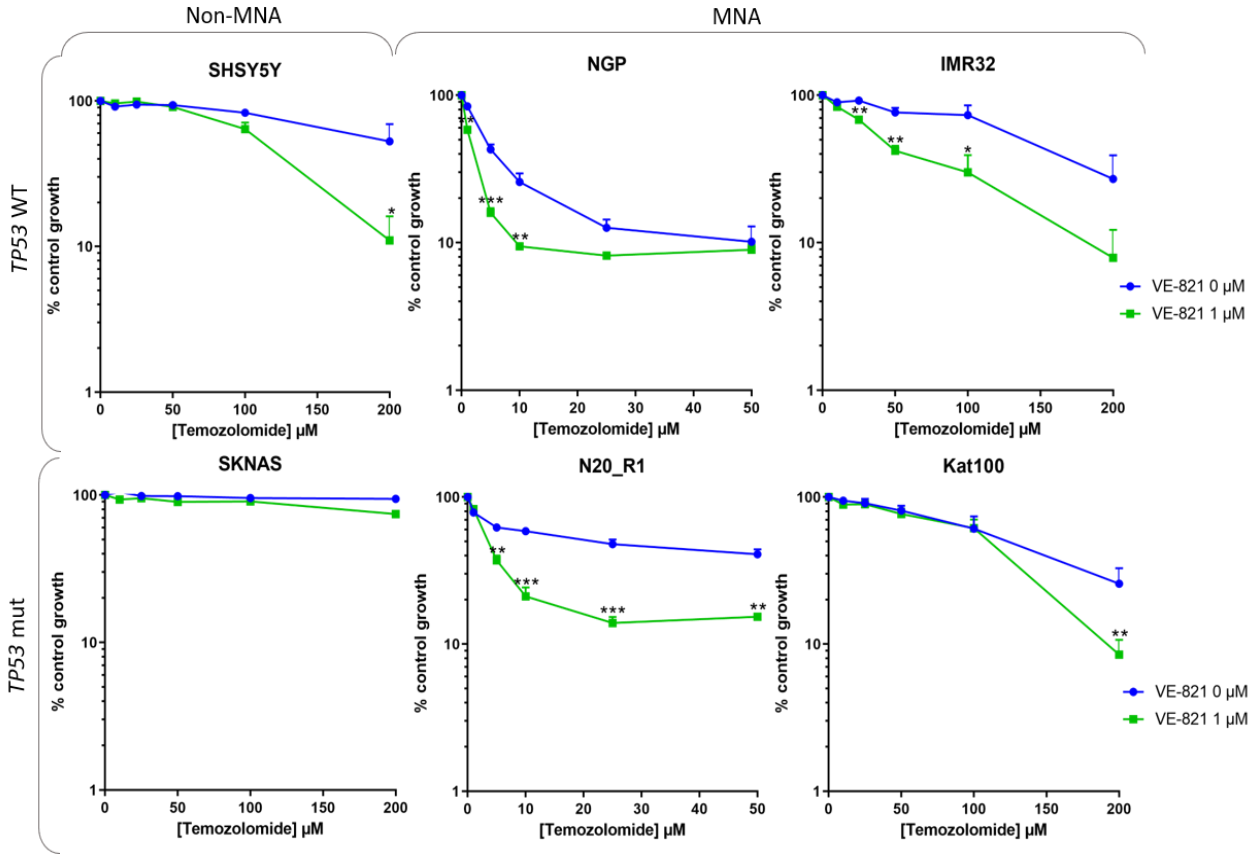

***Figure 6.2**: XTT cell proliferation of the SHSY5Y, SKNAS, NGP, N20_R1, IMR32 and KAT100 neuroblastoma cell lines treated with increasing concentrations of temozolomide alone (blue) or with the addition of 1 µM VE-821 (green). Percentage control growth was normalised to effect of VE-821 alone. Data shown are the mean + SEM from 3 individual experiments. T-test: *p<0.05, ** p<0.01, ***p<0.001, ****p<0.0001. MNA: MYCN amplified, WT: wild type, mut: mutant.*

6.4.2 ATR inhibition in combination with PARP inhibition

To examine the effect of ATR inhibition on PARP inhibitor sensitivity, growth inhibition by increasing concentrations of olaparib alone, and in combination with 0.1 or 1 µM VE-821 was measured by XTT cell proliferation assay in the SHSY5Y and SKNAS cell lines and the NGP/ N20_R1 and IMR32/ KAT100 cell line pairs (**Figure 6.3A**). 1 µM VE-821 significantly sensitised the *MYCN* amplified NGP, N20_R1, IMR32 and KAT100 cell lines to 1 µM olaparib (**Figure 6.3B**). Although not statistically significant, olaparib induced growth inhibition was increased by VE-821 in the non-*MYCN* amplified SHSY5Y and SKNAS cell lines. Synergism between VE-821 and olaparib was determined by combination index analysis (calcusyn) where combination index (CI) <1 indicates synergy. PARP inhibition was synergistic with ATR inhibition in all cell lines, irrespective of *MYCN* or *TP53* status (**Figure 6.3C**).

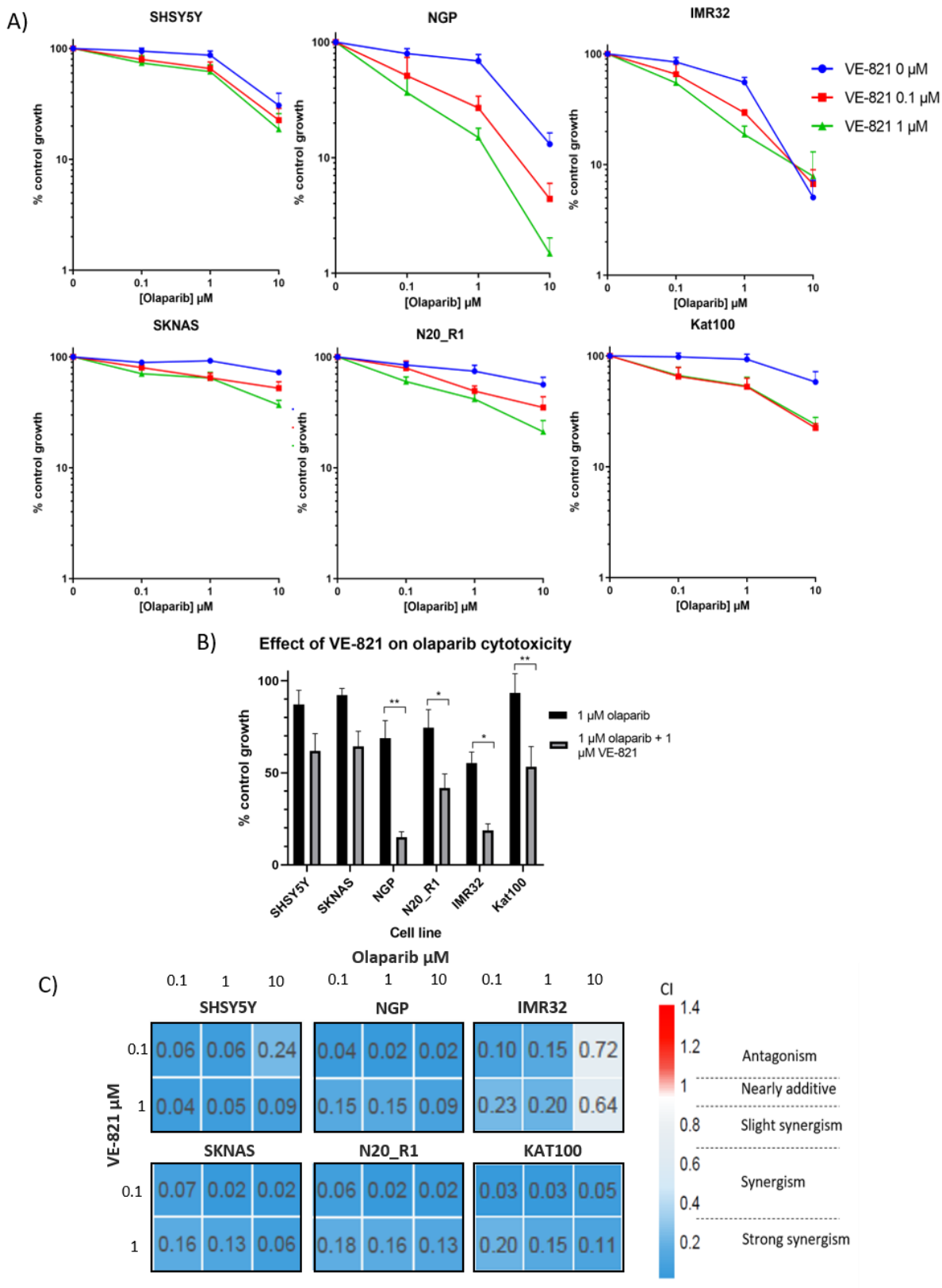

Figure 6.3: *A) XTT cell proliferation of the SHSY5Y, SKNAS, NGP, N20_R1, IMR32 and KAT100 neuroblastoma cell lines treated with 0.1, 1 and 10 µM olaparib alone and with the addition of 0 (blue), 0.1 (red) and 1 (green) µM VE-821. Percentage control growth was normalised to effect of VE-821 alone. Data shown are the mean + SEM from 4 individual experiments. B) Effect of 1 µM VE-821 on cytotoxicity of 1 µM olaparib normalised to the effect of VE-821 alone. Data shown are the mean + SEM from 4 individual experiments. 2-way ANOVA: *p<0.05, ** p<0.01, C) Combination index (CI) values were calculated using CalcuSyn and plotted in a heat map.*

The sensitising effect of VE-821 on olaparib cytotoxicity was confirmed by clonogenic survival assay in the SHSY5Y, SKNAS, NGP and N20_R1 cell lines (**Figure 6.4A**), where 1 μM VE-821 significantly sensitized the *MYCN* amplified NGP and N20_R1 cell lines to 1 μM olaparib but not the non-*MYCN* amplified SHSY5Y and SKNAS cell lines, although percentage survival was decreased (**Figure 6.4B**). As in chapter 5, there was a greater dynamic range in olaparib cytotoxicity when measured by clonogenic survival assay than XTT cell proliferation assay. The greater sensitisation of olaparib in *MYCN* amplified cell lines was much more profound when measured by clonogenic assay, with the percentage survival of NGP and N20_R1 cells in response to 1 μM olaparib being increased 77- and 16-fold respectively in combination with VE-821, compared to 4.6- and 1.79-fold respectively when analysed by XTT (**Table 6.1**). Synergism between VE-821 and olaparib was also confirmed at lower concentrations (< 1 μM) by clonogenic assay (**Figure 6.4C**). However, there is some antagonism (CI>1) seen at the highest olaparib concentration in the SHY5Y and N20_R1 cell lines, which is reflected in the overlapping survival curves (**Figure 6.4A**). There is also antagonism in the NGP cell line following treatment with 0.1 μM VE-81 and 1 μM olaparib, which is not reflected in the graph.

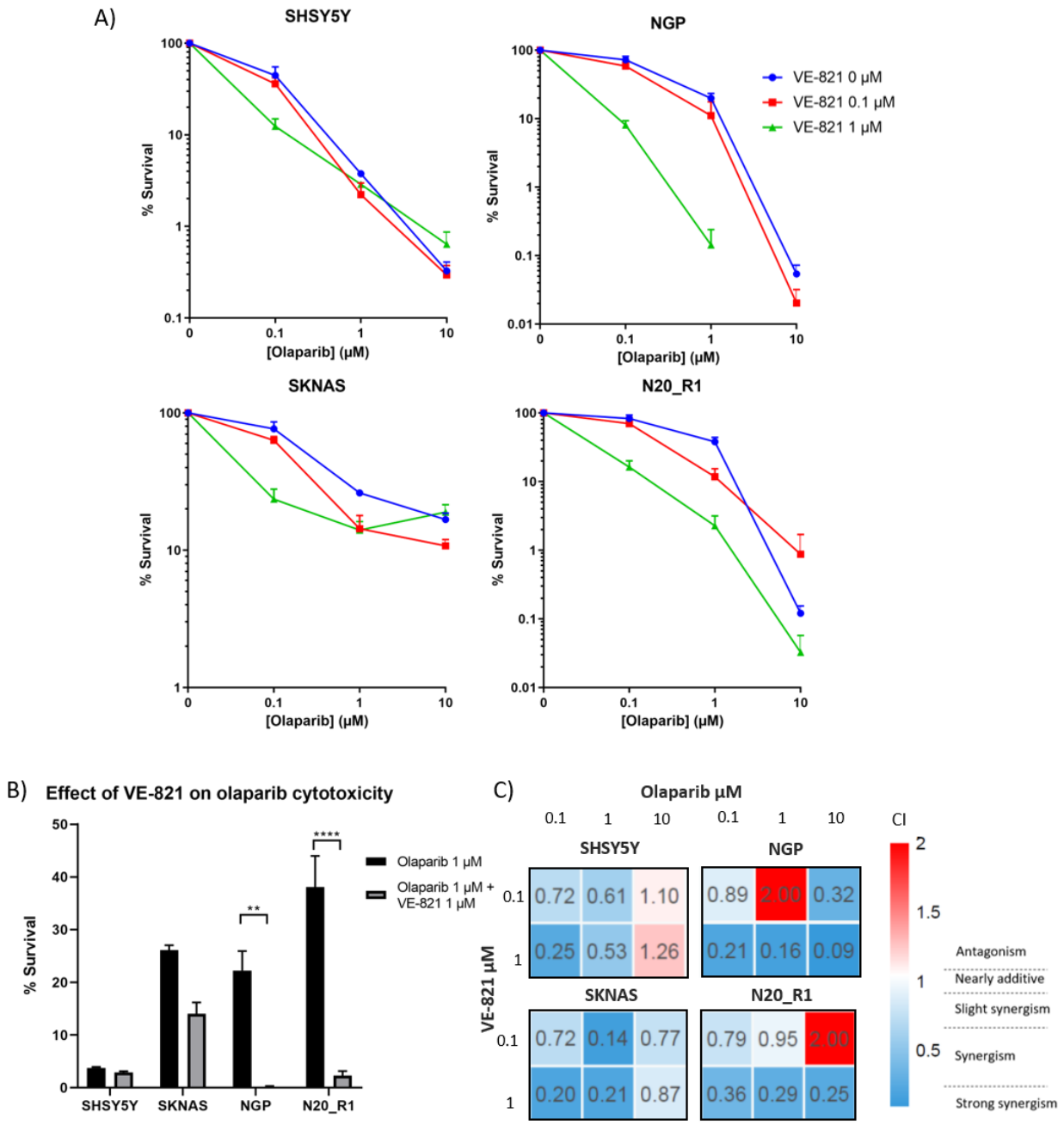

Figure 6.4: *A) Clonogenic survival of the SHSY5Y, SKNAS, NGP and N20_R1 neuroblastoma cell lines treated with 0.1, 1 and 10 μM olaparib alone and with the addition of 0 (blue), 0.1 (red) and 1 (green) μM VE-821. Percentage survival was normalised to effect of VE-821 alone. Data shown are the mean + SEM from 3 individual experiments. B) Effect of 1 μM VE-821 on cytotoxicity of 1 μM olaparib normalised to the effect of VE-821 alone. Data shown are the mean + SEM from 3 individual experiments. 2-way ANOVA: ** p<0.01, ****p<0.0001 C) Combination index (CI) values were calculated using CalcuSyn and plotted in a heat map.*

The sensitising effect of ATR inhibition on PARP inhibitor cytotoxicity was confirmed using another ATR inhibitor, AZD6738. Growth inhibition caused by increasing concentrations of olaparib alone, and in combination with 0.1 or 1 μM AZD6738 was measured by XTT cell proliferation assay in the SHSY5Y, SKNAS, NGP and N20_R1 cell lines (**Figure 6.5**). 1 μM AZD6738 significantly sensitized the *TP53* wild type SHSY5Y and NGP cell lines to 1 μM olaparib (**Figure 6.5B**). Although not statistically significant, olaparib induced growth inhibition was increased by AZD6738 in the N20_R1 cell line. AZD6738 had the least sensitising effect on the SKNAS cell line. This is in contrast with sensitisation with VE-821 where there was significant olaparib sensitisation in the NGP and N20_R1 cell lines, but not the SHSY5Y and SKNAS cell lines, although olaparib-induced growth inhibition was increased in combination with VE-821.

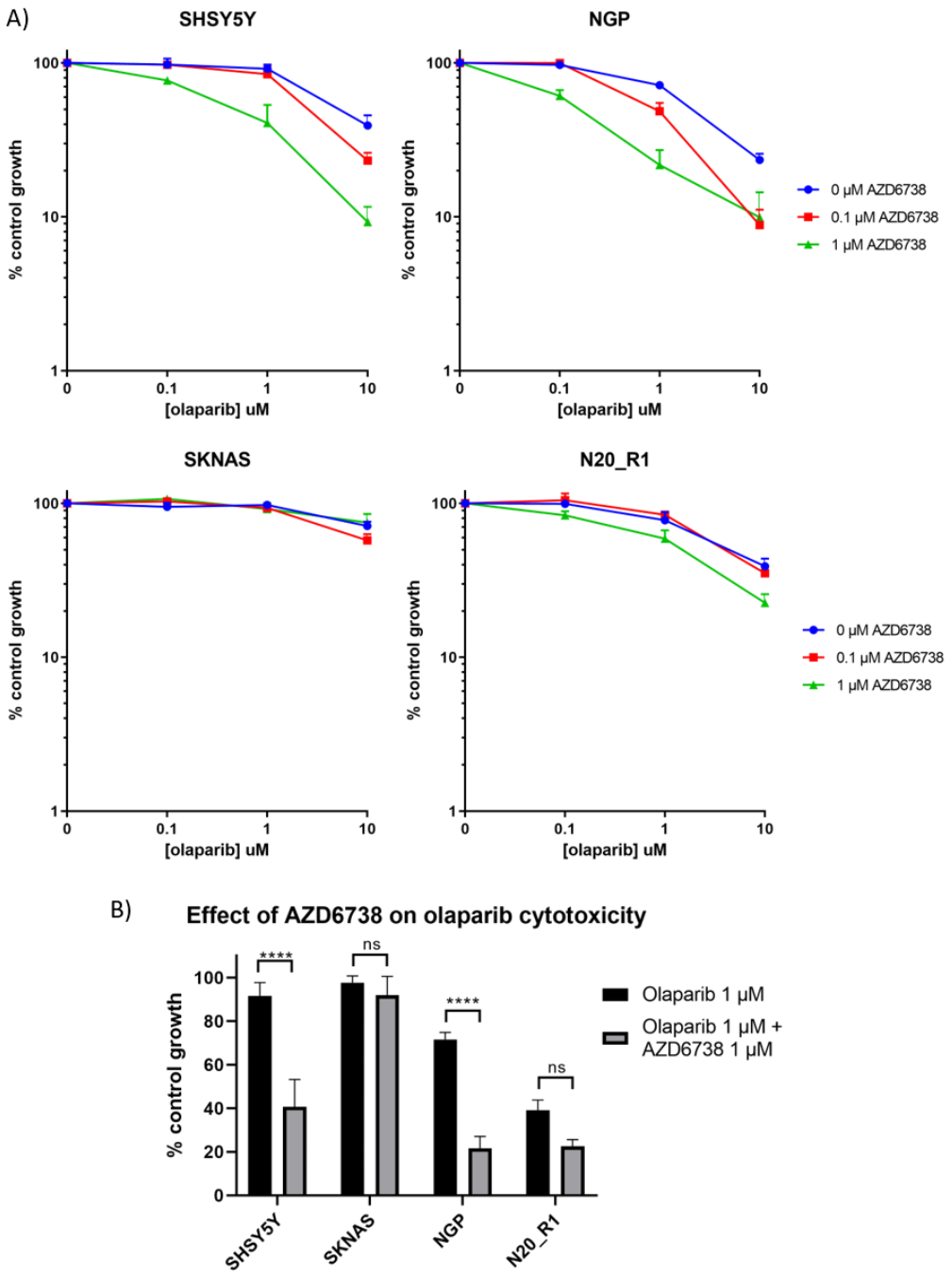

Figure 6.5: *A) XTT cell proliferation of the SHSY5Y, SKNAS, NGP and N20_R1 NB cell lines treated with 0.1, 1 and 10 µM olaparib alone and with the addition of 0 (blue), 0.1 (red) and 1 (green) µM AZD6738. Percentage control growth was normalised to the effect of AZD6738 alone. Data shown are the mean + SEM from 4 individual experiments. B) Effect of 1 µM AZD6738 on cytotoxicity of 1 µM olaparib normalised to the effect of AZD6738 alone. Data shown are the mean + SEM from 4 individual experiments. 2-way ANOVA: ****p<0.0001, ns= not significant.*

The SF of 1 µM olaparib by 1 µM AZD6738 and VE-821 for each cell line by XTT and clonogenic assay is reported in **Table 6.1.**

Table 6.1: Summary of cell line DDR defects and sensitisation factor (SF) of AZD6738 and VE-821 on olaparib cytotoxicity assays.

Cell line	*MYCN* status	*TP53* status	ATM protein expression	AZD6738 SF XTT	VE-821 SF XTT	VE-821 SF clonogenic
SHSY5Y	Non-amp	WT	High	2.25	1.41	1.31
SKNAS	Non-amp	Mutant	High	1.06	1.43	1.86
NGP	Amp	WT	Low	3.30	4.60	77.93
N20_R1	Amp	Mutant	High	1.32	1.79	16.73
IMR32	Amp	WT	Low	-	2.96	-
KAT100	Amp	Mutant	Low	-	1.75	-

6.4.3 Sensitisation by MYCN status/expression

To determine whether MYCN expression impacts the level of sensitisation to olaparib cytotoxicity by ATR inhibition, the SF of 1 µM VE-821 on olaparib induced growth inhibition calculated by XTT assay (**Table 6.1**) was analysed by MYCN protein expression. Although the SF was greater in cell lines expressing high levels of MYCN protein, this did not reach significance (**Figure 6.6A**) but the SF was significantly positively correlated with MYCN protein expression (**Figure 6.6B**).

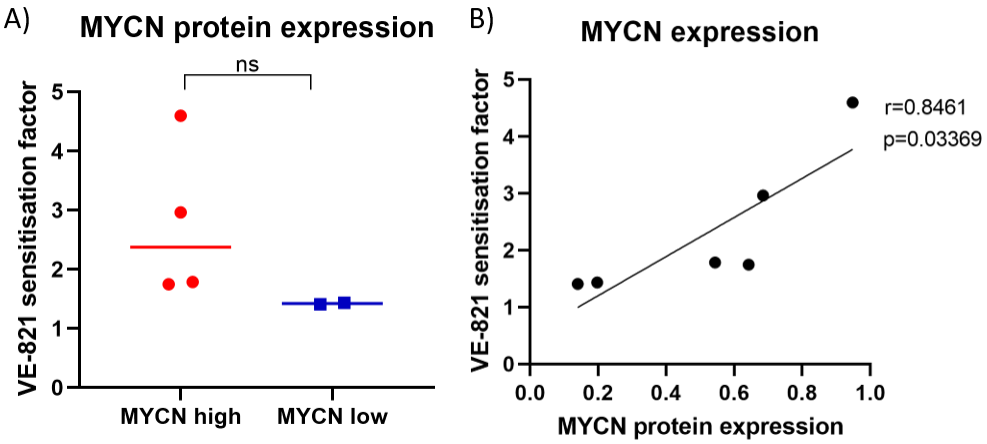

Figure 6.6: *A) Cell lines were split into 2 groups based on MYCN protein expression. VE-821 sensitisation factor calculated by XTT assay (Table 6.1) was plotted for cell lines belonging to each group. B) Correlation of MYCN protein expression vs. VE-821 sensitisation factor.*

To investigate the effect of MYCN expression alone on sensitisation to olaparib cytotoxicity by ATR inhibition, the effect of 1 µM VE-821 on olaparib-induced growth inhibition was

measured by XTT cell proliferation assay in the MYCN expression regulatable cell lines, SHEPtet21N and IMR5/75 shMYCN (**Figure 6.7 A and B**). In both cell lines, the effect of VE-821 on olaparib induced growth inhibition was greater in the MYCN overexpressing cells compared to cells with low MYCN expression (**Figure 6.7C**). The sensitising effect was confirmed by inhibition ATR with AZD6738 (**Figure 6.8**).

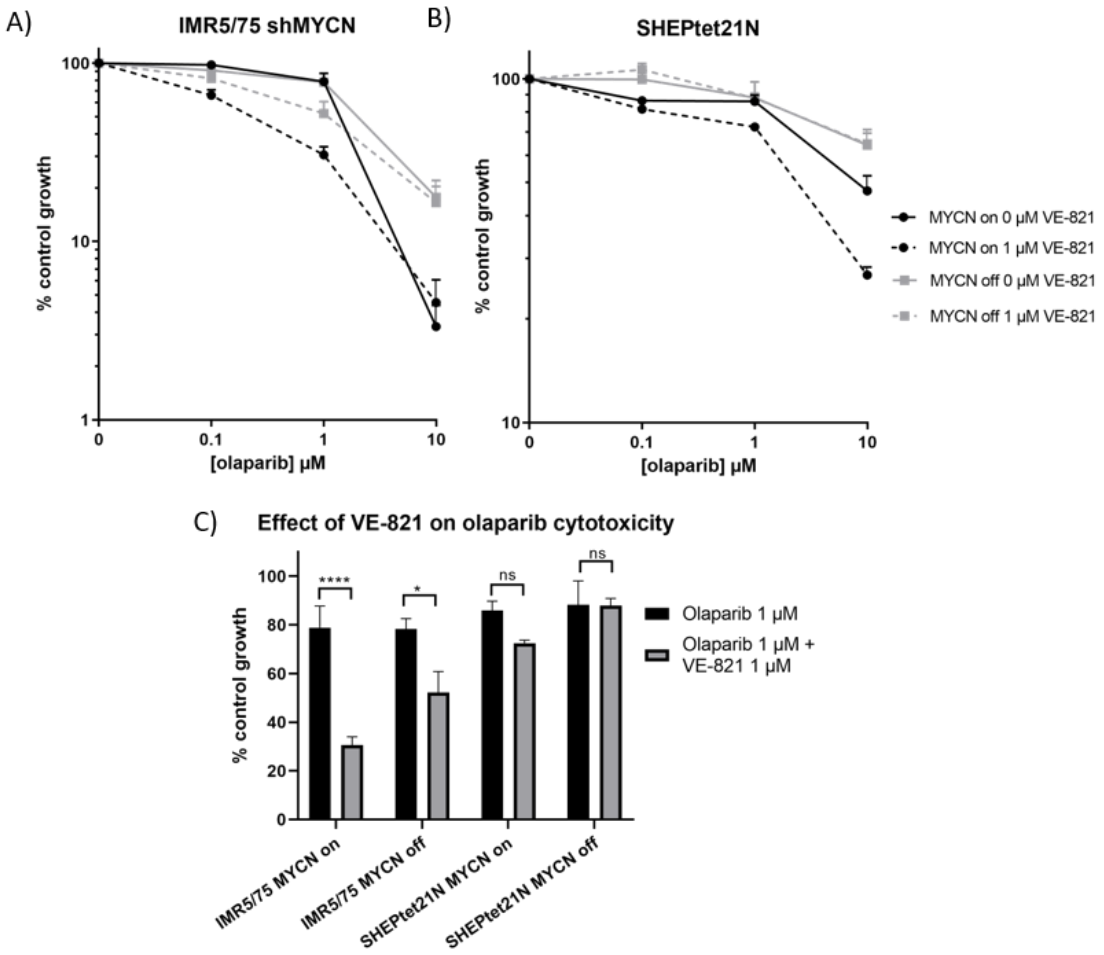

Figure 6.7: *XTT cell proliferation of the A) IMR5/75 shMYCN and B) SHEPtet21N cell lines in MYCN on (black lines) and MYCN off (grey lines) states treated with 0.1, 1 and 10 µM olaparib alone (solid line) and with 1 µM VE-821 (dashed line). Percentage control growth was normalised to the effect of VE-821 alone. Data shown are the mean + SEM from 4 individual experiments. C) Effect of 1 µM VE-821 on cytotoxicity of 1 µM olaparib normalised to the effect of VE-821 alone. Data shown are the mean + SEM from 4 individual experiments. 2- way ANOVA: * p<0.05, ****p<0.0001, ns=not significant*

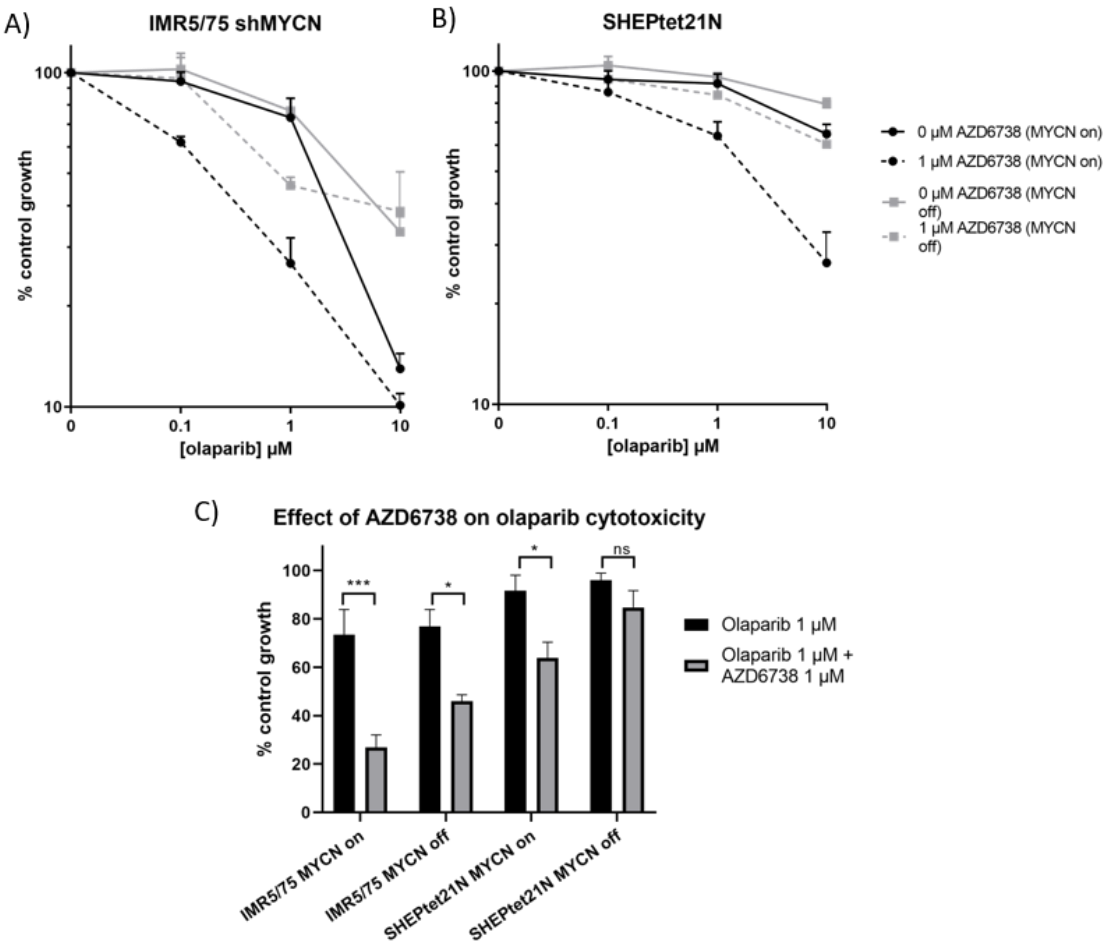

Figure 6.8: *XTT cell proliferation of the A) IMR5/75 shMYCN and B) SHEPtet21N cell lines in MYCN on (black lines) and MYCN off (grey lines) states treated with 0.1, 1 and 10 µM olaparib alone (solid line) and with 1 µM AZD6738 (dashed line). Percentage control growth was normalised to the effect of AZD6738 alone. Data shown are the mean + SEM from 4 individual experiments. C) Effect of 1 µM AZD6738 on cytotoxicity of 1 µM olaparib normalised to the effect of AZD6738 alone. Data shown are the mean + SEM from 4 individual experiments. 2- way ANOVA: * p<0.05, ns=not significant*

6.4.4 Sensitisation by ATM/ p53 status

To determine whether the level of ATM expression impacts sensitisation to olaparib cytotoxicity by ATR inhibition, the SF of VE-821 on olaparib-induced growth inhibition calculated by XTT assay (**Table 6.1**) was analysed by ATM protein expression. The SF was greater in the cell lines expressing low levels of ATM protein (**Figure 6.9A**), although this was not statistically significant. However, there was no correlation between SF and ATM protein expression (**Figure 6.9B**).

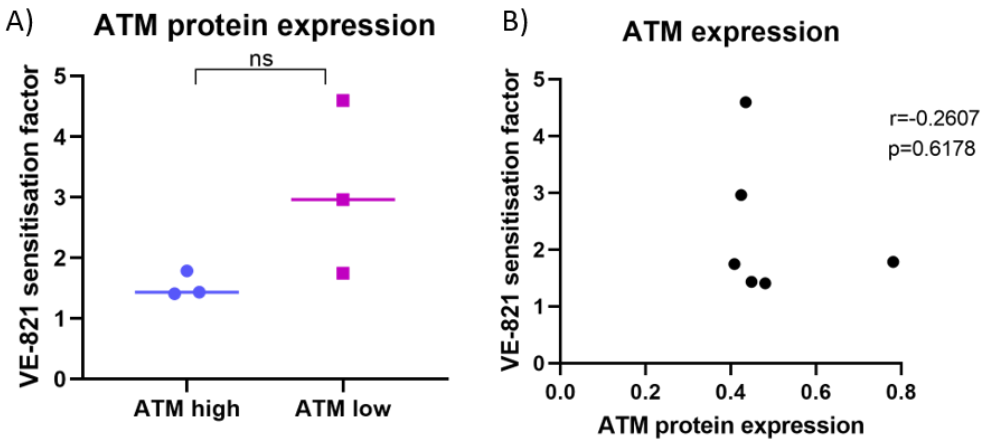

***Figure 6.9**: A) Cell lines were split into 2 groups based on ATM protein expression above (high) or below (low) median expression. VE-821 sensitisation factor calculated by XTT assay (Table 6.1) was plotted for cell lines belonging to each group. B) Correlation of ATM protein expression vs. VE-821 sensitisation factor.*

The effect of *TP53* mutation and p53 protein expression on olaparib sensitisation by VE-821 was analysed using six cell lines. The SF was greater in *TP53* wild type cell lines (**Figure 6.10**), although this was not statistically significant.

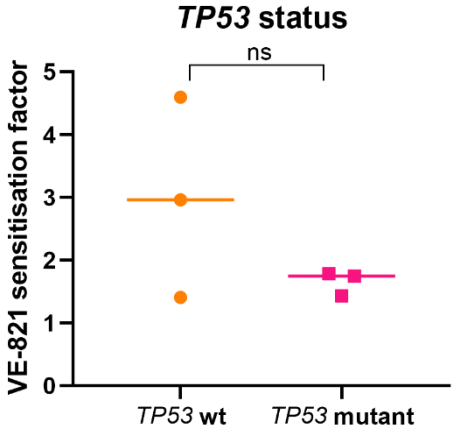

***Figure 6.10:** Cell lines were split into 2 groups based on TP53 mutation status. VE-821 sensitisation factor calculated by XTT assay (Table 6.1) was plotted for cell lines belonging to each group. wt: wild type.*

6.4.5 PARP and ATR inhibitors have the greatest effect on cell proliferation when co-administered

To examine if inhibiting PARP prior to ATR, or vice versa, has a greater effect on growth inhibition or survival of NB cell lines, XTT cell proliferation and clonogenic survival assays were carried out on the SHSY5Y, SKNAS and NGP cell lines treated with combined VE-821 and olaparib for 72 hours or after pre-treatment with either VE-821 or olaparib for 24 hours

followed by exposure to olaparib or VE-821, respectively, for 72 hours (**Figure 6.11**). Although growth inhibition and cell death were increased when cells were pre-treated with either VE-821 or olaparib, the greatest effect was seen when cells were treated with both inhibitors at the same time.

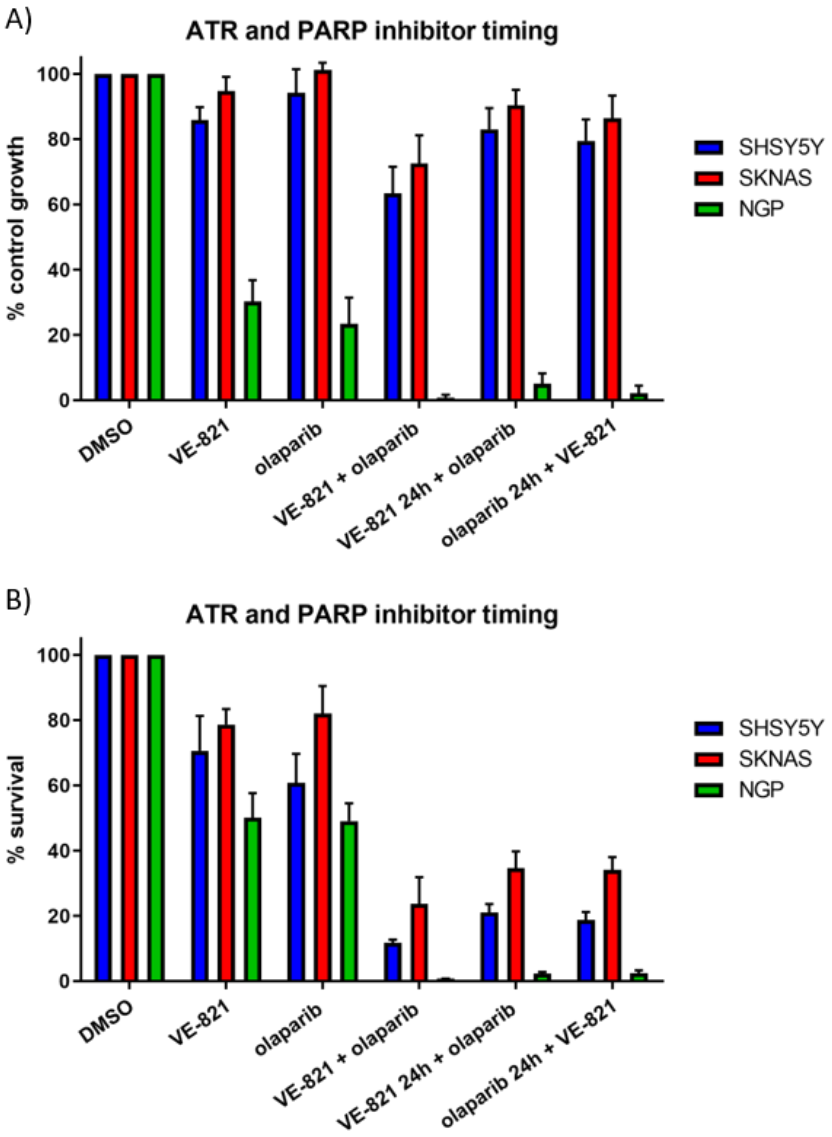

***Figure 6.11**: Percentage control growth (A) or percentage survival (B), measured by XTT cell proliferation or clonogenic survival assays respectively, of the SHSY5Y, SKNAS and NGP cell lines after treatment with 1 µM VE-821 and/or 1 µM olaparib for 72 hours. In the two columns on the far right, cells were pre-treated with either 1 µM VE-821 or 1 µM olaparib for 24 hours before addition of the other inhibitor. Data are mean + SEM of 3 individual experiments.*

6.4.6 Effect of ATR and PARP inhibition on cell cycle

To examine the effect of PARP and ATR inhibition on the cell cycle, the cell cycle phase distribution of asynchronous SHSY5Y, SKNAS and NGP cells were analysed after treatment with VE-821 and/or olaparib for 24 hours (**Figure 6.12**). Olaparib treatment alone increased the proportion of cells in S and G2 phase in all cell lines, suggesting activation of S and G2 checkpoint arrest. This was not observed in cells treated with both olaparib and VE-821, suggesting loss of S and G2 checkpoint arrest. VE-821 alone had little effect on the proportion of cells in each cell cycle phase compared to control.

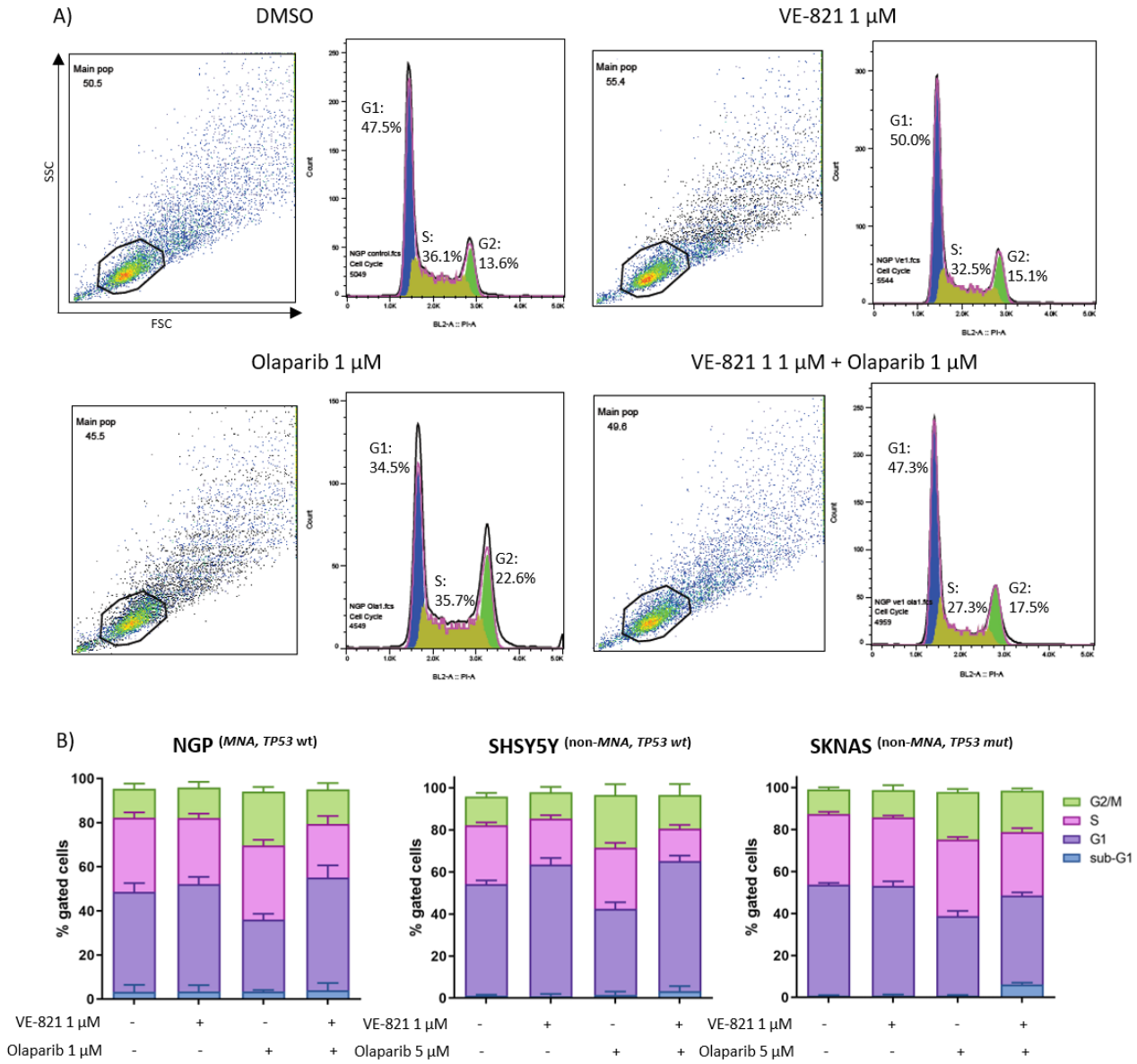

Figure 6.12: *Cell cycle analysis using propidium iodide (PI) in response to ATR and PARP inhibition A) Representative forward and side scatter density plots and PI density histograms of gated population for NGP cells treated with 1 µM VE-821 and/or 1 µM olaparib for 24 hours. B) Cell cycle phase distribution of SHSY5Y, SKNAS and NGP cell lines treated with 5 µM (SHSY5Y and SKNAS) or 1 µM (NGP) olaparib in combination with 1 µM VE-821 for 24 hours. Data are mean + SEM from 3 independent experiments. MNA: MYCN amplified, wt: wild type, mut: mutant*

To confirm that ATR inhibition abrogates olaparib induced S and G2 checkpoints, the effect of VE-821 and olaparib on the cell cycle was also analysed by incorporation of bromodeoxyuridine (BrdU), to label S phase cells, in these cell lines (**Figure 6.13**). The proportion of cells in each cell cycle phase after treatment with VE-821 and/or olaparib was

similar to when analysed with PI alone, confirming the loss of olaparib induced S and G2 checkpoint arrest with the addition of VE-821.

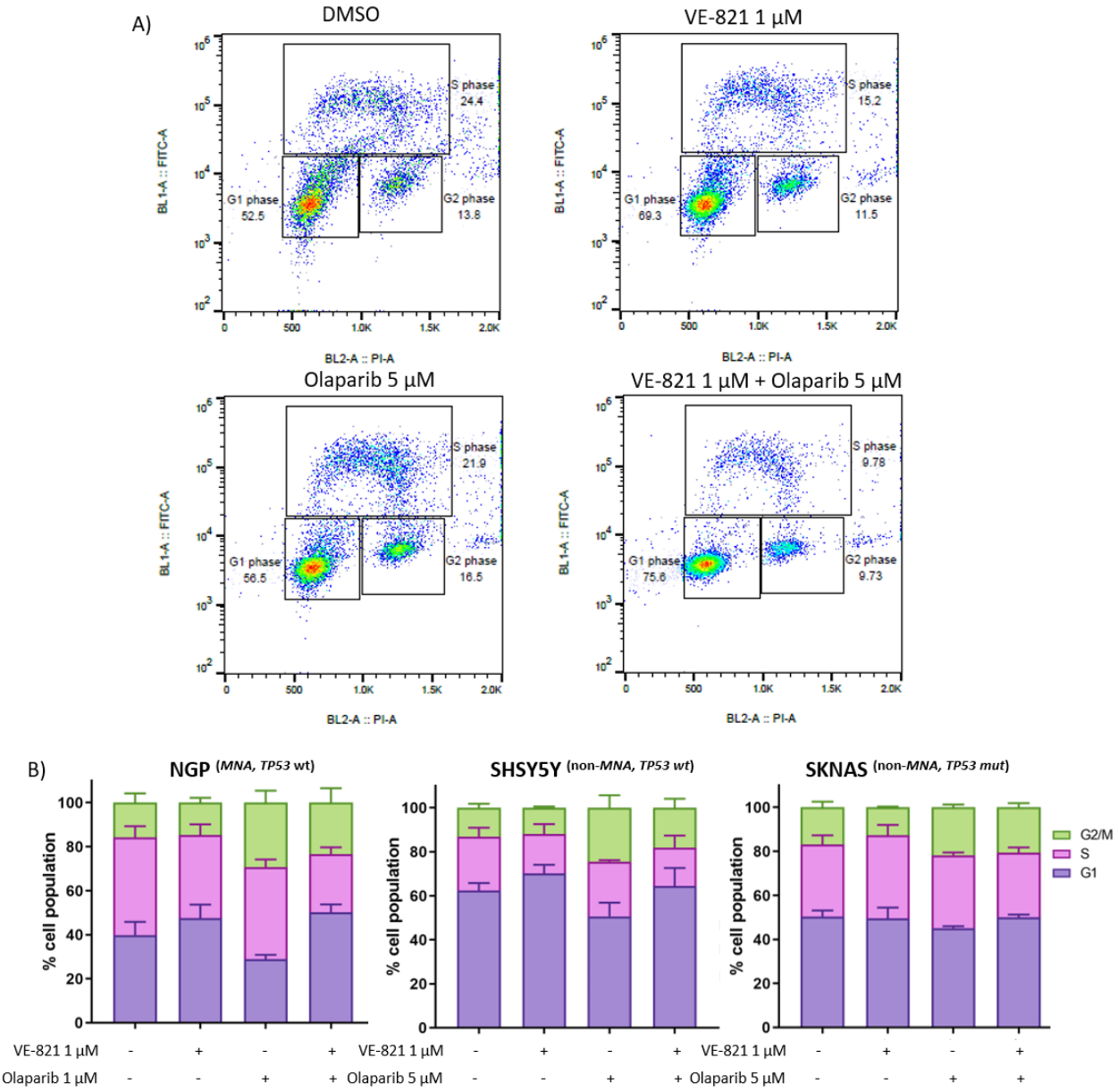

Figure 6.13: Cell cycle analysis using BrdU (FITC) and propidium iodide (PI) in response to ATR and PARP inhibition. A) Representative PI vs FITC intensity plots for SHSY5Y cells treated with 1 µM VE-821 and/or 5 µM olaparib for 24 hours. Populations representing each cell cycle phase were gated as shown. B) Cell cycle phase distribution of SHSY5Y, SKNAS and NGP cell lines treated with 5 µM (SHSY5Y and SKNAS) or 1 µM (NGP) olaparib in combination with 1 µM VE-821 for 24 h. Data are mean + SEM from 3 independent experiments. MNA: MYCN amplified, wt: wild type, mut: mutant

The effect of MYCN overexpression on cell cycle arrest in response to ATR and PARP inhibition was analysed by assessing the cell cycle phase distribution of the SHEPtet21N and IMR5/75

shMYCN MYCN regulatable expression cell lines (**Figure 6.14**). The proportion of control cells in S and G2 phase is greater in the MYCN overexpressing cells of both cell lines compared to cells expressing lower MYCN protein levels. Treatment with VE-821 resulted in an increase the proportion of MYCN overexpressing cells in G1 phase. The effect of ATR and PARP inhibition on the proportion of cells in each cell cycle phase was much less in IMR5/75 shMYCN cells expressing low levels of MYCN protein compared to high levels. A change in cell cycle distribution was only seen in the SHEPtet21N MYCN off cells when treated with both inhibitors.

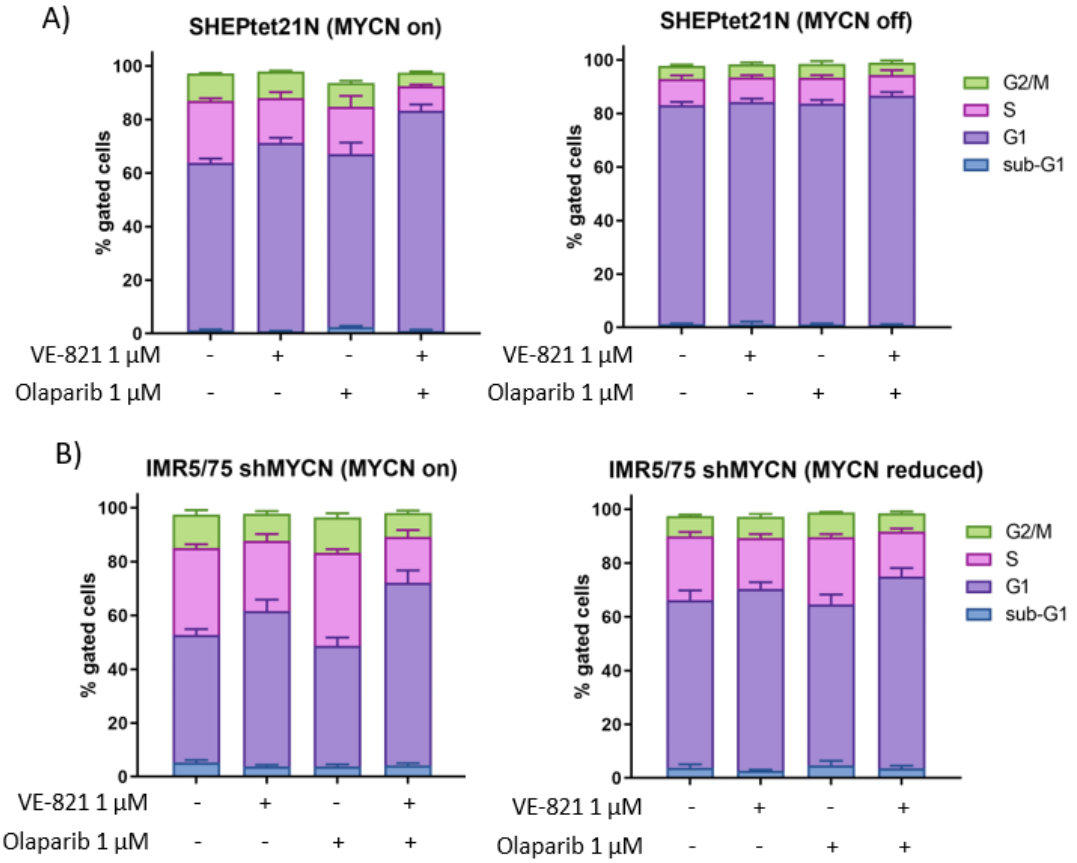

Figure 6.14: *Cell cycle analysis using propidium iodide of the A) SHEPtet21N and B) IMR5/75 shMYCN MYCN regulatable expression cell lines in both MYCN states treated with 1 µM VE-821 and/or 1 µM olaparib for 24 hours. Data are mean + SEM from 3 independent experiments.*

6.4.7 Replication stress

The effect of ATR and PARP inhibition on replication stress was assessed by Western blot analysis of $H2AX^{S139}$ (γH2AX) and $RPA2^{S8}$ phosphorylation in NGP, SKNAS and SHSY5Y cells

after treatment with 10 µM olaparib with and without 0.3, 1 or 3 µM VE-821 for 24 hours (**Figure 6.15**). Expression of γH2AX increased with increasing VE-821 concentration in combination with 10 µM olaparib in all cell lines. This was also the case with RPA2^{S8} phosphorylation, except for SHSY5Y, in which the phosphorylation decreased after treatment with 1 and 3 µM VE-821.

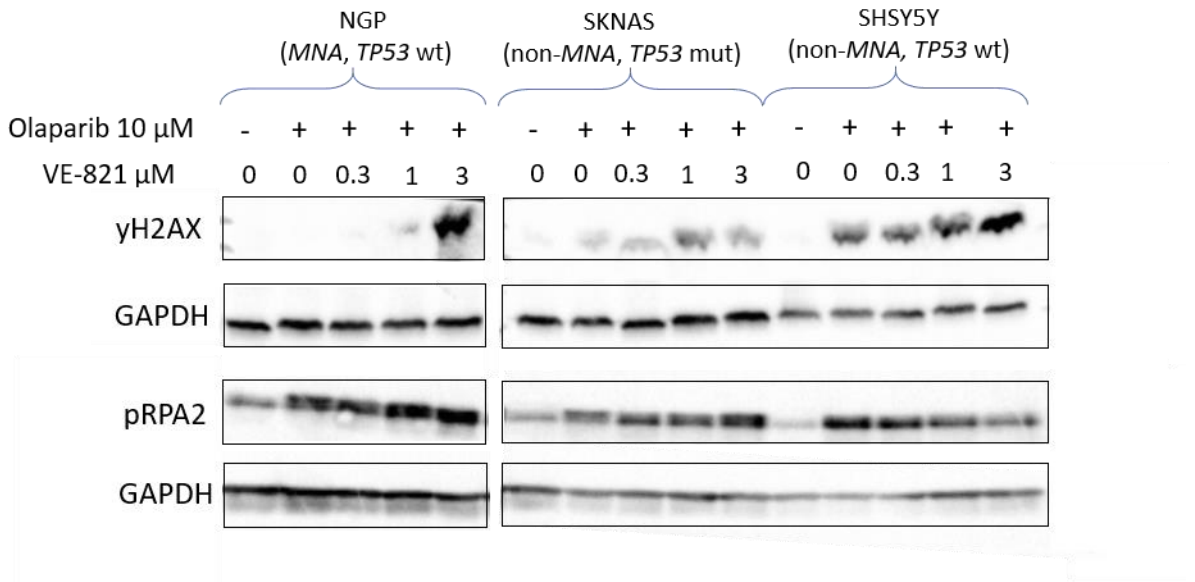

Figure 6.15: *Western blot analysis of γH2AX and phospho-RPA^{S8} (pRPA2^{S8}) in the NGP, SKNAS and SHSY5Y cell lines after treatment with 10 µM olaparib with and without 0.3, 1 or 3 µM VE-821 for 24 hours. GAPDH was used as a control for protein loading.*

To determine if RPA2^{S8} or H2AX phosphorylation could be developed as a pharmacodynamic biomarker of dual ATR and PARP inhibition, pRPA2^{S8} and γH2AX foci formation were measured by immunofluorescence after treatment with 10 µM olaparib and/or 1 µM VE-821 in SHSY5Y, SKNAS, NGP and N20_R1 cell lines. Representative γH2AX and pRPA2^{S8} foci images from the NGP cell line, and merged images from the N20_R1, SHSY5Y and SKNAS cell lines, treated with 1 µM VE-821, 10 µM olaparib or both are shown in **Figure 6.16A and B** respectively. The average number of foci per cell for each treatment is quantified in **Figure 6.17.**

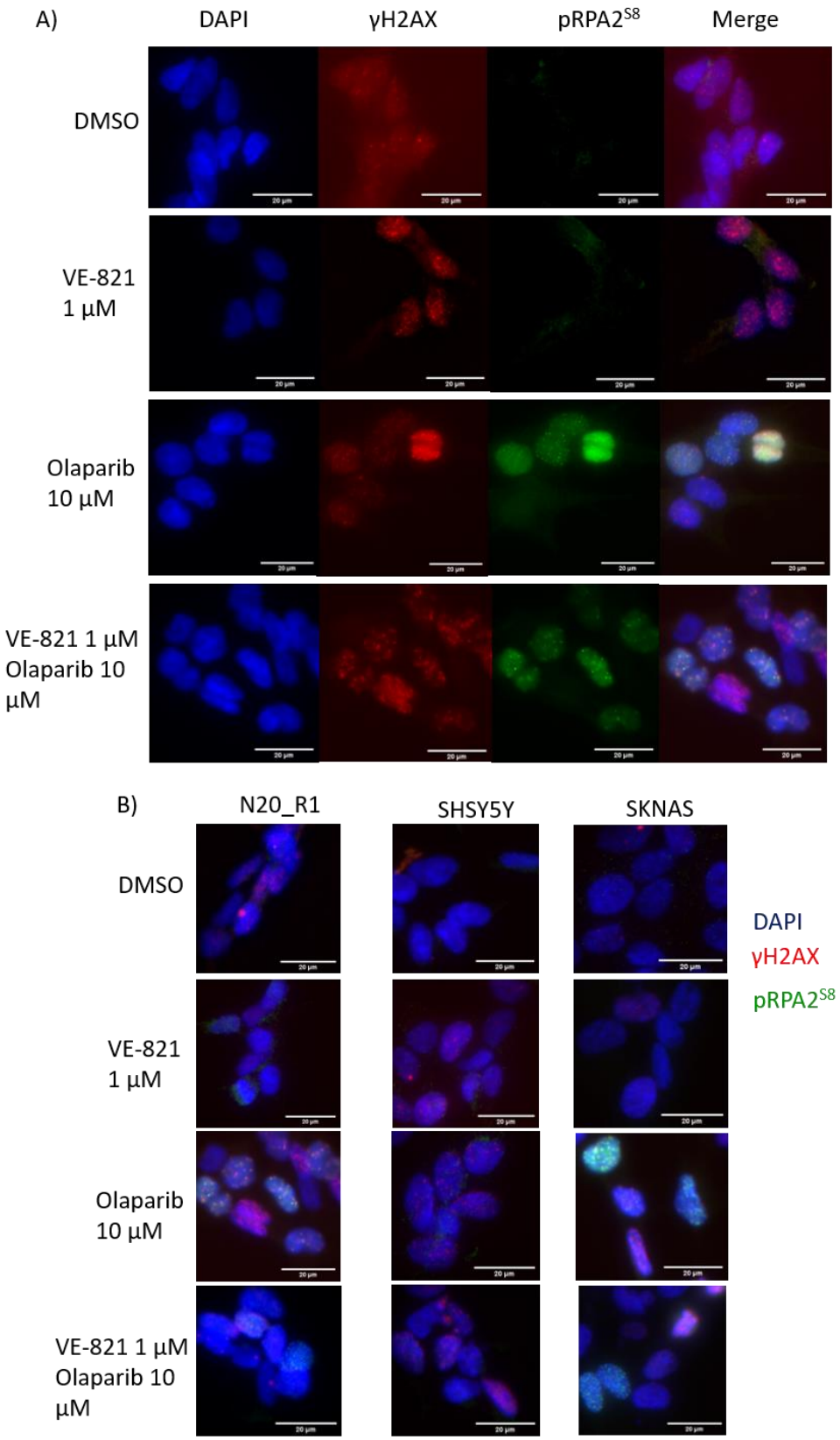

***Figure 6.16**: A) Representative γH2AX and pRPA2^{S8} foci images from the NGP cell line treated with 1 µM VE-821, 10 µM olaparib or both for 24 hours. B) Representative merged γH2AX and pRPA2^{S8} foci images from the N20_R1, SHSY5Y and SKNAS cell lines treated with 1 µM VE-821, 10 µM olaparib or both for 24 hours. Scale bars represent 20 µm.*

Treatment with 10 µM olaparib caused a significant increase in RS in all cell lines when measured by γH2AX foci but only in SKNAS, NGP and N20_R1 cells when measured by pRPA^{S8} foci (**Figure 6.17A and B**). γH2AX nuclear fluorescence did not increase as substantially as foci number in response to 10 µM olaparib, potentially indicating that the number of stalled replication forks was increased (**Figure 6.17C**). VE-821 alone had little or no effect on pRPA2^{S8} or γH2AX foci number and generally resulted in a reduction of olaparib-induced foci (**Figure 6.17B**). Intensity of γH2AX nuclear fluorescence significantly increased in response to olaparib in combination with VE-821 (**Figure 6.17C**).

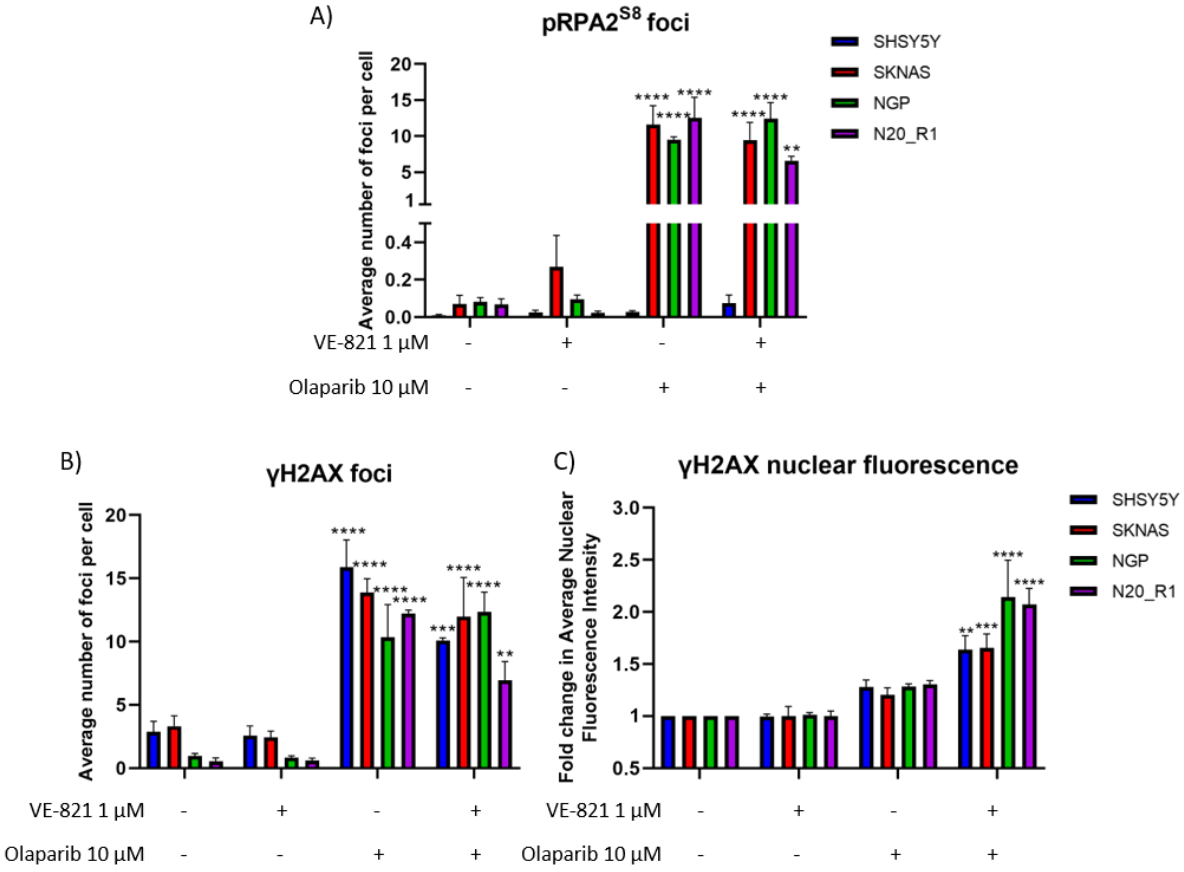

***Figure 6.17**: Average number of pRPA2^{S8} (A), γH2AX (B) foci per cell and fold change in mean γH2AX total nuclear fluorescence intensity (C) for SHSY5Y, SKNAS, NGP and N20_R1 cell lines treated with 1 µM VE-821, 10 µM olaparib or both. Data are mean + SEM from 3 independent experiments. * p<0.05, ** p<0.01, *** p<0.001, **** p<0.0001, 2-way ANOVA difference from control (DMSO).*

6.4.8 Homologous recombination

To examine the effect of PARP and ATR inhibition on HRR, RAD51 and γH2AX foci formation was measured by immunofluorescence after treatment with 10 µM olaparib and/or 1 µM VE-821 in SHSY5Y, SKNAS, NGP and N20_R1 cell lines. Representative γH2AX and Rad51 foci images from the NGP cell line, and merged images from the N20_R1, SHSY5Y and SKNAS cell lines, treated with 1 µM VE-821, 10 µM olaparib or both are shown in **Figure 6.18 A and B** respectively. Treatment with olaparib induced a significant increase in Rad51 foci formation in all cell lines except SKNAS, which was suppressed with the addition of VE-821 (**Figure 6.19A**). Interestingly, SKNAS cells are relatively resistant to both olaparib and VE-821. The formation of γH2AX foci was used to identify cells which sustained DNA damage from ATR and/or PARP inhibition (**Figure 6.19B**).

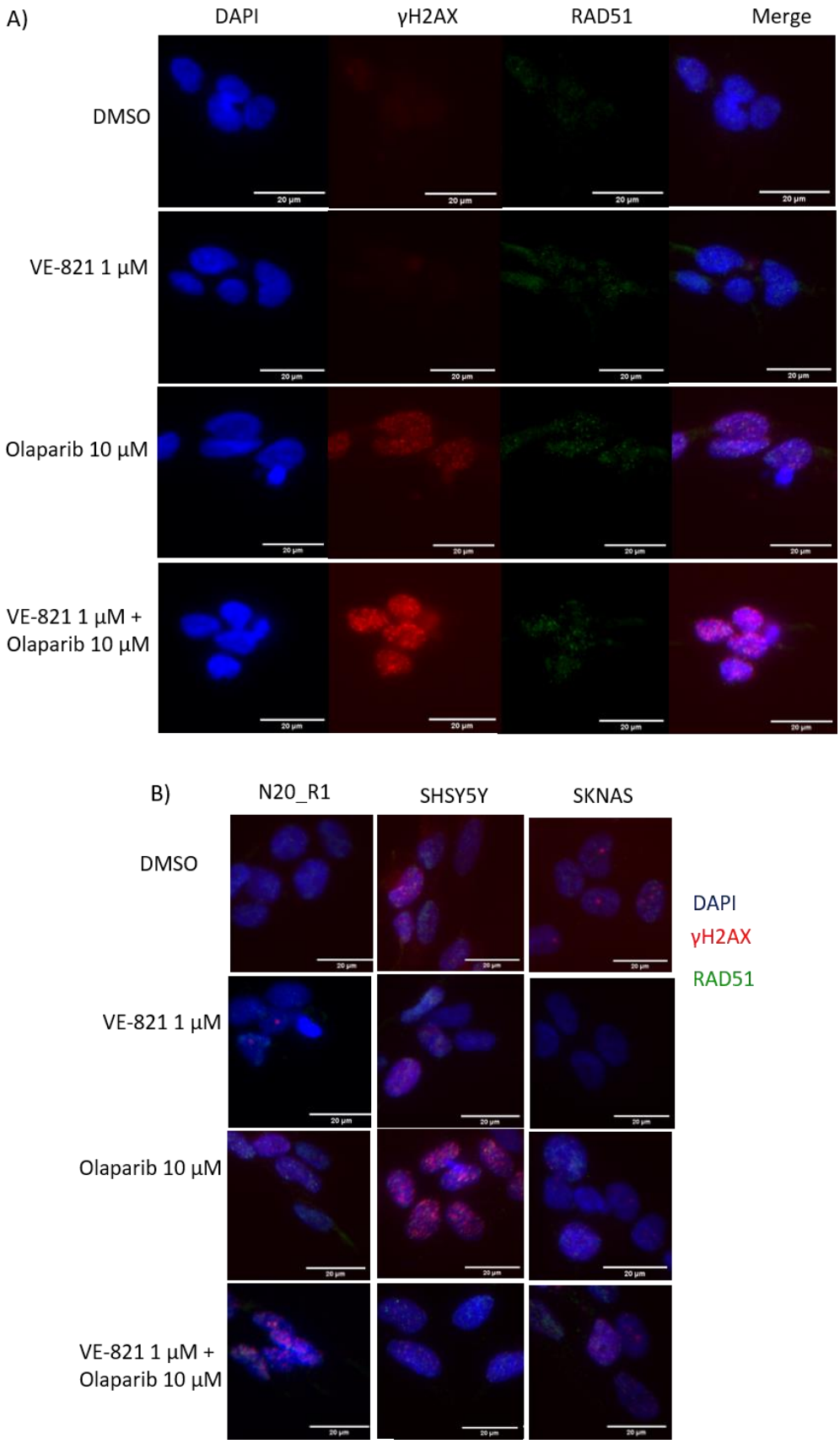

Figure 6.18: *A) Representative γH2AX and Rad51 foci images from the NGP cell line treated with 1 µM VE-821, 10 µM olaparib or both for 24 hours. B) Representative merged γH2AX and Rad51 foci images from the N20_R1, SHSY5Y and SKNAS cell lines treated with 1 µM VE-821, 10 µM olaparib or both for 24 hours. Scale bars represent 20 µm.*

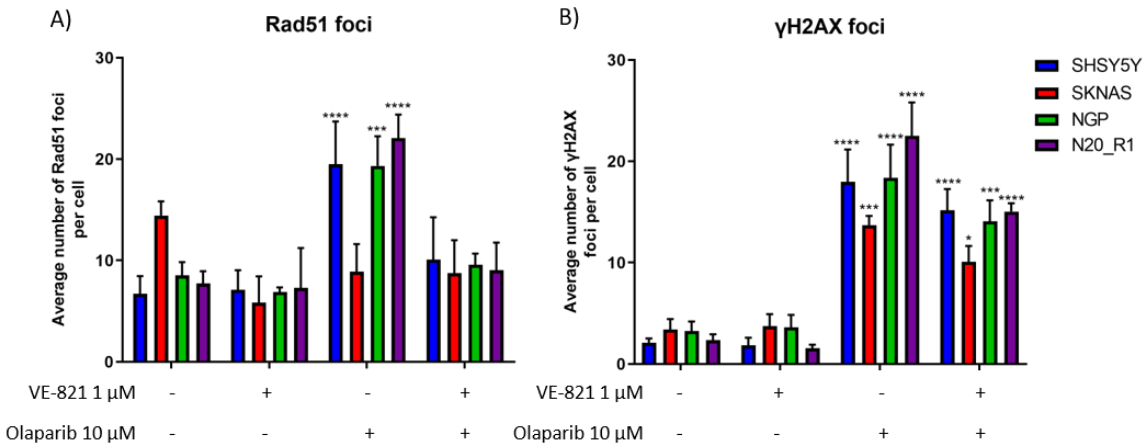

Figure 6.19: *Average number of Rad51 (A) and γH2AX (B) foci per cell for SHSY5Y, SKNAS, NGP and N20_R1 cell lines treated with 1 µM VE-821, 10 µM olaparib or both. Data are mean + SEM from 4 independent experiments. * p<0.05, ** p<0.01, *** p<0.001, **** p<0.0001, 2-way ANOVA difference from control (DMSO).*

6.5 Discussion

In this chapter, ATR inhibition was shown to sensitise NB cell lines to temozolomide and topotecan induced growth inhibition and olaparib cytotoxicity. ATR inhibition abrogated olaparib induced S and G2 checkpoint arrest, further increased olaparib-induced RS and suppressed HRR.

6.5.1 ATR inhibitors sensitize NB cells to topotecan and temozolomide

Topotecan and temozolomide are included in current treatment regimens for NB. Here, the effect of ATR inhibition on topotecan and temozolomide induced growth inhibition was examined in a panel of cell lines. ATR inhibition with 1 μM VE-821 potentiated topotecan induced growth inhibition in all cell lines (**Figure 6.1**). No obvious relationship between *MYCN* amplification status and sensitisation to topotecan was observed here, but sensitisation seemed to be greater in *TP53* mutant cell lines. *TP53* mutant cell lines were more resistant to topotecan in this study, and reported previously (Daniel *et al.*, 2009; Chaturvedi *et al.*, 2016), and therefore the sensitising effect of ATR inhibition is easier to observe. The role of p53 deficiency in sensitisation by ATR inhibition has been reported previously to sensitise colon and breast carcinoma cells to Top1 poisons, with p53-deficient cells showing the greatest sensitisation (Jossé *et al.*, 2014). The combination of ATR and Top1 inhibitors is being tested in several adult clinical trials (identifiers: NCT03896503, NCT04535401, NCT02487095, NCT02595931, NCT04514497 https://www.clinicaltrials.gov/).

Temozolomide-induced growth inhibition was potentiated by 1 μM VE-821 in all cell lines except SKNAS cells, which are very resistant to temozolomide by virtue of high MGMT expression (Wagner *et al.*, 2007). There was no obvious effect of *TP53* or *MYCN* status on temozolomide sensitisation (**Figure 6.2**) in these cell lines. ATR inhibition with NU6027 was shown to enhance temozolomide sensitivity in p53-deficient ovarian cancer cell lines (Peasland *et al.*, 2011). Expanding this study to include more cell lines of varying *MYCN* and *TP53* status may reveal a relationship between these factors and sensitisation by ATR inhibition.

There is extensive preclinical data regarding the potentiation of topotecan and temozolomide by PARP inhibitors (reviewed in (Dréan *et al.*, 2016)), including in NB (Daniel *et al.* 2009;

Sanmartin *et al.* 2017). However, the combination of PARP inhibitors with conventional chemotherapy in adults leads to increased adverse effects, especially significant haematological toxicity, resulting in subsequent dose reductions of both the PARP inhibitor and the combined cytotoxic chemotherapy (Zhou *et al.*, 2017; LaFargue *et al.*, 2019). It is possible that combining ATR inhibition with systemic chemotherapy may result in intolerable off-target effects, especially in paediatric patients, which limit the clinical development of these combinations.

6.5.2 ATR inhibitors synergistic with PARP inhibition in NB

The combination of ATR and PARP inhibition in NB cell lines was analysed here. Inhibition of ATR with 1 µM VE-821 and PARP inhibition with 1 µM olaparib was synergistic in all cell lines when analysed by XTT cell proliferation assay and clonogenic survival (**Figures 6.3 and 6.4**). Enhancement of olaparib-induced growth inhibition by ATR inhibition was confirmed using AZD6738 in the SHSY5Y, SKNAS, NGP and N20_R1 cell lines (**Figure 6.5**). AZD6738 had a greater sensitising effect on olaparib-induced growth inhibition in the SHSY5Y cell line than VE-821. The reason behind this is unclear as this cell line was not more sensitive to AZD6738 alone when compared with other cell lines (Chapter 4, **Figure 4.9**) and may be due to differing off target effects of the two different structures of the ATR inhibitors (Rundle *et al.* 2017).

When analysed by MYCN protein expression, fold sensitisation (SF) of olaparib-induced growth inhibition by VE-821 (**Table 6.1**) positively correlated with MYCN protein expression levels (**Figure 6.6**). Examination of olaparib sensitisation by ATR inhibition with both VE-821 and AZD6738 in MYCN expression regulatable cell lines, SHEPtet21N and IMR5/75 shMYCN, confirmed that ATR inhibition had a greater sensitising effect in cells expressing high levels of MYCN (**Figures 6.7 and 6.8**). In chapter 4, MYCN overexpressing cells were shown to display increased sensitivity to ATR inhibition alone, and the increased sensitisation of olaparib may be a reflection of this.

No relationship between ATM protein expression or *TP53* mutation and SF of olaparib-induced growth inhibition by VE-821 was observed. Previous studies in adult cancers have reported greater enhancement of PARP inhibitor sensitivity when combined with ATR inhibition in ATM-deficient cell lines when compared to ATM-proficient cells (Jette *et al.*,

2019; Jette *et al.*, 2020). The range of ATM protein expression in the cell lines used here was very small and limited analysis of the effect of ATM expression on SF. Further analysis with an increased number of cell lines with a broader range of ATM expression, or paired ATM deficient and proficient cell lines, is required before the effect of ATM protein expression on SF can be established in NB.

Treatment with PARP inhibitors is known to have adverse side effects, in particular haematological toxicities (LaFargue *et al.*, 2019). A phase 1 trial combining AZD6738 with olaparib in adults with advanced solid tumours (NCT02264678) reported dose limiting thrombocytopenia and neutropenia in 5/39 and 6/39 of patients in the dose escalation cohorts, leading to a phase 2 recommended doses of AZD6738 160 mg once daily from days 1-7 and Ola 300 mg twice daily continuously over a 28 day cycle (Krebs *et al.*, 2018). Results from an ongoing phase 2 trial of olaparib in combination with AZD6738 at these doses in ovarian cancer (CAPRI trial, NCT03462342) reported that the combination was tolerated in the 12 patients studied, with mostly low-grade toxicities similar to that of olaparib alone (Shah *et al.*, 2020). The toxicity profile of combined ATR and PARP inhibition may be different in paediatric patients and will become apparent after enrolment onto a new arm (arm N) of the E-SMART trial (NCT02813135), combining olaparib with AZD6738, which will open imminently.

6.5.3 Mechanism of synergism between ATR and PARP inhibition

The mechanism underlying synergism between ATR and PARP inhibition in NB was investigated in this chapter by examining the effect of the timing of ATR and PARP inhibition on cytotoxicity, and the effect of olaparib and VE-821 on cell cycle checkpoint activation, expression of RS markers and HRR.

6.5.3.1 Inhibition of ATR and PARP has the greatest cytotoxic effect when inhibited at the same time

To test if there is a greater sensitising effect when ATR is inhibited before or after PARP inhibition, growth inhibition and clonogenic survival of the NGP, SHSY5Y and SKNAS cell lines was measured after combined VE-821 and olaparib treatment following incubation with

either VE-821 or olaparib alone for 24 hours. Interestingly, the greatest cytotoxic effect was seen when cells were treated with both inhibitors together, rather than sequentially (**Figure 6.11**). The mechanism behind this is unclear. Both PARP and ATR have been reported to act at stalled replication forks (Sugimura *et al.*, 2008; Bryant *et al.*, 2009; Saldivar *et al.*, 2017) and dual inhibition results in impaired replication restart and irreparable chromosome breaks. Inhibition of one 24 hours before the other may have slowed proliferation making the cells less sensitive to the second inhibitors.

6.5.3.2 Abrogation of S and G2 checkpoints and impaired HRR upon ATR inhibition further increases olaparib-induced RS

The effect of dual PARP and ATR inhibition on markers of RS, phosphorylation of H2AX^{S139} (γH2AX) and RPA2^{S8} (pRPA2^{S8}) was analysed in this chapter by Western blot and immunofluorescent imaging. RPA2^{S8} is primarily phosphorylated by ATM and DNA-PK in response to DNA damage (Podhorecka *et al.*, 2010), whereas H2AX can be phosphorylated by ATM, DNA-PK and ATR (Liu *et al.*, 2012). Treatment with 10 µM olaparib induced expression of γH2AX and pRPA2^{S8} (**Figures 6.15, 6.16 and 6.17**), consistent with previous reports of PARP inhibitor induced RS in NB cells (Colicchia *et al.*, 2017; King *et al.*, 2020), which increased when combined with VE-821 in a dose dependent manner in the NGP and SHSY5Y cell lines when analysed by Western blotting. When analysed by immunofluorescence, the number of olaparib-induced pRPA2^{S8} foci increased with the addition of 1 µM VE-821 in the NGP cell lines but decreased in the N20_R1 and SKNAS cell lines. There was a significant increase in the number of γH2AX foci in all cell lines after treatment with 10 µM olaparib, which decreased with the addition of VE-821 in all cell lines except NGP (**Figure 6.17B**). ATR inhibition has been shown previously to result in a reduction of UV- or 4NQO-induced γH2AX foci (Chen *et al.*, 2015b). However, measurement of total nuclear fluorescent intensity of γH2AX staining revealed that the γH2AX signal was significantly increased when cells were treated with both olaparib and VE-821 compared to untreated in all cell lines (**Figure 6.17C**), which is consistent with the increase in γH2AX expression observed by Western blot (**Figure 6.15**). Whereas γH2AX foci formation localises DNA double strand breaks, pan-nuclear γH2AX staining, which can be picked up by measuring total nuclear fluorescence, is associated with the persistence of complex DNA lesions and apoptosis (Meyer *et al.*, 2013; Ding *et al.*, 2016). This is consistent

with the hypothesis that dual PARP and ATR inhibition will lead to increased replication fork stalling and collapse, and chromosome breakage due to collisions between unrepaired DNA breaks and replication and transcription machinery. Furthermore, pan-nuclear γH2AX formation has been shown to be mediated by ATM and DNA-PK and should be unaffected by ATR inhibition.

Measurement of γH2AX fluorescence intensity may be useful as a pharmacodynamic biomarker of dual ATR and PARP inhibition in clinical samples from the upcoming arm of E-SMART combining AZD6738 with olaparib.

In the SHSY5Y cell line, olaparib induced RPA2^{S8} phosphorylation decreased with increasing concentrations of VE-821 and there was no significant increase in the pRPA2^{S8} foci after treatment with 10 μM olaparib in the SHSY5Y cell line. It is unclear why pRPA2^{S8} foci formation were unable to be detected in this cell lines when RPA2^{S8} phosphorylation in response to olaparib was detected by Western blot analysis.

Cell cycle analysis revealed that PARP inhibition with olaparib increased the proportion of cells in S and G2 phase for each cell line suggesting activation of S and G2 checkpoint arrest (**Figures 6.12 and 6.13**), confirming previous reports of PARP inhibitor-induced checkpoint activation (Murai *et al.*, 2012; Jelinic and Levine, 2014) and accounts for the significant increase in RS foci by immunofluorescence signalling to cell cycle arrest and DNA repair pathways. This olaparib-induced S and G2 arrest was not observed after treatment with olaparib in combination with VE-821, suggesting an attenuation of activation of these checkpoints. A reduction of the number of cells in S and G2 phase compared to untreated cells was also observed in the NGP and SHSY5Y cell lines after treatment with VE-821 alone, suggesting that abrogation of these checkpoints contributes to sensitivity to ATR inhibition alone. ATR inhibition has been shown previously to attenuate S and G2 checkpoint arrest (Peasland *et al.*, 2011; Kim *et al.*, 2017; Middleton *et al.*, 2018) and result in an increase in cell death by mitotic catastrophe as cells divide with unrepaired DNA breaks (Toledo *et al.*, 2017). The SKNAS cell line showed the least difference in the percentage of cells in each cell cycle phase after ATR and/or PARP inhibition compared to untreated cells. As SKNAS is the most resistant to both these inhibitors, exploring the mechanism behind the lack of response in this cell line may reveal novel mechanisms of resistance.

In both the MYCN expression regulatable cell lines, there were fewer cells in G1 phase in untreated MYCN overexpressing cells compared to cells with reduced MYCN expression (**Figure 6.14**), suggesting that the signalling to S phase initiation is very strong in cells expressing high levels of MYCN. ATR inhibition with VE-821 alone reduced the number of cells in S and G2 phases, which was more profound in combination with olaparib, in the MYCN overexpressing cells. Neither inhibitor had much effect on the cell cycle profiles of the cells expressing low levels of MYCN, which is likely due to slower proliferation rates, allowing more time to repair or bypass olaparib-induced damage. MYCN overexpressing cells are more reliant on the S and G2 phase checkpoints, as the G1 checkpoint is often evaded by strong signalling to S phase progression (Bell *et al.*, 2006; Evans *et al.*, 2015; Ryl *et al.*, 2017). Attenuation of these checkpoints by ATR inhibition likely contributes to the increased olaparib sensitisation of MYCN amplified cell lines by VE-821.

HRR is required to maintain genome integrity during the repair of replication associated breaks and is critical for the repair of toxic PARP inhibitor-induced DNA breaks during S phase (Wyman *et al.*, 2004; Bryant *et al.*, 2005). ATR inhibition by VE-821 resulted in a reduction of olaparib-induced Rad51 foci, a marker of HRR, in both *MYCN* amplified and non-*MYCN* amplified cell lines (**Figure 6.18**), confirming previous reports of impaired HRR function after loss or inhibition of ATR (Peasland *et al.*, 2011; Buisson *et al.*, 2017; Yazinski *et al.*, 2017). Persistence of PARP inhibitor-induced breaks would lead to prolonged activation of DDR pathways, perhaps resulting in the increase in yH2AX signal intensity observed after dual PARP and ATR inhibition by immunofluorescence.

However, the non-*MYCN* amplified SKNAS cell line, did not show increased Rad51 after PARP inhibition and would be considered HRR-defective. HRR-defective cells are usually highly sensitive to PARP inhibitors, but the SKNAS cell line is the most resistant to olaparib out of the cell lines analysed in this study. Further exploration into the genetics of the SKNAS cell line may reveal novel resistance mechanisms to both PARP and ATR inhibitors.

Measurement of replication fork progression by DNA fibre assay would confirm definitively the effect of dual PARP and ATR inhibition on RS (Nieminuszczy *et al.*, 2016), and the persistence of PARP inhibitor-induced DNA damage could be measured by COMET assay (Møller, 2018). DNA fibre and comet assays could have been performed in the context of this

study but were not feasible due to time constraints. However, these techniques require live cells and are too labour intensive to be feasible in routine analysis of clinic samples.

6.6 Conclusion

ATR inhibition sensitises NB cell lines to temozolomide and topotecan induced growth inhibition and olaparib cytotoxicity. ATR inhibition synergises with PARP inhibition by further increasing PARP inhibitor induced RS through impaired S and G2 cell cycle arrest and attenuation of HRR.

Chapter 7: General Discussion

7.1 Replication stress has a key role in sensitivity to DDR inhibitors

The overall aim of this research was to identify determinants of sensitivity to ATR and PARP inhibition, alone and in combination, in preclinical models of HR-NB. Studies in other cancer types have identified DNA repair defects and increased RS, through overexpression of oncogenes, as contributors of sensitivity to inhibitors of ATR and/or PARP. The baseline level of RS and baseline activity and functional responses of DDR kinases ATM and ATR was characterised in a panel of NB cell lines as well the mutation and/or deletion status of genes which may be synthetically lethal with PARP or ATR inhibition.

A common genetic abnormality in NB is amplification of the *MYCN* oncogene, present in 50% of HR-NB tumours. In chapter 3, *MYCN* amplification was confirmed in 6 cell lines by SNP array analysis (**Figure 3.2**) and was associated with high MYCN protein expression (**Figure 3.6**). MYCN expression significantly positively correlated with CHK1 and PARP1 protein expression in these cell lines (**Figure 3.8**), and MYCN knockdown in regulatable cell lines was associated with a decrease in CHK1 expression and ATR expression and activity (**Figure 4.3**). Taken together, these data confirm previous reports of MYCN expression leading to increased ATR pathway activity (Colicchia *et al.*, 2017). King *et al.* recently showed that MYCN overexpression directly decreased replication fork progression and increased fork stalling by DNA fiber assay, a clear indicator of RS (King *et al.*, 2020).

The ATR inhibitor VE-821 was significantly more toxic to *MYCN* amplified cell lines, or cell lines with high MYCN expression (**Figures 4.6 and 4.7**). Cell lines with high baseline activity of ATR (CHK1^{S345} phosphorylation) and high CHK1 protein expression were also significantly more sensitive to VE-21 (**Figure 4.14**). As CHK1 protein levels correlate with MYCN protein expression, and high MYCN protein levels increase ATR expression and activity, the increased toxicity is likely due to the effect of MYCN overexpression. Analysis of more non-*MYCN* amplified cell lines would be required to determine if high CHK1 expression or ATR activity independently predict sensitivity to ATR inhibition.

MYCN amplification or overexpression was not significantly predictive of sensitivity to the PARP inhibitor olaparib in this study (**Figures 5.3 and 5.4**). However, cells with high baseline

ATR activity and CHK1 protein expression were significantly more sensitive to olaparib (**Figure 5.11**), suggesting that ATR pathway activation does result in vulnerability to PARP inhibition.

MYCN amplified NB cell lines have been shown to be sensitive to inhibition of checkpoint kinases acting downstream of ATR, CHK1 and WEE1 (Xu *et al.*, 2011; Russell *et al.*, 2013; Lowery *et al.*, 2017; Ando *et al.*, 2019). Inhibition of these kinases provides additional methods of targeting the RS response in NB.

Amplification of other oncogenes, such as *ALK* (2p23), *MDM2* (12q15) and *CDK4* (12p14), have been reported, occurring in up to 3% of *MYCN*-amplified and 1% of non-*MYCN* amplified tumours, and are associated with overexpression of the respective protein (Wang *et al.*, 2013; Amoroso *et al.*, 2020). Although rare, the presence of amplicons other than *MYCN* identifies a subset of HR-NB patients with especially poor survival rates, denoted ultra-high-risk (Depuydt *et al.*, 2018). Constitutive *ALK* activation, though gene amplification and overexpression or mutation, likely increases RS via mitogen signalling through the RAS-MAPK and PI3K-AKT-mTOR pathways. Overexpression of MDM2 and CDK4 results in G1 checkpoint dysfunction through preventing accumulation of p53 and uncoupling Rb from E2F allowing transcription of S-phase initiation factors, respectively (Nag *et al.*, 2013; Topacio *et al.*, 2019). Loss of G1 checkpoint control leads to DNA damage being carried into S phase, where it blocks replication, leading to fork stalling, collapse, and chromosome breakage.

SNP array analysis confirmed co-amplified of *ALK* and *MYCN* in the IMR32/ KAT100 cell line pair and amplification *MDM2* and *CDK4*, in addition to *MYCN*, in the NGP/N20_R1 cell line pair. It is unclear if these additional amplicons contribute to ATR and PARP inhibitor toxicity in these cell lines.

Another common genetic abnormality, present in around 30% of NB tumours, is unbalanced loss of chromosome 11q, often including allelic deletion of the *ATM, CHK1, MRE11*, and *H2AFX* DDR genes. Deletion of 11q was confirmed in 7/10 of the cell lines studied here, all of which included *ATM*, *CHK1* and *H2AX* (**Figure 3.3**). However, 11q deletion was not associated with reduced ATM or CHK1 protein expression in these cell lines when analysed by Western blot (**Figure 3.6C and F**). Additionally, there was no correlation between ATM and CHK1 protein expression, suggesting that there was no relationship between loss of one copy of these genes and protein expression in these cell lines. This is in contrast to previous studies which have

reported reduced ATM mRNA and protein expression in 11q deleted NB cells (Mandriota *et al.*, 2015; Sanmartín *et al.*, 2017). In two of the cell lines with the lowest ATM expression, IMR32 and NMB, mutation in *ATM* was detected by next generation panel sequencing (Chapter 3). No ATM function (ATM^{S1981} auto-phosphorylation or $CHK2^{T68}$ phosphorylation) was detected in response to doxorubicin in these cell lines (**Figure 3.11**). Mutation in an *ATM* splice site was identified in the IGRN91 cell line, which also showed no ATM function in response to doxorubicin. In this study, VE-821 was significantly more toxic to cell lines with low ATM protein expression (below median expression) or loss of function in ATM than cell lines with functional ATM (**Figure 4.10**). However, all cell lines with low ATM protein were also *MYCN* amplified. MYCN expression has been shown to lead to downregulation of ATM through upregulation of the micro RNA, miR-421 (Hu *et al.*, 2010; Mansour *et al.*, 2013). Although it is likely that *ATM* loss further increased dependency on ATR in these cell lines making them extremely vulnerable to its inhibition, it is difficult to differentiate the effect of ATM loss from the effect of MYCN overexpression. Again, further analysis of non-*MYCN* amplified cell lines would be required to determine if low ATM expression alone is enough to determine sensitivity to ATR inhibitors.

RS though loss of G1 checkpoint control has been hypothesised to increase sensitivity to ATR inhibition. In addition to oncogenic signalling, defects in the p53 pathway result in defective G1 checkpoint arrest, allowing cells to progress into S phase with damaged DNA. Molecular abnormalities resulting in p53 pathways dysfunction in the panel of cell lines studied here were characterised in chapter 3. Five out of ten of the cell lines studied here have a mutation in *TP53,* and all of these cell lines failed to show p53 activity (p21 upregulation) in response to doxorubicin, with the exception of IGRN91 which retained some function. In addition to mutation, *TP53* deletion through 17p loss was observed in the SKNAS and IGRN91 cell lines (see Appendix 1). Mutation of *TP53* is rare at diagnosis but is observed in up to 15% of relapsed NB tumours (Carr-Wilkinson *et al.*, 2010) and is associated with inferior prognosis.

MDM2 amplification in the NGP *TP53* wild type cell line likely disrupts p53 function by targeting it for protein degradation. Like *TP53* mutations, *MDM2* amplification is rare in NB and is not associated with tumour stage or survival (Carr-Wilkinson *et al.*, 2010). Indirect p53 pathway inactivation through homozygous deletion of *CDKN2A*, which codes for $p14^{ARF}$, an

inhibitor of MDM2, has been identified in up to 5% of NB tumours at diagnosis, increasing to ~20% in relapsed biopsies (Carr-Wilkinson *et al.*, 2010; Dreidax *et al.*, 2014).

In this study, no significant difference in sensitivity to VE-821 or olaparib was observed when cell lines were analysed by *TP53* mutation status or p53 function. In fact, in paired cell lines, *TP53* mutant cells were more resistant to VE-821 than the *TP53* wild type ones (**Figure 4.9**), an observation also made by Middleton *et al.* using isogenic breast and colorectal cancer cell lines (Middleton *et al.*, 2018). A recent study showed that p53 knockout was associated with suppression of RS responses, increased origin firing and decreased DNA breakage in response to mitogen and nucleotide deprivation (Benedict *et al.*, 2018), suggesting a mechanism behind increased resistance to ATR inhibitor monotherapy.

A small number of heterozygous mutations in genes affecting the DDR were also detected in these cell lines, including *BRCA2* in the GIMEN cell line (**Table 3.5**). Although associated with ATR and/or PARP inhibitor sensitivity in other cancers, the effect of these mutations in NB cannot be determined from this study. These mutations are extremely rare and may provide rationale for inclusion in basket trials based on molecular markers for precision medicine.

To summarise, MYCN-induced ATR pathway activation results in vulnerability to ATR inhibition in NB cells. RS caused by other oncogenic signalling pathways or defective DNA repair may also contribute to sensitivity to ATR and PARP inhibitors.

7.2 Mechanisms of synergy between ATR and PARP inhibition

In chapter 6, ATR inhibition with VE-821 sensitised NB cell lines to the cytotoxic effect of the PARP inhibitor olaparib, which was synergistic in all cell lines. Fold sensitisation by VE-821 significantly positively correlated with MYCN protein expression (**Figure 6.6**), which is likely due to these cells being under increased RS when treated. Olaparib was shown to activate ATR signalling and increase RS markers (**Figure 4.8, Figures 6.15-18**), consistent with previous reports of PARP inhibition enhancing RS in *MYCN* amplified cells (Colicchia *et al.*, 2017; King *et al.*, 2020).

PARP inhibition induces S and G2 cell cycle arrest (**Figures 6.12 and 6.13** and reported previously (Murai *et al.*, 2012; Jelinic and Levine, 2014)). Delayed cell cycle progression is required to allow time for repair of the PARP-DNA complexes and persistent single strand

lesions due to impaired BER prior to replication, or collapsed replication forks due to collisions with replication machinery. The ATR pathway is crucial for the induction of S and G2 arrest, especially in the absence of ATM and p53 signalling, and inhibition abrogates checkpoint arrest (**Figures 6.12 and 6.13** and reported previously (Peasland *et al.*, 2011; Maya-Mendoza *et al.*, 2015; Kim *et al.*, 2017; Middleton *et al.*, 2018)). *MYCN* amplified cells have an increased reliance on the S and G2 phase for the repair of DNA damage as the G1/S transition is accelerated (Bell *et al.*, 2006; Evans *et al.*, 2015; Ryl *et al.*, 2017), which likely contributes to the increased sensitisation by VE-821 in MYCN overexpressing cells.

To test if PARP and/or ATR inhibition leads to the accumulation of damage in S-phase, γH2AX intensity could be correlated with proliferating cell nuclear antigen (PCNA) or BrdU by immunofluorescent imaging or flow cytometry. PCNA and incorporation of BrdU are markers of active DNA replication. In addition, analysis of single and double strand DNA breaks, by comet assay (Møller, 2018), in cells treated with PARP and/or ATR inhibitors will reveal if combined inhibition results in an increase in DNA breaks or delayed DNA repair.

In chapter 6, ATR inhibition by VE-821 was shown to impair HRR in both *MYCN* amplified and non-amplified cell lines (**Figure 6.18 and 19**), confirming previous reports of impaired HRR function after loss or inhibition of ATR (Peasland *et al.*, 2011; Buisson *et al.*, 2017; Yazinski *et al.*, 2017). VE-821 resulted in a reduction in olaparib-induced $RPA2^{S8}$ phosphorylation, which is required to initiate HRR after replication arrest (Shi *et al.*, 2010). Inducing HRR defects, or "BRCAness", by targeting HRR or replication fork protection pathways is being explored in many adult cancer models to increase sensitivity of BRCA proficient tumours to PARP inhibitors (Byrum *et al.*, 2019). This concept underlies the synergy observed between ATR and PARP inhibitors in this study.

S and G2 checkpoint abrogation and HRR deficiency increase the probability of cell death by mitotic catastrophe, also known as death by mitotic failure, as cells divide with unrepaired DNA breaks (Vitale *et al.*, 2011). Mitotic defects can be measured by quantifying the percentage of cells with micronuclei or anaphase bridge formation. Cell death by apoptosis can also be measured using techniques such as TUNEL or caspase assays or measuring annexin-V staining by flow cytometry.

7.3 Future directions

A particular strength of this study is that the effect of PARP and ATR inhibition was analysed by two cytotoxicity assays in both paired cell lines and in a panel of cell lines with diverse molecular characteristics. High MYCN expression was confirmed to be a robust marker of sensitivity to ATR inhibition when analysed by genomic status and protein expression level. Expanding the cell line panel may reveal that PARP inhibition is significantly more toxic to MYCN-amplified cell lines, as suggested by the current work in matched cell lines and reported previously (Colicchia *et al.*, 2017; King *et al.*, 2020).

Genomic, proteomic and functional evaluation of ATM and p53 revealed that protein expression level is not always consistent with genetic status or function, and loss of ATM protein expression and/or function may determine sensitivity to ATR inhibition. However, the relatively small size of the cell line panel, with only 4/10 being non-*MYCN* amplified, meant that the role ATM protein expression has in sensitivity to ATR and PARP inhibition could not be separated from the effect of *MYCN* status. Exploring ATM loss using more non-MNA cell lines will determine if low ATM protein expression is independently associated with sensitivity to these inhibitors.

Synergism between PARP and ATR inhibitors was confirmed in NB cell lines using two different ATR inhibitors, VE-821 and AZD6738, in both cell proliferation and clonogenic survival assay. Synergy was observed in all cell lines independently of MYCN or p53 status. While some mechanistic analysis of synergy was presented in chapter 6, some questions remain unanswered. Further work to establish the effect of dual inhibition on DNA damage and repair dynamics, by Comet assay for example, and correlation of DNA damage and S phase markers will provide insight into why cells are especially vulnerable to inhibition of both proteins. Knockdown of PARP and/or ATR, using siRNA or shRNA mediated techniques, will reveal if the presence of the protein is required for synergy, for example PARP trapping on DNA, or just loss of catalytic function.

A thorough *in vivo* investigation of ATR inhibitors, as monotherapy and in combination with PARP inhibition, preferably in patient derived xenograft (PDX) mouse models, is required to establish efficacy in both *MYCN* amplified and non-*MYCN* amplified tumours.

7.4 Translating to the clinic

The data presented in this thesis supports further development of ATR and PARP inhibitors for the treatment of HR-NB, especially patients with *MYCN* amplified tumours. These inhibitors have been introduced in combination with existing therapy regimens e.g. PARP inhibition and irinotecan, in the first instance.

7.4.1 Potential combinations with existing treatment regimens

In chapter 6, ATR inhibition with VE-821 sensitised NB cells to the topoisomerase I poison topotecan, independent of *MYCN* or *TP53* status (**Figure 6.1**). VE-821 also sensitised NB cells to temozolomide (**Figure 6.2**), with the exception of the SKNAS cell line which is particularly resistant due to high MGMT expression (Wagner *et al.*, 2007; Chen *et al.*, 2015a).

PARP inhibitors have been shown previously to sensitise NB cells to topotecan and temozolomide (Daniel *et al.* 2009; Sanmartin *et al.* 2017). Results of the recent ESMART trial (NCT02813135) investigating olaparib in combination with irinotecan in relapsed or refractory paediatric solid tumours harbouring defects in DDR genes, including NB, showed that the combination was well tolerated and induced partial responses in 3/23, including one case of NB, and disease stabilisation in 8/23 patients (Gatz *et al.*, 2019). The phase 2 part of this trial is ongoing.

In addition to Top1 poisons and temozolomide, ATR inhibition has been shown to sensitise cells to platinum-based agents (Hall *et al.*, 2014; Middleton *et al.*, 2018; Shi *et al.*, 2018; Wengner *et al.*, 2020), including NB in the Paediatric Preclinical Testing Program (Kurmasheva *et al.*, 2018), and the nucleoside analogue gemcitabine (Liu *et al.*, 2017b; Fordham *et al.*, 2018). Gemcitabine is not currently included in NB treatment regimens, but cisplatin and carboplatin are given during induction therapy as part of the rapid COJEC protocol (NCT04221035). PARP inhibition has also been shown to sensitise NB cell lines to carboplatin (Norris *et al.*, 2014). Introduction of ATR or PARP inhibitors to current induction regimens may increase the efficacy of these agents and reduce the number of cycles required to induce remission.

The combination of PARP inhibitors with conventional chemotherapy in adult trials have resulted in increased adverse effects, especially significant haematological toxicity, resulting

in subsequent dose reductions of both the PARP inhibitor and the combined cytotoxic chemotherapy (Zhou *et al.*, 2017; LaFargue *et al.*, 2019). Results from a recent phase 1 trial investigating M6620 in combination with topotecan in adult advanced solid tumours reported that 11/21 patients required dose reductions due to neutropenia, thrombocytopenia or decreased creatinine clearance (Thomas *et al.*, 2018). However, tolerable doses were established and the phase 2 efficacy arm of this trial is ongoing (NCT03896503).

ATR and PARP inhibitors have also been shown to sensitise a variety of cancer cells to ionising radiation (Fujisawa *et al.*, 2015; Dillon *et al.*, 2017; Lesueur *et al.*, 2017; Middleton *et al.*, 2018; Wengner *et al.*, 2020), including in preclinical models of NB (Mueller *et al.*, 2013; Nile *et al.*, 2016). Ionising radiation induces many single and double strand DNA lesions, and cells rely on ATR and PARP signalling pathways for effective cell cycle arrest and repair of damaged DNA for survival. Radiotherapy is considered to be more targeted than systemic chemotherapy, as radiation can be directed towards the tumour, therefore combining with ATR or PARP inhibition should result in fewer toxicities. Radiotherapy is currently given to the site of the primary tumour after resection during the consolidation phase of HR-NB treatment. In addition to standard radiotherapy, NB patients may receive targeted molecular radiotherapy with iodine-131-labelled meta-iodobenzylguanidine (^{131}I-mIBG), a noradrenaline mimetic which specifically targets cells expressing the noradrenaline transporter (George *et al.*, 2016).

Overall, combining ATR or PARP inhibitors with chemo- and radiotherapy has great potential for the treatment of HR-NB. Further exploration, especially in *in vivo* models, is required to identify the most synergistic, and hopefully efficacious combinations.

7.4.2 Biomarker development

In order to identify patients who may benefit from PARP and/or ATR inhibitors, robust predictive biomarkers of sensitivity are required. For clinical trials, there is ongoing debate about whether maximum tolerated dose (MTD) or the dose required to inhibit the enzyme in the tumour cells, known as optimal biological dose (OBD), which is likely to be much lower than the MTD, should be used to guide recommended doses. For PARP and ATR inhibitors the OBD may be sufficient for anti-tumour responses, especially in combination with other DNA

damaging agents. Therefore, pharmacodynamic (PD) biomarkers are also required to confirm target inhibition.

7.4.2.1 Predictive biomarkers

The evidence reported here and previously suggest that *MYCN* amplified NB cells are vulnerable to inhibition of ATR alone and in combination with PARP inhibitors. *MYCN* amplification is screened for at diagnosis as part of risk classification. Here, high MYCN protein expression was shown to be predictive of sensitivity to these inhibitors. NB tumour cells can express high levels of MYCN protein in the absence of amplification, as demonstrated in the SJNB1 cell line (Chapter 3), therefore staining tumour biopsies for MYCN expression by immunohistochemistry (IHC) may identify patients with *MYCN* non-amplified tumours who may benefit from treatment with PARP and/or ATR inhibitors.

Sensitivity to ATR or PARP inhibition was also associated with high baseline ATR activity (CHK1^{S345} phosphorylation) and high CHK1 protein expression in this study. Optimising staining for these markers in NB tumours could also be used to stratify patients who may respond to these inhibitors.

Low ATM protein expression was associated with sensitivity to ATR inhibition. *ATM* loss is currently used to select patient cohorts to receive ATR inhibitors as part of clinical trials (NCT03718091, NCT02264678). From the data presented in this thesis, measuring the level of ATM protein expression in tumours may be useful to identify patients who would benefit in the absence of an inactivating *ATM* mutation.

Investigation of these markers in HR-NB tissue microarrays (TMA) was planned as part of this project but could not be completed due to time restrictions and would be required to determine if the range of expression in NB is broad enough to be used as a biomarker.

In addition to the markers identified in this thesis, studies by other research groups have suggested that expression of nuclear restriction factor SLFN11 may determine sensitivity to PARP inhibition, but resistance to ATR inhibition, in a variety of cancer types (Murai *et al.*, 2016; Murai *et al.*, 2019).

Mutations in *ATM* were associated with loss of function in this study. Although rare, screening for mutations in known DDR genes by targeted sequencing may also predict response to these inhibitors in the emerging era of personalised medicine.

7.4.2.2 Pharmacodynamic biomarkers

PD biomarkers are required to guide dose escalation of inhibitors and confirm that ATR and/or PARP is inhibited in tumour tissue. The most selective marker of ATR inhibitor activity is $CHK1^{S345}$ phosphorylation (pCHK1) (Chen *et al.*, 2015b). A reduction in pCHK1 levels was used in chapter 4 to confirm inhibition of ATR in cell lines after treatment with VE-821 (**Figure 4.8**). However, analysis of ATR inhibition by reduced pCHK1 levels has generally been investigated after ATR has been activated by other agents, and although there may be some baseline activation in NB, particularly in *MYCN* amplified tumours, it is likely that the dynamic range of baseline pCHK1 is not enough to be useful as a marker for monotherapy. Loss of pCHK1 signal could be useful when studying ATR inhibition in peripheral blood mononuclear cells (PBMCs) or IHC of biopsy specimens from patients undergoing combinations with PARP inhibitors or RS-inducing chemotherapy, which activate ATR. However, it is unlikely there would be a chemotherapy alone specimen to compare with, especially for IHC, so it would be difficult to say if it had been induced and inhibited or not induced. Ex vivo analysis of ATR inhibition in PBMC treated with DNA damaging agents could be used as a surrogate for measuring inhibition in the tumour (Chen *et al.*, 2015b).

Phosphorylation of $H2AX^{S139}$ (γH2AX) has been used to analyse the effect of ATR inhibition in the clinic (Thomas *et al.*, 2018; Yap *et al.*, 2020). However, the level of γH2AX induced by genotoxic agents generally decreases after ATR inhibition (**Figures 6.16-6.19** and shown previously (Chen *et al.*, 2015b; Thomas *et al.*, 2018)). PARP inhibition has been shown to increase γH2AX foci formation and staining, and γH2AX is used a marker of PARP inhibitor induced DNA damage (Redon *et al.*, 2010).

PARP inhibition is measured by the reduction in poly-ADP ribose (PAR) compared to control (Plummer *et al.*, 2008). Baseline expression of PAR is generally visible in NB cell lines (Nile *et al.*, 2016; King *et al.*, 2020) but *ex vivo* PARP inhibition in PBMCs after activation with other

agents may be required for dose escalation, as a surrogate for target inhibition in the tumour (Plummer *et al.*, 2008).

Further pharmacodynamic evaluation of these markers in response to PARP and/or ATR is required before they can be used guide OBD in clinical trials. In the meantime, MTDs will be continued to be used in the absence of reliable PD biomarkers to examine efficacy of these inhibitors in the clinic.

7.5 Summary and conclusion

The data presented in this thesis demonstrates that increased ATR pathway activity is a key determinant of sensitivity to ATR inhibitors in NB cell lines. *MYCN* amplification is associated with MYCN protein overexpression and increased ATR pathway activation. *MYCN* amplification is present in 50% HR-NB tumours, representing a large proportion of NB patients who may benefit therapeutically from these inhibitors. ATR inhibition sensitises NB cells to RS-inducing agents, such as topotecan, temozolomide, and the PARP inhibitor olaparib, and is synergistic with olaparib inhibition, independent of *MYCN* status. Mechanistically, ATR impairs HRR and abrogates S and G2 checkpoint arrest induced by PARP inhibition, exacerbating RS and increasing cell death. ATR inhibitor sensitivity in NB is summarised in **Figure 7.1**.

Although further work is required to develop robust and reliable predictive and PD biomarkers, the work presented here provides strong rationale for the introduction of ATR and PARP inhibitors to HR-NB treatment regimens to try and improve survival in this aggressive childhood cancer.

7.6 Graphical conclusion

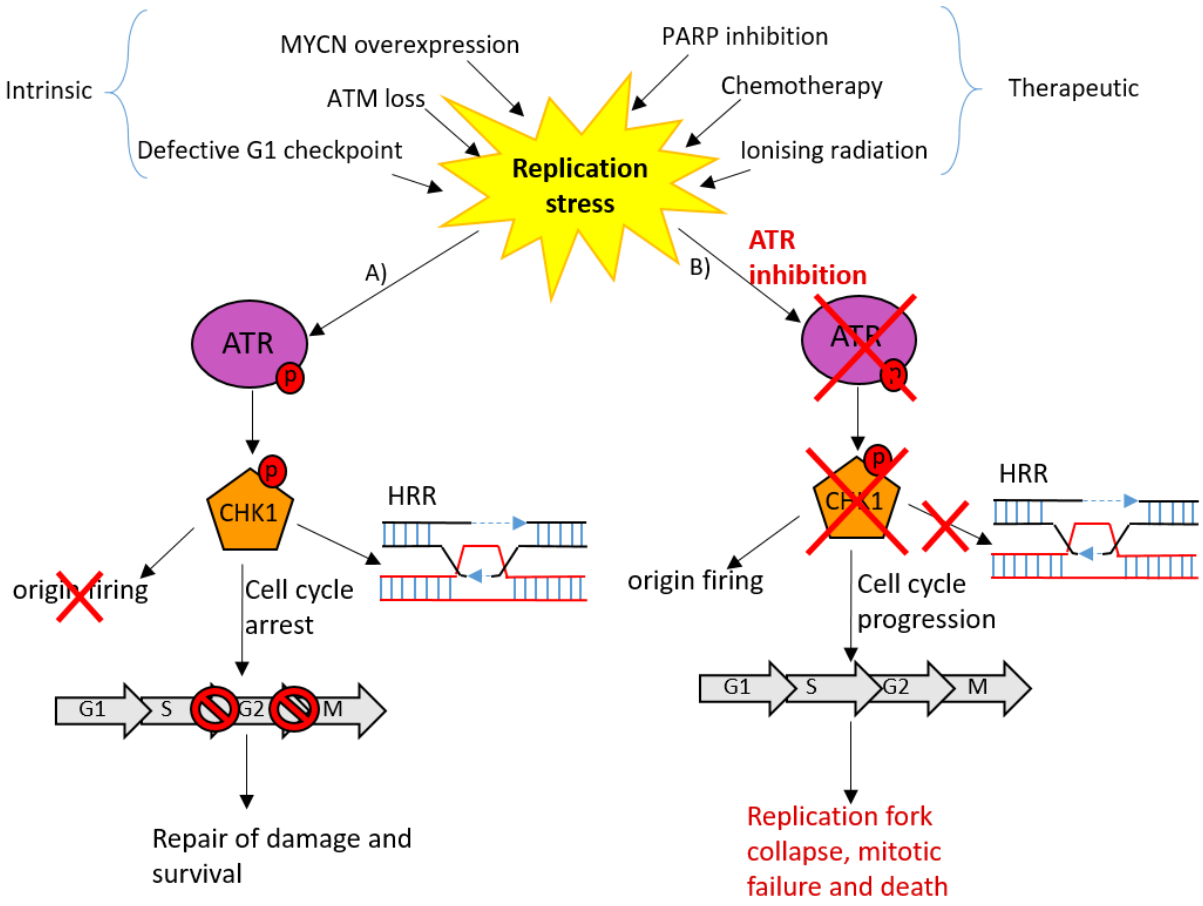

Figure 7.1: *Increased replication stress in neuroblastoma tumours, caused by intrinsic features or induced therapeutically, activates ATR signalling, leading to cell cycle arrest, decreased replication origin firing and DNA repair via homologous recombination repair (HRR) (pathway A). Inhibition of ATR impairs HRR and abrogates cell cycle arrest and allows new origin firing, leading to replication fork collapse, mitotic failure, and death (pathway B).*

References

Adzhubei, I., Jordan, D.M. and Sunyaev, S.R. (2013) 'Predicting functional effect of human missense mutations using PolyPhen-2', *Current protocols in human genetics*, Chapter 7, pp. Unit7.20-Unit7.20.

Agrawal, A., Yang, J., Murphy, R.F. and Agrawal, D.K. (2006) 'Regulation of the p14ARF-Mdm2-p53 pathway: An overview in breast cancer', *Experimental and Molecular Pathology*, 81(2), pp. 115-122.

Alver, R.C., Chadha, G.S. and Blow, J.J. (2014) 'The contribution of dormant origins to genome stability: From cell biology to human genetics', *DNA Repair*, 19(100), pp. 182-189.

Amoroso, L., Ognibene, M., Morini, M., Conte, M., Di Cataldo, A., Tondo, A., D'Angelo, P., Castellano, A., Garaventa, A., Lasorsa, V.A., Podestà, M., Capasso, M. and Pezzolo, A. (2020) 'Genomic coamplification of CDK4/MDM2/FRS2 is associated with very poor prognosis and atypical clinical features in neuroblastoma patients', *Genes, Chromosomes and Cancer*, 59(5), pp. 277-285.

Ando, K., Nakamura, Y., Nagase, H., Nakagawara, A., Koshinaga, T., Wada, S. and Makishima, M. (2019) 'Co-Inhibition of the DNA Damage Response and CHK1 Enhances Apoptosis of Neuroblastoma Cells', *International journal of molecular sciences*, 20(15), p. 3700.

Aparicio, T., Baer, R. and Gautier, J. (2014) 'DNA double-strand break repair pathway choice and cancer', *DNA repair*, 19, pp. 169-175.

Attiyeh, E.F., London, W.B., Mossé, Y.P., Wang, Q., Winter, C., Khazi, D., McGrady, P.W., Seeger, R.C., Look, A.T., Shimada, H., Brodeur, G.M., Cohn, S.L., Matthay, K.K. and Maris, J.M. (2005) 'Chromosome 1p and 11q Deletions and Outcome in Neuroblastoma', *New England Journal of Medicine*, 353(21), pp. 2243-2253.

Austen, B., Skowronska, A., Baker, C., Powell, J.E., Gardiner, A., Oscier, D., Majid, A., Dyer, M., Siebert, R. and Taylor, A.M. (2007) 'Mutation status of the residual ATM allele is an important determinant of the cellular response to chemotherapy and survival in patients with chronic lymphocytic leukemia containing an 11q deletion', *Journal of Clinical Oncology*, 25(34), pp. 5448-5457.

Avitabile, M., Lasorsa, V.A., Cantalupo, S., Cardinale, A., Cimmino, F., Montella, A., Capasso, D., Haupt, R., Amoroso, L., Garaventa, A., Quattrone, A., Corrias, M.V., Iolascon, A. and Capasso, M. (2020) 'Association of PARP1 polymorphisms with response to chemotherapy in patients with high-risk neuroblastoma', *Journal of Cellular and Molecular Medicine*, 24(7), pp. 4072-4081.

Azarova, A.M., Gautam, G. and George, R.E. (2011) 'Emerging importance of ALK in neuroblastoma', *Seminars in Cancer Biology*, 21(4), pp. 267-275.

Barone, G., Anderson, J., Pearson, A.D.J., Petrie, K. and Chesler, L. (2013) 'New Strategies in Neuroblastoma: Therapeutic Targeting of MYCN and ALK', *Clinical Cancer Research*, 19(21), pp. 5814-5821.

Basta, N.O., Halliday, G.C., Makin, G., Birch, J., Feltbower, R., Bown, N., Elliott, M., Moreno, L., Barone, G., Pearson, A.D.J., James, P.W., Tweddle, D.A. and McNally, R.J.Q. (2016) 'Factors associated with recurrence and survival length following relapse in patients with neuroblastoma', *British Journal Of Cancer*, 115, p. 1048.

Beckett, E. (2019) 'A genome-wide study of an unfavourable subgroup of intermediate-risk neuroblastoma', *MRes Thesis, Newcastle University, Newcaslte Upon Tyne*.

Bell, E., Chen, L., Liu, T., Marshall, G.M., Lunec, J. and Tweddle, D.A. (2010) 'MYCN oncoprotein targets and their therapeutic potential', *Cancer Letters*, 293(2), pp. 144-157.

Bell, E., Premkumar, R., Carr, J., Lu, X., Lovat, P.E., Kees, U.R., Lunec, J. and Tweddle, D. (2006) 'The Role of MYCN in the Failure of MYCN Amplified Neuroblastoma Cell Lines to G1 Arrest After DNA Damage', *Cell Cycle*, 5(22), pp. 2639-2647.

Benedict, B., van Harn, T., Dekker, M., Hermsen, S., Kucukosmanoglu, A., Pieters, W., Delzenne-Goette, E., Dorsman, J.C., Petermann, E., Foijer, F. and Te Riele, H. (2018) 'Loss of p53 suppresses replication-stress-induced DNA breakage in G1/S checkpoint deficient cells', *eLife*, 7, p. e37868.

Berlanga, P., Cañete, A. and Castel, V. (2017) 'Advances in emerging drugs for the treatment of neuroblastoma', *Expert Opinion on Emerging Drugs*, 22(1), pp. 63-75.

Bernadotte, A., Mikhelson, V.M. and Spivak, I.M. (2016) 'Markers of cellular senescence. Telomere shortening as a marker of cellular senescence', *Aging (Albany NY)*, 8(1), pp. 3-11.

Berry, T., Luther, W., Bhatnagar, N., Jamin, Y., Poon, E., Sanda, T., Pei, D., Sharma, B., Vetharoy, W.R., Hallsworth, A., Ahmad, Z., Barker, K., Moreau, L., Webber, H., Wang, W., Liu, Q., Perez-Atayde, A., Rodig, S., Cheung, N.-K., Raynaud, F., Hallberg, B., Robinson, S.P., Gray, N.S., Pearson, A.D.J., Eccles, S.A., Chesler, L. and George, R.E. (2012) 'The ALK(F1174L) mutation potentiates the oncogenic activity of MYCN in neuroblastoma', *Cancer cell*, 22(1), pp. 117-130.

Biedler, J.L., Roffler-Tarlov, S., Schachner, M. and Freedman, L.S. (1978) 'Multiple Neurotransmitter Synthesis by Human Neuroblastoma Cell Lines and Clones', *Cancer Research*, 38(11 Part 1), pp. 3751-3757.

Bieging, K.T., Mello, S.S. and Attardi, L.D. (2014) 'Unravelling mechanisms of p53-mediated tumour suppression', *Nature reviews. Cancer*, 14(5), pp. 359-370.

Binz, N., Shalaby, T., Rivera, P., Shin-ya, K. and Grotzer, M.A. (2005) 'Telomerase inhibition, telomere shortening, cell growth suppression and induction of apoptosis by telomestatin in childhood neuroblastoma cells', *European Journal of Cancer*, 41(18), pp. 2873-2881.

Blanc, E., Goldschneider, D., Ferrandis, E., Barrois, M., Le Roux, G., Leonce, S., Douc-Rasy, S., Bénard, J. and Raguénez, G. (2003) 'MYCN enhances P-gp/MDR1 gene expression in the human metastatic neuroblastoma IGR-N-91 model', *The American journal of pathology*, 163(1), pp. 321-331.

Bollag, G., Clapp, D.W., Shih, S., Adler, F., Zhang, Y.Y., Thompson, P., Lange, B.J., Freedman, M.H., McCormick, F., Jacks, T. and Shannon, K. (1996) 'Loss of NF1 results in activation of the Ras signaling pathway and leads to aberrant growth in haematopoietic cells', *Nat Genet*, 12(2), pp. 144-148.

Bouwman, P. and Jonkers, J. (2012) 'The effects of deregulated DNA damage signalling on cancer chemotherapy response and resistance', *Nat Rev Cancer*, 12(9), pp. 587-598.

Bower, K., Napier, C.E., Cole, S.L., Dagg, R.A., Lau, L.M.S., Duncan, E.L., Moy, E.L. and Reddel, R.R. (2012) 'Loss of Wild-Type ATRX Expression in Somatic Cell Hybrids Segregates with Activation of Alternative Lengthening of Telomeres', *PLoS ONE*, 7(11), p. e50062.

Bown, N., Cotterill, S., Łastowska, M., O'Neill, S., Pearson, A.D.J., Plantaz, D., Meddeb, M., Danglot, G., Brinkschmidt, C., Christiansen, H., Laureys, G., Nicholson, J., Bernheim, A., Betts, D.R., Vandesompele, J., Van Roy, N. and Speleman, F. (1999) 'Gain of Chromosome Arm 17q and Adverse Outcome in Patients with Neuroblastoma', *New England Journal of Medicine*, 340(25), pp. 1954-1961.

Bradbury, A., Hall, S., Curtin, N. and Drew, Y. (2020) 'Targeting ATR as Cancer Therapy: A new era for synthetic lethality and synergistic combinations?', *Pharmacology & Therapeutics*, 207, p. 107450.

Bresler, S.C., Weiser, D.A., Huwe, P.J., Park, J.H., Krytska, K., Ryles, H., Laudenslager, M., Rappaport, E.F., Wood, A.C., McGrady, P.W., Hogarty, M.D., London, W.B., Radhakrishnan, R., Lemmon, M.A. and Mossé, Y.P. (2014) 'ALK mutations confer differential oncogenic activation and sensitivity to ALK inhibition therapy in neuroblastoma', *Cancer cell*, 26(5), pp. 682-694.

Brodeur, G.M. (2003) 'Neuroblastoma: biological insights into a clinical enigma', *Nat Rev Cancer*, 3(3), pp. 203-216.

Brodeur, G.M., Seeger, R.C., Schwab, M., Varmus, H.E. and Bishop, J.M. (1984) 'Amplification of N-myc in untreated human neuroblastomas correlates with advanced disease stage', *Science*, 224, pp. 1121-1124.

Brodeur, G.M., Sekhon, G.S. and Goldstein, M.N. (1977) 'Chromosomal aberrations in human neuroblastomas', *Cancer*, 40(5), pp. 2256-2263.

Brooks, G.A., Stopfer, J.E., Erlichman, J., Davidson, R., Nathanson, K.L. and Domchek, S.M. (2006) 'Childhood cancer in families with and without BRCA1 or BRCA2 mutations ascertained at a high-risk breast cancer clinic', *Cancer Biology & Therapy*, 5(9), pp. 1098-1102.

Bryant, H.E., Petermann, E., Schultz, N., Jemth, A.-S., Loseva, O., Issaeva, N., Johansson, F., Fernandez, S., McGlynn, P. and Helleday, T. (2009) 'PARP is activated at stalled forks to mediate Mre11-dependent replication restart and recombination', *The EMBO Journal*, 28(17), pp. 2601-2615.

Bryant, H.E., Schultz, N., Thomas, H.D., Parker, K.M., Flower, D., Lopez, E., Kyle, S., Meuth, M., Curtin, N.J. and Helleday, T. (2005) 'Specific killing of BRCA2-deficient tumours with inhibitors of poly(ADP-ribose) polymerase', *Nature*, 434(7035), pp. 913-917.

Buisson, R., Niraj, J., Rodrigue, A., Ho, C.K., Kreuzer, J., Foo, T.K., Hardy, E.J.L., Dellaire, G., Haas, W., Xia, B., Masson, J.-Y. and Zou, L. (2017) 'Coupling of Homologous Recombination and the Checkpoint by ATR', *Molecular cell*, 65(2), pp. 336-346.

Burrell, R.A., McClelland, S.E., Endesfelder, D., Groth, P., Weller, M.-C., Shaikh, N., Domingo, E., Kanu, N., Dewhurst, S.M., Gronroos, E., Chew, S.K., Rowan, A.J., Schenk, A., Sheffer, M., Howell, M., Kschischo, M., Behrens, A., Helleday, T., Bartek, J., Tomlinson, I.P. and Swanton, C. (2013) 'Replication stress links structural and numerical cancer chromosomal instability', *Nature*, 494(7438), pp. 492-496.

Byers, L.A., Wang, J., Nilsson, M.B., Fujimoto, J., Saintigny, P., Yordy, J., Giri, U., Peyton, M., Fan, Y.H., Diao, L., Masrorpour, F., Shen, L., Liu, W., Duchemann, B., Tumula, P., Bhardwaj, V., Welsh, J., Weber, S., Glisson, B.S., Kalhor, N., Wistuba, I.I., Girard, L., Lippman, S.M., Mills, G.B., Coombes, K.R., Weinstein, J.N., Minna, J.D. and Heymach, J.V. (2012) 'Proteomic Profiling Identifies Dysregulated

Pathways in Small Cell Lung Cancer and Novel Therapeutic Targets Including PARP1', *Cancer Discovery*, 2(9), pp. 798-811.

Byrum, A.K., Vindigni, A. and Mosammaparast, N. (2019) 'Defining and Modulating 'BRCAness'', *Trends in Cell Biology*, 29(9), pp. 740-751.

Caldecott, K.W. (2003) 'XRCC1 and DNA strand break repair', *DNA Repair*, 2(9), pp. 955-969.

Caldecott, K.W. (2008) 'Single-strand break repair and genetic disease', 9, p. 619.

Campbell, K., Gastier-Foster, J.M., Mann, M., Naranjo, A.H., Van Ryn, C., Bagatell, R., Matthay, K.K., London, W.B., Irwin, M.S., Shimada, H., Granger, M.M., Hogarty, M.D., Park, J.R. and DuBois, S.G. (2017) 'Association of MYCN copy number with clinical features, tumor biology, and outcomes in neuroblastoma: A report from the Children's Oncology Group', *Cancer*, 123(21), pp. 4224-4235.

Cardnell, R.J., Feng, Y., Diao, L., Fan, Y.-H., Masrorpour, F., Wang, J., Shen, Y., Mills, G.B., Minna, J.D., Heymach, J.V. and Byers, L.A. (2013) 'Proteomic Markers of DNA Repair and PI3K Pathway Activation Predict Response to the PARP Inhibitor BMN 673 in Small Cell Lung Cancer', *Clinical Cancer Research*, 19(22), pp. 6322-6328.

Carén, H., Abel, F., Kogner, P. and Martinsson, T. (2008) 'High incidence of DNA mutations and gene amplifications of the ALK gene in advanced sporadic neuroblastoma tumours', *Biochemical Journal*, 416(2), pp. 153-159.

Carpenter, E.L. and Mossé, Y.P. (2012) 'Targeting ALK in neuroblastoma—preclinical and clinical advancements', *Nature reviews. Clinical oncology*, 9(7), pp. 391-399.

Carr-Wilkinson, J., O'Toole, K., Wood, K.M., Challen, C.C., Baker, A.G., Board, J.R., Evans, L., Cole, M., Cheung, N.-K.V., Boos, J., Köhler, G., Leuschner, I., Pearson, A.D.J., Lunec, J. and Tweddle, D.A. (2010) 'High Frequency of p53/MDM2/p14ARF Pathway Abnormalities in Relapsed Neuroblastoma', *Clinical cancer research : an official journal of the American Association for Cancer Research*, 16(4), pp. 1108-1118.

Carr, J., Bell, E., Pearson, A.D.J., Kees, U.R., Beris, H., Lunec, J. and Tweddle, D.A. (2006) 'Increased Frequency of Aberrations in the p53/MDM2/p14ARF Pathway in Neuroblastoma Cell Lines Established at Relapse', *Cancer Research*, 66(4), pp. 2138-2145.

Carrozza, M.J., Stefanick, D.F., Horton, J.K., Kedar, P.S. and Wilson, S.H. (2009) 'PARP inhibition during alkylation-induced genotoxic stress signals a cell cycle checkpoint response mediated by ATM', *DNA repair*, 8(11), pp. 1264-1272.

Chaturvedi, N.K., McGuire, T.R., Coulter, D.W., Shukla, A., McIntyre, E.M., Sharp, J.G. and Joshi, S.S. (2016) 'Improved therapy for neuroblastoma using a combination approach: superior efficacy with vismodegib and topotecan', *Oncotarget*, 7(12), pp. 15215-15229.

Chayka, O., D'Acunto, C.W., Middleton, O., Arab, M. and Sala, A. (2015) 'Identification and pharmacological inactivation of the MYCN gene network as a therapeutic strategy for neuroblastic tumor cells', *The Journal of biological chemistry*, 290(4), pp. 2198-2212.

Chen, L., Iraci, N., Gherardi, S., Gamble, L.D., Wood, K.M., Perini, G., Lunec, J. and Tweddle, D.A. (2010) 'p53 is a Direct Transcriptional Target of MYCN in Neuroblastoma', *Cancer research*, 70(4), pp. 1377-1388.

Chen, L., Rousseau, R.F., Middleton, S.A., Nichols, G.L., Newell, D.R., Lunec, J. and Tweddle, D.A. (2015a) 'Pre-clinical evaluation of the MDM2-p53 antagonist RG7388 alone and in combination with chemotherapy in neuroblastoma', *Oncotarget*, 6(12), pp. 10207-10221.

Chen, T., Middleton, F.K., Falcon, S., Reaper, P.M., Pollard, J.R. and Curtin, N.J. (2015b) 'Development of pharmacodynamic biomarkers for ATR inhibitors', *Molecular Oncology*, 9(2), pp. 463-472.

Chen, Y., Takita, J., Choi, Y.L., Kato, M., Ohira, M., Sanada, M., Wang, L., Soda, M., Kikuchi, A., Igarashi, T., Nakagawara, A., Hayashi, Y., Mano, H. and Ogawa, S. (2008) 'Oncogenic mutations of ALK kinase in neuroblastoma', *Nature*, 455(7215), pp. 971-974.

Cheung, N.-K.V., Zhang, J., Lu, C., Parker, M., Bahrami, A., Tickoo, S.K., Heguy, A., Pappo, A.S., Federico, S., Dalton, J., Cheung, I.Y., Ding, L., Fulton, B., Wang, J., Chen, X., Becksfort, J., Wu, J., Billups, C.A., Ellison, D., Mardis, E.R., Wilson, R.K., Downing, J.R. and Dyer, M.A. (2012) 'Association of Age at Diagnosis and Genetic Mutations in Patients with Neuroblastoma', *JAMA : the journal of the American Medical Association*, 307(10), pp. 1062-1071.

Cheung, N.K. and Dyer, M.A. (2013) 'Neuroblastoma: developmental biology, cancer genomics and immunotherapy', *Nat Rev Cancer*, 13(6), pp. 397-411.

Choi, M., Kipps, T. and Kurzrock, R. (2016) 'ATM Mutations in Cancer: Therapeutic Implications', *Molecular Cancer Therapeutics*, 15(8), pp. 1781-1791.

Choi, Y., Sims, G.E., Murphy, S., Miller, J.R. and Chan, A.P. (2012) 'Predicting the functional effect of amino acid substitutions and indels', *PloS one*, 7(10), pp. e46688-e46688.

Ciccia, A. and Elledge, S.J. (2010) 'The DNA Damage Response: Making it safe to play with knives', *Molecular cell*, 40(2), pp. 179-204.

Cimprich, K.A. and Cortez, D. (2008) 'ATR: an essential regulator of genome integrity', *Nature reviews. Molecular cell biology*, 9(8), p. 616.

Clynes, D., Higgs, D.R. and Gibbons, R.J. (2013) 'The chromatin remodeller ATRX: a repeat offender in human disease', *Trends in Biochemical Sciences*, 38(9), pp. 461-466.

Cohn, S.L., Pearson, A.D.J., London, W.B., Monclair, T., Ambros, P.F., Brodeur, G.M., Faldum, A., Hero, B., Iehara, T. and Machin, D. (2009) 'The International Neuroblastoma Risk Group (INRG) classification system: an INRG task force report', *Journal of clinical oncology*, 27(2), pp. 289-297.

Cole, K.A., Huggins, J., Laquaglia, M., Hulderman, C.E., Russell, M.R., Bosse, K., Diskin, S.J., Attiyeh, E.F., Sennett, R., Norris, G., Laudenslager, M., Wood, A.C., Mayes, P.A., Jagannathan, J., Winter, C., Mosse, Y.P. and Maris, J.M. (2011) 'RNAi screen of the protein kinome identifies checkpoint kinase 1 (CHK1) as a therapeutic target in neuroblastoma', *Proceedings of the National Academy of Sciences*, 108(8), pp. 3336-3341.

Cole, K.A., Pal, S., Kudgus, R.A., Ijaz, H., Liu, X., Minard, C.G., Pawel, B.R., Maris, J.M., Haas-Kogan, D.A., Voss, S.D., Berg, S.L., Reid, J.M., Fox, E. and Weigel, B.J. (2020) 'Phase I Clinical Trial of the

Wee1 Inhibitor Adavosertib (AZD1775) with Irinotecan in Children with Relapsed Solid Tumors: A COG Phase I Consortium Report (ADVL1312)', *Clinical cancer research : an official journal of the American Association for Cancer Research*, 26(6), pp. 1213-1219.

Colicchia, V., Petroni, M., Guarguaglini, G., Sardina, F., Sahún-Roncero, M., Carbonari, M., Ricci, B., Heil, C., Capalbo, C. and Belardinilli, F. (2017) 'PARP inhibitors enhance replication stress and cause mitotic catastrophe in MYCN-dependent neuroblastoma', *Oncogene*, 36(33), pp. 4682-4691.

Collins, S. and Groudine, M. (1982) 'Amplification of endogenous myc-related DNA sequences in a human myeloid leukaemia cell line', *Nature*, 298(5875), pp. 679-681.

Cornaglia-Ferraris, P., Ponzoni, M., Montaldo, P., Mariottini, G.L., Donti, E., Di Martino, D. and Tonini, G.P. (1990) 'A New Human Highly Tumorigenic Neuroblastoma Cell Line with Undetectable Expression of N-myc', *Pediatric Research*, 27(1), pp. 1-6.

Crowder, R.N. and El-Deiry, W.S. (2012) 'Caspase-8 regulation of TRAIL-mediated cell death', *Exp Oncol*, 34(3), pp. 160-164.

Curtin, N.J. (2012) 'DNA repair dysregulation from cancer driver to therapeutic target', *Nat Rev Cancer*, 12(12), pp. 801-17.

Curtin, N.J. and Szabo, C. (2020) 'Poly(ADP-ribose) polymerase inhibition: past, present and future', *Nature Reviews Drug Discovery*, 19(10), pp. 711-736.

Dang, C.V., O'Donnell, K.A., Zeller, K.I., Nguyen, T., Osthus, R.C. and Li, F. (2006) 'The c-Myc target gene network', *Seminars in Cancer Biology*, 16(4), pp. 253-264.

Daniel, R.A., Rozanska, A.L., Thomas, H.D., Mulligan, E.A., Drew, Y., Castelbuono, D.J., Hostomsky, Z., Plummer, E.R., Boddy, A.V., Tweddle, D.A., Curtin, N.J. and Clifford, S.C. (2009) 'Inhibition of Poly(ADP-Ribose) Polymerase-1 Enhances Temozolomide and Topotecan Activity against Childhood Neuroblastoma', *Clinical Cancer Research*, 15(4), pp. 1241-1249.

Darzynkiewicz, Z. (2010) 'Cytometry of the cell cycle: In search for perfect methodology for DNA content analysis in tissue specimens', *Cell cycle (Georgetown, Tex.)*, 9(17), pp. 3395-3396.
Davidoff, A.M. (2012) 'Neuroblastoma', *Seminars in Pediatric Surgery*, 21(1), pp. 2-14.

Deans, A.J. and West, S.C. (2011) 'DNA interstrand crosslink repair and cancer', *Nature Reviews Cancer*, 11(7), pp. 467-480.

Deckbar, D., Birraux, J., Krempler, A., Tchouandong, L., Beucher, A., Walker, S., Stiff, T., Jeggo, P. and Löbrich, M. (2007) 'Chromosome breakage after G2 checkpoint release', *The Journal of cell biology*, 176(6), pp. 749-755.

Deeg, K.I., Chung, I., Bauer, C. and Rippe, K. (2016) 'Cancer Cells with Alternative Lengthening of Telomeres Do Not Display a General Hypersensitivity to ATR Inhibition', *Frontiers in oncology*, 6, pp. 186-186.

Defferrari, R., Mazzocco, K., Ambros, I.M., Ambros, P.F., Bedwell, C., Beiske, K., Benard, J., Berbegall, A.P., Bown, N., Combaret, V., Couturier, J., Erminio, G., Gambini, C., Garaventa, A., Gross, N., Haupt, R., Kohler, J., Jeison, M., Lunec, J., Marques, B., Martinsson, T., Noguera, R., Parodi, S., Schleiermacher, G., Tweddle, D.A., Valent, A., Van Roy, N., Vicha, A., Villamon, E. and Tonini, G.P.

(2015) 'Influence of segmental chromosome abnormalities on survival in children over the age of 12 months with unresectable localised peripheral neuroblastic tumours without MYCN amplification', *Br J Cancer*, 112(2), pp. 290-295.

Delia, D., Piane, M., Buscemi, G., Savio, C., Palmeri, S., Lulli, P., Carlessi, L., Fontanella, E. and Chessa, L. (2004) 'MRE11 mutations and impaired ATM-dependent responses in an Italian family with ataxia-telangiectasia-like disorder', *Human Molecular Genetics*, 13(18), pp. 2155-2163.

Depuydt, P., Boeva, V., Hocking, T.D., Cannoodt, R., Ambros, I.M., Ambros, P.F., Asgharzadeh, S., Attiyeh, E.F., Combaret, V., Defferrari, R., Fischer, M., Hero, B., Hogarty, M.D., Irwin, M.S., Koster, J., Kreissman, S., Ladenstein, R., Lapouble, E., Laureys, G., London, W.B., Mazzocco, K., Nakagawara, A., Noguera, R., Ohira, M., Park, J.R., Pötschger, U., Theissen, J., Tonini, G.P., Valteau-Couanet, D., Varesio, L., Versteeg, R., Speleman, F., Maris, J.M., Schleiermacher, G. and De Preter, K. (2018) 'Genomic Amplifications and Distal 6q Loss: Novel Markers for Poor Survival in High-risk Neuroblastoma Patients', *JNCI: Journal of the National Cancer Institute*, pp. djy022-djy022.

Dillon, M.T., Barker, H.E., Pedersen, M., Hafsi, H., Bhide, S.A., Newbold, K.L., Nutting, C.M., McLaughlin, M. and Harrington, K.J. (2017) 'Radiosensitization by the ATR Inhibitor AZD6738 through Generation of Acentric Micronuclei', *Molecular cancer therapeutics*, 16(1), pp. 25-34.

Ding, D., Zhang, Y., Wang, J., Zhang, X., Gao, Y., Yin, L., Li, Q., Li, J. and Chen, H. (2016) 'Induction and inhibition of the pan-nuclear gamma-H2AX response in resting human peripheral blood lymphocytes after X-ray irradiation', *Cell Death Discovery*, 2(1), p. 16011.

do Valle, Í.F., Giampieri, E., Simonetti, G., Padella, A., Manfrini, M., Ferrari, A., Papayannidis, C., Zironi, I., Garonzi, M., Bernardi, S., Delledonne, M., Martinelli, G., Remondini, D. and Castellani, G. (2016) 'Optimized pipeline of MuTect and GATK tools to improve the detection of somatic single nucleotide polymorphisms in whole-exome sequencing data', *BMC Bioinformatics*, 17(12), p. 341.

Downs, K.M., Martin, G.R. and Bishop, J.M. (1989) 'Contrasting patterns of myc and N-myc expression during gastrulation of the mouse embryo', *Genes Dev*, 3(6), pp. 860-9.

Dréan, A., Lord, C.J. and Ashworth, A. (2016) 'PARP inhibitor combination therapy', *Critical Reviews in Oncology/Hematology*, 108(Supplement C), pp. 73-85.

Dreidax, D., Bannert, S., Henrich, K.-O., Schröder, C., Bender, S., Oakes, C.C., Lindner, S., Schulte, J.H., Duffy, D., Schwarzl, T., Saadati, M., Ehemann, V., Benner, A., Pfister, S., Fischer, M. and Westermann, F. (2014) 'p19-INK4d inhibits neuroblastoma cell growth, induces differentiation and is hypermethylated and downregulated in MYCN-amplified neuroblastomas', *Human Molecular Genetics*, 23(25), pp. 6826-6837.

Drummond, C.J., Esfandiari, A., Liu, J., Lu, X., Hutton, C., Jackson, J., Bennaceur, K., Xu, Q., Makimanejavali, A.R., Bello, F.D., Piergentili, A., Newell, D.R., Hardcastle, I.R., Griffin, R.J. and Lunec, J. (2016) 'TP53 mutant MDM2-amplified cell lines selected for resistance to MDM2-p53 binding antagonists retain sensitivity to ionizing radiation', *Oncotarget*, 7(29), pp. 46203-46218.

Duan, X.-F. and Zhao, Q. (2017) 'TERT-mediated and ATRX-mediated Telomere Maintenance and Neuroblastoma', *Journal of Pediatric Hematology/Oncology*.

Dunham, M.A., Neumann, A.A., Fasching, C.L. and Reddel, R.R. (2000) 'Telomere maintenance by recombination in human cells', *Nat Genet*, 26(4), pp. 447-450.

Durinck, K. and Speleman, F. (2018) 'Epigenetic regulation of neuroblastoma development', *Cell and Tissue Research*, 372(2), pp. 309-324.

Dutto, I., Scalera, C. and Prosperi, E. (2018) 'CREBBP and p300 lysine acetyl transferases in the DNA damage response', *Cellular and Molecular Life Sciences*, 75(8), pp. 1325-1338.
Eilers, M. and Eisenman, R.N. (2008) 'Myc's broad reach', *Genes & Development*, 22(20), pp. 2755-2766.

Eleveld, T.F., Oldridge, D.A., Bernard, V., Koster, J., Daage, L.C., Diskin, S.J., Schild, L., Bentahar, N.B., Bellini, A., Chicard, M., Lapouble, E., Combaret, V., Legoix-Ne, P., Michon, J., Pugh, T.J., Hart, L.S., Rader, J., Attiyeh, E.F., Wei, J.S., Zhang, S., Naranjo, A., Gastier-Foster, J.M., Hogarty, M.D., Asgharzadeh, S., Smith, M.A., Guidry Auvil, J.M., Watkins, T.B.K., Zwijnenburg, D.A., Ebus, M.E., van Sluis, P., Hakkert, A., van Wezel, E., van der Schoot, C.E., Westerhout, E.M., Schulte, J.H., Tytgat, G.A., Dolman, M.E.M., Janoueix-Lerosey, I., Gerhard, D.S., Caron, H.N., Delattre, O., Khan, J., Versteeg, R., Schleiermacher, G., Molenaar, J.J. and Maris, J.M. (2015) 'Relapsed neuroblastomas show frequent RAS-MAPK pathway mutations', *Nat Genet*, 47(8), pp. 864-871.

Esposito, M.R., Aveic, S., Seydel, A. and Tonini, G.P. (2017) 'Neuroblastoma treatment in the post-genomic era', *Journal of Biomedical Science*, 24, p. 14.

Evans, L., Chen, L., Milazzo, G., Gherardi, S., Perini, G., Willmore, E., Newell, D.R. and Tweddle, D.A. (2015) 'SKP2 is a direct transcriptional target of MYCN and a potential therapeutic target in neuroblastoma', *Cancer Letters*, 363(1), pp. 37-45.

Faraoni, I., Compagnone, M., Lavorgna, S., Angelini, D.F., Cencioni, M.T., Piras, E., Panetta, P., Ottone, T., Dolci, S., Venditti, A., Graziani, G. and Lo-Coco, F. (2015) 'BRCA1, PARP1 and γH2AX in acute myeloid leukemia: Role as biomarkers of response to the PARP inhibitor olaparib', *Biochimica et Biophysica Acta (BBA) - Molecular Basis of Disease*, 1852(3), pp. 462-472.

Federico, S.M., Pappo, A.S., Sahr, N., Sykes, A., Campagne, O., Stewart, C.F., Clay, M.R., Bahrami, A., McCarville, M.B., Kaste, S.C., Santana, V.M., Helmig, S., Gartrell, J., Shelat, A., Brennan, R.C., Hawkins, D., Godwin, K., Bishop, M.W., Furman, W.L. and Stewart, E. (2020) 'A phase I trial of talazoparib and irinotecan with and without temozolomide in children and young adults with recurrent or refractory solid malignancies', *European Journal of Cancer*, 137, pp. 204-213.

Ferrandis, E. and Bénard, J. (1993) 'Activation of the human mdr1 gene promoter in differentiated neuroblasts', *International Journal of Cancer*, 54(6), pp. 987-991.

Fikaris, A.J., Lewis, A.E., Abulaiti, A., Tsygankova, O.M. and Meinkoth, J.L. (2006) 'Ras triggers ataxia-telangiectasia-mutated and Rad-3-related activation and apoptosis through sustained mitogenic signaling', *J Biol Chem*, 281(46), pp. 34759-67.

Flynn, R.L., Cox, K.E., Jeitany, M., Wakimoto, H., Bryll, A.R., Ganem, N.J., Bersani, F., Pineda, J.R., Suvà, M.L., Benes, C.H., Haber, D.A., Boussin, F.D. and Zou, L. (2015) 'Alternative Lengthening of Telomeres Renders Cancer Cells Hypersensitive to ATR Inhibitors', *Science (New York, N.Y.)*, 347(6219), pp. 273-277.

Fordham, S.E., Blair, H.J., Elstob, C.J., Plummer, R., Drew, Y., Curtin, N.J., Heidenreich, O., Pal, D., Jamieson, D., Park, C., Pollard, J., Fields, S., Milne, P., Jackson, G.H., Marr, H.J., Menne, T., Jones, G.L.

and Allan, J.M. (2018) 'Inhibition of ATR acutely sensitizes acute myeloid leukemia cells to nucleoside analogs that target ribonucleotide reductase', *Blood advances*, 2(10), pp. 1157-1169.

Fortini, P. and Dogliotti, E. (2007) 'Base damage and single-strand break repair: Mechanisms and functional significance of short- and long-patch repair subpathways', *DNA Repair*, 6(4), pp. 398-409.

Freed-Pastor, W.A. and Prives, C. (2012) 'Mutant p53: one name, many proteins', *Genes & development*, 26(12), pp. 1268-1286.

Fu, D., Calvo, J.A. and Samson, L.D. (2012) 'Balancing repair and tolerance of DNA damage caused by alkylating agents', *Nature Reviews Cancer*, 12(2), pp. 104-120.

Fujisawa, H., Nakajima, N.I., Sunada, S., Lee, Y., Hirakawa, H., Yajima, H., Fujimori, A., Uesaka, M. and Okayasu, R. (2015) 'VE-821, an ATR inhibitor, causes radiosensitization in human tumor cells irradiated with high LET radiation', *Radiation oncology (London, England)*, 10, pp. 175-175.

Gagou, M.E., Zuazua-Villar, P. and Meuth, M. (2010) 'Enhanced H2AX phosphorylation, DNA replication fork arrest, and cell death in the absence of Chk1', *Molecular biology of the cell*, 21(5), pp. 739-752.

Gaillard, H., García-Muse, T. and Aguilera, A. (2015) 'Replication stress and cancer', *Nature Reviews Cancer*, 15, p. 276.

Gamble, L.D., Kees, U.R., Tweddle, D.A. and Lunec, J. (2012) 'MYCN sensitizes neuroblastoma to the MDM2-p53 antagonists Nutlin-3 and MI-63', *Oncogene*, 31(6), pp. 752-763.

Gatz, S.A., Rubino, J., Rossoni, C., Andre, N., Aerts, I., Thebaud, E., Nebchi, S., Rondof, W., Hübschmann, D., Mortimer, P.G., Paoletti, X., Vassal, G. and Geoerger, B. (2019) 'AcSé-ESMART: European Proof of Concept Therapeutic Stratification Trial of Molecular Anomalies in Relapsed or Refractory Tumors in Children and Adolescents–Arm D: Olaparib and irinotecan', *Journal of Clinical Oncology*, 37(15_suppl), pp. 10047-10047.

Gavande, N.S., VanderVere-Carozza, P.S., Hinshaw, H.D., Jalal, S.I., Sears, C.R., Pawelczak, K.S. and Turchi, J.J. (2016) 'DNA repair targeted therapy: The past or future of cancer treatment?', *Pharmacology & Therapeutics*, 160, pp. 65-83.

George, R.E., Sanda, T., Hanna, M., Fröhling, S., Luther, W., Zhang, J., Ahn, Y., Zhou, W., London, W.B., McGrady, P., Xue, L., Zozulya, S., Gregor, V., Webb, T.R., Gray, N.S., Gilliland, D.G., Diller, L., Greulich, H., Morris, S.W., Meyerson, M. and Look, A.T. (2008) 'Activating mutations in ALK provide a therapeutic target in neuroblastoma', *Nature*, 455(7215), pp. 975-978.

George, S.L., Falzone, N., Chittenden, S., Kirk, S.J., Lancaster, D., Vaidya, S.J., Mandeville, H., Saran, F., Pearson, A.D.J., Du, Y., Meller, S.T., Denis-Bacelar, A.M. and Flux, G.D. (2016) 'Individualized 131I-mIBG therapy in the management of refractory and relapsed neuroblastoma', *Nuclear medicine communications*, 37(5), pp. 466-472.

George, S.L., Lorenzi, F., King, D., Hartlieb, S., Campbell, J., Pemberton, H., Toprak, U.H., Barker, K., Tall, J., da Costa, B.M., van den Boogaard, M.L., Dolman, M.E.M., Molenaar, J.J., Bryant, H.E., Westermann, F., Lord, C.J. and Chesler, L. (2020a) 'Therapeutic vulnerabilities in the DNA damage response for the treatment of ATRX mutant neuroblastoma', *EBioMedicine*, 59, p. 102971.

George, S.L., Parmar, V., Lorenzi, F., Marshall, L.V., Jamin, Y., Poon, E., Angelini, P. and Chesler, L. (2020b) 'Novel therapeutic strategies targeting telomere maintenance mechanisms in high-risk neuroblastoma', *Journal of Experimental & Clinical Cancer Research*, 39(1), p. 78.

Gilardini Montani, M.S., Prodosmo, A., Stagni, V., Merli, D., Monteonofrio, L., Gatti, V., Gentileschi, M.P., Barilà, D. and Soddu, S. (2013) 'ATM-depletion in breast cancer cells confers sensitivity to PARP inhibition', *Journal of Experimental & Clinical Cancer Research*, 32(1), p. 95.

Goldman, S.C., Chen, C.Y., Lansing, T.J., Gilmer, T.M. and Kastan, M.B. (1996) 'The p53 signal transduction pathway is intact in human neuroblastoma despite cytoplasmic localization', *The American journal of pathology*, 148(5), pp. 1381-1385.

Goldschneider, D., Blanc, E., Raguénez, G., Barrois, M., Legrand, A., Le Roux, G., Haddada, H., Bénard, J. and Douc-Rasy, S. (2004) 'Differential response of p53 target genes to p73 overexpression in SH-SY5Y neuroblastoma cell line', *Journal of Cell Science*, 117(2), pp. 293-301.

Goldschneider, D., Horvilleur, E., Plassa, L.-F., Guillaud-Bataille, M., Million, K., Wittmer-Dupret, E., Danglot, G., de Thé, H., Bénard, J., May, E. and Douc-Rasy, S. (2006) 'Expression of C-terminal deleted p53 isoforms in neuroblastoma', *Nucleic acids research*, 34(19), pp. 5603-5612.

Gossen, M. and Bujard, H. (1992) 'Tight control of gene expression in mammalian cells by tetracycline-responsive promoters', *Proceedings of the National Academy of Sciences of the United States of America*, 89(12), pp. 5547-5551.

Gossen, M., Freundlieb, S., Bender, G., Muller, G., Hillen, W. and Bujard, H. (1995) 'Transcriptional activation by tetracyclines in mammalian cells', *Science*, 268(5218), pp. 1766-1769.

Gu, L., Chu, P., Lingeman, R., McDaniel, H., Kechichian, S., Hickey, R.J., Liu, Z., Yuan, Y.-C., Sandoval, J.A., Fields, G.B. and Malkas, L.H. (2015) 'The Mechanism by Which MYCN Amplification Confers an Enhanced Sensitivity to a PCNA-Derived Cell Permeable Peptide in Neuroblastoma Cells', *EBioMedicine*, 2(12), pp. 1923-1931.

Gur, H., Ozen, F., Can Saylan, C. and Atasever-Arslan, B. (2017) 'Dinutuximab in the Treatment of High-Risk Neuroblastoma in Children', *Clinical Medicine Insights: Therapeutics*, 9, p. 1179559X17719106.

Hahn, W.C. and Meyerson, M. (2001) 'Telomerase activation, cellular immortalization and cancer', *Annals of Medicine*, 33(2), pp. 123-129.

Hall, A.B., Newsome, D., Wang, Y., Boucher, D.M., Eustace, B., Gu, Y., Hare, B., Johnson, M.A., Milton, S., Murphy, C.E., Takemoto, D., Tolman, C., Wood, M., Charlton, P., Charrier, J.-D., Furey, B., Golec, J., Reaper, P.M. and Pollard, J.R. (2014) 'Potentiation of tumor responses to DNA damaging therapy by the selective ATR inhibitor VX-970', *Oncotarget*, 5(14), pp. 5674-5685.

Hallberg, B. and Palmer, R.H. (2013) 'Mechanistic insight into ALK receptor tyrosine kinase in human cancer biology', *Nat Rev Cancer*, 13(10), pp. 685-700.

Hanahan, D. and Weinberg, R.A. (2000) 'The Hallmarks of Cancer', *Cell*, 100(1), pp. 57-70.

Hanahan, D. and Weinberg, Robert A. (2011) 'Hallmarks of Cancer: The Next Generation', *Cell*, 144(5), pp. 646-674.

Harper, J.W. and Elledge, S.J. (2007) 'The DNA damage response: ten years after', *Molecular cell*, 28(5), pp. 739-745.

Helson, L., Verma, M. and Helson, C. (1983) 'Vitamin E and human neuroblastoma', in *Modulation and Mediation of Cancer by Vitamins*. Karger Publishers, pp. 258-265.

Henssen, A.G., Koche, R., Zhuang, J., Jiang, E., Reed, C., Eisenberg, A., Still, E., MacArthur, I.C., Rodríguez-Fos, E., Gonzalez, S., Puiggròs, M., Blackford, A.N., Mason, C.E., de Stanchina, E., Gönen, M., Emde, A.-K., Shah, M., Arora, K., Reeves, C., Socci, N.D., Perlman, E., Antonescu, C.R., Roberts, C.W.M., Steen, H., Mullen, E., Jackson, S.P., Torrents, D., Weng, Z., Armstrong, S.A. and Kentsis, A. (2017a) 'PGBD5 promotes site-specific oncogenic mutations in human tumors', *Nature Genetics*, 49(7), pp. 1005-1014.

Henssen, A.G., Reed, C., Jiang, E., Garcia, H.D., von Stebut, J., MacArthur, I.C., Hundsdoerfer, P., Kim, J.H., de Stanchina, E., Kuwahara, Y., Hosoi, H., Ganem, N.J., Dela Cruz, F., Kung, A.L., Schulte, J.H., Petrini, J.H. and Kentsis, A. (2017b) 'Therapeutic targeting of PGBD5-induced DNA repair dependency in pediatric solid tumors', *Science Translational Medicine*, 9(414).

Herriott, A., Tudhope, S.J., Junge, G., Rodrigues, N., Patterson, M.J., Woodhouse, L., Lunec, J., Hunter, J.E., Mulligan, E.A., Cole, M., Allinson, L.M., Wallis, J.P., Marshall, S., Wang, E., Curtin, N.J. and Willmore, E. (2015) 'PARP1 expression, activity and ex vivo sensitivity to the PARP inhibitor, talazoparib (BMN 673), in chronic lymphocytic leukaemia', *Oncotarget*, 6(41), pp. 43978-43991.

Hertwig, F., Peifer, M. and Fischer, M. (2016) 'Telomere maintenance is pivotal for high-risk neuroblastoma', *Cell Cycle*, 15(3), pp. 311-312.

Hirning, U., Schmid, P., Schulz, W.A., Rettenberger, G. and Hameister, H. (1991) 'A comparative analysis of N-myc and c-myc expression and cellular proliferation in mouse organogenesis', *Mechanisms of Development*, 33(2), pp. 119-125.

Hochegger, H., Takeda, S. and Hunt, T. (2008) 'Cyclin-dependent kinases and cell-cycle transitions: does one fit all?', *Nature Reviews Molecular Cell Biology*, 9, p. 910.

Hoeijmakers, J.H.J. (2001) 'Genome maintenance mechanisms for preventing cancer', *Nature*, 411(6835), pp. 366-374.

Hogarty, M.D. (2003) 'The requirement for evasion of programmed cell death in neuroblastomas with MYCN amplification', *Cancer Letters*, 197(1), pp. 173-179.

Horn, H.F. and Vousden, K.H. (2007) 'Coping with stress: multiple ways to activate p53', *Oncogene*, 26(9), pp. 1306-1316.

Hu, H., Du, L., Nagabayashi, G., Seeger, R.C. and Gatti, R.A. (2010) 'ATM is down-regulated by N-Myc-regulated microRNA-421', *Proceedings of the National Academy of Sciences of the United States of America*, 107(4), pp. 1506-1511.

Hyun, S.-Y. and Jang, Y.-J. (2015) 'p53 activates G_1 checkpoint following DNA damage by doxorubicin during transient mitotic arrest', *Oncotarget*, 6(7), pp. 4804-4815.

Iwahara, T., Fujimoto, J., Wen, D., Cupples, R., Bucay, N., Arakawa, T., Mori, S., Ratzkin, B. and Yamamoto, T. (1997) 'Molecular characterization of ALK, a receptor tyrosine kinase expressed specifically in the nervous system', *Oncogene*, 14(4).

Jackson, C.B., Noorbakhsh, S.I., Sundaram, R.K., Kalathil, A.N., Ganesa, S., Jia, L., Breslin, H., Burgenske, D.M., Gilad, O., Sarkaria, J.N. and Bindra, R.S. (2019) 'Temozolomide Sensitizes MGMT-Deficient Tumor Cells to ATR Inhibitors', *Cancer research*, 79(17), pp. 4331-4338.

Janoueix-Lerosey, I., Lequin, D., Brugieres, L., Ribeiro, A., de Pontual, L., Combaret, V., Raynal, V., Puisieux, A., Schleiermacher, G., Pierron, G., Valteau-Couanet, D., Frebourg, T., Michon, J., Lyonnet, S., Amiel, J. and Delattre, O. (2008) 'Somatic and germline activating mutations of the ALK kinase receptor in neuroblastoma', *Nature*, 455(7215), pp. 967-970.

Jelinic, P. and Levine, D.A. (2014) 'New Insights into PARP Inhibitors' Effect on Cell Cycle and Homology-Directed DNA Damage Repair', *Molecular Cancer Therapeutics*, 13(6), pp. 1645-1654.

Jette, N.R., Kumar, M., Radhamani, S., Arthur, G., Goutam, S., Yip, S., Kolinsky, M., Williams, G.J., Bose, P. and Lees-Miller, S.P. (2020) 'ATM-Deficient Cancers Provide New Opportunities for Precision Oncology', *Cancers*, 12(3), p. 687.

Jette, N.R., Radhamani, S., Arthur, G., Ye, R., Goutam, S., Bolyos, A., Petersen, L.F., Bose, P., Bebb, D.G. and Lees-Miller, S.P. (2019) 'Combined poly-ADP ribose polymerase and ataxia-telangiectasia mutated/Rad3-related inhibition targets ataxia-telangiectasia mutated-deficient lung cancer cells', *British journal of cancer*, 121(7), pp. 600-610.

Jia, P. and Zhao, Z. (2017) 'Impacts of somatic mutations on gene expression: an association perspective', *Briefings in bioinformatics*, 18(3), pp. 413-425.

Jossé, R., Martin, S.E., Guha, R., Ormanoglu, P., Pfister, T.D., Reaper, P.M., Barnes, C.S., Jones, J., Charlton, P., Pollard, J.R., Morris, J., Doroshow, J.H. and Pommier, Y. (2014) 'ATR inhibitors VE-821 and VX-970 sensitize cancer cells to topoisomerase i inhibitors by disabling DNA replication initiation and fork elongation responses', *Cancer research*, 74(23), pp. 6968-6979.

Kakarougkas, A. and Jeggo, P.A. (2014) 'DNA DSB repair pathway choice: an orchestrated handover mechanism', *The British Journal of Radiology*, 87(1035), p. 20130685.

Karakaidos, P., Karagiannis, D. and Rampias, T. (2020) 'Resolving DNA Damage: Epigenetic Regulation of DNA Repair', *Molecules (Basel, Switzerland)*, 25(11), p. 2496.

Karnitz, L.M. and Zou, L. (2015) 'Molecular Pathways: Targeting ATR in Cancer Therapy', *Clinical cancer research : an official journal of the American Association for Cancer Research*, 21(21), pp. 4780-4785.

Kastan, M.B., Zhan, Q., El-Deiry, W.S., Carrier, F., Jacks, T., Walsh, W.V., Plunkett, B.S., Vogelstein, B. and Fornace, A.J. (1992) 'A mammalian cell cycle checkpoint pathway utilizing p53 and GADD45 is defective in ataxia-telangiectasia', *Cell*, 71(4), pp. 587-597.

Kaufmann, T., Strasser, A. and Jost, P.J. (2012) 'Fas death receptor signalling: roles of Bid and XIAP', *Cell Death and Differentiation*, 19(1), pp. 42-50.

Kawashima, M., Kojima, M., Ueda, Y., Kurihara, S. and Hiyama, E. (2016) 'Telomere biology including TERT rearrangements in neuroblastoma: a useful indicator for surgical treatments', *Journal of Pediatric Surgery*, 51(12), pp. 2080-2085.

Keshelava, N., Zuo, J.J., Waidyaratne, N.S., Triche, T.J. and Reynolds, C.P. (2000) 'p53 mutations and loss of p53 function confer multidrug resistance in neuroblastoma', *Medical and Pediatric Oncology*, 35(6), pp. 563-568.

Kim, H., George, E., Ragland, R., Rafail, S., Zhang, R., Krepler, C., Morgan, M., Herlyn, M., Brown, E. and Simpkins, F. (2017) 'Targeting the ATR/CHK1 Axis with PARP Inhibition Results in Tumor Regression in BRCA-Mutant Ovarian Cancer Models', *Clinical cancer research : an official journal of the American Association for Cancer Research*, 23(12), pp. 3097-3108.

Kim, H., Xu, H., George, E., Hallberg, D., Kumar, S., Jagannathan, V., Medvedev, S., Kinose, Y., Devins, K., Verma, P., Ly, K., Wang, Y., Greenberg, R.A., Schwartz, L., Johnson, N., Scharpf, R.B., Mills, G.B., Zhang, R., Velculescu, V.E., Brown, E.J. and Simpkins, F. (2020) 'Combining PARP with ATR inhibition overcomes PARP inhibitor and platinum resistance in ovarian cancer models', *Nature Communications*, 11(1), p. 3726.

King, D., Li, X.D., Almeida, G.S., Kwok, C., Gravells, P., Harrison, D., Burke, S., Hallsworth, A., Jamin, Y., George, S., Robinson, S.P., Lord, C.J., Poon, E., Yeomanson, D., Chesler, L. and Bryant, H.E. (2020) 'MYCN expression induces replication stress and sensitivity to PARP inhibition in neuroblastoma', *Oncotarget*, 11(23), pp. 2141-2159.

Koppen, A., Ait-Aissa, R., Koster, J., van Sluis, P.G., Øra, I., Caron, H.N., Volckmann, R., Versteeg, R. and Valentijn, L.J. (2007) 'Direct regulation of the minichromosome maintenance complex by MYCN in neuroblastoma', *European Journal of Cancer*, 43(16), pp. 2413-2422.

Kotsantis, P., Petermann, E. and Boulton, S.J. (2018) 'Mechanisms of Oncogene-Induced Replication Stress: Jigsaw Falling into Place', *Cancer Discovery*, 8(5), pp. 537-555.

Krebs, M.G., Lopez, J., El-Khoueiry, A., Bang, Y.-J., Postel-Vinay, S., Abida, W., Carter, L., Xu, W., Im, S.-A., Pierce, A., Frewer, P., Berges, A., Cheung, S.Y.A., Stephens, C., Felicetti, B., Dean, E. and Hollingsworth, S.J. (2018) 'Abstract CT026: Phase I study of AZD6738, an inhibitor of ataxia telangiectasia Rad3-related (ATR), in combination with olaparib or durvalumab in patients (pts) with advanced solid cancers', *Cancer Research*, 78(13 Supplement), pp. CT026-CT026.

Krokan, H.E. and Bjørås, M. (2013) 'Base Excision Repair', *Cold Spring Harbor Perspectives in Biology*, 5(4), p. a012583.

Kubota, E., Williamson, C.T., Ye, R., Elegbede, A., Peterson, L., Lees-Miller, S.P. and Bebb, D.G. (2014) 'Low ATM protein expression and depletion of p53 correlates with olaparib sensitivity in gastric cancer cell lines', *Cell cycle (Georgetown, Tex.)*, 13(13), pp. 2129-2137.

Kurmasheva, R.T., Kurmashev, D., Reynolds, C.P., Kang, M., Wu, J., Houghton, P.J. and Smith, M.A. (2018) 'Initial testing (stage 1) of M6620 (formerly VX-970), a novel ATR inhibitor, alone and combined with cisplatin and melphalan, by the Pediatric Preclinical Testing Program', *Pediatric Blood & Cancer*, 65(2), pp. e26825-n/a.

Kwok, M., Davies, N., Agathanggelou, A., Smith, E., Oldreive, C., Petermann, E., Stewart, G., Brown, J., Lau, A., Pratt, G., Parry, H., Taylor, M., Moss, P., Hillmen, P. and Stankovic, T. (2016) 'ATR inhibition

induces synthetic lethality and overcomes chemoresistance in TP53- or ATM-defective chronic lymphocytic leukemia cells', *Blood*, 127(5), pp. 582-595.

LaFargue, C.J., Dal Molin, G.Z., Sood, A.K. and Coleman, R.L. (2019) 'Exploring and comparing adverse events between PARP inhibitors', *The Lancet. Oncology*, 20(1), pp. e15-e28.

Lakoma, A., Barbieri, E., Agarwal, S., Jackson, J., Chen, Z., Kim, Y., McVay, M., Shohet, J.M. and Kim, E.S. (2015) 'The MDM2 small-molecule inhibitor RG7388 leads to potent tumor inhibition in p53 wild-type neuroblastoma', *Cell Death Discovery*, 1, p. 15026.

Lasorsa, V.A., Formicola, D., Pignataro, P., Cimmino, F., Calabrese, F.M., Mora, J., Esposito, M.R., Pantile, M., Zanon, C., De Mariano, M., Longo, L., Hogarty, M.D., de Torres, C., Tonini, G.P., Iolascon, A. and Capasso, M. (2016) 'Exome and deep sequencing of clinically aggressive neuroblastoma reveal somatic mutations that affect key pathways involved in cancer progression', *Oncotarget*, 7(16), pp. 21840-21852.

Lawlor, D., Martin, P., Busschots, S., Thery, J., O'leary, J.J., Hennessy, B.T. and Stordal, B., 2014. PARP Inhibitors as P-glyoprotein Substrates. *Journal of pharmaceutical sciences*, *103*(6), pp.1913-1920.

Lee, S.H., Kim, J.-S., Zheng, S., Huse, J.T., Bae, J.S., Lee, J.W., Yoo, K.H., Koo, H.H., Kyung, S., Park, W.-Y. and Sung, K.W. (2017) 'ARID1B alterations identify aggressive tumors in neuroblastoma', *Oncotarget*, 8(28), pp. 45943-45950.

Lesueur, P., Chevalier, F., Austry, J.-B., Waissi, W., Burckel, H., Noël, G., Habrand, J.-L., Saintigny, Y. and Joly, F. (2017) 'Poly-(ADP-ribose)-polymerase inhibitors as radiosensitizers: a systematic review of pre-clinical and clinical human studies', *Oncotarget*, 8(40), pp. 69105-69124.

Liu, D., Keijzers, G. and Rasmussen, L.J. (2017a) 'DNA mismatch repair and its many roles in eukaryotic cells', *Mutation Research/Reviews in Mutation Research*, 773, pp. 174-187.

Liu, J., Zhang, C., Hu, W. and Feng, Z. (2015) 'Tumor suppressor p53 and its mutants in cancer metabolism', *Cancer letters*, 356(2), pp. 197-203.

Liu, S., Ge, Y., Wang, T., Edwards, H., Ren, Q., Jiang, Y., Quan, C. and Wang, G. (2017b) 'Inhibition of ATR potentiates the cytotoxic effect of gemcitabine on pancreatic cancer cells through enhancement of DNA damage and abrogation of ribonucleotide reductase induction by gemcitabine', *Oncology reports*, 37(6), pp. 3377-3386.

Liu, S., Opiyo, S.O., Manthey, K., Glanzer, J.G., Ashley, A.K., Amerin, C., Troksa, K., Shrivastav, M., Nickoloff, J.A. and Oakley, G.G. (2012) 'Distinct roles for DNA-PK, ATM and ATR in RPA phosphorylation and checkpoint activation in response to replication stress', *Nucleic acids research*, 40(21), pp. 10780-10794.

Lloyd, R.L., Wijnhoven, P.W.G., Ramos-Montoya, A., Wilson, Z., Illuzzi, G., Falenta, K., Jones, G.N., James, N., Chabbert, C.D., Stott, J., Dean, E., Lau, A. and Young, L.A. (2020) 'Combined PARP and ATR inhibition potentiates genome instability and cell death in ATM-deficient cancer cells', *Oncogene*, 39(25), pp. 4869-4883.

London, W.B., Bagatell, R., Weigel, B.J., Fox, E., Guo, D., Van Ryn, C., Naranjo, A. and Park, J.R. (2017) 'Historical time to disease progression and progression-free survival in patients with

recurrent/refractory neuroblastoma treated in the modern era on Children's Oncology Group early-phase trials', *Cancer*, 123(24), pp. 4914-4923.

London, W.B., Castel, V., Monclair, T., Ambros, P.F., Pearson, A.D.J., Cohn, S.L., Berthold, F., Nakagawara, A., Ladenstein, R.L., Iehara, T. and Matthay, K.K. (2011) 'Clinical and biologic features predictive of survival after relapse of neuroblastoma: a report from the International Neuroblastoma Risk Group project', *Journal of clinical oncology : official journal of the American Society of Clinical Oncology*, 29(24), pp. 3286-3292.

Look, A.T., Hayes, F.A., Shuster, J.J., Douglass, E.C., Castleberry, R.P., Bowman, L.C., Smith, E.I. and Brodeur, G.M. (1991) 'Clinical relevance of tumor cell ploidy and N-myc gene amplification in childhood neuroblastoma: a Pediatric Oncology Group study', *Journal of Clinical Oncology*, 9(4), pp. 581-591.

Lopes, M.C., Joyce, C., Ritchie, G.R.S., John, S.L., Cunningham, F., Asimit, J. and Zeggini, E. (2012) 'A combined functional annotation score for non-synonymous variants', *Human heredity*, 73(1), pp. 47-51.

Lord, C.J. and Ashworth, A. (2016) 'BRCAness revisited', *Nature Reviews Cancer*, 16(2), pp. 110-120.

Lord, C.J. and Ashworth, A. (2017) 'PARP inhibitors: Synthetic lethality in the clinic', *Science (New York, N.Y.)*, 355(6330), pp. 1152-1158.

Löser, D.A., Shibata, A., Shibata, A.K., Woodbine, L.J., Jeggo, P.A. and Chalmers, A.J. (2010) 'Sensitization to radiation and alkylating agents by inhibitors of poly(ADP-ribose) polymerase is enhanced in cells deficient in DNA double-strand break repair', *Molecular cancer therapeutics*, 9(6), pp. 1775-1787.

Lowery, C.D., Dowless, M., Renschler, M., Blosser, W., VanWye, A.B., Stephens, J.R., Iversen, P.W., Lin, A.B., Beckmann, R.P., Krytska, K., Cole, K.A., Maris, J.M., Hawkins, D.S., Rubin, B.P., Kurmasheva, R.T., Houghton, P.J., Gorlick, R., Kolb, E.A., Kang, M.H., Reynolds, C.P., Erickson, S.W., Teicher, B.A., Smith, M.A. and Stancato, L.F. (2019) 'Broad Spectrum Activity of the Checkpoint Kinase 1 Inhibitor Prexasertib as a Single Agent or Chemopotentiator Across a Range of Preclinical Pediatric Tumor Models', *Clinical Cancer Research*, 25(7), pp. 2278-2289.

Lowery, C.D., VanWye, A.B., Dowless, M., Blosser, W., Falcon, B.L., Stewart, J., Stephens, J., Beckmann, R.P., Bence Lin, A. and Stancato, L.F. (2017) 'The Checkpoint Kinase 1 Inhibitor Prexasertib Induces Regression of Preclinical Models of Human Neuroblastoma', *Clinical Cancer Research*, 23(15), pp. 4354-4363.

Lutz, W., Stöhr, M., Schürmann, J., Wenzel, A., Löhr, A. and Schwab, M. (1996) 'Conditional expression of N-myc in human neuroblastoma cells increases expression of alpha-prothymosin and ornithine decarboxylase and accelerates progression into S-phase early after mitogenic stimulation of quiescent cells', *Oncogene*, 13(4), pp. 803-12.

Lyu, X., Chastain, M. and Chai, W. (2019) 'Genome-wide mapping and profiling of γH2AX binding hotspots in response to different replication stress inducers', *BMC Genomics*, 20(1), p. 579.

Ma, M., Zhao, K., Wu, W., Sun, R. and Fei, J. (2014) 'Dynamic expression of N-myc in mouse embryonic development using an enhanced green fluorescent protein reporter gene in the N-myc locus', *Development, Growth & Differentiation*, 56(2), pp. 152-160.

Mac, S.M., D'Cunha, C.A. and Farnham, P.J. (2000) 'Direct recruitment of N-myc to target gene promoters', *Molecular carcinogenesis*, 29(2), pp. 76-86.

Mahaney, Brandi L., Meek, K. and Lees-Miller, Susan P. (2009) 'Repair of ionizing radiation-induced DNA double-strand breaks by non-homologous end-joining', *Biochemical Journal*, 417(3), p. 639.

Mandriota, S.J., Valentijn, L.J., Lesne, L., Betts, D.R., Marino, D., Boudal-Khoshbeen, M., London, W.B., Rougemont, A.-L., Attiyeh, E.F. and Maris, J.M. (2015) 'Ataxia-telangiectasia mutated (ATM) silencing promotes neuroblastoma progression through a MYCN independent mechanism', *Oncotarget*, 6(21), p. 18558.

Mansour, W.Y., Bogdanova, N.V., Kasten-Pisula, U., Rieckmann, T., Köcher, S., Borgmann, K., Baumann, M., Krause, M., Petersen, C., Hu, H., Gatti, R.A., Dikomey, E., Dörk, T. and Dahm-Daphi, J. (2013) 'Aberrant overexpression of miR-421 downregulates ATM and leads to a pronounced DSB repair defect and clinical hypersensitivity in SKX squamous cell carcinoma', *Radiotherapy and Oncology*, 106(1), pp. 147-154.

Maréchal, A. and Zou, L. (2013) 'DNA Damage Sensing by the ATM and ATR Kinases', *Cold Spring Harbor Perspectives in Biology*, 5(9), p. a012716.

Maris, J.M. (2010) 'Recent advances in neuroblastoma', *New England Journal of Medicine*, 362(23), pp. 2202-2211.

Maris, J.M., Guo, C., White, P.S., Hogarty, M.D., Thompson, P.M., Stram, D.O., Gerbing, R., Matthay, K.K., Seeger, R.C. and Brodeur, G.M. (2001) 'Allelic deletion at chromosome bands 11q14–23 is common in neuroblastoma', *Pediatric Blood & Cancer*, 36(1), pp. 24-27.

Marteijn, J.A., Lans, H., Vermeulen, W. and Hoeijmakers, J.H.J. (2014) 'Understanding nucleotide excision repair and its roles in cancer and ageing', *Nature Reviews Molecular Cell Biology*, 15, p. 465.

Massague, J. (2004) 'G1 cell-cycle control and cancer', *Nature*, 432(7015), pp. 298-306.

Mathur, R. (2018) 'ARID1A loss in cancer: Towards a mechanistic understanding', *Pharmacology & Therapeutics*, 190, pp. 15-23.

Matthay, K.K., Maris, J.M., Schleiermacher, G., Nakagawara, A., Mackall, C.L., Diller, L. and Weiss, W.A. (2016) 'Neuroblastoma', *Nature Reviews Disease Primers*, 2, p. 16078.

Maya-Mendoza, A., Ostrakova, J., Kosar, M., Hall, A., Duskova, P., Mistrik, M., Merchut-Maya, J.M., Hodny, Z., Bartkova, J., Christensen, C. and Bartek, J. (2015) 'Myc and Ras oncogenes engage different energy metabolism programs and evoke distinct patterns of oxidative and DNA replication stress', *Molecular oncology*, 9(3), pp. 601-616.

McCluskey, A.G., Mairs, R.J., Tesson, M., Pimlott, S.L., Babich, J.W., Gaze, M.N., Champion, S. and Boyd, M. (2012) 'Inhibition of poly(ADP-Ribose) polymerase enhances the toxicity of 131I-metaiodobenzylguanidine/topotecan combination therapy to cells and xenografts that express the noradrenaline transporter', *J Nucl Med*, 53(7), pp. 1146-54.

McKee, A.E. and Thiele, C.J. (2006) 'Targeting caspase 8 to reduce the formation of metastases in neuroblastoma', *Expert Opinion on Therapeutic Targets*, 10(5), pp. 703-708.

Meyer, B., Voss, K.-O., Tobias, F., Jakob, B., Durante, M. and Taucher-Scholz, G. (2013) 'Clustered DNA damage induces pan-nuclear H2AX phosphorylation mediated by ATM and DNA-PK', *Nucleic acids research*, 41(12), pp. 6109-6118.

Michelena, J., Lezaja, A., Teloni, F., Schmid, T., Imhof, R. and Altmeyer, M. (2018) 'Analysis of PARP inhibitor toxicity by multidimensional fluorescence microscopy reveals mechanisms of sensitivity and resistance', *Nature Communications*, 9(1), p. 2678.

Middleton, F.K., Patterson, M.J., Elstob, C.J., Fordham, S., Herriott, A., Wade, M.A., McCormick, A., Edmondson, R., May, F.E.B., Allan, J.M., Pollard, J.R. and Curtin, N.J. (2015) 'Common cancer-associated imbalances in the DNA damage response confer sensitivity to single agent ATR inhibition', *Oncotarget*, 6(32), pp. 32396-32409.

Middleton, F.K., Pollard, J.R. and Curtin, N.J. (2018) 'The Impact of p53 Dysfunction in ATR Inhibitor Cytotoxicity and Chemo- and Radiosensitisation', *Cancers*, 10(8), p. 275.

Min, A., Im, S.-A., Jang, H., Kim, S., Lee, M., Kim, D.K., Yang, Y., Kim, H.-J., Lee, K.-H., Kim, J.W., Kim, T.-Y., Oh, D.-Y., Brown, J., Lau, A., O'Connor, M.J. and Bang, Y.-J. (2017) 'AZD6738, A Novel Oral Inhibitor of ATR, Induces Synthetic Lethality with ATM Deficiency in Gastric Cancer Cells', *Molecular Cancer Therapeutics*, 16(4), pp. 566-577.

Mlakar, V., Mlakar, S.J., Lopez, G., Maris, J.M., Ansari, M. and Gumy-Pause, F. (2017) '11q deletion in neuroblastoma: a review of biological and clinical implications', *Molecular cancer*, 16(1), p. 114.

Molenaar, J.J., Koster, J., Zwijnenburg, D.A., van Sluis, P., Valentijn, L.J., van der Ploeg, I., Hamdi, M., van Nes, J., Westerman, B.A., van Arkel, J., Ebus, M.E., Haneveld, F., Lakeman, A., Schild, L., Molenaar, P., Stroeken, P., van Noesel, M.M., Ora, I., Santo, E.E., Caron, H.N., Westerhout, E.M. and Versteeg, R. (2012) 'Sequencing of neuroblastoma identifies chromothripsis and defects in neuritogenesis genes', *Nature*, 483(7391), pp. 589-593.

Møller, P. (2018) 'The comet assay: ready for 30 more years', *Mutagenesis*, 33(1), pp. 1-7.

Monclair, T., Brodeur, G.M., Ambros, P.F., Brisse, H.J., Cecchetto, G., Holmes, K., Kaneko, M., London, W.B., Matthay, K.K., Nuchtern, J.G., von Schweinitz, D., Simon, T., Cohn, S.L. and Pearson, A.D.J. (2009) 'The International Neuroblastoma Risk Group (INRG) Staging System: An INRG Task Force Report', *Journal of Clinical Oncology*, 27(2), pp. 298-303.

Morales, J.C., Li, L., Fattah, F.J., Dong, Y., Bey, E.A., Patel, M., Gao, J. and Boothman, D.A. (2014) 'Review of Poly (ADP-ribose) Polymerase (PARP) Mechanisms of Action and Rationale for Targeting in Cancer and Other Diseases', *Critical reviews in eukaryotic gene expression*, 24(1), pp. 15-28.

Morris, S.W., Naeve, C., Mathew, P., James, P.L., Kirstein, M.N., Cui, X. and Witte, D.P. (1997) 'ALK, the chromosome 2 gene locus altered by the t (2; 5) in non-Hodgkin's lymphoma, encodes a novel neural receptor tyrosine kinase that is highly related to leukocyte tyrosine kinase (LTK)', *Oncogene*, 14(18).

Morrison, D.K. (2012) 'MAP kinase pathways', *Cold Spring Harbor perspectives in biology*, 4(11), p. a011254.

Mossé, Y.P. (2016) 'Anaplastic Lymphoma Kinase as a Cancer Target in Pediatric Malignancies', *Clinical Cancer Research*, 22(3), pp. 546-552.

Mossë, Y.P., Laudenslager, M., Longo, L., Cole, K.A., Wood, A., Attiyeh, E.F., Laquaglia, M.J., Sennett, R., Lynch, J.E., Perri, P., Laureys, G., Speleman, F., Hakonarson, H., Torkamani, A., Schork, N.J., Brodeur, G.M., Tonini, G.P., Rappaport, E., Devoto, M. and Maris, J.M. (2008) 'Identification of ALK as the Major Familial Neuroblastoma Predisposition Gene', *Nature*, 455(7215), pp. 930-935.

Mouw, K.W. and D'Andrea, A.D. (2014) 'Crosstalk between the nucleotide excision repair and Fanconi anemia/BRCA pathways', *DNA Repair*, 19(Supplement C), pp. 130-134.

Mueller, S., Bhargava, S., Molinaro, A.M., Yang, X., Kolkowitz, I., Olow, A., Wehmeijer, N., Orbach, S., Chen, J. and Matthay, K.K. (2013) 'Poly (ADP-Ribose) polymerase inhibitor MK-4827 together with radiation as a novel therapy for metastatic neuroblastoma', *Anticancer research*, 33(3), pp. 755-762.

Mullen, P. (2004) 'PARP Cleavage as a Means of Assessing Apoptosis', in Langdon, S.P. (ed.) *Cancer Cell Culture: Methods and Protocols*. Totowa, NJ: Humana Press, pp. 171-181.

Murai, J., Feng, Y., Yu, G.K., Ru, Y., Tang, S.-W., Shen, Y. and Pommier, Y. (2016) 'Resistance to PARP inhibitors by SLFN11 inactivation can be overcome by ATR inhibition', *Oncotarget*, 7(47), pp. 76534-76550.

Murai, J., Huang, S.-y.N., Das, B.B., Renaud, A., Zhang, Y., Doroshow, J.H., Ji, J., Takeda, S. and Pommier, Y. (2012) 'Trapping of PARP1 and PARP2 by Clinical PARP Inhibitors', *Cancer Research*, 72(21), pp. 5588-5599.

Murai, J., Thomas, A., Miettinen, M. and Pommier, Y. (2019) 'Schlafen 11 (SLFN11), a restriction factor for replicative stress induced by DNA-targeting anti-cancer therapies', *Pharmacology & therapeutics*, 201, pp. 94-102.

Murga, M., Campaner, S., Lopez-Contreras, A.J., Toledo, L.I., Soria, R., Montaña, M.F., D'Artista, L., Schleker, T., Guerra, C. and Garcia, E. (2011) 'Exploiting oncogene-induced replicative stress for the selective killing of Myc-driven tumors', *Nature structural & molecular biology*, 18(12), pp. 1331-1335.

Nag, S., Qin, J., Srivenugopal, K.S., Wang, M. and Zhang, R. (2013) 'The MDM2-p53 pathway revisited', *Journal of biomedical research*, 27(4), pp. 254-271.

Napier, C.E., Huschtscha, L.I., Harvey, A., Bower, K., Noble, J.R., Hendrickson, E.A. and Reddel, R.R. (2015) 'ATRX represses alternative lengthening of telomeres', *Oncotarget*, 6(18), pp. 16543-16558.

Nau, M.M., Brooks, B.J., Battey, J., Sausville, E., Gazdar, A.F., Kirsch, I.R., McBride, O.W., Bertness, V., Hollis, G.F. and Minna, J.D. (1985) 'L-myc, a new myc-related gene amplified and expressed in human small cell lung cancer', *Nature*, 318(6041), pp. 69-73.

Newman, E.A., Chukkapalli, S., Bashllari, D., Thomas, T.T., Van Noord, R.A., Lawlor, E.R., Hoenerhoff, M.J., Opipari, A.W. and Opipari, V.P. (2017) 'Alternative NHEJ pathway proteins as components of MYCN oncogenic activity in human neural crest stem cell differentiation: implications for neuroblastoma initiation', *Cell death & disease*, 8(12), pp. 3208-3208.

Newman, E.A., Lu, F., Bashllari, D., Wang, L., Opipari, A.W. and Castle, V.P. (2015) 'Alternative NHEJ Pathway Components Are Therapeutic Targets in High-Risk Neuroblastoma', *Molecular Cancer Research*, 13(3), pp. 470-482.

Nieminuszczy, J., Schwab, R.A. and Niedzwiedz, W. (2016) 'The DNA fibre technique – tracking helicases at work', *Methods*, 108, pp. 92-98.

Nile, D.L., Rae, C., Hyndman, I.J., Gaze, M.N. and Mairs, R.J. (2016) 'An evaluation in vitro of PARP-1 inhibitors, rucaparib and olaparib, as radiosensitisers for the treatment of neuroblastoma', *BMC cancer*, 16(1), p. 621.

Norris, R.E., Adamson, P.C., Nguyen, V.T. and Fox, E. (2014) 'Preclinical evaluation of the PARP inhibitor, olaparib, in combination with cytotoxic chemotherapy in pediatric solid tumors', *Pediatric blood & cancer*, 61(1), pp. 145-150.

Onitake, Y., Hiyama, E., Kamei, N., Yamaoka, H., Sueda, T. and Hiyama, K. (2009) 'Telomere biology in neuroblastoma: telomere binding proteins and alternative strengthening of telomeres', *Journal of Pediatric Surgery*, 44(12), pp. 2258-2266.

Osajima-Hakomori, Y., Miyake, I., Ohira, M., Nakagawara, A., Nakagawa, A. and Sakai, R. (2005) 'Biological role of anaplastic lymphoma kinase in neuroblastoma', *The American journal of pathology*, 167(1), pp. 213-222.

Ossovskaya, V., Koo, I.C., Kaldjian, E.P., Alvares, C. and Sherman, B.M. (2010) 'Upregulation of Poly (ADP-Ribose) Polymerase-1 (PARP1) in Triple-Negative Breast Cancer and Other Primary Human Tumor Types', *Genes & Cancer*, 1(8), pp. 812-821.

Ozenne, P., Eymin, B., Brambilla, E. and Gazzeri, S. (2010) 'The ARF tumor suppressor: Structure, functions and status in cancer', *International Journal of Cancer*, 127(10), pp. 2239-2247.

Padovan-Merhar, O.M., Raman, P., Ostrovnaya, I., Kalletla, K., Rubnitz, K.R., Sanford, E.M., Ali, S.M., Miller, V.A., Mossé, Y.P., Granger, M.P., Weiss, B., Maris, J.M. and Modak, S. (2016) 'Enrichment of Targetable Mutations in the Relapsed Neuroblastoma Genome', *PLoS genetics*, 12(12), pp. e1006501-e1006501.

Påhlman, S. and Mohlin, S. (2018) 'Hypoxia and hypoxia-inducible factors in neuroblastoma', *Cell and tissue research*, 372(2), pp. 269-275.

Paige, A.J.W. (2003) 'Redefining tumour suppressor genes: exceptions to the two-hit hypothesis', *Cellular and Molecular Life Sciences CMLS*, 60(10), pp. 2147-2163.

Park, J.R., Bagatell, R., London, W.B., Maris, J.M., Cohn, S.L., Mattay, K.M., Hogarty, M. and on behalf of the, C.O.G.N.C. (2013) 'Children's Oncology Group's 2013 blueprint for research: Neuroblastoma', *Pediatric Blood & Cancer*, 60(6), pp. 985-993.

Park, Y., Chui, M.H., Suryo Rahmanto, Y., Yu, Z.-C., Shamanna, R.A., Bellani, M.A., Gaillard, S., Ayhan, A., Viswanathan, A., Seidman, M.M., Franco, S., Leung, A.K.L., Bohr, V.A., Shih, I.-M. and Wang, T.-L. (2019) 'Loss of ARID1A in Tumor Cells Renders Selective Vulnerability to Combined Ionizing Radiation and PARP Inhibitor Therapy', *Clinical Cancer Research*, 25(18), pp. 5584-5594.

Paull, T. (2015) 'Mechanisms of ATM Activation', *Annual Review of Biochemistry*, 84(1), pp. 711-

738.

Payne, S. and Miles, D. (2008) *Mechanisms of anticancer drugs*. CRC press.

Peasland, A., Wang, L.Z., Rowling, E., Kyle, S., Chen, T., Hopkins, A., Cliby, W.A., Sarkaria, J., Beale, G., Edmondson, R.J. and Curtin, N.J. (2011) 'Identification and evaluation of a potent novel ATR inhibitor, NU6027, in breast and ovarian cancer cell lines', *British Journal of Cancer*, 105(3), pp. 372-381.

Peifer, M., Hertwig, F., Roels, F., Dreidax, D., Gartlgruber, M., Menon, R., Krämer, A., Roncaioli, J.L., Sand, F., Heuckmann, J.M., Ikram, F., Schmidt, R., Ackermann, S., Engesser, A., Kahlert, Y., Vogel, W., Altmüller, J., Nürnberg, P., Thierry-Mieg, J., Thierry-Mieg, D., Mariappan, A., Heynck, S., Mariotti, E., Henrich, K.-O., Glöckner, C., Bosco, G., Leuschner, I., Schweiger, M.R., Savelyeva, L., Watkins, S.C., Shao, C., Bell, E., Höfer, T., Achter, V., Lang, U., Theissen, J., Volland, R., Saadati, M., Eggert, A., de Wilde, B., Berthold, F., Peng, Z., Zhao, C., Shi, L., Ortmann, M., Büttner, R., Perner, S., Hero, B., Schramm, A., Schulte, J.H., Herrmann, C., O'Sullivan, R.J., Westermann, F., Thomas, R.K. and Fischer, M. (2015) 'Telomerase activation by genomic rearrangements in high-risk neuroblastoma', *Nature*, 526(7575), pp. 700-704.

Perwein, T., Lackner, H., Sovinz, P., Benesch, M., Schmidt, S., Schwinger, W. and Urban, C. (2011) 'Survival and late effects in children with stage 4 neuroblastoma', *Pediatric blood & cancer*, 57(4), pp. 629-635.

Petroni, M., Sardina, F., Heil, C., Sahún-Roncero, M., Colicchia, V., Veschi, V., Albini, S., Fruci, D., Ricci, B., Soriani, A., Di Marcotullio, L., Screpanti, I., Gulino, A. and Giannini, G. (2016) 'The MRN complex is transcriptionally regulated by MYCN during neural cell proliferation to control replication stress', *Cell death and differentiation*, 23(2), pp. 197-206.

Petroni, M., Sardina, F., Infante, P., Bartolazzi, A., Locatelli, E., Fabretti, F., Di Giulio, S., Capalbo, C., Cardinali, B., Coppa, A., Tessitore, A., Colicchia, V., Sahùn Roncero, M., Belardinilli, F., Di Marcotullio, L., Soddu, S., Comes Franchini, M., Petricci, E., Gulino, A. and Giannini, G. (2018) 'MRE11 inhibition highlights a replication stress-dependent vulnerability of MYCN-driven tumors', *Cell death & disease*, 9(9), pp. 895-895.

Pfeiffer, R., Brabeck, C. and Bürkle, A. (1999) 'Quantitative Nonisotopic Immuno-Dot-Blot Method for the Assessment of Cellular Poly(ADP-ribosyl)ation Capacity', *Analytical Biochemistry*, 275(1), pp. 118-122.

Pietras, A., Gisselsson, D., Ora, I., Noguera, R., Beckman, S., Navarro, S. and Påhlman, S. (2008) 'High levels of HIF-2alpha highlight an immature neural crest-like neuroblastoma cell cohort located in a perivascular niche', *J Pathol*, 214(4), pp. 482-8.

Pires, I.M., Bencokova, Z., Milani, M., Folkes, L.K., Li, J.-L., Stratford, M.R., Harris, A.L. and Hammond, E.M. (2010) 'Effects of acute versus chronic hypoxia on DNA damage responses and genomic instability', *Cancer research*, 70(3), pp. 925-935.

Plummer, R., Jones, C., Middleton, M., Wilson, R., Evans, J., Olsen, A., Curtin, N., Boddy, A., McHugh, P., Newell, D., Harris, A., Johnson, P., Steinfeldt, H., Dewji, R., Wang, D., Robson, L. and Calvert, H. (2008) 'Phase I study of the poly(ADP-ribose) polymerase inhibitor, AG014699, in combination with temozolomide in patients with advanced solid tumors', *Clinical cancer research : an official journal of the American Association for Cancer Research*, 14(23), pp. 7917-7923.

Podhorecka, M., Skladanowski, A. and Bozko, P. (2010) 'H2AX Phosphorylation: Its Role in DNA Damage Response and Cancer Therapy', *Journal of Nucleic Acids*, 2010, p. 920161.

Pommier, Y., O'Connor, M.J. and de Bono, J. (2016) 'Laying a trap to kill cancer cells: PARP inhibitors and their mechanisms of action', *Sci Transl Med*, 8(362), p. 362ps17.

Primo, L.M.F. and Teixeira, L.K. (2020) 'DNA replication stress: oncogenes in the spotlight', *Genetics and Molecular Biology*, 43.

Prior, I.A., Lewis, P.D. and Mattos, C. (2012) 'A comprehensive survey of Ras mutations in cancer', *Cancer research*, 72(10), pp. 2457-2467.

Prochownik, E.V. and Vogt, P.K. (2010) 'Therapeutic Targeting of Myc', *Genes & Cancer*, 1(6), pp. 650-659.

Pugh, T.J., Morozova, O., Attiyeh, E.F., Asgharzadeh, S., Wei, J.S., Auclair, D., Carter, S.L., Cibulskis, K., Hanna, M., Kiezun, A., Kim, J., Lawrence, M.S., Lichenstein, L., McKenna, A., Pedamallu, C.S., Ramos, A.H., Shefler, E., Sivachenko, A., Sougnez, C., Stewart, C., Ally, A., Birol, I., Chiu, R., Corbett, R.D., Hirst, M., Jackman, S.D., Kamoh, B., Khodabakshi, A.H., Krzywinski, M., Lo, A., Moore, R.A., Mungall, K.L., Qian, J., Tam, A., Thiessen, N., Zhao, Y., Cole, K.A., Diamond, M., Diskin, S.J., Mosse, Y.P., Wood, A.C., Ji, L., Sposto, R., Badgett, T., London, W.B., Moyer, Y., Gastier-Foster, J.M., Smith, M.A., Auvil, J.M.G., Gerhard, D.S., Hogarty, M.D., Jones, S.J.M., Lander, E.S., Gabriel, S.B., Getz, G., Seeger, R.C., Khan, J., Marra, M.A., Meyerson, M. and Maris, J.M. (2013) 'The genetic landscape of high-risk neuroblastoma', *Nature genetics*, 45(3), pp. 279-284.

Rampias, T., Karagiannis, D., Avgeris, M., Polyzos, A., Kokkalis, A., Kanaki, Z., Kousidou, E., Tzetis, M., Kanavakis, E., Stravodimos, K., Manola, K.N., Pantelias, G.E., Scorilas, A. and Klinakis, A. (2019) 'The lysine-specific methyltransferase KMT2C/MLL3 regulates DNA repair components in cancer', *EMBO reports*, 20(3), p. e46821.

Reaper, P.M., Griffiths, M.R., Long, J.M., Charrier, J.-D., MacCormick, S., Charlton, P.A., Golec, J.M.C. and Pollard, J.R. (2011) 'Selective killing of ATM-or p53-deficient cancer cells through inhibition of ATR', *Nature chemical biology*, 7(7), pp. 428-430.

Redon, C.E., Nakamura, A.J., Zhang, Y.-W., Ji, J.J., Bonner, W.M., Kinders, R.J., Parchment, R.E., Doroshow, J.H. and Pommier, Y. (2010) 'Histone gammaH2AX and poly(ADP-ribose) as clinical pharmacodynamic biomarkers', *Clinical cancer research : an official journal of the American Association for Cancer Research*, 16(18), pp. 4532-4542.

Reva, B., Antipin, Y. and Sander, C. (2011) 'Predicting the functional impact of protein mutations: application to cancer genomics', *Nucleic acids research*, 39(17), pp. e118-e118.

Rivlin, N., Brosh, R., Oren, M. and Rotter, V. (2011) 'Mutations in the p53 Tumor Suppressor Gene: Important Milestones at the Various Steps of Tumorigenesis', *Genes & Cancer*, 2(4), pp. 466-474.

Rohban, S. and Campaner, S. (2015) 'Myc induced replicative stress response: How to cope with it and exploit it', *Biochimica et Biophysica Acta (BBA) - Gene Regulatory Mechanisms*, 1849(5), pp. 517-524.

Ross, R.A., Spengler, B.A. and Biedler, J.L. (1983) 'Coordinate Morphological and Biochemical Interconversion of Human Neuroblastoma Cells2', *JNCI: Journal of the National Cancer Institute*, 71(4), pp. 741-747.

Rueden, C.T., Schindelin, J., Hiner, M.C., DeZonia, B.E., Walter, A.E., Arena, E.T. and Eliceiri, K.W. (2017) 'ImageJ2: ImageJ for the next generation of scientific image data', *BMC Bioinformatics*, 18(1), p. 529.

Rundle, S., Bradbury, A., Drew, Y. and Curtin, N.J. (2017) 'Targeting the ATR-CHK1 Axis in Cancer Therapy', *Cancers*, 9(5), p. 41.

Russell, K.J., Wiens, L.W., Demers, G.W., Galloway, D.A., Plon, S.E. and Groudine, M. (1995) 'Abrogation of the G2 checkpoint results in differential radiosensitization of G1 checkpoint-deficient and G1 checkpoint-competent cells', *Cancer research*, 55(8), pp. 1639-1642.

Russell, M.R., Levin, K., Rader, J., Belcastro, L., Li, Y., Martinez, D., Pawel, B., Shumway, S.D., Maris, J.M. and Cole, K.A. (2013) 'Combination therapy targeting the Chk1 and Wee1 kinases shows therapeutic efficacy in neuroblastoma', *Cancer research*, 73(2), pp. 776-784.

Ryl, T., Kuchen, E.E., Bell, E., Shao, C., Flórez, A.F., Mönke, G., Gogolin, S., Friedrich, M., Lamprecht, F., Westermann, F. and Höfer, T. (2017) 'Cell-Cycle Position of Single MYC-Driven Cancer Cells Dictates Their Susceptibility to a Chemotherapeutic Drug', *Cell Systems*, 5(3), pp. 237-250.e8.

Saldivar, J., Cortez, D. and Cimprich, K. (2017) *The essential kinase ATR: ensuring faithful duplication of a challenging genome*.

Sale, J.E. (2013) 'Translesion DNA Synthesis and Mutagenesis in Eukaryotes', *Cold Spring Harbor Perspectives in Biology*, 5(3), p. a012708.

Sangster-Guity, N., Conrad, B.H., Papadopoulos, N. and Bunz, F. (2011) 'ATR mediates cisplatin resistance in a p53 genotype-specific manner', *Oncogene*, 30(22), pp. 2526-2533.

Sanmartín, E., Muñoz, L., Piqueras, M., Sirerol, J.A., Berlanga, P., Cañete, A., Castel, V. and de Mora, J.F. (2017) 'Deletion of 11q in neuroblastomas drives sensitivity to PARP inhibition', *Clinical Cancer Research*, p. clincanres. 0593.2017.

Santarpia, L., Lippman, S.L. and El-Naggar, A.K. (2012) 'Targeting the Mitogen-Activated Protein Kinase RAS-RAF Signaling Pathway in Cancer Therapy', *Expert opinion on therapeutic targets*, 16(1), pp. 103-119.

Santiago, T., Tarek, N., Boulos, F., Hayes, C., Jeha, S., Raimondi, S. and Rodriguez-Galindo, C. (2019) 'Correlation Between MYCN Gene Status and MYCN Protein Expression in Neuroblastoma: A Pilot Study To Propose the Use of MYCN Immunohistochemistry in Limited-Resource Areas', *Journal of Global Oncology*, (5), pp. 1-7.

Sausen, M., Leary, R.J., Jones, S., Wu, J., Reynolds, C.P., Liu, X., Blackford, A., Parmigiani, G., Diaz, L.A., Jr., Papadopoulos, N., Vogelstein, B., Kinzler, K.W., Velculescu, V.E. and Hogarty, M.D. (2013) 'Integrated genomic analyses identify ARID1A and ARID1B alterations in the childhood cancer neuroblastoma', *Nature genetics*, 45(1), pp. 12-17.

Schleiermacher, G., Javanmardi, N., Bernard, V., Leroy, Q., Cappo, J., Rio Frio, T., Pierron, G., Lapouble, E., Combaret, V. and Speleman, F. (2014) 'Emergence of new ALK mutations at relapse of neuroblastoma', *Journal of Clinical Oncology*, 32(25), pp. 2727-2734.

Schleiermacher, G., Michon, J., Ribeiro, A., Pierron, G., Mosseri, V., Rubie, H., Munzer, C., Bénard, J., Auger, N., Combaret, V., Janoueix-Lerosey, I., Pearson, A., Tweddle, D.A., Bown, N., Gerrard, M., Wheeler, K., Noguera, R., Villamon, E., Cañete, A., Castel, V., Marques, B., de Lacerda, A., Tonini, G.P., Mazzocco, K., Defferrari, R., de Bernardi, B., di Cataldo, A., van Roy, N., Brichard, B., Ladenstein, R., Ambros, I., Ambros, P., Beiske, K., Delattre, O. and Couturier, J. (2011) 'Segmental chromosomal alterations lead to a higher risk of relapse in infants with MYCN-non-amplified localised unresectable/disseminated neuroblastoma (a SIOPEN collaborative study)', *British Journal of Cancer*, 105(12), pp. 1940-1948.

Schleiermacher, G., Mosseri, V., London, W.B., Maris, J.M., Brodeur, G.M., Attiyeh, E., Haber, M., Khan, J., Nakagawara, A., Speleman, F., Noguera, R., Tonini, G.P., Fischer, M., Ambros, I., Monclair, T., Matthay, K.K., Ambros, P., Cohn, S.L. and Pearson, A.D.J. (2012) 'Segmental chromosomal alterations have prognostic impact in neuroblastoma: a report from the INRG project', *Br J Cancer*, 107(8), pp. 1418-1422.

Schleiermacher, G., Raynal, V., Janoueix-Lerosey, I., Combaret, V., Aurias, A. and Delattre, O. (2004) 'Variety and complexity of chromosome 17 translocations in neuroblastoma', *Genes, Chromosomes and Cancer*, 39(2), pp. 143-150.

Schmitt, A., Knittel, G., Welcker, D., Yang, T.-P., George, J., Nowak, M., Leeser, U., Büttner, R., Perner, S., Peifer, M. and Reinhardt, H.C. (2017) '*ATM* Deficiency Is Associated with Sensitivity to PARP1- and ATR Inhibitors in Lung Adenocarcinoma', *Cancer Research*, 77(11), pp. 3040-3056.

Schoonen, P.M., Kok, Y.P., Wierenga, E., Bakker, B., Foijer, F., Spierings, D.C.J. and van Vugt, M.A.T.M. (2019) 'Premature mitotic entry induced by ATR inhibition potentiates olaparib inhibition-mediated genomic instability, inflammatory signaling, and cytotoxicity in BRCA2-deficient cancer cells', *Molecular oncology*, 13(11), pp. 2422-2440.

Schoppy, D.W. and Brown, E.J. (2012) 'Chk'ing p53-deficient breast cancers', *J Clin Invest*, 122(4), pp. 1202-5.

Schoppy, D.W., Ragland, R.L., Gilad, O., Shastri, N., Peters, A.A., Murga, M., Fernandez-Capetillo, O., Diehl, J.A. and Brown, E.J. (2012) 'Oncogenic stress sensitizes murine cancers to hypomorphic suppression of ATR', *The Journal of Clinical Investigation*, 122(1), pp. 241-252.

Schramm, A., Köster, J., Assenov, Y., Althoff, K., Peifer, M., Mahlow, E., Odersky, A., Beisser, D., Ernst, C., Henssen, A.G., Stephan, H., Schröder, C., Heukamp, L., Engesser, A., Kahlert, Y., Theissen, J., Hero, B., Roels, F., Altmüller, J., Nürnberg, P., Astrahantseff, K., Gloeckner, C., De Preter, K., Plass, C., Lee, S., Lode, H.N., Henrich, K.-O., Gartlgruber, M., Speleman, F., Schmezer, P., Westermann, F., Rahmann, S., Fischer, M., Eggert, A. and Schulte, J.H. (2015) 'Mutational dynamics between primary and relapse neuroblastomas', *Nature Genetics*, 47(8), pp. 872-877.

Schwab, M., Alitalo, K., Klempnauer, K.-H., Varmus, H.E., Bishop, J.M., Gilbert, F., Brodeur, G., Goldstein, M. and Trent, J. (1983) 'Amplified DNA with limited homology to myc cellular oncogene is shared by human neuroblastoma cell lines and a neuroblastoma tumour', *Nature*, 305(5931), pp. 245-248.

Shah, P.D., Zarrin, H., Wethington, S., Latif, N., Martin, L., Rodriguez, D., Elkins, K., Giuntoli, R., Burger, R., Tanyi, J., Morgan, M., Domchek, S.M., Gailliard, S., Armstrong, D.K. and Simpkins, F. (2020) 'Abstract A72: Combination ATR and PARP inhibitor (CAPRI) for recurrent, platinum-resistant ovarian cancer', *Clinical Cancer Research*, 26(13 Supplement), pp. A72-A72.

Shaltiel, I.A., Krenning, L., Bruinsma, W. and Medema, R.H. (2015) 'The same, only different – DNA damage checkpoints and their reversal throughout the cell cycle', *Journal of Cell Science*, 128(4), pp. 607-620.

Shay, J.W. and Bacchetti, S. (1997) 'A survey of telomerase activity in human cancer', *European Journal of Cancer*, 33(5), pp. 787-791.

Shi, Q., Shen, L.-Y., Dong, B., Fu, H., Kang, X.-Z., Yang, Y.-B., Dai, L., Yan, W.-P., Xiong, H.-C., Liang, Z. and Chen, K.-N. (2018) 'The identification of the ATR inhibitor VE-822 as a therapeutic strategy for enhancing cisplatin chemosensitivity in esophageal squamous cell carcinoma', *Cancer Letters*, 432, pp. 56-68.

Shi, W., Feng, Z., Zhang, J., Gonzalez-Suarez, I., Vanderwaal, R.P., Wu, X., Powell, S.N., Roti Roti, J.L., Gonzalo, S. and Zhang, J. (2010) 'The role of RPA2 phosphorylation in homologous recombination in response to replication arrest', *Carcinogenesis*, 31(6), pp. 994-1002.

Shiloh, Y. and Ziv, Y. (2013) 'The ATM protein kinase: regulating the cellular response to genotoxic stress, and more', *Nature Reviews Molecular Cell Biology*, 14, p. 197.

Shimada, H., Ambros, I.M., Dehner, L.P., Hata, J., Joshi, V.V., Roald, B., Stram, D.O., Gerbing, R.B., Lukens, J.N., Matthay, K.K. and Castleberry, R.P. (1999) 'The International Neuroblastoma Pathology Classification (the Shimada system)', *Cancer*, 86(2), pp. 364-72.

Sim, N.-L., Kumar, P., Hu, J., Henikoff, S., Schneider, G. and Ng, P.C. (2012) 'SIFT web server: predicting effects of amino acid substitutions on proteins', *Nucleic acids research*, 40(Web Server issue), pp. W452-W457.

Smits, V.A. and Gillespie, D.A. (2015) 'DNA damage control: regulation and functions of checkpoint kinase 1', *Febs j*, 282(19), pp. 3681-92.

Southgate, H.E.D., Chen, L., Curtin, N.J. and Tweddle, D.A. (2020) 'Targeting the DNA Damage Response for the Treatment of High Risk Neuroblastoma', *Frontiers in Oncology*, 10(371).

Spitz, R., Hero, B., Simon, T. and Berthold, F. (2006) 'Loss in Chromosome 11q Identifies Tumors with Increased Risk for Metastatic Relapses in Localized and 4S Neuroblastoma', *Clinical Cancer Research*, 12(11), pp. 3368-3373.

Spivak, G. (2015) 'Nucleotide excision repair in humans', *DNA repair*, 36, pp. 13-18.

Squire, C.J., Dickson, J.M., Ivanovic, I. and Baker, E.N. (2005) 'Structure and Inhibition of the Human Cell Cycle Checkpoint Kinase, Wee1A Kinase: An AtypicalTyrosine Kinase with a Key Role in CDK1 Regulation', *Structure*, 13(4), pp. 541-550.

Staker, B.L., Hjerrild, K., Feese, M.D., Behnke, C.A., Burgin, A.B. and Stewart, L. (2002) 'The mechanism of topoisomerase I poisoning by a camptothecin analog', *Proceedings of the National Academy of Sciences*, 99(24), pp. 15387-15392.

Stiller, C. (2007) *Childhood cancer in Britain: incidence, survival, mortality*. Oxford University Press.

Stolz, A. and Bastians, H. (2013) 'Therapeutic S and G2 checkpoint override causes centromere fragmentation in mitosis', *Cell cycle (Georgetown, Tex.)*, 12(12), pp. 1826-1827.

Ström, C.E., Johansson, F., Uhlén, M., Szigyarto, C.A.-K., Erixon, K. and Helleday, T. (2011) 'Poly (ADP-ribose) polymerase (PARP) is not involved in base excision repair but PARP inhibition traps a single-strand intermediate', *Nucleic acids research*, 39(8), pp. 3166-3175.

Stupack, D.G., Teitz, T., Potter, M.D., Mikolon, D., Houghton, P.J., Kidd, V.J., Lahti, J.M. and Cheresh, D.A. (2006) 'Potentiation of neuroblastoma metastasis by loss of caspase-8', *Nature*, 439(7072), pp. 95-99.

Su, J.M., Thompson, P., Adesina, A., Li, X.-N., Kilburn, L., Onar-Thomas, A., Kocak, M., Chyla, B., McKeegan, E., Warren, K.E., Goldman, S., Pollack, I.F., Fouladi, M., Chen, A., Giranda, V., Boyett, J., Kun, L. and Blaney, S.M. (2014) 'A phase I trial of veliparib (ABT-888) and temozolomide in children with recurrent CNS tumors: a pediatric brain tumor consortium report', *Neuro-oncology*, 16(12), pp. 1661-1668.

Subhash, V.V., Tan, S.H., Yeo, M.S., Yan, F.L., Peethala, P.C., Liem, N., Krishnan, V. and Yong, W.P. (2016) 'ATM Expression Predicts Veliparib and Irinotecan Sensitivity in Gastric Cancer by Mediating P53-Independent Regulation of Cell Cycle and Apoptosis', *Molecular Cancer Therapeutics*, 15(12), pp. 3087-3096.

Sugimura, K., Takebayashi, S.-I., Taguchi, H., Takeda, S. and Okumura, K. (2008) 'PARP-1 ensures regulation of replication fork progression by homologous recombination on damaged DNA', *The Journal of cell biology*, 183(7), pp. 1203-1212.

Takagi, M., Yoshida, M., Nemoto, Y., Tamaichi, H., Tsuchida, R., Seki, M., Uryu, K., Hoshino, N., Nishii, R., Miyamoto, S., Saito, M., Shimizu, T., Hanada, R., Kaneko, H., Fukao, T., Koyama, T., Shiraishi, Y., Chiba, K., Tanaka, H., Miyano, S., Sato, Y., Fujii, Y., Kataoka, K., Okuno, Y., Yoshida, K., Morio, T., Oka, A., Ohira, M., Hayashi, Y., Nakagawara, A., Ogawa, S., Mizutani, S. and Takita, J. (2017) 'Loss of DNA Damage Response in Neuroblastoma and Utility of a PARP Inhibitor', *JNCI: Journal of the National Cancer Institute*, 109(11).

Tanaka, T., Higashi, M., Kimura, K., Wakao, J., Fumino, S., Iehara, T., Hosoi, H., Sakai, T. and Tajiri, T. (2016) 'MEK inhibitors as a novel therapy for neuroblastoma: Their in vitro effects and predicting their efficacy', *Journal of Pediatric Surgery*, 51(12), pp. 2074-2079.

Tate, J.G., Bamford, S., Jubb, H.C., Sondka, Z., Beare, D.M., Bindal, N., Boutselakis, H., Cole, C.G., Creatore, C., Dawson, E., Fish, P., Harsha, B., Hathaway, C., Jupe, S.C., Kok, C.Y., Noble, K., Ponting, L., Ramshaw, C.C., Rye, C.E., Speedy, H.E., Stefancsik, R., Thompson, S.L., Wang, S., Ward, S., Campbell, P.J. and Forbes, S.A. (2019) 'COSMIC: the Catalogue Of Somatic Mutations In Cancer', *Nucleic acids research*, 47(D1), pp. D941-D947.

Taylor, E.M. and Lindsay, H.D. (2016) 'DNA replication stress and cancer: cause or cure?', *Future Oncology*, 12(2), pp. 221-237.

Teitz, T., Lahti, J.M. and Kidd, V.J. (2001) 'Aggressive childhood neuroblastomas do not express caspase-8: an important component of programmed cell death', *Journal of molecular medicine*, 79(8), pp. 428-436.

Thiele, C.J. (1999) 'Neuroblastoma', in Masters, J.R.W. and Palsson, B. (eds.) *Human Cell Culture: Cancer Cell Lines Part 1*. Dordrecht: Springer Netherlands, pp. 21-53.

Thomas, A., Redon, C.E., Sciuto, L., Padiernos, E., Ji, J., Lee, M.-J., Yuno, A., Lee, S., Zhang, Y., Tran, L., Yutzy, W., Rajan, A., Guha, U., Chen, H., Hassan, R., Alewine, C.C., Szabo, E., Bates, S.E., Kinders, R.J., Steinberg, S.M., Doroshow, J.H., Aladjem, M.I., Trepel, J.B. and Pommier, Y. (2018) 'Phase I Study of ATR Inhibitor M6620 in Combination With Topotecan in Patients With Advanced Solid Tumors', *Journal of clinical oncology : official journal of the American Society of Clinical Oncology*, 36(16), pp. 1594-1602.

Thompson, J., Zamboni, W.C., Cheshire, P.J., Lutz, L., Luo, X., Li, Y., Houghton, J.A., Stewart, C.F. and Houghton, P.J. (1997) 'Efficacy of systemic administration of irinotecan against neuroblastoma xenografts', *Clinical Cancer Research*, 3(3), pp. 423-431.

Toledo, L., Neelsen, K.J. and Lukas, J. (2017) 'Replication Catastrophe: When a Checkpoint Fails because of Exhaustion', *Molecular Cell*, 66(6), pp. 735-749.

Toledo, L.I., Murga, M., Zur, R., Soria, R., Rodriguez, A., Martinez, S., Oyarzabal, J., Pastor, J., Bischoff, J.R. and Fernandez-Capetillo, O. (2011) 'A cell-based screen identifies ATR inhibitors with synthetic lethal properties for cancer-associated mutations', *Nature structural & molecular biology*, 18(6), pp. 721-727.

Topacio, B.R., Zatulovskiy, E., Cristea, S., Xie, S., Tambo, C.S., Rubin, S.M., Sage, J., Kõivomägi, M. and Skotheim, J.M. (2019) 'Cyclin D-Cdk4,6 Drives Cell-Cycle Progression via the Retinoblastoma Protein's C-Terminal Helix', *Molecular Cell*, 74(4), pp. 758-770.e4.

Trigg, R.M. and Turner, S.D. (2018) 'ALK in Neuroblastoma: Biological and Therapeutic Implications', *Cancers*, 10(4), p. 113.

Tumilowicz, J.J., Nichols, W.W., Cholon, J.J. and Greene, A.E. (1970) 'Definition of a Continuous Human Cell Line Derived from Neuroblastoma', *Cancer Research*, 30(8), pp. 2110-2118.

Turner, N.C., Lord, C.J., Iorns, E., Brough, R., Swift, S., Elliott, R., Rayter, S., Tutt, A.N. and Ashworth, A. (2008) 'A synthetic lethal siRNA screen identifying genes mediating sensitivity to a PARP inhibitor', *The EMBO Journal*, 27(9), pp. 1368-1377.

Tweddle, D.A., Malcolm, A.J., Bown, N., Pearson, A.D.J. and Lunec, J. (2001) 'Evidence for the Development of p53 Mutations after Cytotoxic Therapy in a Neuroblastoma Cell Line', *Cancer Research*, 61(1), pp. 8-13.

Ulaner, G.A., Hu, J.-F., Vu, T.H., Giudice, L.C. and Hoffman, A.R. (1998) 'Telomerase Activity in Human Development Is Regulated by Human Telomerase Reverse Transcriptase (hTERT) Transcription and by Alternate Splicing of hTERT Transcripts', *Cancer Research*, 58(18), pp. 4168-4172.

Valentijn, L.J., Koster, J., Haneveld, F., Aissa, R.A., van Sluis, P., Broekmans, M.E.C., Molenaar, J.J., van Nes, J. and Versteeg, R. (2012) 'Functional MYCN signature predicts outcome of neuroblastoma

irrespective of MYCN amplification', *Proceedings of the National Academy of Sciences of the United States of America*, 109(47), pp. 19190-19195.

Valentijn, L.J., Koster, J., Zwijnenburg, D.A., Hasselt, N.E., van Sluis, P., Volckmann, R., van Noesel, M.M., George, R.E., Tytgat, G.A.M. and Molenaar, J.J. (2015) 'TERT rearrangements are frequent in neuroblastoma and identify aggressive tumors', *Nature genetics*, 47(12), pp. 1411-1414.

Van Maerken, T., Ferdinande, L., Taildeman, J., Lambertz, I., Yigit, N., Vercruysse, L., Rihani, A., Michaelis, M., Cinatl, J., Cuvelier, C.A., Marine, J.-C., De Paepe, A., Bracke, M., Speleman, F. and Vandesompele, J. (2009) 'Antitumor Activity of the Selective MDM2 Antagonist Nutlin-3 Against Chemoresistant Neuroblastoma With Wild-Type p53', *JNCI: Journal of the National Cancer Institute*, 101(22), pp. 1562-1574.

Van Maerken, T., Rihani, A., Dreidax, D., De Clercq, S., Yigit, N., Marine, J.-C., Westermann, F., De Paepe, A., Vandesompele, J. and Speleman, F. (2011) 'Functional Analysis of the p53 Pathway in Neuroblastoma Cells Using the Small-Molecule MDM2 Antagonist Nutlin-3', *Molecular Cancer Therapeutics*, 10(6), pp. 983-993.

Van Roy, N., Van Limbergen, H., Vandesompele, J., Van Gele, M., Poppe, B., Salwen, H., Laureys, G., Manoel, N., De Paepe, A. and Speleman, F. (2001) 'Combined M-FISH and CGH analysis allows comprehensive description of genetic alterations in neuroblastoma cell lines', *Genes, Chromosomes and Cancer*, 32(2), pp. 126-135.

Vandesompele, J., Michels, E., De Preter, K., Menten, B., Schramm, A., Eggert, A., Ambros, P.F., Combaret, V., Francotte, N., Antonacci, F., De Paepe, A., Laureys, G., Speleman, F. and Van Roy, N. (2008) 'Identification of 2 putative critical segments of 17q gain in neuroblastoma through integrative genomics', *International Journal of Cancer*, 122(5), pp. 1177-1182.

Vaser, R., Adusumalli, S., Leng, S.N., Sikic, M. and Ng, P.C. (2016) 'SIFT missense predictions for genomes', *Nature Protocols*, 11(1), pp. 1-9.

Villamón, E., Berbegall, A.P., Piqueras, M., Tadeo, I., Castel, V., Djos, A., Martinsson, T., Navarro, S. and Noguera, R. (2013) 'Genetic instability and intratumoral heterogeneity in neuroblastoma with MYCN amplification plus 11q deletion', *PLoS One*, 8(1), p. e53740.

Vitale, I., Galluzzi, L., Castedo, M. and Kroemer, G. (2011) 'Mitotic catastrophe: a mechanism for avoiding genomic instability', *Nature Reviews Molecular Cell Biology*, 12(6), pp. 385-392.

Vogelstein, B., Lane, D. and Levine, A.J. (2000) 'Surfing the p53 network', *Nature*, 408(6810), pp. 307-310.

Wagner, L.M., McLendon, R.E., Yoon, K.J., Weiss, B.D., Billups, C.A. and Danks, M.K. (2007) 'Targeting Methylguanine-DNA Methyltransferase in the Treatment of Neuroblastoma', *Clinical Cancer Research*, 13(18), pp. 5418-5425.

Walsh, M.F., Kennedy, J., Harlan, M., Kentsis, A., Shukla, N., Musinsky, J., Roberts, S., Kung, A.L., Robson, M., Kushner, B.H., Meyers, P. and Offit, K. (2017) 'Germline BRCA2 mutations detected in pediatric sequencing studies impact parents' evaluation and care', *Cold Spring Harbor molecular case studies*, 3(6), p. a001925.

Wang, C., Jette, N., Moussienko, D., Bebb, D.G. and Lees-Miller, S.P. (2017) 'ATM-Deficient Colorectal Cancer Cells Are Sensitive to the PARP Inhibitor Olaparib', *Translational oncology*, 10(2), pp. 190-196.

Wang, M., Zhou, C., Sun, Q., Cai, R., Li, Y., Wang, D. and Gong, L. (2013) 'ALK amplification and protein expression predict inferior prognosis in neuroblastomas', *Experimental and Molecular Pathology*, 95(2), pp. 124-130.

Wang, X., Zou, L., Lu, T., Bao, S., Hurov, K.E., Hittelman, W.N., Elledge, S.J. and Li, L. (2006) 'Rad17 Phosphorylation Is Required for Claspin Recruitment and Chk1 Activation in Response to Replication Stress', *Molecular Cell*, 23(3), pp. 331-341.

Weber, A.M. and Ryan, A.J. (2015) 'ATM and ATR as therapeutic targets in cancer', *Pharmacology & Therapeutics*, 149(Supplement C), pp. 124-138.

Weiss, W.A., Aldape, K., Mohapatra, G., Feuerstein, B.G. and Bishop, J.M. (1997) 'Targeted expression of MYCN causes neuroblastoma in transgenic mice', *The EMBO Journal*, 16(11), pp. 2985-2995.

Wengner, A.M., Siemeister, G., Lücking, U., Lefranc, J., Wortmann, L., Lienau, P., Bader, B., Bömer, U., Moosmayer, D., Eberspächer, U., Golfier, S., Schatz, C.A., Baumgart, S.J., Haendler, B., Lejeune, P., Schlicker, A., von Nussbaum, F., Brands, M., Ziegelbauer, K. and Mumberg, D. (2020) 'The Novel ATR Inhibitor BAY 1895344 Is Efficacious as Monotherapy and Combined with DNA Damage–Inducing or Repair–Compromising Therapies in Preclinical Cancer Models', *Molecular Cancer Therapeutics*, 19(1), pp. 26-38.

Westermann, F., Muth, D., Benner, A., Bauer, T., Henrich, K.-O., Oberthuer, A., Brors, B., Beissbarth, T., Vandesompele, J., Pattyn, F., Hero, B., König, R., Fischer, M. and Schwab, M. (2008) 'Distinct transcriptional MYCN/c-MYC activities are associated with spontaneous regression or malignant progression in neuroblastomas', *Genome Biology*, 9(10), p. R150.

Weston, V.J., Oldreive, C.E., Skowronska, A., Oscier, D.G., Pratt, G., Dyer, M.J.S., Smith, G., Powell, J.E., Rudzki, Z., Kearns, P., Moss, P.A.H., Taylor, A.M.R. and Stankovic, T. (2010) 'The PARP inhibitor olaparib induces significant killing of ATM-deficient lymphoid tumor cells in vitro and in vivo', *Blood*, 116(22), pp. 4578-4587.

Williamson, C.T., Kubota, E., Hamill, J.D., Klimowicz, A., Ye, R., Muzik, H., Dean, M., Tu, L., Gilley, D., Magliocco, A.M., McKay, B.C., Bebb, D.G. and Lees-Miller, S.P. (2012) 'Enhanced cytotoxicity of PARP inhibition in mantle cell lymphoma harbouring mutations in both ATM and p53', *EMBO molecular medicine*, 4(6), pp. 515-527.

Williamson, C.T., Miller, R., Pemberton, H.N., Jones, S.E., Campbell, J., Konde, A., Badham, N., Rafiq, R., Brough, R., Gulati, A., Ryan, C.J., Francis, J., Vermulen, P.B., Reynolds, A.R., Reaper, P.M., Pollard, J.R., Ashworth, A. and Lord, C.J. (2016) 'ATR inhibitors as a synthetic lethal therapy for tumours deficient in ARID1A', *Nature Communications*, 7(1), p. 13837.

Woodfield, S.E., Zhang, L., Scorsone, K.A., Liu, Y. and Zage, P.E. (2016) 'Binimetinib inhibits MEK and is effective against neuroblastoma tumor cells with low NF1 expression', *BMC Cancer*, 16, p. 172.

Wu, R.-C., Wang, T.-L. and Shih, I.-M. (2014) 'The emerging roles of ARID1A in tumor suppression', *Cancer biology & therapy*, 15(6), pp. 655-664.

Wyman, C., Ristic, D. and Kanaar, R. (2004) 'Homologous recombination-mediated double-strand break repair', *DNA Repair*, 3(8), pp. 827-833.

Xu, H., Cheung, I.Y., Wei, X.X., Tran, H., Gao, X. and Cheung, N.-K.V. (2011) 'Checkpoint kinase inhibitor synergizes with DNA-damaging agents in G1 checkpoint-defective neuroblastoma', *International Journal of Cancer*, 129(8), pp. 1953-1962.

Xue, C., Haber, M., Flemming, C., Marshall, G.M., Lock, R.B., MacKenzie, K.L., Gurova, K.V., Norris, M.D. and Gudkov, A.V. (2007) 'p53 determines multidrug sensitivity of childhood neuroblastoma', *Cancer research*, 67(21), pp. 10351-10360.

Yao, Y. and Dai, W. (2014) 'Genomic Instability and Cancer', *Journal of carcinogenesis & mutagenesis*, 5, p. 1000165.

Yap, T.A., Tan, D.S., Terbuch, A., Caldwell, R., Guo, C., Goh, B.C., Heong, V., Haris, N.R.M., Bashir, S., Drew, Y., Hong, D.S., Meric-Bernstam, F., Wilkinson, G., Hreiki, J., Wengner, A.M., Bladt, F., Schlicker, A., Ludwig, M., Zhou, Y., Liu, L., Bordia, S., Plummer, R., Lagkadinou, E. and de Bono, J.S. (2020) 'First-in-Human Trial of the Oral Ataxia Telangiectasia and Rad3-Related Inhibitor BAY 1895344 in Patients with Advanced Solid Tumors', *Cancer Discovery*, pp. CD-20-0868.

Yazinski, S.A., Comaills, V., Buisson, R., Genois, M.-M., Nguyen, H.D., Ho, C.K., Todorova Kwan, T., Morris, R., Lauffer, S., Nussenzweig, A., Ramaswamy, S., Benes, C.H., Haber, D.A., Maheswaran, S., Birrer, M.J. and Zou, L. (2017) 'ATR inhibition disrupts rewired homologous recombination and fork protection pathways in PARP inhibitor-resistant BRCA-deficient cancer cells', *Genes & Development*, 31(3), pp. 318-332.

Zaremba, T., Ketzer, P., Cole, M., Coulthard, S., Plummer, E.R. and Curtin, N.J. (2009) 'Poly(ADP-ribose) polymerase-1 polymorphisms, expression and activity in selected human tumour cell lines', *British Journal of Cancer*, 101(2), pp. 256-262.

Zeineldin, M., Federico, S., Chen, X., Fan, Y., Xu, B., Stewart, E., Zhou, X., Jeon, J., Griffiths, L., Nguyen, R., Norrie, J., Easton, J., Mulder, H., Yergeau, D., Liu, Y., Wu, J., Van Ryn, C., Naranjo, A., Hogarty, M.D., Kamiński, M.M., Valentine, M., Pruett-Miller, S.M., Pappo, A., Zhang, J., Clay, M.R., Bahrami, A., Vogel, P., Lee, S., Shelat, A., Sarthy, J.F., Meers, M.P., George, R.E., Mardis, E.R., Wilson, R.K., Henikoff, S., Downing, J.R. and Dyer, M.A. (2020) 'MYCN amplification and ATRX mutations are incompatible in neuroblastoma', *Nature Communications*, 11(1), p. 913.

Zeman, M.K. and Cimprich, K.A. (2014) 'Causes and Consequences of Replication Stress', *Nature cell biology*, 16(1), pp. 2-9.

Zhang, B., Yin, C.P., Zhao, Q. and Yue, S.W. (2014) 'Upregulation of HIF-1α by hypoxia protect neuroblastoma cells from apoptosis by promoting survivin expression', *Asian Pac J Cancer Prev*, 15(19), pp. 8251-7.

Zhang, J., Dai, Q., Park, D. and Deng, X. (2016) 'Targeting DNA Replication Stress for Cancer Therapy', *Genes*, 7(8), p. 51.

Zhao, Y., Yu, H. and Hu, W. (2014) 'The regulation of MDM2 oncogene and its impact on human cancers', *Acta Biochimica et Biophysica Sinica*, 46(3), pp. 180-189.

Zhou, J.X., Feng, L.J. and Zhang, X. (2017) 'Risk of severe hematologic toxicities in cancer patients treated with PARP inhibitors: a meta-analysis of randomized controlled trials', *Drug design, development and therapy*, 11, pp. 3009-3017.

Zhu, S., Lee, J.-S., Guo, F., Shin, J., Perez-Atayde, A.R., Kutok, J.L., Rodig, S.J., Neuberg, D.S., Helman, D., Feng, H., Stewart, R.A., Wang, W., George, R.E., Kanki, J.P. and Look, A.T. (2012) 'Activated ALK Collaborates with MYCN in Neuroblastoma Pathogenesis', *Cancer Cell*, 21(3), pp. 362-373.

Appendix 1: SNP array cell lines

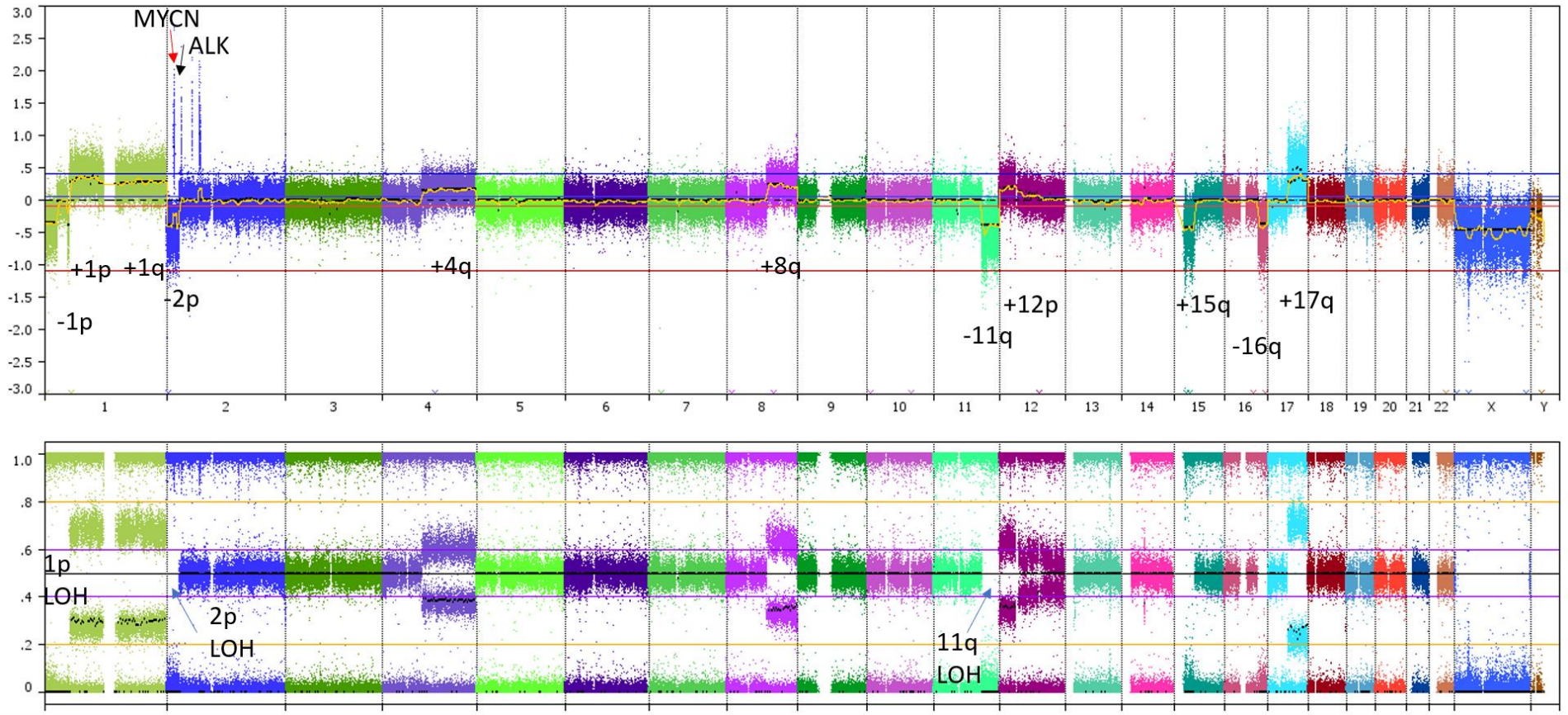

Figure 1: SNP array for IMR32 cell line. Log2 ratio representing amplicons and numerical and segmental chromosomal aberrations (NCAs and SCAs) (top) and the B allele frequency (BAF) shows segmental heterozygosity (bottom). The following criteria was used: chromosomal gain ≥+0.15; chromosomal loss ≤-0.25, gene amplification > 0.7 and SCA cut off ≥3Mb.

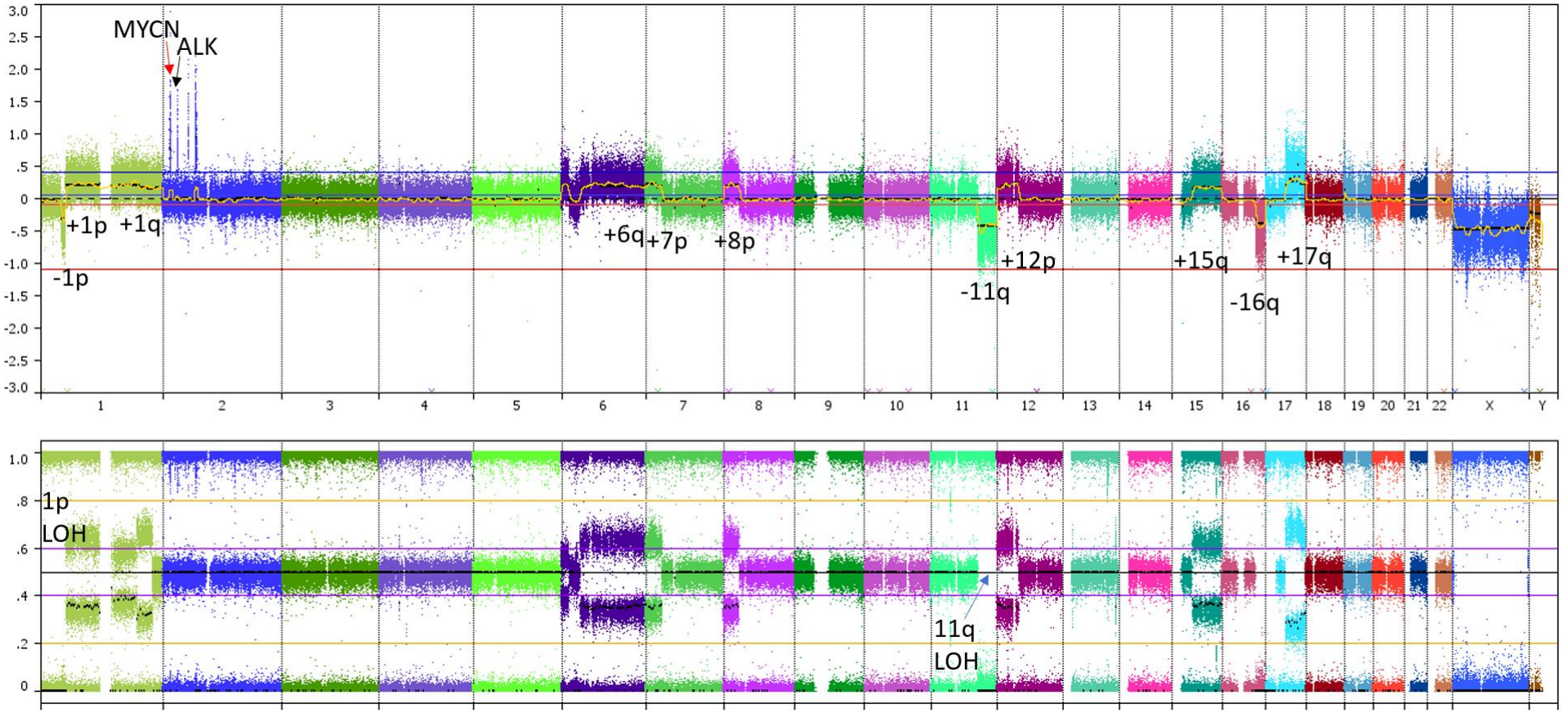

Figure2: SNP array for KAT100 cell line. Log2 ratio representing amplicons and numerical and segmental chromosomal aberrations (NCAs and SCAs) (top) and the B allele frequency (BAF) shows segmental heterozygosity (bottom). The following criteria was used: chromosomal gain ≥+0.15; chromosomal loss ≤-0.25, gene amplification > 0.7 and SCA cut off ≥3Mb.

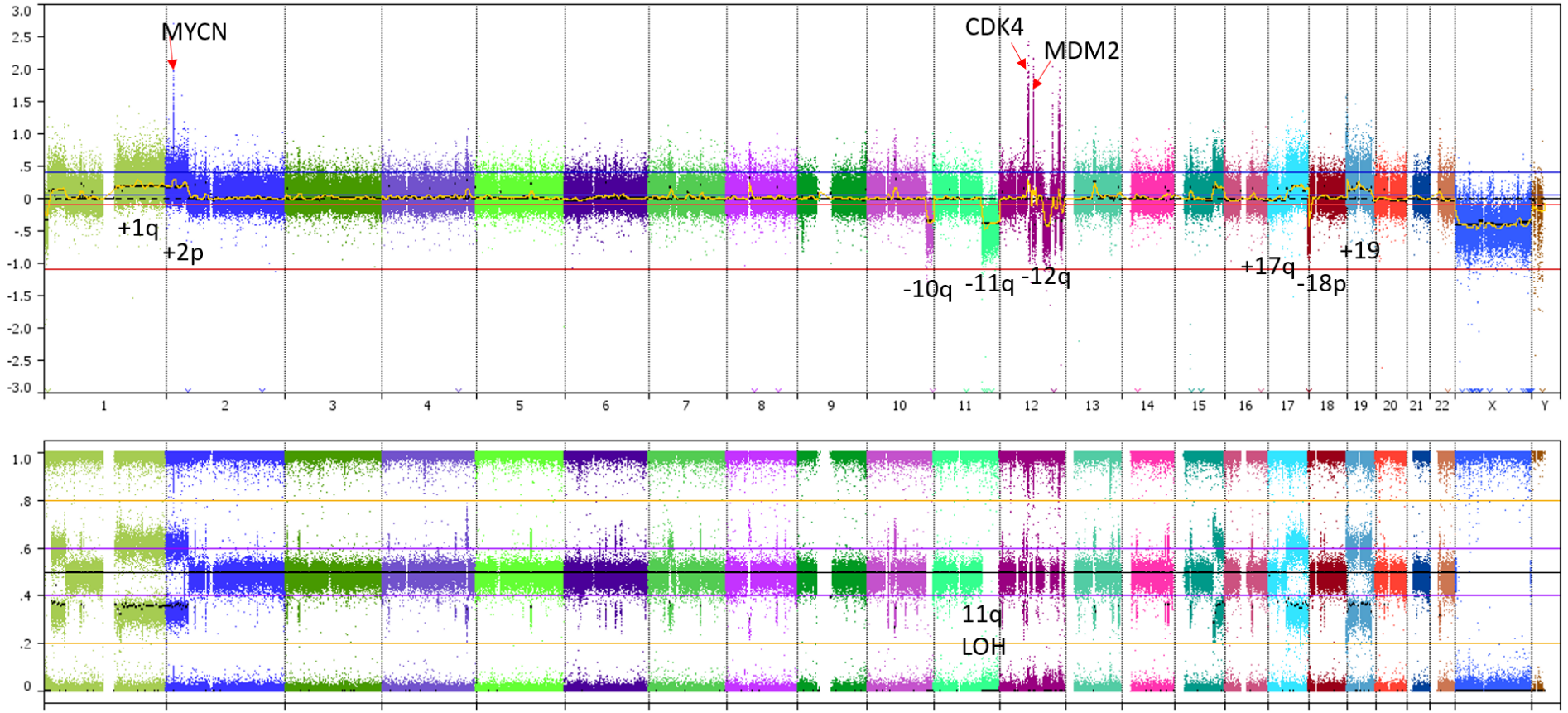

Figure 3: SNP array for NGP cell line. Log2 ratio representing amplicons and numerical and segmental chromosomal aberrations (NCAs and SCAs) (top) and the B allele frequency (BAF) shows segmental heterozygosity (bottom). The following criteria was used: chromosomal gain ≥+0.15; chromosomal loss ≤-0.25, gene amplification > 0.7 and SCA cut off ≥3Mb.

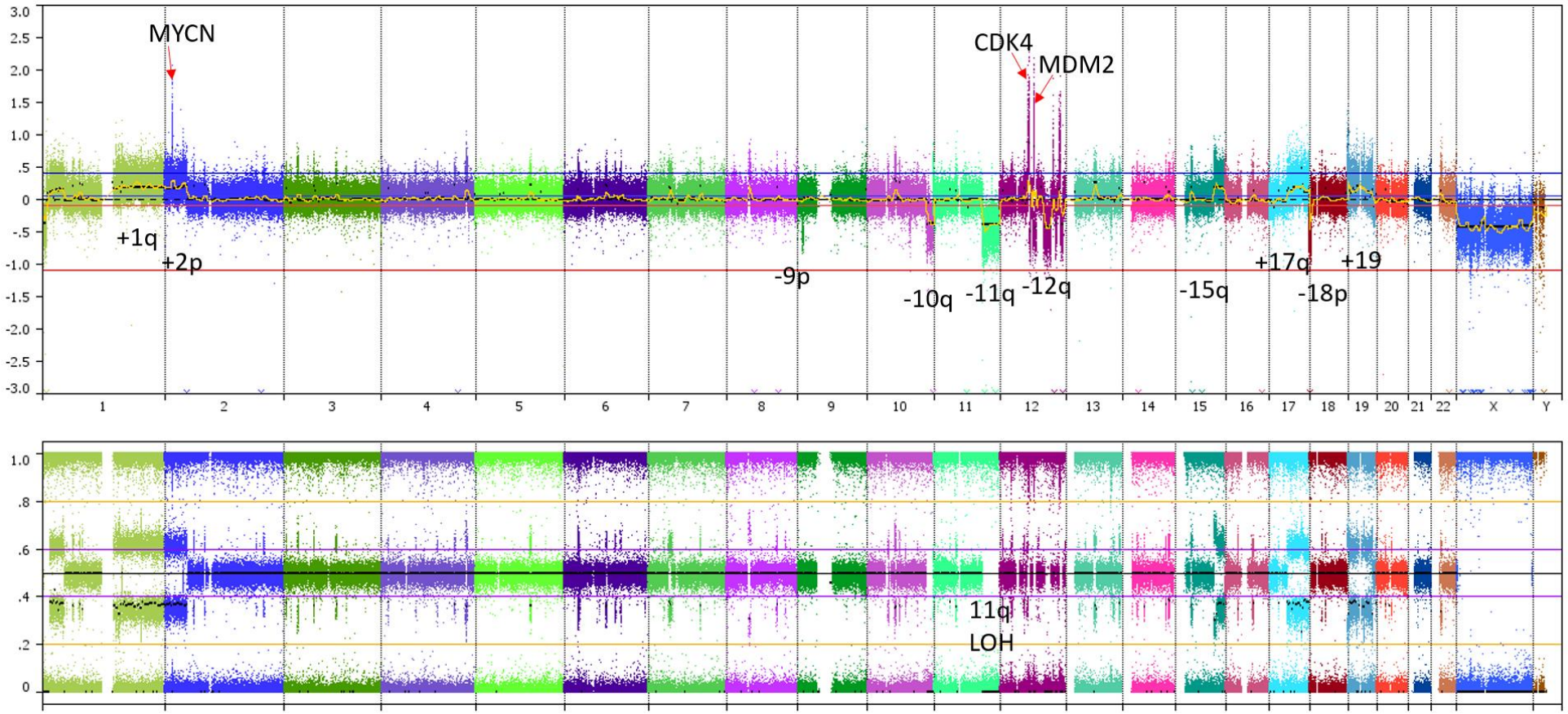

Figure 4: SNP array for N20_R1 cell line. Log2 ratio representing amplicons and numerical and segmental chromosomal aberrations (NCAs and SCAs) (top) and the B allele frequency (BAF) shows segmental heterozygosity (bottom). The following criteria was used: chromosomal gain ≥+0.15; chromosomal loss ≤-0.25, gene amplification > 0.7 and SCA cut off ≥3Mb.

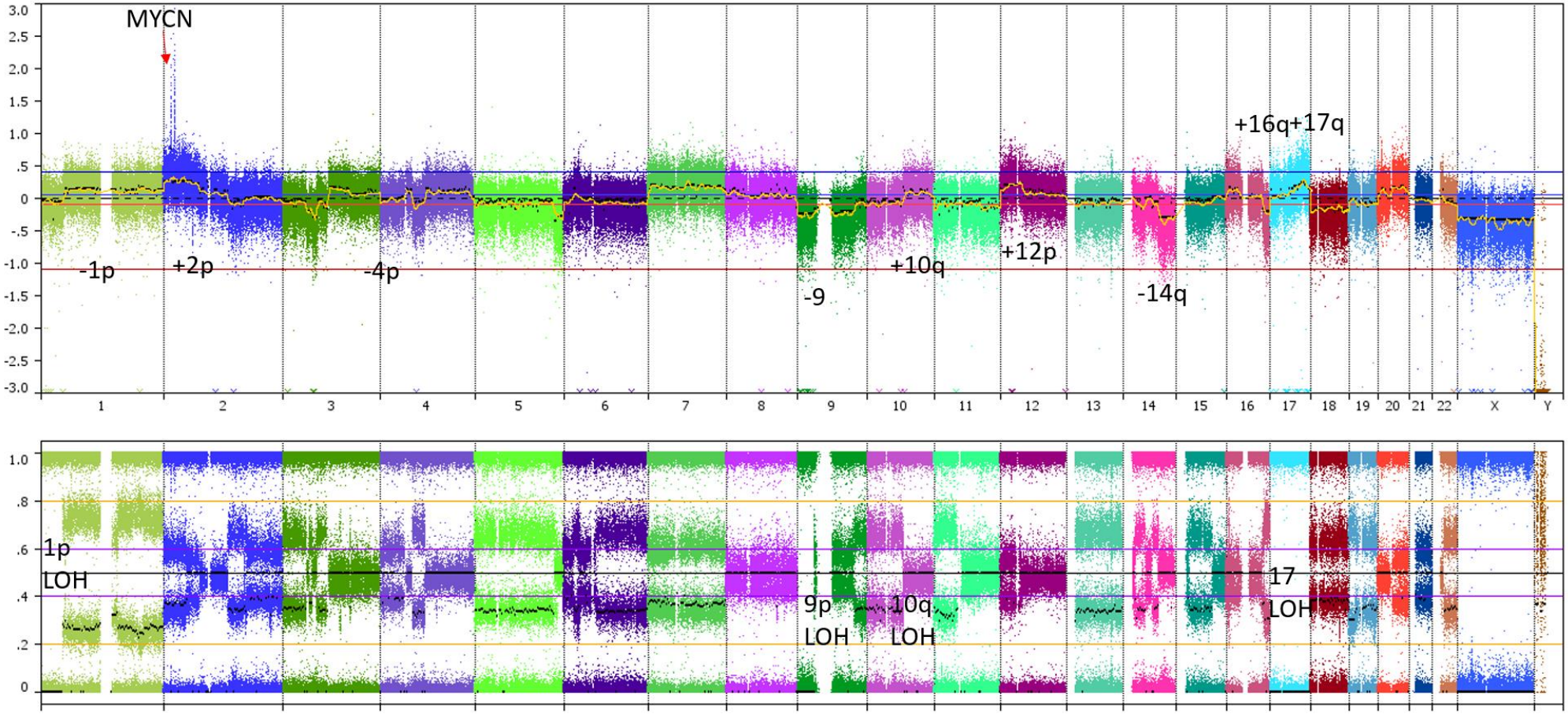

Figure 5: SNP array for NMB cell line. Log2 ratio representing amplicons and numerical and segmental chromosomal aberrations (NCAs and SCAs) (top) and the B allele frequency (BAF) shows segmental heterozygosity (bottom). The following criteria was used: chromosomal gain ≥+0.15; chromosomal loss ≤-0.25, gene amplification > 0.7 and SCA cut off ≥3Mb.

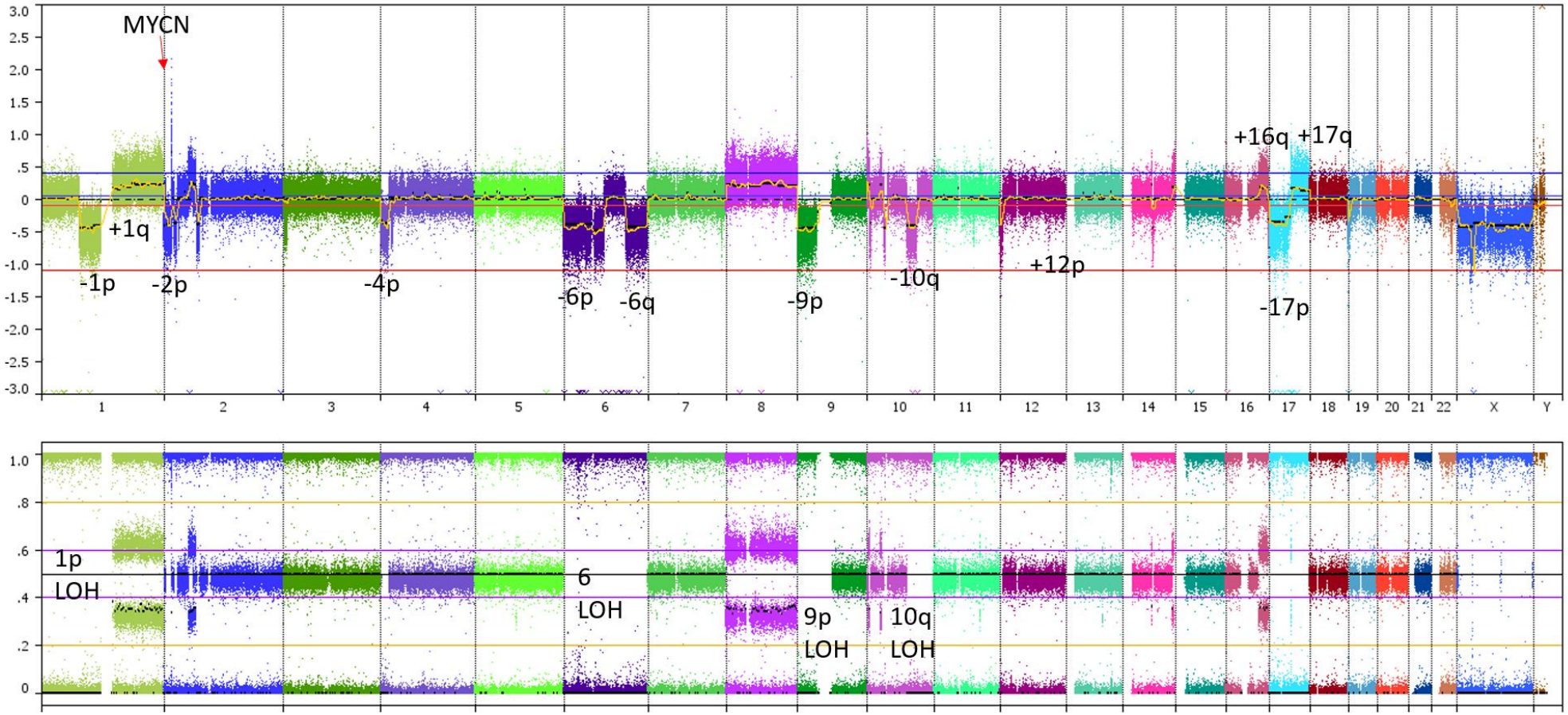

Figure 615: SNP array for IGRN91 cell line. Log2 ratio representing amplicons and numerical and segmental chromosomal aberrations (NCAs and SCAs) (top) and the B allele frequency (BAF) shows segmental heterozygosity (bottom). The following criteria was used: chromosomal gain ≥+0.15; chromosomal loss ≤-0.25, gene amplification > 0.7 and SCA cut off ≥3Mb.

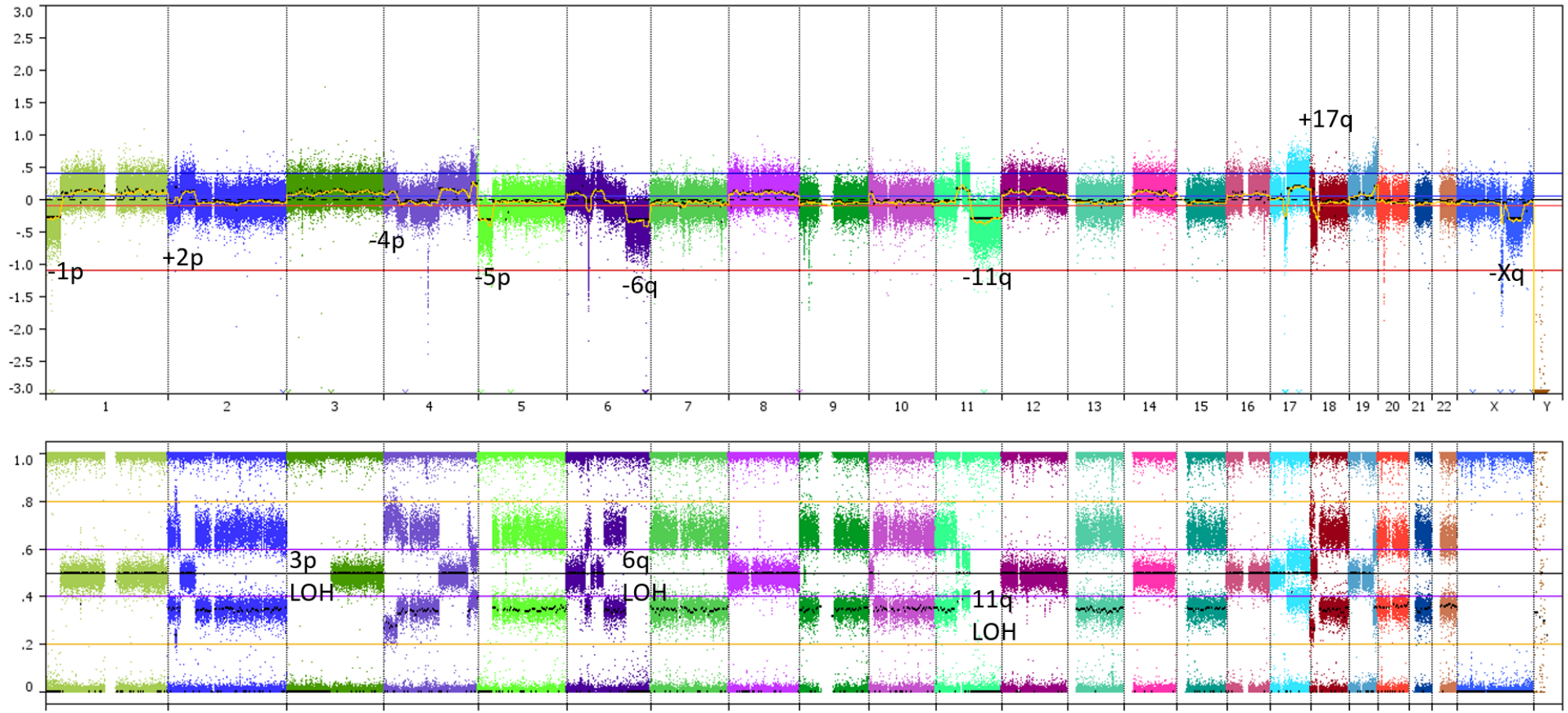

Figure 7: SNP array for GIMEN cell line. Log2 ratio representing amplicons and numerical and segmental chromosomal aberrations (NCAs and SCAs) (top) and the B allele frequency (BAF) shows segmental heterozygosity (bottom). The following criteria was used: chromosomal gain ≥+0.15; chromosomal loss ≤-0.25, gene amplification > 0.7 and SCA cut off ≥3Mb.

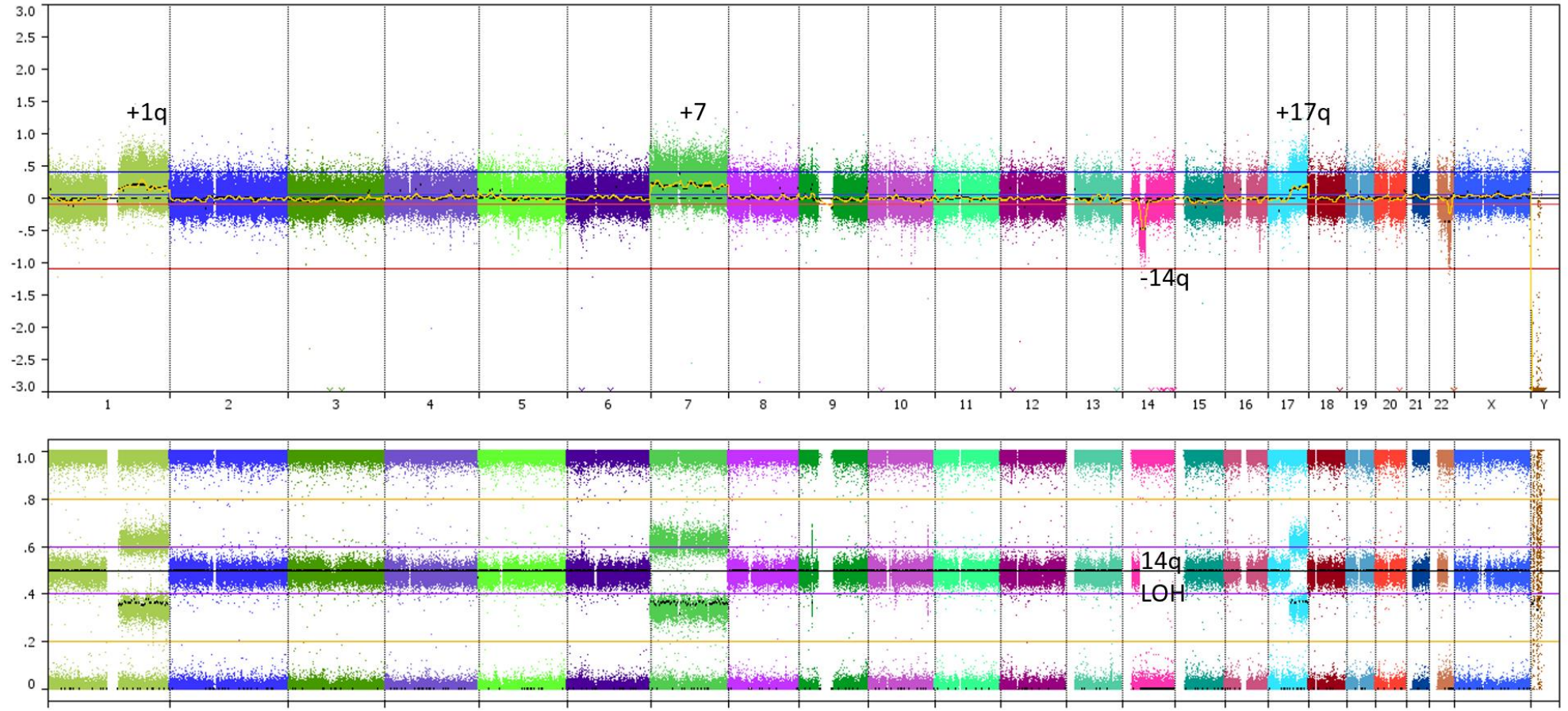

Figure 8: SNP array for SHSY5Y cell line. Log2 ratio representing amplicons and numerical and segmental chromosomal aberrations (NCAs and SCAs) (top) and the B allele frequency (BAF) shows segmental heterozygosity (bottom). The following criteria was used: chromosomal gain ≥+0.15; chromosomal loss ≤-0.25, gene amplification > 0.7 and SCA cut off ≥3Mb.

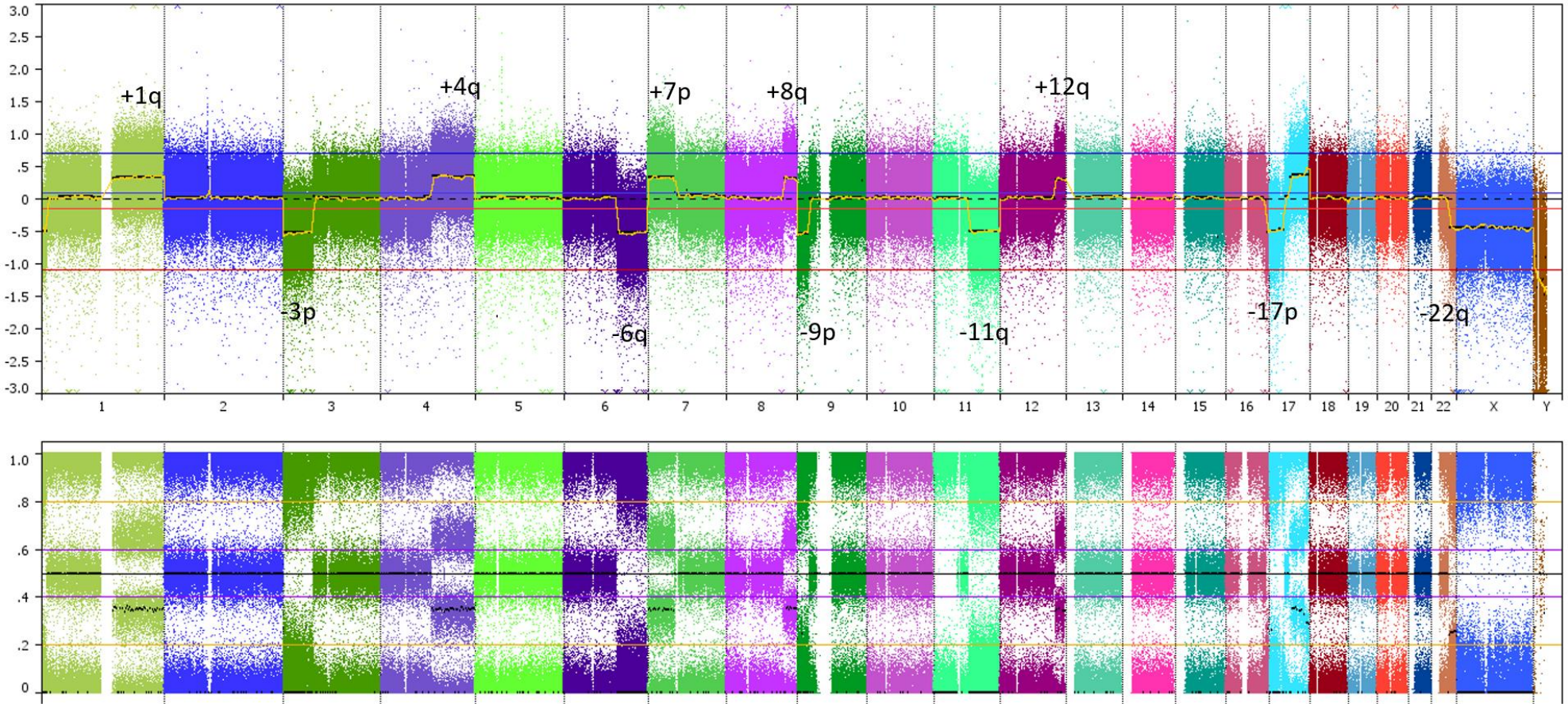

Figure 9: SNP array for SKNAS cell line. Log2 ratio representing amplicons and numerical and segmental chromosomal aberrations (NCAs and SCAs) (top) and the B allele frequency (BAF) shows segmental heterozygosity (bottom). The following criteria was used: chromosomal gain ≥+0.15; chromosomal loss ≤-0.25, gene amplification > 0.7 and SCA cut off ≥3Mb.

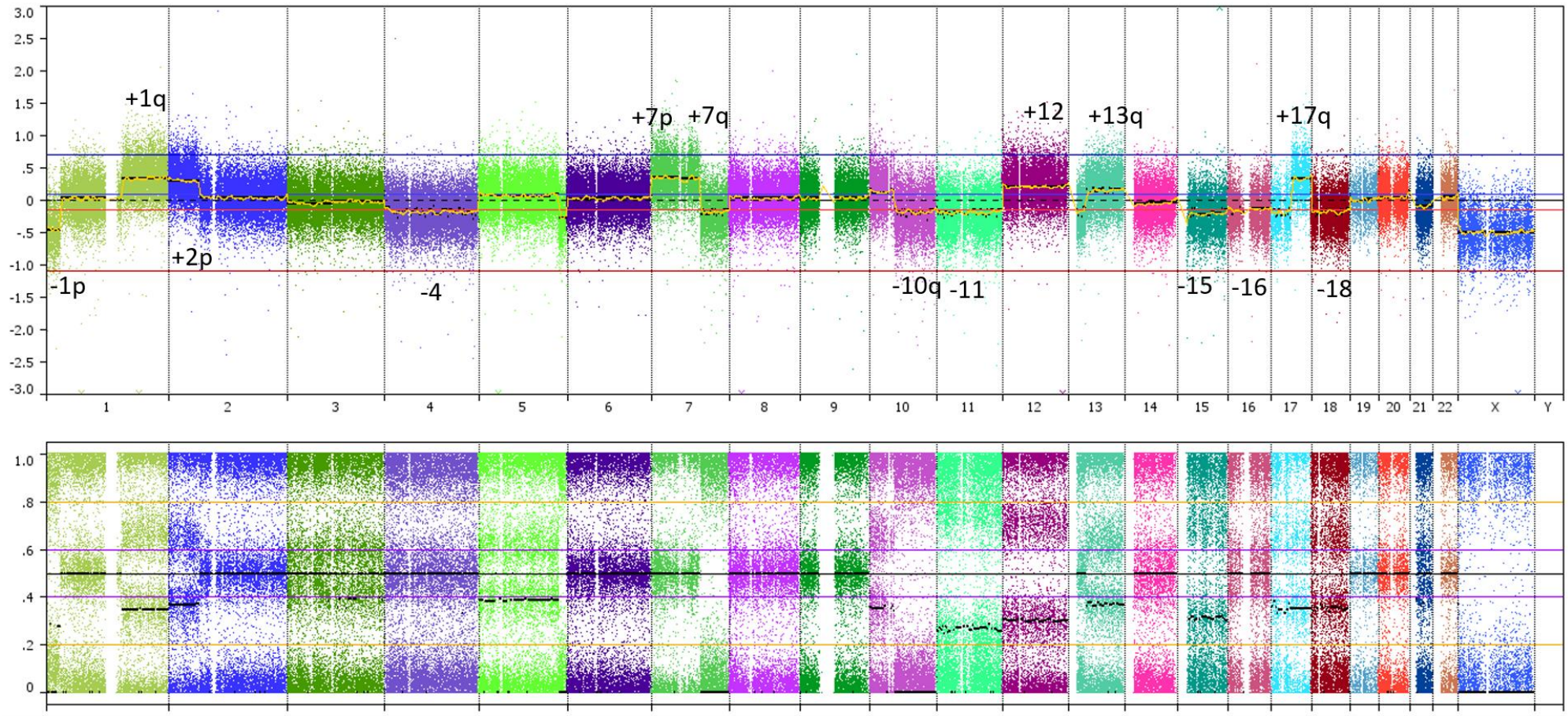

Figure 10: SNP array for the tetraploid SJNB1 cell line. Log2 ratio representing amplicons and numerical and segmental chromosomal aberrations (NCAs and SCAs) (top) and the B allele frequency (BAF) shows segmental heterozygosity (bottom). The following criteria was used: chromosomal gain ≥+0.15; chromosomal loss ≤-0.25, gene amplification > 0.7 and SCA cut off ≥3Mb.

Appendix 2: Whole exome sequencing paired cell lines

Table 7: Parental cell lines specific mutations identified by whole exome sequencing. Mutations predicted to affect the DDR are highlighted in yellow.

Cell Line	Genes	Codes for	AA Change	Variant Effect	SIFT class (score)
IMR32	*CLCA2*	Calcium-activated chloride channel regulator 2	P536L	missense_variant	Deleterious (1.000)
IMR32	*RPRD2*	Regulation of nuclear pre-mRNA domain-containing protein 2	S597*	stop_gained	-
IMR32	*YY1AP1*	YY1-associated protein 1	V527F	missense_variant	Deleterious (1.000)
IMR32	*FMO3*	Dimethylaniline monooxygenase [N-oxide-forming] 3	G162E	missense_variant, splice_region_variant	Deleterious (1.000)
IMR32	*HMCN1*	Hemicentin-1	-	splice_region_variant,intron_variant	-
IMR32	*FCAMR*	High affinity immunoglobulin alpha and immunoglobulin mu Fc receptor	Q535K	missense_variant	Deleterious (0.998)
IMR32	*CRYBG3*	Very large A-kinase anchor protein	G569*	stop_gained	-
IMR32	*CCDC80*	Coiled-coil domain-containing protein 80	K329N	missense_variant	Deleterious (0.989)
IMR32	*ZSWIM6*	Zinc finger SWIM domain-containing protein 6	R717W	missense_variant	Deleterious (1.000)
IMR32	*PDE6A*	Phosphodiesterase 6A	-	splice_donor_variant	-
IMR32	*PLEKHG1*	Pleckstrin homology domain-containing family G member 1	E55*	stop_gained	-
IMR32	*CASD1*	N-acetylneuraminate 9-O-acetyltransferase	R461Q	missense_variant	Deleterious (1.000)
IMR32	*MUC12*	Mucin-12	S71I	missense_variant	Deleterious (0.999)
IMR32	*NOS3*	Nitrix oxide synthase 1	-	splice_region_variant,intron_variant	-
IMR32	*TDRD7*	Tudor domain-containing protein 7	W932C	missense_variant	Deleterious (1.000)
IMR32	*QSER1*	Glutamine and serine-rich protein 1	S364R	missense_variant	Deleterious (0.990)
IMR32	*ATM*	Serine-protein kinase ATM	V2716A	missense_variant	Deleterious (1.000)

IMR32	*PDE6H*	Phosphodiesterase 6H	-	splice_region_variant,intron_variant	-
IMR32	*SLC38A2*	Sodium-coupled neutral amino acid transporter 2	G216V	missense_variant, splice_region_variant	Deleterious (1.000)
IMR32	*OSBPL8*	Oxysterol Binding Protein Like 8	S203*	stop_gained	-
IMR32	*PRKAB1*	Protein Kinase AMP-Activated Non-Catalytic Subunit Beta 1	P208Q	missense_variant	Deleterious (1.000)
IMR32	*RNF6*	Ring Finger Protein 6	R135I	missense_variant	Deleterious (1.000)
IMR32	*SERPINA 12*	Serpin Family A Member 12 (protease inhibitors)	K155N	missense_variant	Deleterious (0.999)
IMR32	*DMXL2*	DmX-like protein 2	C781F	missense_variant	Deleterious (1.000)
IMR32	*IQGAP1*	IQ Motif Containing GTPase Activating Protein 1	E1578G	missense_variant	Deleterious (1.000)
IMR32	*ACSM2A*	Acyl-CoA Synthetase Medium Chain Family Member 2A	Q91H	missense_variant	Deleterious (0.989)
IMR32	*SGSM2*	Small G Protein Signaling Modulator 2	N852S	missense_variant	Deleterious (0.989)
IMR32	*OR1D5*	Olfactory Receptor Family 1 Subfamily D Member 5	W149C	missense_variant	Deleterious (0.999)
IMR32	*NXPH3*	Neurexophilin 3	G185V	missense_variant	Deleterious (0.996)
IMR32	*USP32*	Ubiquitin Specific Peptidase 32	A717S	missense_variant	Deleterious (0.989)
IMR32	*FCGBP*	Fc Fragment Of IgG Binding Protein	G1190V	missense_variant	Deleterious (1.000)
IMR32	*TFF3*	Trefoil Factor 3	C72*	stop_gained	-

Table 8: Daughter cell lines specific mutations identified by whole exome sequencing. Mutations predicted to affect the DDR are highlighted in yellow.

Cell Line	Genes	Codes for	AA Change	Variant Effect	SIFT class (score)
KAT100	*DNM3*	Dynamin 3	R850L	missense_variant	Deleterious (1.000)
KAT100	*CEP350*	Centrosomal Protein 350	V188F	missense_variant	Deleterious (0.989)
KAT100	*OPTC*	Opticin	I304F	missense_variant	Deleterious (1.000)
KAT100	*ZNF670*	Zinc Finger Protein 670	S88*	stop_gained	-
KAT100	*IGKV4-1*	Immunoglobulin Kappa Variable 4-1	Q68H	missense_variant	Deleterious (0.999)
KAT100	*GZMA*	Granzyme A	A67S	missense_variant	Deleterious (1.000)
KAT100	*CEP120*	Centrosomal Protein 120	K561E	missense_variant	Deleterious (0.999)
KAT100	*MDC1*	Mediator Of DNA Damage Checkpoint 1	Q1463H	missense_variant	Deleterious (1.000)
KAT100	*PRPH2*	Peripherin 2	P210T	missense_variant	Deleterious (1.000)
KAT100	*RUNX2*	RUNX Family Transcription Factor 2	M39R	missense_variant	Deleterious (0.999)
KAT100	*TTYH3*	Tweety Family Member 3 (chloride channel)	-	splice_region_variant,intron_variant	-
KAT100	*OSBPL3*	Oxysterol Binding Protein Like 3	R279I	missense_variant	Deleterious (0.999)
KAT100	*FANCG*	Fanconi anemia group G protein	C75*	stop_gained	-
KAT100	*PPRC1*	PPARG Related Coactivator 1	L1375F	missense_variant	Deleterious (1.000)
KAT100	*TRIM49B*	Tripartite Motif Containing 49B	R408*	stop_gained	-
KAT100	*OR1S2*	Olfactory Receptor Family 1 Subfamily S Member 2	P223L	missense_variant	Deleterious (1.000)
KAT100	*KLRF2*	Killer Cell Lectin Like Receptor F2	I175M	missense_variant	Deleterious (0.990)
KAT100	*SRGAP1*	SLIT-ROBO Rho GTPase Activating Protein 1	-	splice_region_variant,intron_variant	-
KAT100	*INF2*	Inverted Formin, FH2 And WH2 Domain Containing	Q366*	stop_gained	-
KAT100	*PLCB2*	Phospholipase C Beta 2	G534V	missense_variant, splice_region_variant	Deleterious (0.999)
KAT100	*MYO5C*	Myosin VC	E1077*	stop_gained	-
KAT100	*UNC13C*	Unc-13 Homolog C	G798*	stop_gained	-
KAT100	*CD19*	B-lymphocyte antigen CD19	E527*	stop_gained	-

KAT100	*TP53*	Tumour suppressor protein 53	C135F	missense_variant	Deleterious (1.000)
KAT100	*HSD17B1*	Hydroxysteroid 17-Beta Dehydrogenase 1	G136*	stop_gained	-
KAT100	*RBL1*	RB Transcriptional Corepressor Like 1	L206F	missense_variant	Deleterious (1.000)
KAT100	*NLGN3*	Neuroligin 3	F546L	missense_variant	Deleterious (1.000)
KAT100	*SLC9B1P1*	Putative SLC9B1-like protein SLC9B1P1	K222*	stop_gained	-
N20R1	*CLCNKA*	Chloride Voltage-Gated Channel Ka	T492N	missense_variant	Deleterious (1.000)
N20R1	*GBP4*	Guanylate Binding Protein 4	L272Q	missense_variant	Deleterious (1.000)
N20R1	*RFX5*	DNA-binding protein RFX5	V565G	missense_variant	Deleterious (1.000)
N20R1	*IGFN1*	Immunoglobulin Like And Fibronectin Type III Domain Containing 1	E2796D	missense_variant	Deleterious (0.989)
N20R1	*BROX*	BRO1 domain-containing protein BROX	K158N	missense_variant, splice_region_variant	Deleterious (0.998)
N20R1	*ANKRD36C*	Ankyrin Repeat Domain 36C	R1582T	missense_variant	Neutral(0.977)
N20R1	*IL18R1*	Interleukin 18 Receptor 1	L400F	missense_variant	Deleterious (1.000)
N20R1	*DNAH7*	Dynein Axonemal Heavy Chain 7	V1183A	missense_variant	Deleterious (0.996)
N20R1	*ACAD9*	Acyl-CoA Dehydrogenase Family Member 9	A176S	missense_variant	Deleterious (1.000)
N20R1	*NUDT6*	Nudix Hydrolase 6	R90*	stop_gained	-
N20R1	*FKBP6*	Inactive peptidyl-prolyl cis-trans isomerase FKBP6	S74Y	missense_variant	Deleterious (1.000)
N20R1	*KMT2C*	Lysine methyltransferase 2C	G908C	missense_variant	Deleterious (1.000)
N20R1	*WDFY4*	WD repeat- and FYVE domain-containing protein 4	G1342E	missense_variant	Deleterious (1.000)
N20R1	*LDHAL6A*	Lactate Dehydrogenase A Like 6A	L165M	missense_variant	Deleterious (1.000)
N20R1	*DAGLA*	Diacylglycerol Lipase Alpha	S12Y	missense_variant	Deleterious (1.000)
N20R1	*CDAN1*	Codanin 1	P560Q	missense_variant	Deleterious (1.000)
N20R1	*CENPN*	Centromere Protein N	S195I	missense_variant	Deleterious (1.000)
N20R1	*TP53*	Tumour suppressor protein 53	P152T	missense_variant	Deleterious (1.000)
N20R1	*TP53*	Tumour suppressor protein 53	P98H	missense_variant	Deleterious (1.000)

N20R1	*TCEB3C*	Elongin-A3 member B	E379D	missense_variant	Deleterious (0.999)
N20R1	*KHSRP*	Far upstream element-binding protein 2	R394S	missense_variant, splice_region_variant	Deleterious (0.989)
N20R1	*ZC3H4*	Zinc finger CCCH domain-containing protein 4	G431*	stop_gained	-
N20R1	*SSC5D*	Soluble scavenger receptor cysteine-rich domain-containing protein SSC5D	E1348*	stop_gained	-
N20R1	*ZSCAN5A*	Zinc finger and SCAN domain-containing protein 5A	D270G	missense_variant	Deleterious (0.996)
N20R1	*GNAS*	Guanine nucleotide-binding protein G(s) subunit alpha isoforms Xlas	K943N	missense_variant	Deleterious (1.000)

Appendix 3: Publications

Publications:

Southgate HED, Chen L, Tweddle DA, Curtin NJ. ATR Inhibition Potentiates PARP Inhibitor Cytotoxicity in High Risk Neuroblastoma Cell Lines by Multiple Mechanisms. Cancers (Basel). 2020 Apr 28;12(5):1095. doi: 10.3390/cancers12051095. PMID: 32354033; PMCID: PMC7281288.

Southgate HED, Chen L, Curtin NJ, Tweddle DA. Targeting the DNA Damage Response for the Treatment of High Risk Neuroblastoma. Front Oncol. 2020 Apr 3;10:371. doi: 10.3389/fonc.2020.00371. PMID: 32309213; PMCID: PMC7145987.

Smith HL, **Southgate H**, Tweddle DA, Curtin NJ. DNA damage checkpoint kinases in cancer. Expert Rev Mol Med. 2020 Jun 8;22:e2. doi: 10.1017/erm.2020.3. PMID: 32508294.

Conference Presentations

AACR virtual conference 2, 2020 - Poster presentation – Title: Preclinical investigation of ATR inhibition alone and in combination with PARP inhibition in high risk neuroblastoma

NCRI 2019, Glasgow – Poster presentation – Title: PARP inhibition increases replication stress in pre-clinical models of high risk neuroblastoma and synergises with inhibition of ATR

PARP conference 2019, Budapest – Poster presentation – Title: PARP inhibition causes replication stress in preclinical models of high risk neuroblastoma and synergises with inhibition of ATR.

EORTIC-NCI-AACR Symposium 2018, Dublin – Poster presentation - Title: Preclinical evaluation of the ATR inhibitor VE-821 alone and in combination with the PARP inhibitor olaparib in neuroblastoma